UNIVERSITÀ DEGLI STUDI FIRENZE

DOTTORATO DI RICERCA IN Area del Farmaco e Trattamenti Innovativi, Curriculum Scienze Farmaceutiche

CICLO XXXV

COORDINATORE Prof. Carla Ghelardini

Application of advanced mass spectrometry techniques for the development of analytical methods to study molecules of pharmaceutical and biological interest

Settore Scientifico Disciplinare CHIM/08

Dottorando
Dott. *Marco Pallecchi*

(firma)

Tutore
Prof. *Gianluca Bartolucci*

(firma)

Coordinatore
Prof. *Carla Ghelardini*

(firma)

Anni 2019/2022

INDEX

1. AIMS OF THE PROJECT 1
2. INTRODUCTION TO MASS SPECTROMETRY 4
2.1. SAMPLE INTRODUCTION 5
2.2. ION SOURCES 6
2.2.1. ELECTRON IONIZATION (EI) 6
2.2.2. CHEMICAL IONIZATION (CI) 9
2.2.3. ELECTROSPRAY IONIZATION (ESI) 10
2.3. MASS ANALYZERS 13
2.3.1. QUADRUPOLE MASS ANALYZER 13
2.3.2. QUADRUPOLE ION TRAP 15
2.3.3. ORBITRAP® 16
2.4. TANDEM MASS SPECTROMETRY (MS/MS) 18
2.5. MS/MS BY TRIPLE QUADRUPOLE 19
2.6. CHROMATOGRAPHY 21
2.6.1. GAS CHROMATOGRAPHY 21
2.6.2. LIQUID CHROMATOGRAPHY 23
2.6.3. CHROMATOGRAPHY PARAMETERS 25
3. PROJECT 1: APPLICATION OF LEDA ALGORITHM FOR THE RECOGNITION OF PG-P AND CARBONIC ANHYDRASE HYBRID INHIBITORS AND EVALUATION OF THEIR PLASMA STABILITY BY HPLC-MS/MS ANALYSIS 30
3.1. INTRODUCTION 33
3.2. MATHERIAL AND METHODS 42
3.2.1. CHEMICALS 42
3.2.1. CHROMATOGRAPHY 42
3.2.2. MASS SPECTROMETRY PARAMETER 43
3.2.3. STANDARD SOLUTION, CALIBRATION CURVES AND SAMPLE PREPARATION 44
3.2.4. VALIDATION OF HPLC-MS/MS METHOD 46
3.2.5. MS/MS EXPERIMENTS 46
3.2.6. LEDA ALGORITHM 47
3.3. RESULTS 48
3.3.1. CHROMATOGRAPHY 48

3.3.2. COLLISION-INDUCED DISSOSIATION STUDY 52
3.3.3. LINEARITY AND LOD 59
3.3.4. MATRIX EFFECT, RECOVERY, AND LEDA RELIABILITY 61
3.3.5. ACCURACY AND PRECISION 65
3.3.6. CHEMICAL STABILITY TEST 66
3.4. CONCLUSION 74
3.5. FURTHER APPLICATIONS 78
4. PROJECT 2: DEVELOPMENT OF AN ID/GC-MS METHOD FOR THE QUANTITATIVE EVALUATION OF FATTY ACIDS IN PLASMA TO CONFRONT HEALTHY PATIENTS AND COLORECTAL CANCER PATIENTS 99
4.1. INTRODUCTION 100
4.2. MATHERIAL AND METHODS 102
4.2.1. CHEMICALS 102
4.2.2. CHROMATOGRAPHY 103
4.2.3. MASS SPECTROMETRY METHOD 103
4.2.4. STANDARD SOLUTIONS AND SAMPLES PREPARATION 104
4.3. RESULTS 108
4.3.1. CHROMATOGRAPHY 108
4.3.2. MASS SPECTROMETRY PARAMETER 109
4.3.3. SAMPLE ANALYSIS 110
4.4. CONCLUSION 121
4.5. FURTHER APPLICATIONS 121
5. PROJECT 3: DEVELOPMENT OF AN ID/2D-HILIC-HPLC-MS/MS METHOD TO DETERMINE HISTAMINE FOR STUDYING THE EFFECT OF N-PALMITOYLETHANOLAMINE ON MORPHINE TOLERANCE 123
5.1. INTRODUCTION 124
5.2. MATHERIAL AND METHODS 125
5.2.1. CHEMICALS 125
5.2.2. CHROMATOGRAPHY 125
5.2.3. MASS SPECTROMETRY PARAMETER 128
5.2.4. STANDARD SOLUTION, CALIBRATION CURVES AND SAMPLE PREPARATION 128
5.2.5. VALIDATION OF HPLC-MS/MS METHOD 129

5.3. RESULTS 130
5.3.1. CHROMATOGRAPHY 130
5.3.2. MASS SPECTROMETRY ANALYSIS 131
5.3.3. LINEARITY, LOD, LOQ AND VALIDATION 133
5.3.4. SAMPLES ANALYSIS 135
5.4. CONCLUSIONS 137
5.5. FURTHER APPLICATIONS 138
6 PROJECT 4 : EVALUATION OF CID FRAGMENTATION OF LEU-ENKEPHALIN IN A LINEAR TRIPLE QUADRUPOLE VARYING THE PRESSURE AND THE COLLISION GAS INSIDE THE COLLISION CELL (WORK IN PROGRESS) 141
6.1 INTRODUCTION 142
6.2 MATERIAL AND METHODS 144
6.2.1 CHEMICALS 144
6.2.2 MASS SPECTROMETRY PARAMETERS 145
6.2.3 SAMPLE PREPARATION 147
6.2.4 DATA PROCESSING 147
6.3 RESULTS 148
6.3.1 RESULTS DISCUSSION 148
6.3.2 PERSPECTIVE 156
7 CONCLUSIONS 157
8 BIBLIOGRAPHY 159

LIST OF ABBREVIATION

ABC	ATP Binding Cassette
ADE	high-grade dysplasia adenoma
APCI	Atmospheric-Pressure Chemical Ionization
APPI	Atmospheric Pressure Photo Ionization
AR	Asymmetry Factor
CA	carbonic anhydrase
CD	Celiac Disease
CE	Capillary electrophoresis
CI	Chemical Ionization
CID	Collision Induced Dissociation
CRC	ColonRectal Cancer
CV	Collision Voltage
Da	Dalton
DC	Direct Current
DR	Drug Resistance
EI	Electron Ionization
ERMS	Energy Resolved Mass Spectrometry
ESI	Electrospray Ionization Source
FAB	Fast Atom Bombardment
FD	Field Desorption
FFA	Free Fatty Acid
FM	Fibromyalgia
FT-ICR	Fourier Transform-Ion Cyclotron Resonance
GC	gas chromatography
GM	Gut Microbiota
GPCR	G-protein coupled receptor
H	plate height
hCA	human Carbonic Anhydrase
HDAC	Histone Deacetylases
HILIC	Hydrophylic Interaction chromatography

H-pl	Human Plasma
HPLC	high-performance liquid chromatogrpahy
IBD	Intestinal Bowel disease
ID	Isotopic Dilution
IEX	Ion Exchange chromatography
IM	Ion Mobility
IS	Internal Standard
IT	Ion Traps
k	retention factor
KEE	Ketoprofen Ethyl Ester
KM	Michaelis-Menten constant
LEDA	Linear Equation of Deconvolution Analysis
LLE	Liquid-liquid extraction
LOD	Limit Of Detection
LOQ	Limit Of Quantitation
LRP	Lung Resistance-related Protein
m/z	mass to charge
MALDI	Matrix Assisted Laser Desorption Ionization
MC	mast cell
MCFA	Medium Chain Fatty Acid
MDR	Multiple Drug Resistance
ME	Matrix Effect
MRM	Multiple Reaction Monitoring
MTBE	Methyl-t-butyl ether
MW	Molecular Weight
N	Number of plates
NPLC	Normal Phase Liquid Chromatography
NSAIDs-CAIs Hybrids	Nonsteroidal Anti-Inflammatory Drugs and Carbonic Anhydrase Inhibitors
PAR	Peak Area Ratio
PBS	Phosphate Buffer Saline
PD	Plasma Desorption

PEA	N-palmitoylethanolamine
P-gp	P-glycoprotein
Pi	Product Ion
PLS-DA	Partial Least Squares Discriminant Analysis
PT	Proton Transfer
PTR	Proton Transfer Reaction
Q	Quadrupole
QqQ	triple quadrupole
R	resolution (chromatography)
R^2	Determination coeffiecient
RE	Recovery
RF	Radio Frequency
Ri	Reference Ion
RPLC	Reverse Phase Liquid Chromatography
RSD	Relative Standard Deviation
SCFA	Short Chain Fatty Acid
SD	Standard Deviation
SDY-I	Standard Deviation of y-intercept
SEC	Size Exclusion Chromatography
SFC	Supercritical Fluid Chromatography
SIMS	Secondary Ion Mass Spectrometry
SPE	Solid Phase Extraction
SRM	Single Reaction Monitoring
$t_{1/2}$	half-life
ToF	Time of Flight
Tr	retention time
α	selectivity

1. AIMS OF THE PROJECT

The potential of mass spectrometry techniques in pharmaceutical and biomedical fields are well documented. The high specificity, selectivity, and sensitivity of mass spectrometry coupled with chromatography (gas and/or liquid mobile phases) affords the study of compounds either alone or in mixtures, as well as in complex matrices. In last decades mass spectrometry was employed as selected analytical method for several different investigations such as stability of a drug in different matrices (buffers, plasma etc.), evaluation of possible biomarkers to characterize a disease or even determine the concentration of a specific compound (analyte) in a biological media [1].

The aim of this PhD project was to use Mass Spectrometry as a technique to develop analytical methods to perform studies in the pharmaceutical and biological fields. In fact, all the work done in these three years consists of different projects all carried out by using mass spectrometry coupled with chromatography. In the next chapter will be introduced mass spectrometry and chromatography. Then each project will be deepened in its specific chapter.

It is well known that there are different combinations of mass spectrometer systems, so in order to better explain all the works done a general scheme was made considering, also, the instruments available in the laboratory (Figure 1.1).

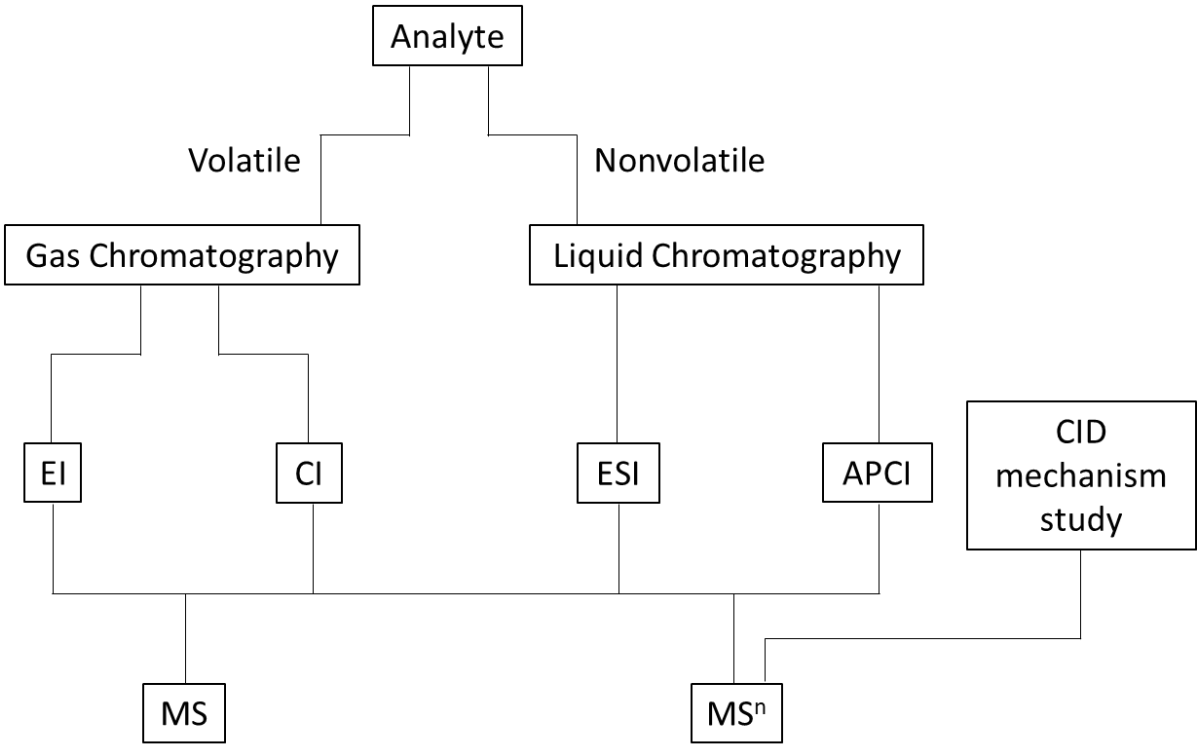

Figure 1.1: Generic scheme that introduces each different project

This scheme will help the reader to understand the choice of the best combination between chromatography and mass spectrometry in order to obtain the best performance from each project. Another important goal was the achievement of a high productivity trying to develop simple sample preparation and the fastest run time analysis without losing in specificity, sensitivity, and accuracy. Since most of the work done during my PhD experience were carried out by using MS/MS methods through Collision Induced Dissociation (CID) experiments it was decided to perform a further project (the number 4), under the supervision of Prof. Memboeuf from the Universitè of Bretagne Occidentale to deepen this mechanism that promote the formation of the product ion. In fact, usually the fragmentation of the precursor ion is achieved by using a curtain of an inert gas at a given pressure, inside the collision cell. Thus, it was deemed interesting to explore the influences of different inert gases and their pressure inside the collision cell to the CID mechanism. In detail this thesis consists of four distinct projects each one will be developed with the sections as follows:

1. Introduction;
2. Material and Methods;
3. Results;
4. Conclusions.

The four different projects are the following:

1. Application of LEDA algorithm for the recognition of PG-P and Carbonic Anhydrase hybrids inhibitors and evaluation of their plasma stability by HPLC-MS/MS analysis;
2. Development of an ID/GC-MS method for the quantitative evaluation of fatty acids in plasma to confront healthy patients and colorectal cancer patients;
3. Development of an ID/2D-HILIC-HPLC-MS/MS method to determine histamine for study the effect of N-palmitoylethanolamine on morphine tolerance;
4. Evaluation of CID fragmentation of Leu-enkephalin in a linear triple quadrupole varying the pressure and the collision gas inside the collision cell (abroad experience at Universitè de Bretagne Occidentale, work in progress).

The final goal is to highlight the versatility of the MS techniques and also its large potential in both pharmaceutical and biological studies.

2. INTRODUCTION TO MASS SPECTROMETRY

Mass Spectrometry (MS) is an analytical technique that can be used to detect and determine the amount of a specific or more analytes in the processed samples[2]. Furthermore, can be also used to establish the elemental composition and/or some characteristic of the molecular structure of a studied compound. It is mandatory that the analytes are ionized and in the gas phase in order to be separated, according to their individual *mass-to-charge ratio (m/z)* values and revealed by the detector (e.g. electron- or photo-multiplier). Moreover, to avoid the interference with the characteristics of the ions (e.g. energetic content or structural information) and keep the background signal as low as possible, this instrument has to work under vacuum. Since the ionized analytes are charged particles, their position in the space can be manipulated by using electric or magnetic fields (or both). Therefore, it is important to specify that the unit of measurement in the mass spectrometer is the *m/z*, then if only one charge is present on the ion this value is equal to the mass. Generally, the ionization process of each compound involves the formation of several ions (such as fragmented and isotopologues ions) that, with their separation and detection, compose the mass spectrum of the analyte. A mass spectrum is a relative ion abundance (Y-axis) vs *m/z* (X-axis) chart, characterize by a base peak (the most abundant ion) with which the other ions are compared. It is worth to highlight that the mass spectrometer is usually coupled with a separating system such as Gas Chromatography (GC), High-Performance Liquid Chromatography (HPLC), Supercritical Fluid Chromatography (SFC), Capillary Electrophoresis (CE) etc. This is recommended in the case of samples containing two or more isomers that often give the same *m/z* ion signals.

A mass spectrometer is composed by:

- an ion source, that can be represented as the origin of the gas phase ions;
- a *m/z* analyzer, that is the portion of the instrument responsible for discrimination of ions according to their individual *m/z* values;
- the detector, that generates the signals that are a recording of the *m/z* values and abundances of the ions;
- the vacuum system, that remove molecules, thereby providing a collision-free path for the ions from the ion source to the detector);
- the computer, that coordinates the functions of the individual components and records and stores the data.

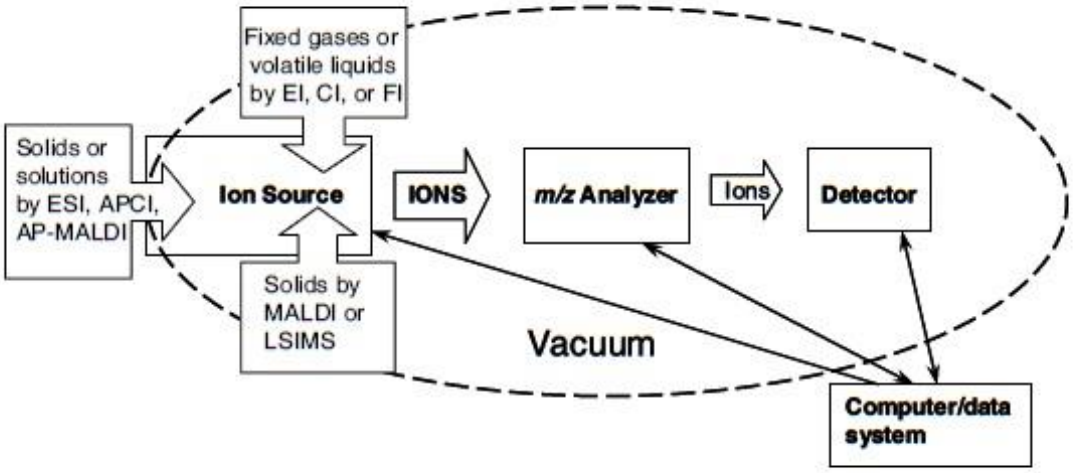

Figure 2.1: general scheme of a mass spectrometer

MS is widely used in any scientific area, however, is a crucial technique in the pharmaceutical and clinical fields.

Any mass spectrometer can be made up by a combination of different sources and analyzers and it depends also on the different separation system used. For example, GC is usually coupled with the mass spectrometer by an Electron Ionization (EI) or Chemical Ionization (CI) considering that the sample is already in the gas-phase while the HPLC is usually coupled with an Electrospray Ionization source (ESI) or an Atmospheric-Pressure Chemical Ionization (APCI) where the sample, carried by a liquid, is also evaporated. In the following chapters will be deepened the sources and analyzers that composed the instruments use for all the developed projects.

2.1. SAMPLE INTRODUCTION

The analyzed sample can be a liquid, a solid or a gas; in regards the solid samples, they are placed at the top of the probe, which is introduced in the vacuum chamber through an entrance and subsequently the sample is evaporated or sublimated by heating. Otherwise, liquids or gasses can be introduced with a calibrated syringe or by special valve systems, that let the sample to access to the ionization source without have contact with the external atmosphere. In all cases described the quantity of the sample used are extremely low, such as nano- or picograms, that are 10^{-9}-10^{-12} grams. As already mentioned, to obtain a spectrum of a single

compound from a mixture sample is appropriate to equip the spectrometer with a separative system, like GC or HPLC, to distinguish the components. These analytical techniques, known as GC-MS and HPLC-MS, are extremely useful in the analysis of mixtures or complicated matrices.

2.2. ION SOURCES

Ionization process occurs inside the ion source and could be done by different techniques. The source must be chosen according to the compounds in study because is it possible to obtain different spectra. Based on the energy involved, the ionization methods can be classified in two major classes.

- Hard Ionization, that operates at high energy, obtaining a boosted fragmentation:
    - Electron Ionization (EI);
- Soft Ionization, that operates at low energy, obtaining a low number of fragments or none:
    - Chemical Ionization (CI);
    - Fast Atom Bombardment (FAB);
    - Secondary Ion Mass Spectrometry (SIMS);
    - Plasma Desorption (PD);
    - Matrix Assisted Laser Desorption Ionization (MALDI);
    - Field Desorption (FD);
    - Electrospray Ionization (ESI);
    - Atmospheric-Pressure Chemical Ionization (APCI)
    - Atmospheric Pressure Photoionization Ionization (APPI)

Among these techniques, we used EI, CI and ESI ion sources to develop the analytical methods for my PhD projects.

2.2.1. ELECTRON IONIZATION (EI)

Widely used in mass spectrometry, Electron ionization (EI) is still the most classic ionization technique that is based in the production of the molecular ions from gas-phase analytes by the

interaction with high energetic electron (70 eV)[2]. The ionization mechanism can be represented as follows:

$$M + e^- \rightarrow [M]^{\cdot +} + 2e^-$$

The neutral molecules (M) arrived in the source interact with an electron beam at 70eV producing the molecular ions ($[M]^{\cdot +}$). The interaction with the electrons involves the transfer of a high amount of energy on the new formed molecular ion; then the excess of this energy can be used to break one or more chemical bond. Therefore, not only the molecules are ionized but the excess energy obtained is dissipated through the breakage of one or more bonds (fragmentation). The result of this interaction leads to the formation in the ion source of a complex mixture of ions, both positive and negative, and neutral species. The cleavage of the analyte molecular ion leads to the formation of fragment ions in a reproducible way, which results in a "fingerprint" of the analyte. Because of the uniqueness of these "chemical fingerprints", commercially available libraries containing hundreds of thousands of standard EI mass spectra can be used to facilitate identification of unknown compounds [1]. This source usually works at a pressure of 10^{-6} Torr and can be usually connected to a GC, while very difficult is the coupling with the HPLC. Generally, in the EI, only positive ions are detected because their abundance is higher respect to the negative ions, non-ionized and neutral molecules, instead, are removed by the vacuum system of the instrument. Positive ions are guided to the analyzer maintaining the ion source at positive potential and focalizing the ion beam through appropriate potentials. These are applied to a sequence of lens located between the source and the analyzer. The role of the Repeller, to which a positive potential is applied, is to cause the expulsion of the positive ions. In the contrary, the electrons are attracted on the Trap, positively charged **(**Figure 2.2).

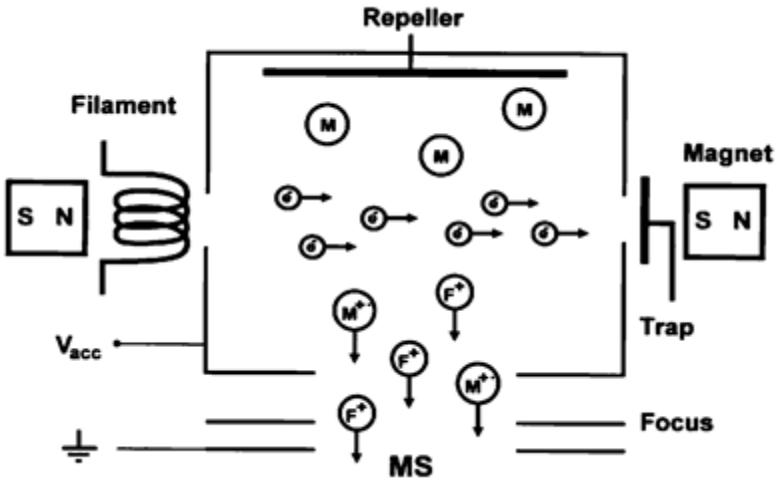

Figure 2.2: EI source representation

The following example represents the ionization of methanol:

$$CH_3OH + e^- \rightarrow [CH_3OH]^{\cdot+} + 2e^-$$

The symbol "$^{\cdot+}$" represents the radical cation, that is an unpaired electron. The imparted energy to the ion and its resulting instability led to a further breaking, with the formation of molecules and/or neutral radical, that are not revealed by the instrument, or a radical cation (fragment ions). In the case of methanol, it will obtain:

$$[CH_3OH]^{\cdot+}(molecular\ ion) \rightarrow [CH_2OH]^{+}(fragment\ ion) + H^{\cdot}$$

$$[CH_3OH]^{\cdot+}(molecular\ ion) \rightarrow [CH_3]^{+}(fragment\ ion) + OH^{\cdot}$$

On their path, molecular ions undergo an acceleration directly proportional to the potential V of the focus lens and they are expelled through an exit with a kinetic energy equal to:

$$zV = \frac{1}{2}mv^2$$

Where:

- *z* is the charge of the ion, usually equal to 1;
- *V* is the potential of the focus lens
- *m* is the mass of the ion;
- *v* is the speed of the ion.

The fragmentation of molecular ion, that often occurs, can represent a disadvantage because the signal of molecular ion is not always revealed, thus the molecular mass of the analyte cannot be determined. For these reasons sometimes is necessary switch the EI ions source to use "soft techniques".

2.2.2. CHEMICAL IONIZATION (CI)

Chemical Ionization (CI) is a mechanism which exploits the reaction between two molecules, a charged one (reactive) and a neutral one (analyte), with a limited energy exchange[2]. Generally, this reaction involves the transfer from the reagent gas, previously ionized ($[GH^+]$) to the neutral molecule to analyze. In Proton Transfer Reaction (PTR), the acidic reagent ($[GH^+]$) gives the proton to the neutral analyte (M) to form the protonated ion of the molecule ($[M+H]^+$):

$$GH^+ + M \rightarrow MH^+ + G$$

The analyte M, in gas-phase, is introduced inside the spectrometer with an excess of reagent gas (for instance methane), who must have a less proton affinity than the one of the molecule in order to be able to provide the proton. Formerly, the gas is ionized by EI, forming the reactive species that will interact with the analyte, giving and/or tearing a proton or an electron. So, summing up, the ion $[M+H]^+$, that has a molecular mass equal to M+1, will be detected in positive ion mode, while the ions $[M-H]^-$ or $[M]^-$ will be detected in negative ion mode. For example, using the methane as reagent gas, it is possible to obtain the following reactive species:

$$[CH_4]^{\bullet+} + CH_4 \rightarrow [CH_5]^+ + CH_3^{\bullet}$$
$$[CH_4]^{\bullet+} + CH_4 \rightarrow [C_2H_5]^+ + H_2 + H^{\bullet}$$

The species $[CH_5]^+$ but especially the cation $[C_2H_5]^+$, being ions with a high tendency to donate a proton, through an acid-base reaction, can basically protonated any organic molecule. This reaction mechanism is called Proton Transfer (PT) and generally is the main process that leads in the positive CI. However, this ionization can involve different reaction mechanisms with other ionic species present in the reactive plasma that leading to the formations of many adduct or even fragment ions of the analyte molecule. Finally, both in EI and CI it is possible to analyze

small compounds (<1200 Da) while for bigger molecular masses, such as polymers or macromolecules, it is commonly used other sources.

2.2.3. ELECTROSPRAY IONIZATION (ESI)

Electrospray ionization or ESI is classified as soft ionization technique, that occurs at atmospheric pressure and in liquid phase (Figure 2.3) and its diffusion and development coincided with the growing of the reversed phase liquid chromatography[2]. Indeed, in this chromatography approach the mobile phase is characterized by the presence of water or its mixture with miscible solvents (generally methanol or acetonitrile) and the ESI functionality is favored by the conductivity properties of water content mobile phases. Furthermore, the water solutions can improve the ionization of the solutes by the modification of their pH value; then, adding a proper volatile compound (acidic or basic) in the mobile phase, it is possible to promote the ionization of solutes by protonation (positive ion) or dissociation (negative ions).

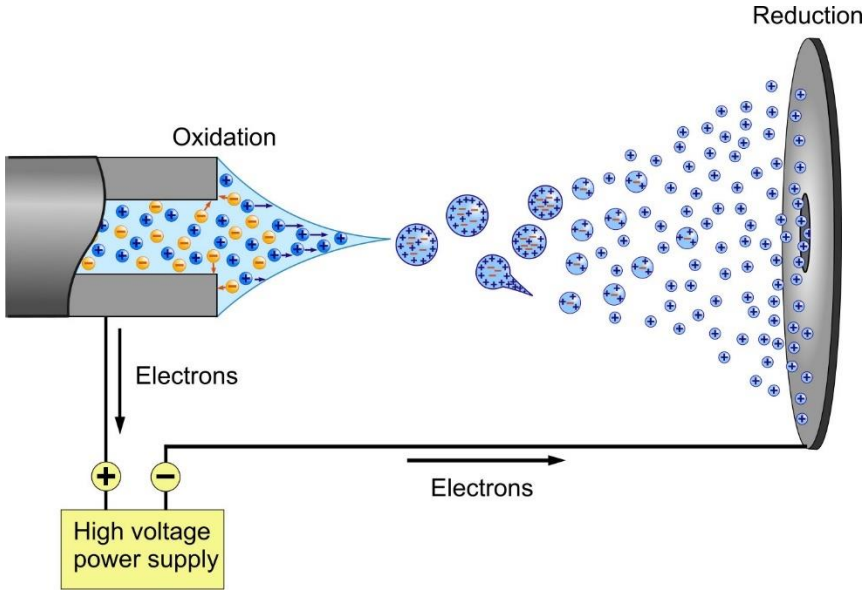

Figure 2.3: ESI representation in positive ion mode

The sample solution is introduced in the source through a conductive capillary tube and came out as an aerosol or spray because of the different pressure between the inside and the outside of the capillary (from high to low pressure). Therefore, the sample solution will tend to expand at the exit of the capillary, dispersing into very small drops (1-2 μm of diameter). A high

potential current (4-5 kV) is applied between the exit of the capillary tube and the orifice entry of the mass spectrometer in order to polarize the ionic solutes of the sample solution and, basing on the electric potential sign applied, it will produce a different disposition of the ion charges. For instance, if the electric potential of the capillary tube is positive, the positive ions of the solution will move away from the surfaces of the capillary and will accumulate in the center of the tube (ion gradient). This ion gradient, induced by the applied electric field, involves two phenomena: 1) the formation of the "Taylor cone" and the variation of the pH value of the solution. In fact, resuming the previous example, if the positive ions of a solutions accumulate in a very small drop and the solution is aqueous or is a mixture containing water, most of the positive ions of the solution are hydronium ($[H_3O]^+$). Therefore, their accumulation in a define space increase their concentration resulting in a decrease of the pH value. This effect leads to the ionization (i.e. protonation) of the neutral compounds solubilized in the solution flowing through the capillary tube. The effect on pH is obviously inverse when it is applied a negative electrical potential. Then, in the Taylor cone, there are the ionic species of the solubilized analytes that must be desolvated and vaporized to introduce them into the mass spectrometer. For this purpose, the spray of the sample solution, once it came out from the capillary, is invested by the hot flow of an inert gas (nebulizer gas). The overall effect, caused by the nebulizer gas and its temperature, lead to a progressive reduction in the average diameter of the drops. It follows that the concentration of both ionic solute and surface charge of the droplet increase until the liquid surface tension is exceeded, causing the so called "Coulomb explosion" (Figure 2.4).

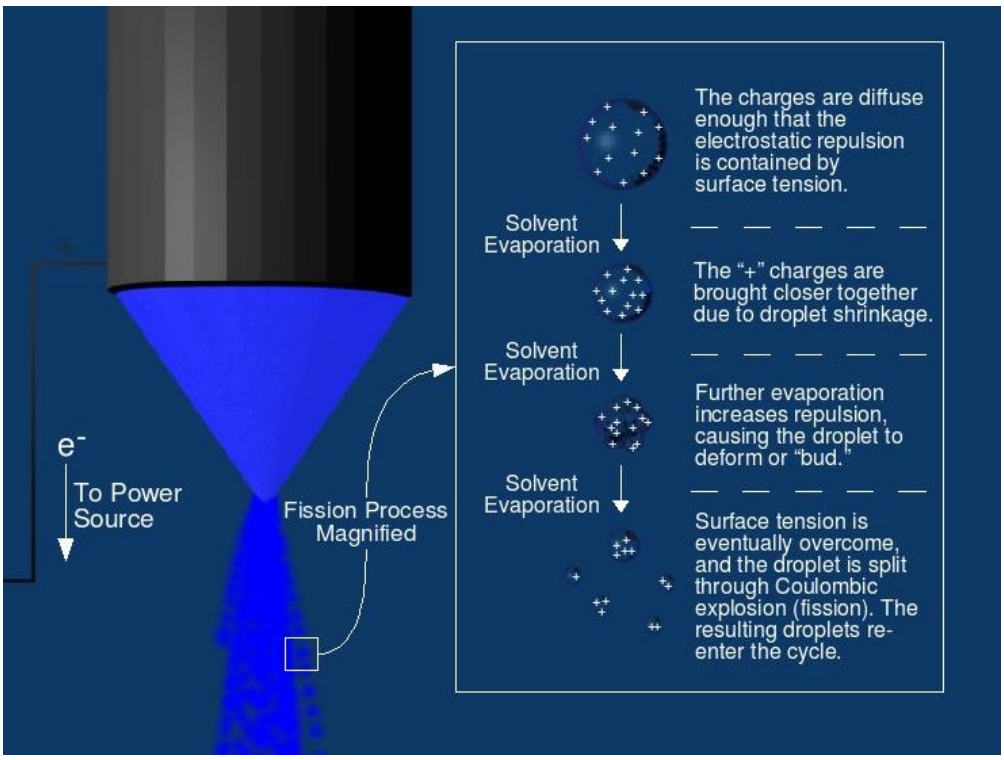

Figure 2.4**:** Coulomb explosion representation.

So, analyte ions in gas-phase are formed and they are pushed by the electrical field through a succession of lens until they reach the low-pressure zone, where they are accelerated to the analyzer. The ESI source is also able to deploy, on the molecule, a number of charges greater than one (usually occur to large molecules like polypeptides or proteins). In this case the value of the denominator increases and the *m/z* ratio decreases allowing the revelation of compounds with a very high molecular mass without losing in sensitivity. In fact, this is a source suitable for most of the compounds, from small organic molecules to macromolecules (such as proteins), as long as they have several ionization sites. Usually, with this source, no fragments are produced, and thus, the spectra obtained are extremely simple and easy to interpret. In fact, the sample solution, already contains the ionized solute; therefore, in the ESI source the ionized analyte is simply desolvated, using the minimum quantity of energy. Furthermore, it is common to observe, in the ESI mass spectra, different types of ions called adduct ions, both positive and negative. This ions are generated, in the Taylor cone, by the molecule adduction with native ions present in the surrounding solution, such as sodium or potassium ($[M+Na]^+$ and $[M+K]^+$ respectively) for positive adduct ions and Chlorine ($[M+Cl]^-$) and formate ($[M+HCOO]^-$) for negative ones. Unfortunately, the ESI source cannot operate in normal phase chromatography or with apolar compound like hydrocarbons; in these cases, it is necessary to change the ion source with APCI or APPI interfaces.

2.3. MASS ANALYZERS

The mass analyzer is a device that uses dispersion or filter methods; for separate the ions depending on their *m/z* ratio or a related property (i.e. cross section). The most diffused mass analyzers are Magnetic and Electric Sectors, Quadrupoles (Q), Ion Traps (IT), Orbitraps®, Time of Flight (ToF) and Fourier Transform-Ion Cyclotron Resonance (FT-ICR).

2.3.1. QUADRUPOLE MASS ANALYZER

In the quadrupole mass analyzer, the ions are separated based on their motion inside the area limited by four cylindrical bars connected with a Direct Current (DC) and a Radio Frequency alternating current (RF)[2]. The four cylindrical bars are arranged longitudinally parallel with a length between 20 and 50 cm (Figure 2.5).

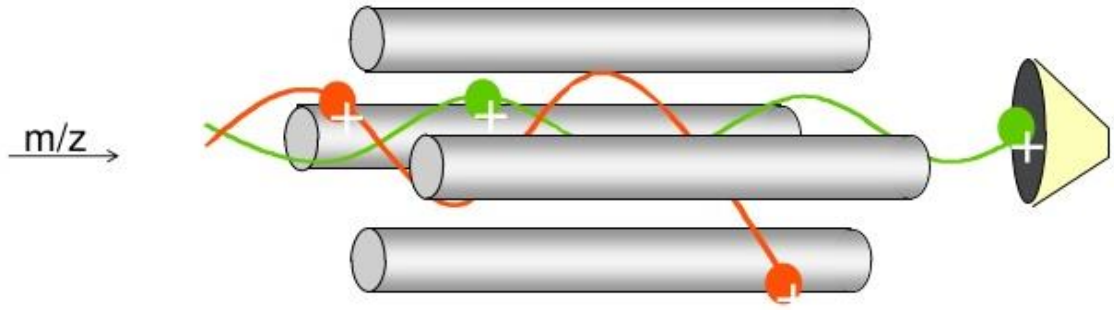

Figure 2.5: Quadrupole scheme

This symmetrical arrangement allows nearly hyperbolic electric fields to be produced according to quadrupole theory. The ions, coming from an ion source, are accelerated (5–15 V) into the central space that constitutes the quadrupole electric field along the longitudinal axis toward the detector. The rods are maintained at an oscillating electric potential, so that, when the two vertical rods have positive potential, the horizontal ones have the negative potential, switching the potential at high frequency (kHz-MHz). Ions travel a different trajectory for each *m/z* value. By adjusting the oscillating electric field, it is possible to select the *m/z* value of the ions that cross the quadrupole; the ions with a different *m/z* will be diverted and cannot reach the detector. To investigate a *m/z* range of ion (scan ion mode), it is necessary to perform a systematic variation of the strength of the fields (DC and RF). Consequently, a series of short time intervals were defined, each characterized by different intensity of both DC and RF electric fields, that

allow the sequential transmission of different *m/z* (a *m/z* value at time) through the mass analyzer (space-based mass analyzer), This is the reason why the quadrupole mass analyzer is also known as quadrupole mass filter. The conditions for stable trajectories can be identified by the Mathieu diagram (Figure 2.6), in which it is possible to distinguish space regions *a*-*q*, where the solutions of the equations of motion are stable or unstable.

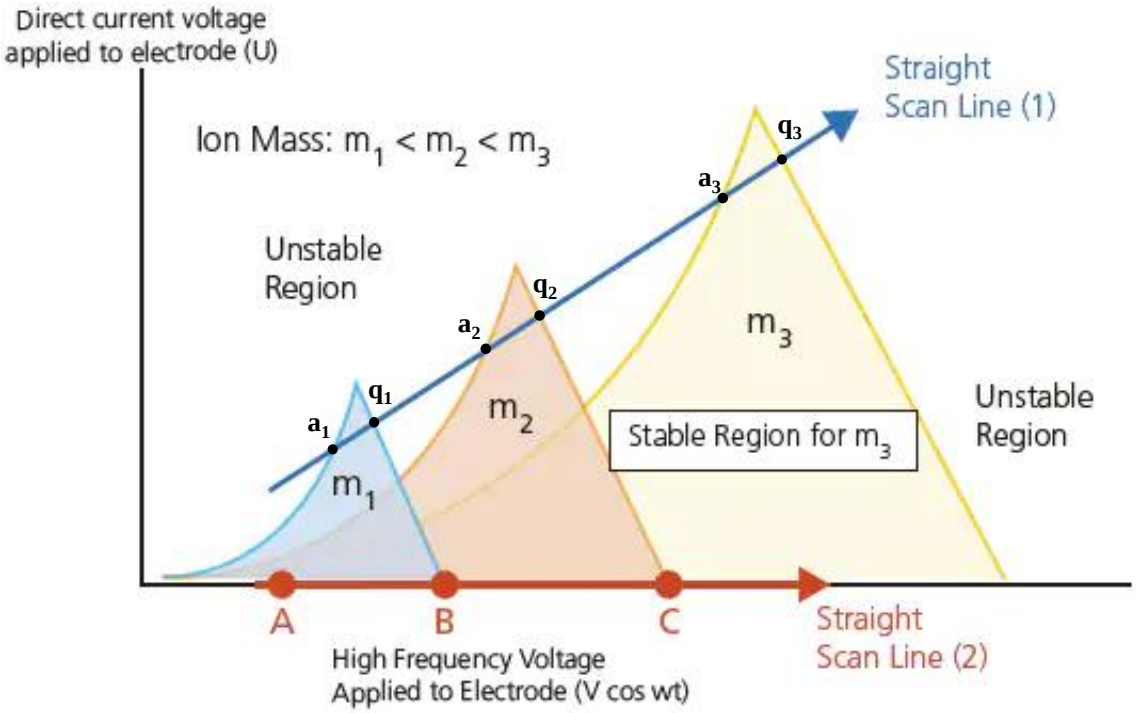

Figure 2.6: Mathieu stability diagram

As might be anticipated from the very large number of a and q values that constitute the colored area in the stability diagram, a quadrupole mass filter could, be operated at any value in the *a*-*q* space corresponding to a point in the shaded region. However, in practice, the values of a and q space are limited by adjusting the RF and DC potentials to a fixed ratio. By fixing the ratio of RF and DC potentials to establish the resolving power, the only values of *a* and *q* space available to ions in the instrument lie along the operating line or scan line (in blue) within the colored region. Therefore, the slope of the scan line represented by the intensities' ratio between DC/RF and their simultaneous variation allow the sequential transfer of the different *m/z* ions in a defined range. In the new and optimized quadrupolar mass filters, the scan time to analyze a range between 10 and 800 Da is inferior to the second, much shorter than the magnetic sector analyzers. It is also possible to vary the slope of the operating scan line in order to modify the selectivity of the mass filter (mass resolution), but this kind of mass analyzer operates generally

at low resolution (1-3·10^3 FWHM), allowing the ions distinction that differ of integer values of *m/z*. An interesting phenomenon occurs when the DC is kept constant or removed by the linear quadrupole; in this case, the scan line come down along the abscissa of the Mathieu diagram, indicating that all ions included in the stability area have stable trajectories. The condition just described represent a different quadrupole system (RF-only quadrupole) that can be used as ions reaction (collision cell) or time-based analyzer (Ion trap or QIT).

2.3.2. QUADRUPOLE ION TRAP

The quadrupole ion trap (QIT) mass analyzers operate based on the same physical principle as quadrupole mass analyzers, but the ions are trapped in stable orbits in a 3-D chamber and are sequentially ejected [3]. The quadrupole ion trap mass analyzer consists of three hyperbolic electrodes: a donut-shaped ring electrode, an entrance endcap electrode, and the exit endcap electrode (Figure 2.7). Both endcap electrodes have a hole in their center through which the ions can travel, and the ring electrode is located midway between the two endcap electrodes. These electrodes form a cavity in which it is possible to trap the ions and analyze them by progressively destabilization during the time (time-based mass analyzer).

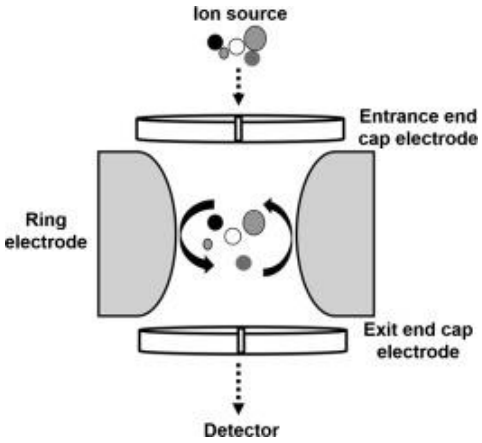

Figure 2.7: Quadrupole ion trap scheme

The primary component of the quadrupole electric field that surrounds the ions is based on radio frequency (RF) potentials applied to the ring electrode. Unlike the transmission quadrupole, that employs a two-dimensional field, the one of the QIT is three dimensional, which means that ions of all *m/z* values are stored in the device, traveling in discrete orbits within the RF

field. These mass analyzers are distinguished due to the use of supplemental alternating potentials applied to the endcaps electrodes that are employed for the destabilization or excitation of the stored ions in the performed MS experiments. Indeed, the ion trap allows the tandem mass spectrometry experiments without involving other mass analyzer, by managing the stored ions in time-based sequential operations. The ion trap operates at a relatively high pressure (about 10^{-3} Torr), achieved by introducing a continuous flow of helium (buffer gas) into the instrument, to obtain an adequate resolution between the ions and acquire stable and reliable mass spectra. The use of buffer gas collisional cools the ions, reducing their rotational and vibrational energies, so the amplitude of their random displacement about the z-axis is diminished; this damping of the ion motions extends the *m/z* range of ions that can be trapped with good efficiency and resolution. Furthermore, the helium can be used as collision gas in the MS/MS or MS^n experiments, by increasing the excitation time to allow the fragmentation of isolated ions (precursor ion).

2.3.3. ORBITRAP®

The orbitrap is a new mass analyzer consist of a specially shaped inner axial (a spindle) and outer coaxial (a barrel) electrodes[2]. Unlike the quadrupole ion trap, which uses a dynamic electric field typically oscillating at ~1 MHz, the Orbitrap uses a static electrostatic field to sustain ion trapping following the specialized dynamic injection pulse. This mass analyzer consists of two electrodes in the form of coaxial axisymmetric electrodes, an outer barrel-shaped surface, and an inner spindle-shaped electrode oriented (Figure 2.8).

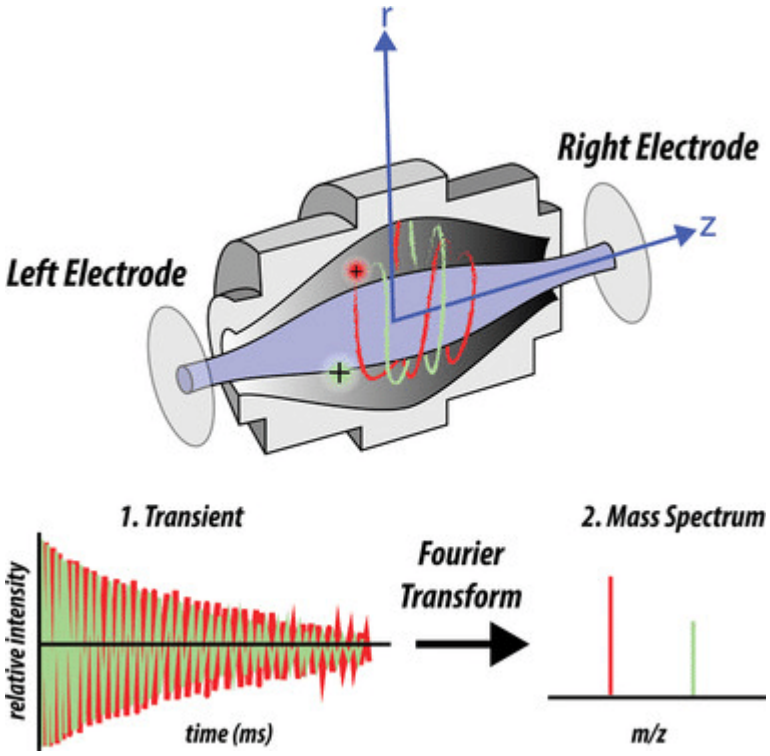

Figure 2.8: Orbitrap representation

A constant electric potential is imposed between these two axisymmetric electrodes. Ions are injected into the mass analyzer at right angles to the z-axis at a nonzero position along the x- and y-axes at an optimal position between the surfaces and displaced from the point of greatest separation of the two surfaces (center of the Orbitrap) along the z-axis. Properly injected ions follow circular orbits above the outer surface of the inner spindle-like electrode but below the inner surface of the barrel-like outer electrode. The radius of the circular orbit is established by balancing an electrodynamic centripetal force with the centrifugal forces acting on the ion related to its initial tangential velocity. Because the electric field between the surfaces of the coaxial electrodes is inhomogeneous in a symmetric manner as a function of position along the z-axis relative to the point of greatest separation between the two surfaces (center of the Orbitrap), the ions have a natural tendency to oscillate axially (i.e., along the z axis). These oscillations produce a complex alternate image current, acquired by the outer electrodes, derived by the sum of each image current created by individual *m/z* ion stored in the Orbitrap. The frequency deconvolution, by using the Fourier Transform (FT) algorithm, of the complex image current allows the reconstruction of the mass spectrum. The resolving power of this analyzer is 100000 at 400 *m/z* for a standard instrument but can reach higher values in the premium ones. Furthermore, the Orbitrap resolving power is proportional to the number of harmonic oscillations of the ions; as a result, the resolving power is inversely proportional to

the square root of *m/z* and proportional to acquisition time. The high resolution provided by this analyzer let the calculation of the accurate mass helping the molecular structure elucidation and can also distinguish isobars compounds without their separation.

2.4. TANDEM MASS SPECTROMETRY (MS/MS)

In tandem mass spectrometry, the instrument is not used only to separate the ions by their *m/z* ratio, but also to isolate one or more ions from a mixture to study their characteristics. For instance, it is possible to evaluate the generated fragments that depend on the structure of the molecules and the conditions used for the analysis. The MS/MS experiment can be summarized in the following fundamental steps (summarized in Figure 2.9):

1. Selection of one ion (Precursor ions);
2. Fragmentation of the precursor ion, through a collision with an inert gas (Collision Induced Dissociation, CID);
3. Analysis of the fragments obtained (Product ions).
4.

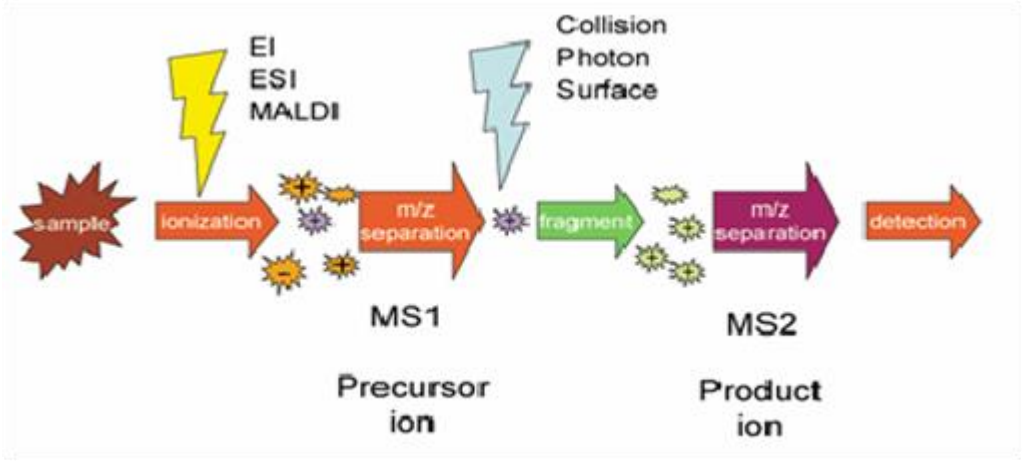

Figure 2.9: how a MS^2 experiment works

Theoretically, to perform a MS/MS experiment, it takes only two analyzers, separated by a collision cell. Practically, merging several analyzers it is possible to obtain a lot more information:

- The quadrupole is characterized by an elevated dynamic range, is cheap and robust but has a limited range of detectable *m/z* values and low resolution. Its use is very common

as *m/z* filter coupled with any other analyzer (Q, Orbitrap; QIT) but also as collision cell, in only-rf mode (Triple Quadrupole, QqQ);

- The Orbitrap and Time of flight (ToF) work in high resolution, so it is possible to calculate the accurate mass, then they are used as second analyzer;
- The ion trap, instead, let to perform MSn. This means that the MS/MS experiments can be carried out in time in a single analyzer. In fact, it is the only one that does not need to be coupled with other analyzers.

Therefore, except for the ion trap, in order to perform MS/MS experiments it needs two or more analyzer in series. The most common combination of analyzers are the following:

- Triple quadrupole (QqQ);
- ToF-ToF;
- Qq-ToF;
- Qq-QIT;
- Quadrupole Ion Trap (QIT)

As it was already said, the ion trap is an exception, because it uses the time variable as tool before revelation (tandem-in-time mass spectrometry). Basically, the MS^n experiments are distributed in time and potentially can be repeated until the exhaustion of the available fragments. Repeating more MS^n analysis steps is useful to identify compounds in complex mixtures and for determine the structure of an analyte, or to increase the sensitivity for in traces dosage. In the next chapter will be deepened the used MS/MS technique for my projects.

2.5. MS/MS BY TRIPLE QUADRUPOLE

The triple quadrupole (QqQ) is a tandem arrangement system in which the first and third quadrupoles are mass-selective (Q) and the second quadrupole (q), operating in the RF-only mode (transmits all ions), works as a collision cell (Figure 2.10)[2].

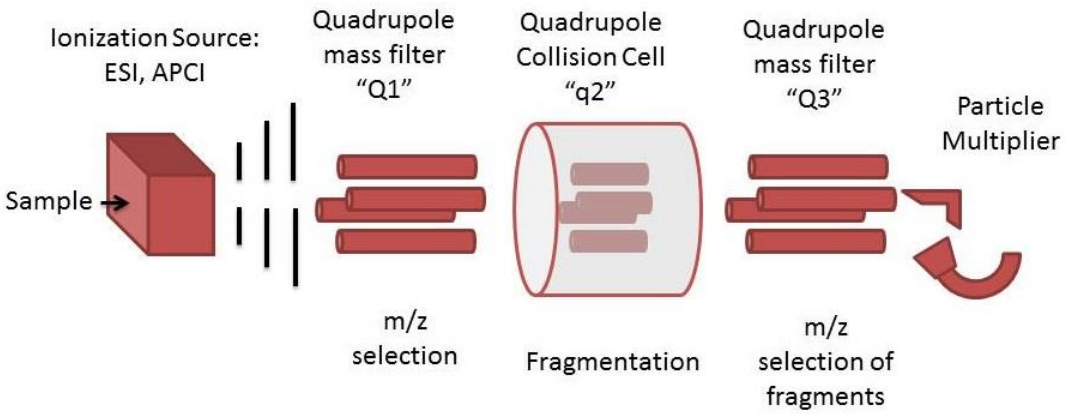

Figure 2.10: MS^2 experiment in QqQ

The first quadrupole is used for selection of precursor ions following any ionization source employed. The precursor ion is transmitted to the collision cell, which manages the residual precursor ions and all the formed product ions, while the third quadrupole provides to analyze all the ions transferred from the collision cell. The pressure in the collision cell will be ~10^{-3} Torr due to the presence of a collision gas (usually Argon or Nitrogen) used to fragment the precursor ion by collision induced dissociation mechanism (CID). There are different MS/MS experiment available with this arrangement:

1. Product Ion Scan: in this case the Q_1 selects a *m/z* ratio and, after its fragmentation, the Q_3 operates a scan of the product ions in a defined *m/z* range. With this experiment is possible, through the analysis of the fragment ions, obtain structural information of the precursor ion;
2. Precursor Ion Scan: in this acquisition mode the Q_1 is in scan mode in a selected *m/z* range, while the Q_3 analyzes only one specific product ion. So, it is possible to determine all the precursor ions that generate a specific fragment ion and identify classes of molecules with similar molecular structure;
3. Neutral Loss: in this experiment both Q1 and Q3 are scanned together, but with a constant mass offset. This allows the selective recognition of all ions which, by fragmentation in q2, lead to the loss of a given neutral fragment (e.g. H2O, NH_3 etc.). Similar to the precursor ion scan, this method is useful in the selective identification of closely related compound in a mixture;
4. Single or Multiple Reaction Monitoring (SRM or MRM): this acquisition is generally coupled with a chromatographic system (gas or liquid) for the multiresidue analysis. The identity of the molecule is known, and the first quadrupole is set on the *m/z* value

of the precursor ion while the third one is set on the *m/z* value of a quantitative fragment and a qualitative fragment (SRM). The time to record each transition is in the order of the microseconds (μs), then, in the elution time of a chromatographic peak, it is possible to record hundreds of transitions to characterize several analytes (MRM). This acquisition mode allows to hypothetically perform multicomponent analysis without losing in specificity and sensitivity.

2.6. CHROMATOGRAPHY

Considering that in several project the mass spectrometer was coupled with a chromatographic system it was deemed necessary to introduce this technique. The chromatography system is composed by a fluid solvent (gas or liquid) called the mobile phase that carries the sample through a system (a column, a capillary tube, a plate, or a sheet) on which a material called the stationary phase is fixed. The mixture of components in the sample are separated based on the different partitioning between the mobile and the stationary phases. The reversible interactions between the analytes and stationary phase, such as dispersion, hydrogen bonding, and dipole–dipole forces govern the separations. When the mobile phase is a gas, the technique is referred to as gas chromatography (GC) and when it is a liquid, the technique is called liquid chromatography (LC). Unlike the sample, which is injected as a discrete and known volume, the mobile phase flows continuously through the chromatographic column, transferring the sample mixture. The separation of the sample components carries out by increasing stepwise their affinity for mobile phase can operate on different parameters depending on the chromatography system considered. The obtained chromatogram profile gives many information on each peak, but the most important are: the retention time (t_r) that, in the used conditions, is characteristic of individual component (qualitative information) and its abundance (integrated area or height), which is related to the concentration of the component in the sample (quantitative information).

2.6.1. GAS CHROMATOGRAPHY

Gas chromatography is the chosen separation method for volatile and thermally stable compounds[4]. In GC, the mobile phase is an inert gas, typically helium (He), nitrogen (N_2), or hydrogen (H_2), delivered from a high-pressure gas tank. The gas is applied in the column and flowing through toward the low-pressure end; then, pressure difference between the head and

ending of the column establishes the flow rate value of mobile phase. Generally, the stationary phase in GC is represented by high-temperature resistant polymer film of 0.25-5 μm thick distributed in the internal wall of a capillary glass column of 0.1 to 0.25 mm of internal diameter and tens meters long (Figure 2.11).

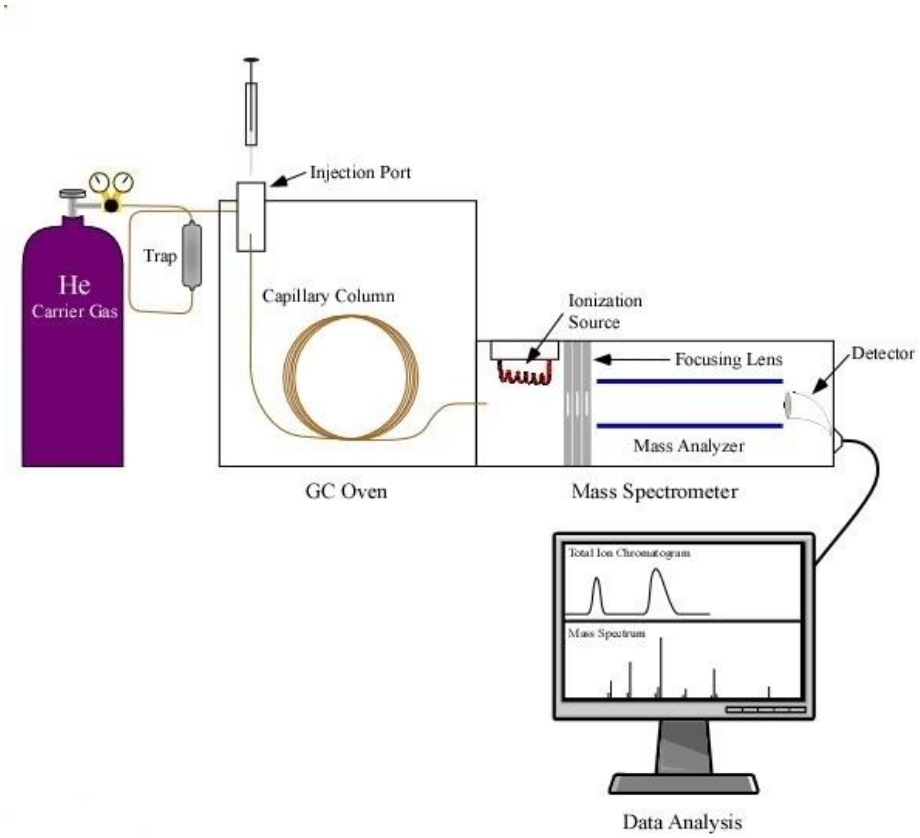

Figure 2.11: generic representation of a GC system

The carrier gas must be inert both with the solutes and the stationary phase, its function is simply to transfer the sample components into the column to undergo the differential interaction with mobile and stationary phases. The equilibrium between the phases can be describe by the distribution constant or partition coefficient (K), described as follows:

$$K = \frac{[solute]_{stat}}{[solute]_{gas}}$$

The retention of the compounds and their separation is characterized by the number and the strength of the interactions that they establish with the stationary phase. The chemical nature (typically apolar) of the GC analyzed compounds indicates the dispersion interactions as the major retention forces, while more specific reversible bonds, such as dipole-dipole and

hydrogen-bonding interactions, giving rise to an additional retention. However, the strength of these interactions, giving rise to an additional retention. However, the strength of these interactions is strongly temperature dependent. Therefore, to manage the separation of a sample complex mixture in a GC system three key parameters must be controlled:

1. temperature;
2. mobile phase velocity;
3. the chemical nature of the stationary phase (e.g., polar versus nonpolar).
4.

2.6.2. LIQUID CHROMATOGRAPHY

Liquid chromatography is used for all thermolabile compounds that cannot be analyzed by gas chromatography such as amino acids, environmental toxins, drugs, surfactants, carbohydrates etc[4]. In this technique, a liquid mobile phase is pumped, by a system of pumps, through a packed column filled with highly porous particles (normally silica) that constitute the stationary phase. The mobile phase transports the analyte molecules through the column, allowing the formation of the interactions between mobile and stationary phases. The surface of the silica particles (stationary phase) interacts with the analyte molecules and cause their retention in the column. The separated compounds, differentially eluted by mobile phase, is detected with a detector, in our case the mass spectrometer. The effectiveness, reliability and diffusion of the liquid chromatography system just described, it suggested its naming as high-performance liquid chromatography or commonly defined HPLC (Figure 2.12).

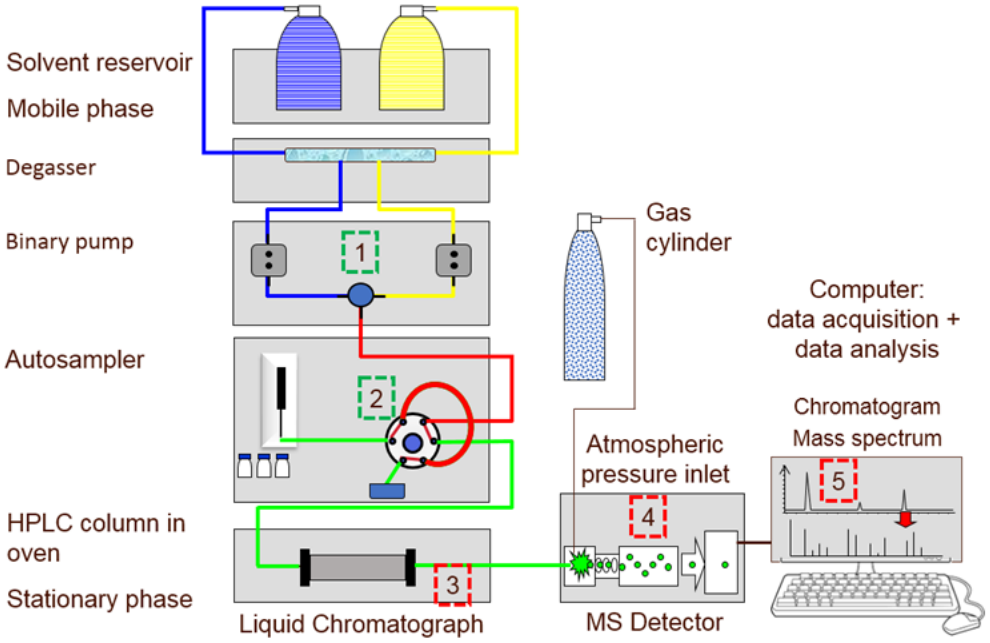

Figure 2.12: generic representation of a HPLC system

The total retention time of any solute is therefore related by its different affinity for the mobile or stationary phase. Molecules that have a high solubility to the mobile phase should be slightly retained, while molecules that have strong interactions with the stationary phase are highly retained. Complex mixtures of molecules can thus be separated because different compounds have different blends of mobile phase and stationary phase affinities. There are many liquid chromatography approaches that can be performed to separate a complex mixture and the most suited depends on the types of solutes. A selection of these approaches are:

1. Normal phase liquid chromatography (NPLC);
2. Reversed-phase liquid chromatography (RPLC);
3. Ion-exchange chromatography (IEX);
4. Hydrophilic interaction chromatography (HILIC);
5. Size exclusion chromatography (SEC);
6. Affinity chromatography.

Considering the project carried out the reversed-phase liquid chromatography and hydrophilic interaction chromatography will be deepened in the following subchapters.

Reversed-phase liquid chromatography (RPLC)

In contrast to the polar stationary phases and nonpolar mobile phases originally used by Tswett and which characterize NPLC, Horvath reversed the polarities of the mobile and stationary phases by using particles modified by linking nonpolar alkane-like molecules. In combination

with this, he proposed polar mobile phases constituted primarily of water or its mixtures with polar organic solvents such as acetonitrile (CAN) and methanol (MeOH). For this reason, these chromatographic methods are referred to as reversed-phase liquid chromatography (RPLC). In the most common RPLC, the surface of the silica particles is modified with alkyl chains (the most representative is the C-18 chains) that can be functionalized with polar moieties (-CN, -NH_2, -diol, etc.). The stationary phase therefore acts somewhat like a thin layer of liquid alkane into which solutes can diffuse and interact. Because the solute is embedded in the stationary phase, the mechanism of retention is solute partitioning between the mobile and stationary phases.

Hydrophilic interaction chromatography (HILIC)

While RPLC can separate a wide range of organic compounds, small polar molecules typically quickly elute in this method due to the high-water content used in the mobile phases. HILIC approach is an alternative mode for separating polar and charged compounds. HILIC, like NPLC, uses polar stationary phases such as silica or short-chain amino, and cyano or more polar phases. Contrary to the RPLC, in HILIC technique, the retention, is achieved by increasing the quantity of organic solvents. The partition mechanism arises from a layer of water that is adsorbed to the particle surface throughout the pores. This creates a liquid layer near the pore surface that is richer in water than is the mobile phase. Polar molecules are attracted to this layer and are thus retained in a partition-like mechanism. The more hydrophilic a solute is, the more it favors partitioning into the immobilized water layer, and thus the more it is retained.

2.6.3. CHROMATOGRAPHY PARAMETERS

The parameters that characterize a chromatographic separation can be summarized as follows:

1. retention time (t_r);
2. retention factor (k);
3. selectivity (α);
4. efficiency (N);
5. resolution (R);
6. asymmetry factor (AR).

The retention time (t_r) can be explained as the time that a molecule spends in the column, from the injection to the detection, and can be represented by the following equation:

$$t_r = t_s + t_m$$

where t_s and t_m are the time spent in the stationary and mobile phases, respectively. More simply, t_r is the time of the chromatogram of the peak related to the molecule. While the retention time is the most fundamental quantity measured, we often convert it into a dimensionless quantity called the retention factor, k, where:

$$k = \frac{t_r - t_m}{t_m}$$

In this case, t_m, represents the time it takes the mobile phase to flow from the start of the column to the detection and it also called "dead time". Anyway, the retention of any single component is typically not of primary importance to a chromatographer, while the idea of separation is much more important. In fact, in chromatography there are a lot of parameters that must be evaluated in order to have the best separation between two or more analytes. These parameters are also important because they can help to understand where to improve in case of an insufficient separation or resolution. Anyway, the degree of separation between any two solutes, A and B, is quantified using a parameter called the separation factor, α.

$$\alpha = \frac{k_B}{k_A}$$

Where "B" is the solute with the longer retention time and higher k. It is also possible to refer to α as "selectivity".

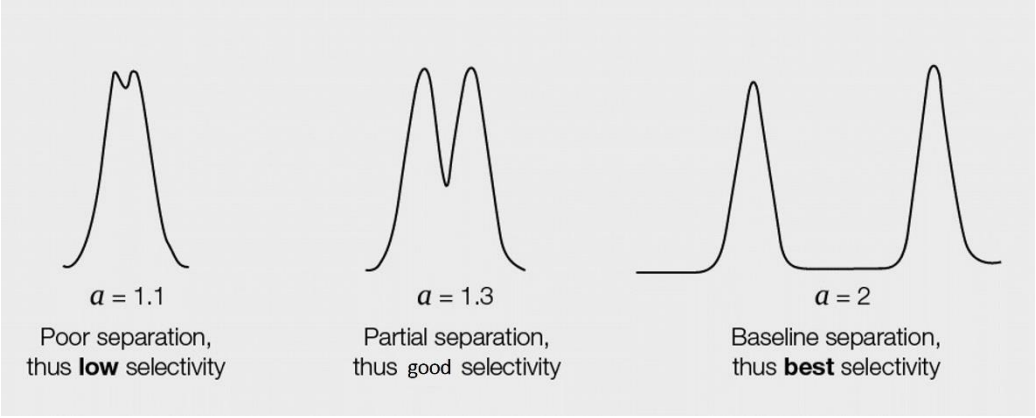

Figure 2.13: Examples of different alphas

More two analytes are well separated, higher will be the α. Another important parameter of chromatography is the width of the peak that can be measured from the baseline (W_b) or from

the half-height ($W_{1/2}$). The efficiency is represented by the *Number of plates* (N) and can be calculated by:

$$N = 5.54 \left(\frac{t_r}{w_{1/2}}\right)^2$$

N is a dimensionless value and can be used to confront different columns with the same length. Higher is the N obtained by a column more is the efficiency. If a confrontation between the efficiency of two columns with different length (L) is needed the *plate height* (H) can be used as parameter:

$$H = \frac{L}{N}$$

When comparing columns in terms of H values, smaller plate heights are better. In fact, high numbers of theoretical plates (large N) and small plate heights (small H) are associated with narrow peaks and generally better resolution than columns with smaller N and correspondingly larger plate heights. The parameter that evaluates the goodness of separation is the *Resolution* (R).

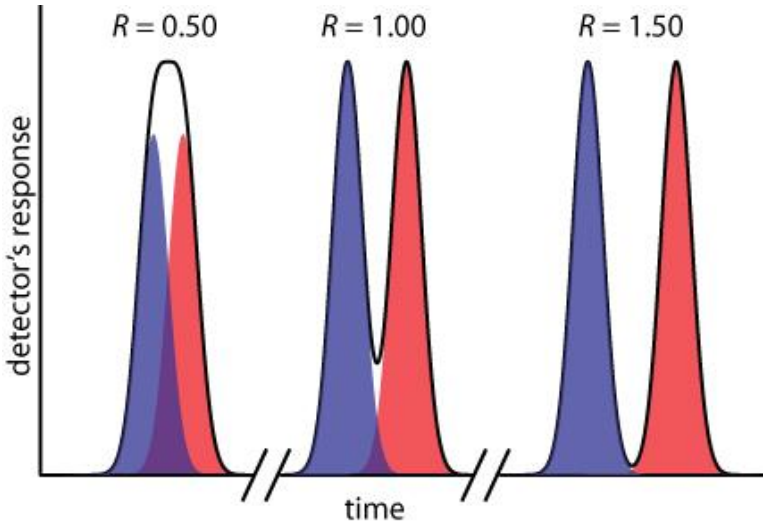

Figure 2.14: Examples of different resolutions in chromatography

R is related to the selectivity and the efficiency of the system, and it is calculated as follows:

$$R = \frac{t_{r2} - t_{r1}}{\frac{1}{2}(W_{b1} + W_{b2})}$$

R is a dimensionless value and can be equal or higher than zero.

Furthermore, peaks are never perfectly symmetrical. In Figure 2.15 is it possible to see an example of symmetric (left peak) and asymmetric peaks (middle and right peak). The middle peak is referred to as “fronted” while the right peak is referred to as “tailed”.

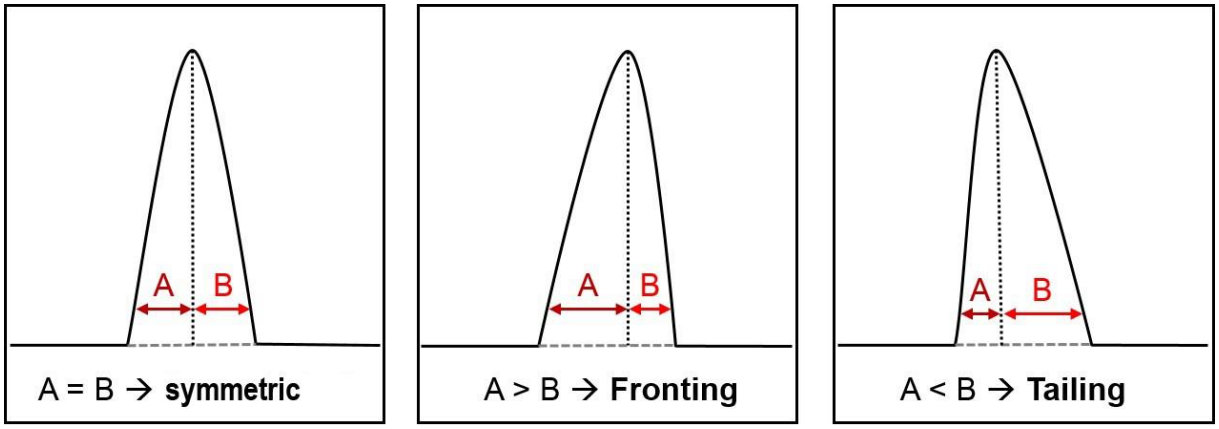

Figure 2.15: Representation of symmetry and asymmetry peaks

The asymmetry is calculated by the asymmetry factor (AF) defined as the ratio of the peak half-widths at a given peak height, often taken at 10% of the total height, leading to:

$$AF = \frac{b}{a}$$

Finally, in order to develop a good chromatography method, selectivity and resolution must be optimized. Symmetry can be evaluated too because can be a critical issue for the separation.

Finally, the chromatographic peak is used to quantify a compound or individual components in a mixture, in fact, the area of the peak (sometimes also the heigh of the peak) is proportional to the concentration of the analyte(s). The most used quantitative technique is that with the internal standard. Internal standards are molecules that generally mimic the behavior of the analyte(s) in study. This means they should have comparable retention (although not identical as this would cause peak overlap) and generally produce similar detector responses as the analyte(s). The role of internal standard is to compensate for variability coming from the method. When the chromatography is coupled with the mass spectrometry the best internal standard is the isotopologue (isotopically enriched with deuterium (^{2}H or D) or carbon-13(^{13}C)) of the analyte to be quantified. In this case they will have the same physico-chemical properties (and same t_r)

but different mass. In case of complex matrices, the isotopologue prevent both the matrix and recovery effect.

3. PROJECT 1: APPLICATION OF LEDA ALGORITHM FOR THE RECOGNITION OF PG-P AND CARBONIC ANHYDRASE HYBRID INHIBITORS AND EVALUATION OF THEIR PLASMA STABILITY BY HPLC-MS/MS ANALYSIS

This project is part of a wider study regarding the design and synthesis of hybrid inhibitors and the results gave a significant support for the development of this topic in the pharmaceutical chemistry field. Hybrid inhibitors are drugs where two or more pharmacophores, that interact with different targets, are linked together obtaining a single molecule able to act towards different enzymatic systems or other receptors[5]. This class of drugs can be decisive, for instance, in case of diseases where there is an overexpression of two or more enzyme systems that must be inhibited [6]. Sometimes this kind of approach can give also an improvement regarding the pharmacokinetic of this drug. Then, in this case, instead to use two different drugs, where each one interacts with its target, it is more convenient to use a hybrid compound. However, their activity can be explained both by their entire structure or by the single active moieties, in case of a linker cleavage. In fact, the project of my graduation thesis consisted of the evaluation of the stability in human plasma of anti-inflammatory drugs and carbonic anhydrase hybrid inhibitors (NSAI-CAI hybrids) because they showed an interesting activity towards both targets in vitro [6] and it was interesting to understand if they were stable in biological matrices used in future studies. Specifically, these hybrids were linked by an amide group that cannot be theoretically hydrolyzed by esterase enzymes present in plasma, so it was very important to evaluate the stability. The results of this study showed that all NSAI-CAI hybrids were stable in the matrices tested, then it was possible to hypothesize that these compounds can reach the target tissues unmodified, opening new perspective on the development of NSAID - CAI hybrids with potential applications in the treatment of inflammation [7]. Due to these results, it was decided to synthesize the same hybrids but with an ester group as a linker to see if they showed different behavior, as the esters can be hydrolyzed by esterases present in diverse tissued [8].

Such promising results obtained with this combination of hybrid inhibitor compounds, fostered us to plan further investigations on different enzymatic system targets. In 2016 it was highlighted the capacity of the inhibition of CA XII to reverse doxorubicin resistance in Multiple Drug Resistance (MDR) cancer cells that overexpress P-gp[9].

Subsequently, hybrids inhibitors able to inhibit carbonic anhydrase XII (CA XII) and p-glycoprotein (P-gp) to fight Multidrug Resistance were hypothesized and synthesized [10]. Some of these compounds showed an interesting dual inhibitory effect in vivo. However, considering

that the two pharmacophores are linked by two ester groups it was deemed necessary to evaluate their stability in human plasma to give support and continue the development of this drugs. Specifically, these twelve new hybrids are divided in six couples of positional isomers therefore, in order to resolve them, a specific chromatographic method, for each pair, might be needed. Generally, this approach may require a longer time to set up the separation method with the evaluation of different chromatographic columns, mobile phases, and elution programs to obtain adequate analytes separation. All these procedures are usually molecule-specific and rarely can be extended to other compounds. Therefore, it was deemed more useful to propose a sole chromatographic method applied for all the analytes, in order to saving time and increase the productivity, then to develop a series of MS/MS conditions that allow the recognition of studied isomer pairs, supporting their chemical stability study. Indeed, in the last two decades, many MS/MS strategies were developed to solve this problem by allowing the characterization and quantification of isomers and/or isobars in mixtures via a standardized approach, applicable to different compounds [11, 12, 13, 14]. Summarizing the reported results, the discrimination between the isomers was achieved by optimizing the selection of precursor ion, its fragmentation through collision induced dissociation (CID) mechanism and the analysis of fragmented ions produced. Each of these phases was explored, developed and tuned to carry out an adequate specificity to distinguish the isomers in the sample without the support of any structural manipulation (i.e. derivatization and isotopic enrichment) or chromatographic separation. The use of the right approach provides many analytical advantages, among which the most important are sensitivity, reliability and faster analysis.

Regarding the topic of isomers recognition, our group proposed and developed an MS/MS post-processing mathematical algorithm named LEDA (Linear Equation of Deconvolution Analysis) that allows the recognition of isomer compounds without their chromatographic separation [15, 16]. Profiting by LEDA features, recently we introduced a methodological approach that simplifies the liquid chromatography (HPLC) parameters, allowing the use of a short column and a fast elution gradient, leading to an increased productivity without losing determination specificity [17]. With this approach, the chromatographic column was used only to avoid or limit the interference of the sample matrix towards the analyte ionization process (matrix effects).

In figure 3.1 is reported the decision flow chart employed to this project.

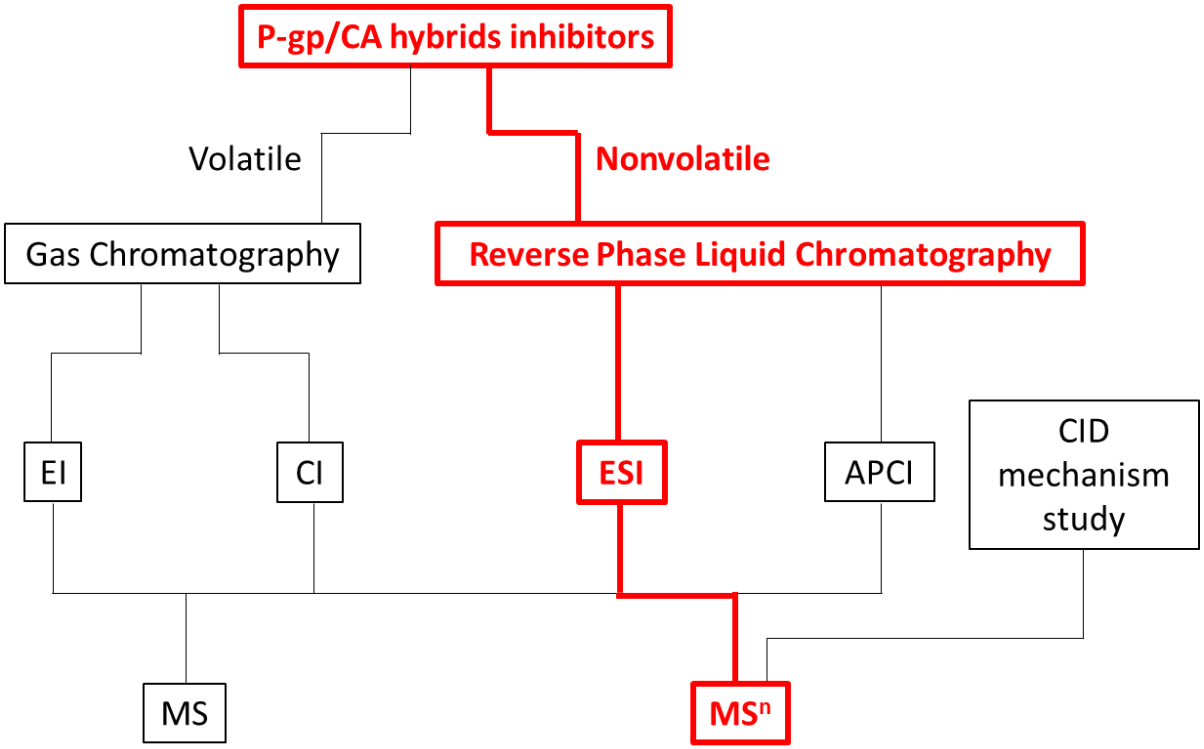

Figure 3.1: scheme of the system employed for Project 1

Commonly the proposed HPLC method achieved a poor efficiency, mainly due to the short column used, and the analyzed isomers are coeluted. Then, to obtain a suitable distinction (analytical specificity) between the isomers and ensure their proper monitoring during the degradation experiment, the MS/MS features of each analyte must be explored. The MS/MS investigations begin with a series of fragmentation studies on the $[M+H]^+$ species at different collision voltages (CVs). The set of MS/MS acquisitions at different CVs is referred as energy resolved mass spectrometry or ERMS experiments. These experiments were carried out by direct infusion of each analyte in product ion scan acquisition to point out the possible intrinsic differences in the molecular stability of the isomers. By processing the data obtained from ERMS experiments, the collision breakdown curves were plotted and the most significant product ions (Pis) for each couple of isomers were selected to set up a proper acquisition MRM method.

In order to evaluate the qualitative-quantitative performances of the algorithm, mixtures at different concentration of isomers pair were prepared and then analyzed. The chromatographic method proposed to this study was developed with a binary solvents elution gradient by using a Phenomenex Luna C18 20 mm length, 2 mm internal diameter and 3 mm particle size. The solvents used were: water:acetonitrile 90:10 solution added with 10 mM formic acid and 5 mM ammonium formate and water:acetonitrile 10:90 solution added with 10 mM formic acid and 5

mM ammonium formate. The elution gradient was set as follows: initial at 90% solvent A, which was then decreased to 10% in 4.0 min, kept for 2.0 min, returned to initial conditions in 0.1 min and maintained for 2.0 min for reconditioning, to a total run time of 8.0 min. Finally, the algorithm proved to be suitable for the recognitions of these isomers even in binary mixtures. Since their structure contains two ester groups, it was important evaluating their chemical stability as a preliminary *in vitro* test; therefore, in this study a series of drug stability experiments was carried out in human plasma (H-pl) and phosphate-buffer saline (PBS) to assess the possible susceptibility of the ester bonds to plasma enzymes or the spontaneous hydrolysis respectively. Drug stability experiments relied on incubation of each analyte, in PBS and H-pl, for different times (0, 30, 60 and 120 minutes) and analyzed with the same method used for the LEDA algorithm experiments. Also, to verify the reliability of proposed HPLC-MS/MS approach, an evaluation of Matrix Effect following Matuszewski protocol was planned.

3.1. INTRODUCTION

In general, Drug Resistance (DR) is a phenomenon widespread at a pharmacological level that led to a diminished or lower activity in the treatment of various pathologies, making them ineffective, useless or even dangerous, as the pathological agents for example may transmit the resistance to other bacteria, fungi, etc.. This mechanism covers the treatment of both infections with antibacterial drugs and tumors with anticancer drugs. Furthermore, this phenomenon develops more quickly if the therapy is not properly done (i.e. wrong doses, inadequate duration of the therapy or unfulfilled time between administrations). Thus, a drug that was effective before, became tolerated by the microorganisms or cancer cells and is no longer effective.

There are two important classes of Drug Resistance: 1) *intrinsic* or *de novo* DR, when cancer cells or microorganisms are naturally resistant to drugs and their resistance manifests since the beginning of the treatment; and 2) *acquired* DR, when cells or microorganisms became insensitive after the beginning of the therapy [18]. Finally, Multidrug Resistance (MDR) can be defined as a phenomenon of acquired resistance, initially observed in cancer cells (in vivo and in vitro) and subsequently found in microorganisms too, that occurs as cross resistance to the action of uncorrelated chemotherapy drugs, thus, with different chemical structure or different mechanisms of action. More specifically, a cancer cell that develop a resistance to a specific class of chemotherapy drug, will also develop a resistance to a different class of anticancer drugs, not related, that never interacted with.

MDR is a complex phenomenon to which can be associated with several biochemical mechanisms, consequently, the target cell can reduce the activity of the anti-cancer drug. The most important ones are:

- Modified activation or drug degradation (the drug is not completely activated or is degraded more quickly) [19];
- Failing of the physiologically mechanism of apoptosis [20];
- Increased efflux of the drug from the intracellular environment to the extracellular one [21];
- Increased of the DNA repair mechanisms [22];
- Modified or altered expression of enzymes and target proteins [23];
- Overexpression of Lung Resistance-related Protein (LRP) [24].

The most MDR forms studied so far are those caused by the overexpression of transport proteins that are able to reduce the intracellular concentration of the anti-cancer drug through active transport. Then, the use of a drug that can inhibit these pumps increases the concentration of the anti-cancer drug inside the cell so its activity on the target cell and avoid the MDR effect. The most studied efflux pump is the P-glycoprotein (P-gp where P stands for permeability) which is part of the ATP Binding Cassette (ABC) transporter family. P-gp uses the energy produced by the hydrolysis of ATP to expel outside of the cell a large variety of cytotoxic compounds characterized by different structure and dimension, and it is made against the concentration gradient. It is overexpressed in many tumors and its elevated expression has been considered the cause of the reduced chemotherapeutic responses in various cancer types including blood and solid cancers [25].

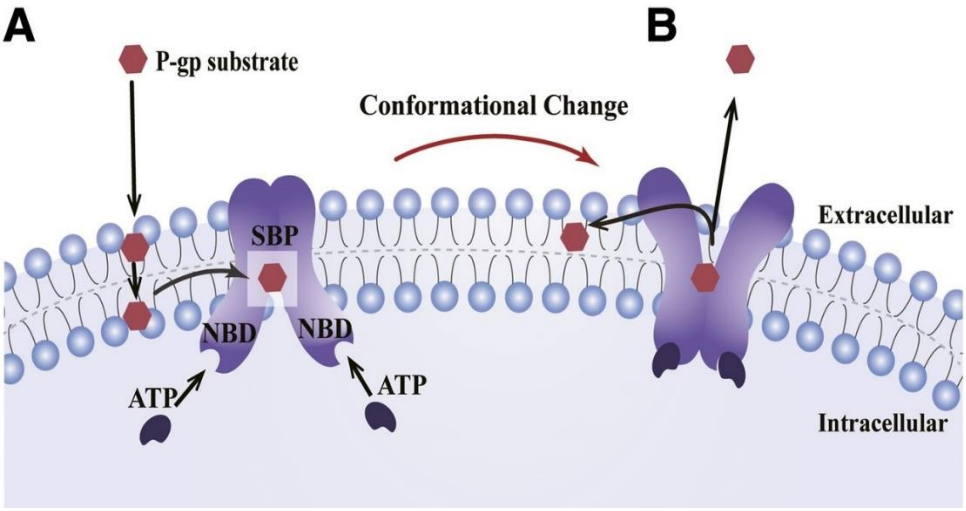

Figure 3.2: P-gp activity

A recent work highlighted that the activity of the efflux transmembrane transporter P-gp could be modulated by Carbonic Anhydrase XII [26]. In fact, Carbonic Anhydrases (CAs) are metalloenzymes that catalyze the conversion of carbon dioxide to bicarbonate and a proton.

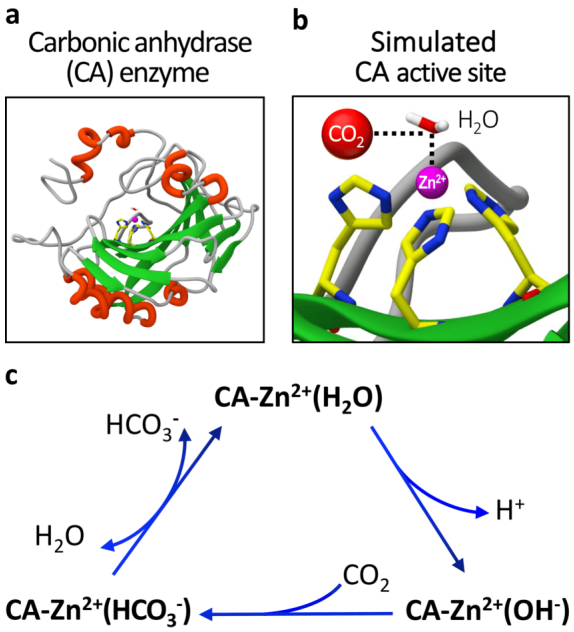

Figure 3.3: CA activity

Their function is essential for the maintenance of pH homeostasis in the organism and also have a metabolic function in many biosynthetic processes. Human CAs (hCAs) is represented by several isoforms and among these, CA IX and XII are extracellular, membrane bound CAs associated with tumor progression and metastases formation [27, 28]. The overexpression of these two isoenzymes is induced in most hypoxic solid tumors by the hypoxia inducible factor 1α (HIF-1α)[29]. Furthermore, the P-gp efflux activity is known to be influenced by intracellular pH, as the optimal pH at which P-gp operates is slightly alkaline. This condition is maintained by the CA XII catalytic activity, which assures the suitable intra- and extracellular pH in tumor cells overexpressing it. CA XII is highly expressed in some chemoresistant P-gp positive cancer cells [26] and its activity is critical for the P-gp efflux function and contribution to MDR. In fact, there are recent evidence that the reduction of pH, caused by the inhibition of CA XII, produces a significant decrease in P-gp ATPase activity [26, 9]. For these reasons, new hybrid compounds able to inhibit both targets were design and synthesized by Professor Teodori's research group. These new hybrid molecules are characterized by the presence of both P-gp and hCA XII binding moieties. Therefore, their structure contains a tertiary amine group carrying two polymethylenic chains of variable length (between 8 and 10 carbon atoms), linked to different

aromatic moieties through two ester bonds. The structures of the analytes in study are the follow:

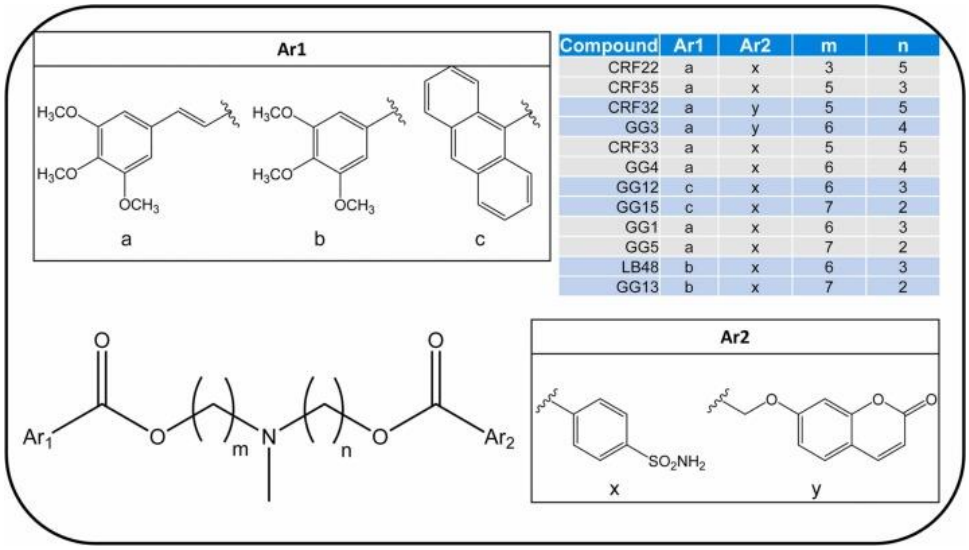

Compound	Ar1	Ar2	m	n
CRF22	a	x	3	5
CRF35	a	x	5	3
CRF32	a	y	5	5
GG3	a	y	6	4
CRF33	a	x	5	5
GG4	a	x	6	4
GG12	c	x	6	3
GG15	c	x	7	2
GG1	a	x	6	3
GG5	a	x	7	2
LB48	b	x	6	3
GG13	b	x	7	2

Figure 3.4: Structures of the compounds in study

The pharmacological activity of the P-gp/CA hybrid inhibitors can be explained considering both the whole structure and/or their single parts (P-gp and CA inhibitors), that can be released by hydrolysis of ester bonds then, a chemical stability study of these compounds towards spontaneous (phosphate buffer saline or PBS) or enzymatic hydrolysis (human plasma) was deemed necessary in order to better comprehend their pharmacokinetic and pharmacodynamic properties. Furthermore, the panel of P-gp/CA hybrid inhibitors is represented by positional isomers with different length of hydrocarbon chain. For this reason, a very high selectivity method was required to avoid any isomer mutual interference. At this point, the main ways of work were two. The first one was to develop a HPLC method at least for each pair of isomers in order to have the right chromatography selectivity. Once the chromatographic method is validated it guarantee a very high specificity, but it needs long time of developing and possibly long columns, different solvents and again, long run time analysis. The second one instead, was to develop a unique HPLC method for all the analytes and a series of MS/MS conditions that allow the recognition of the studied isomer pairs, supporting the chemical stability thus applying a mathematical algorithm called LEDA. In this case, using short columns and fast run time analysis, the productivity increases without losing in specificity. Considering the high number of samples to be prepared, analyzed and processed in order to obtain all the required data to complete the work it was decided to choose the second way.

LEDA algorithm is a mathematical algorithm based on the assumption that a mixture of similarly fragmenting compounds will generate MS/MS spectra that are a combination of fragments from each component summed in proportions to their relative concentration, saying that a mathematical matrix can be used [11]. Then, the relative intensity of product ions and their branching ratios would be different among the isomers. In order to do that, each isomer must be analyzed by ERMS experiments to establish its CID behavior. The ERMS experiments consists of a series of product ion scan analyzes, monitoring all the fragments produced from the precursor ion by increasing stepwise the collision voltage. In Figure 3.5 is reported the graph of the abundances of all ions (precursor and products) acquired during the ERMS experiments on LB48 isomer. The obtained plots (breakdown curves) describe the fragmentation of precursor ion by CID mechanism.

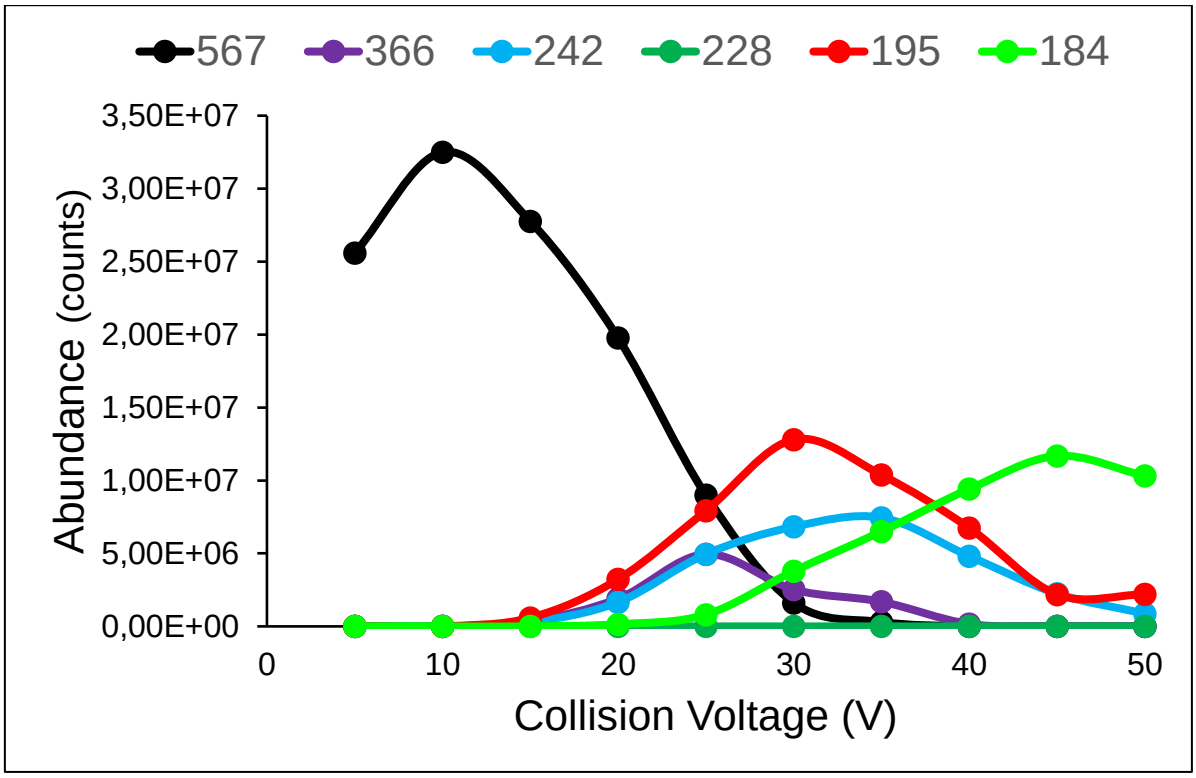

Figure 3.5: Breakdown curves obtained by ERMS experiments on LB48 isomer

The black line represents the behavior of precursor ion in the ERMS experiments; its abundance increases at low collision voltages (5-10 V) until, by continuing the gain of the voltages, decreases stepwise leading to the formation of the product ions (colored lines), that rise to the maximum intensities in the medium-high voltage range. In Figure 3.6 is reported the profiles of the precursor and the sum of the product ions vs collision voltages of LB48 isomer.

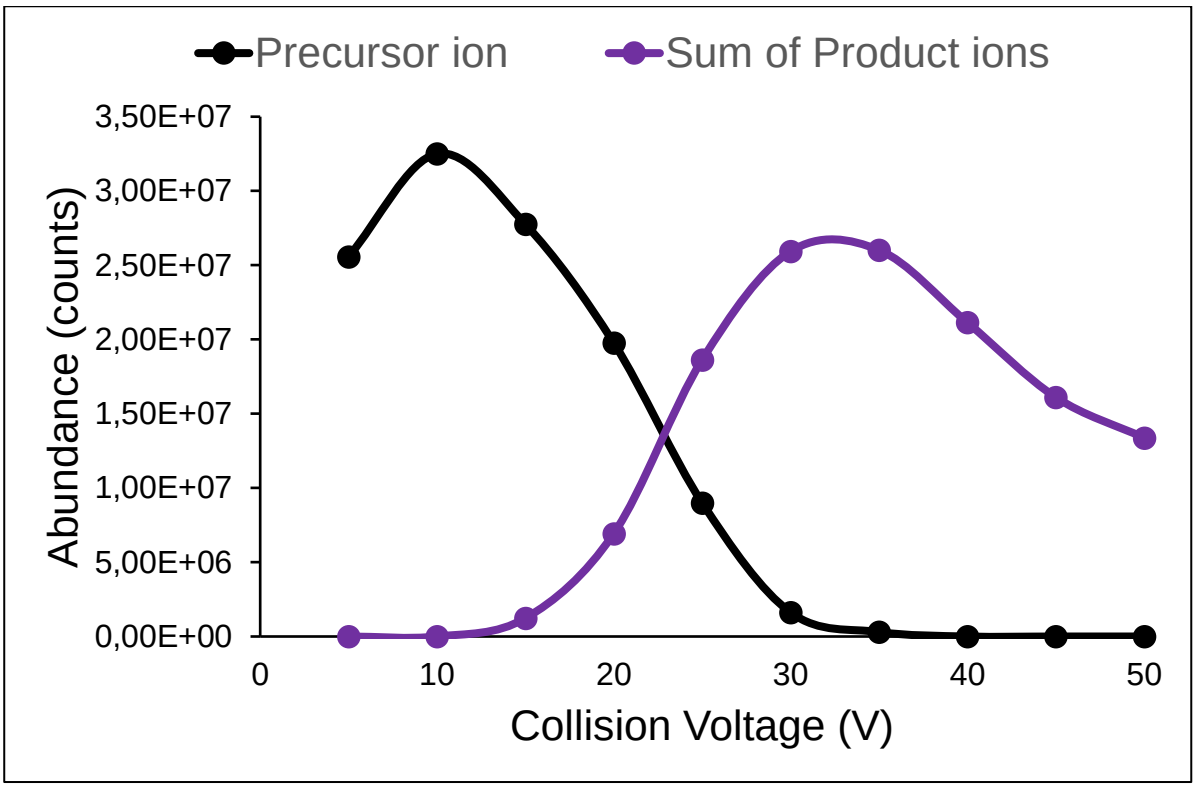

Figure 3.6: Breakdown curves of precursor and sum of product ions by ERMS experiments on LB48 isomer

Worth of note that the abundance of sum of product ions do not achieve the maximum abundance of the precursor ion; therefore, the yield of formation of product ions can be variable, depending on the parameters of CID process (effectiveness of ion transmission, collision gas, its pressure, dimension of collision cell, etc…) and on the intrinsic characteristic of the structure of the analyte. Since the CID parameters are the same for all the analytes processed, by highlighting the differences in the formation yield of the common product ions of similar analytes (e.g., positional isomers), it is possible to find a way to distinguish them. In order to point out, in the graph of breakdown curves, the different formation yield of common product ion between two isomers, it is possible to represent the ion abundance as the relative value respect to the sum of all the ion abundances for each data point. However, this data elaboration neglects the effectiveness of the ions' transmission by the collision cell as the collision voltage applied changes. Indeed, the plots intensity lose some information, i.e. the profile of precursor ion is underestimate while some product ions showed overestimated values at high collision voltages (Figure 3.7).

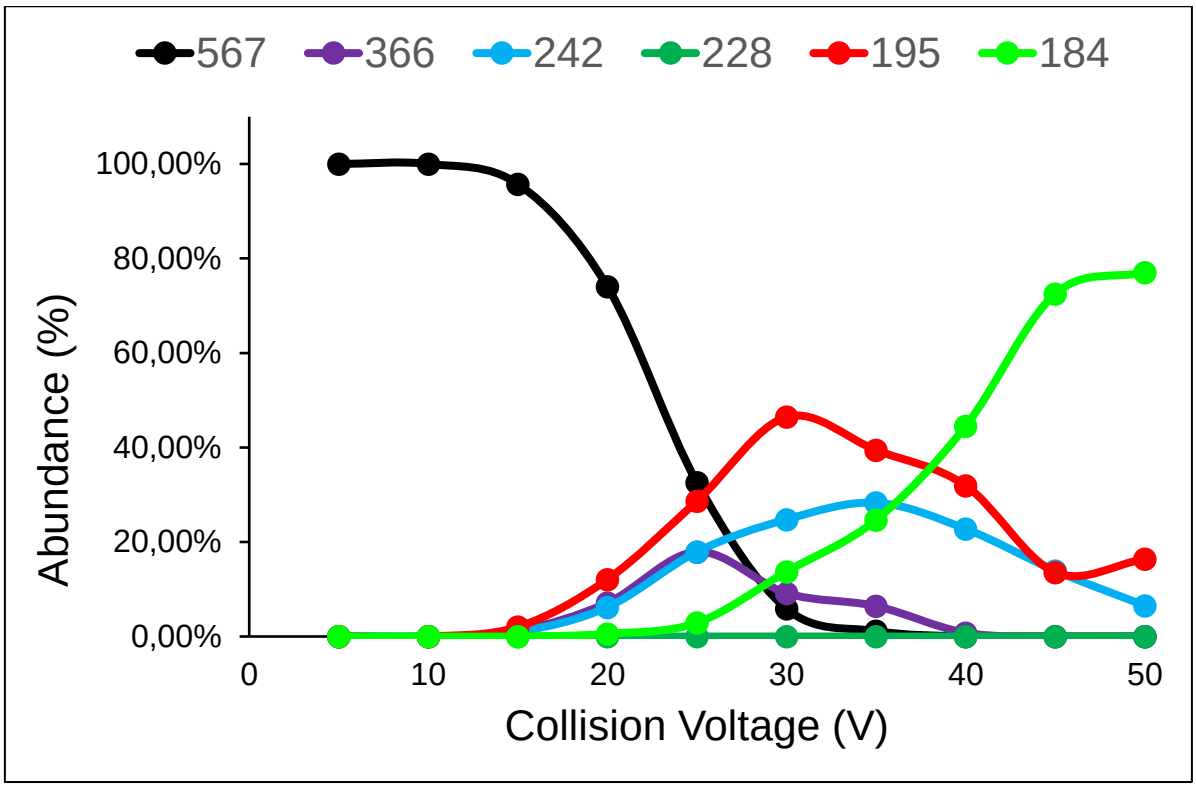

Figure 3.7: Breakdown curves obtained by ERMS experiments on LB48 isomer considering the relative abundance (%) of each ion respect to the sum of all ions revealed vs the collision voltage applied

The figure 3.7 shows a "flatten" precursor ion profile in the 5-15 V collision voltage region while the abundance of 184 *m/z* product ion is "exaggerate" respect to the intensity showed in figure 3.5 (overestimation due to the data elaboration). To obtain reliable data, the relative abundances of the different product ions were calculated with respect to the reference ion abundance (Ri), to avoid possible misleading results due to compound-dependent product ions yield. For this purpose, the precursor ion signal can be acquired as Ri at the CV value corresponding to its highest intensity in the breakdown curve (in this case was 10 V), without any fragmentation process occurred (Figure 3.8).

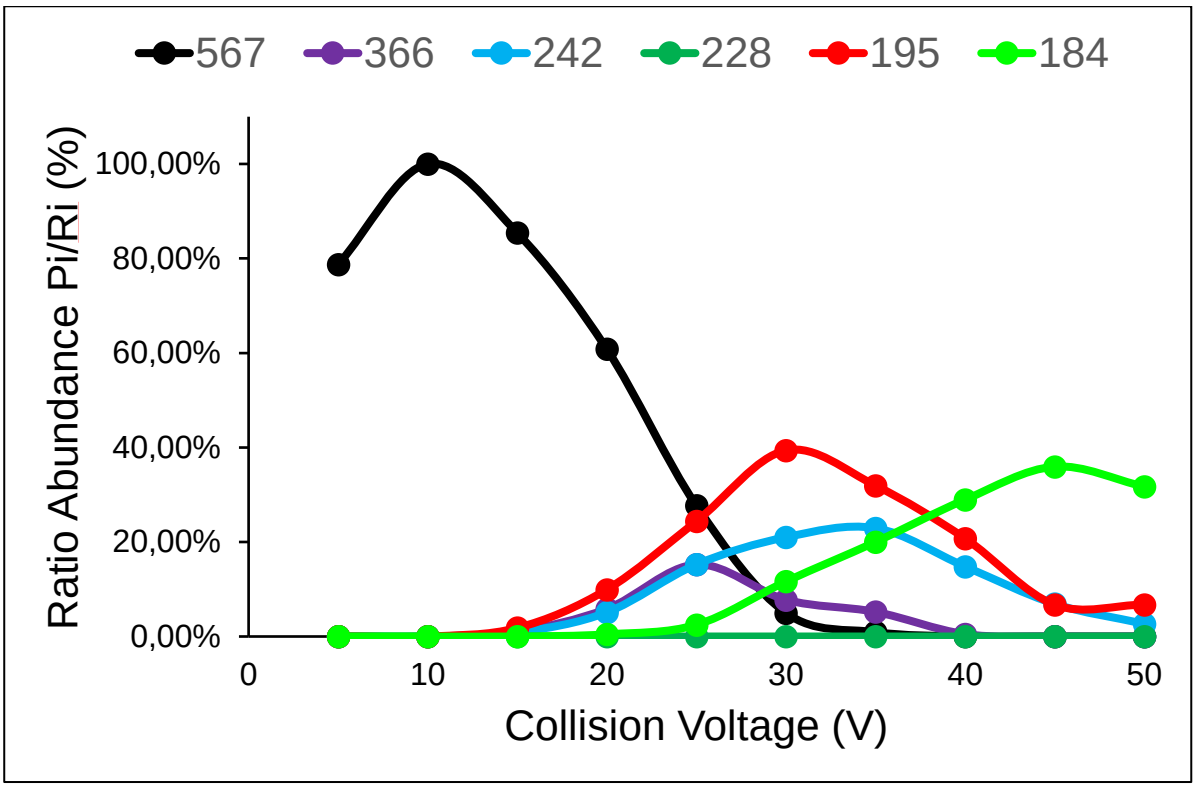

Figure 3.8: Breakdown curves obtained by ERMS experiments on LB48 isomer considering the relative abundance (%) of each ion revealed respect to Ri vs the collision voltage applied.

By this approach, the ratio between the abundance of each product ion (Pi) acquired and the abundance of Ri represents the characteristic yield of the Pi formation at selected CV for the analyzed isomer.

Hence, the ERMS study on the pure isomers allows to emphasize their product ions differences which could be related both on the intensity of the signal or on the variation of the collision voltage abundances distribution. Finally, the MS/MS spectrum obtained by analysis of a mixture of isomers is a combination of the mass spectra of pure components added in proportions corresponding to their relative concentrations. The aims of the mathematical approach present in the LEDA algorithm are to allow the deconvolution of the MS/MS spectrum, to recognize the components present in the sample and to evaluate they quantitative composition, avoiding the support of chromatographic separation. To check the relationship between these ratios and the composition of isomer mixture, a series of standard solutions at different composition of the isomer pair is analyzed. By plotting the obtained intensity ratios from each mixture versus its theoretical composition, a linear correlation occurs that confirm the possibility of recognition of isomers by only elaboration of MS/MS data (Figure 3.9).

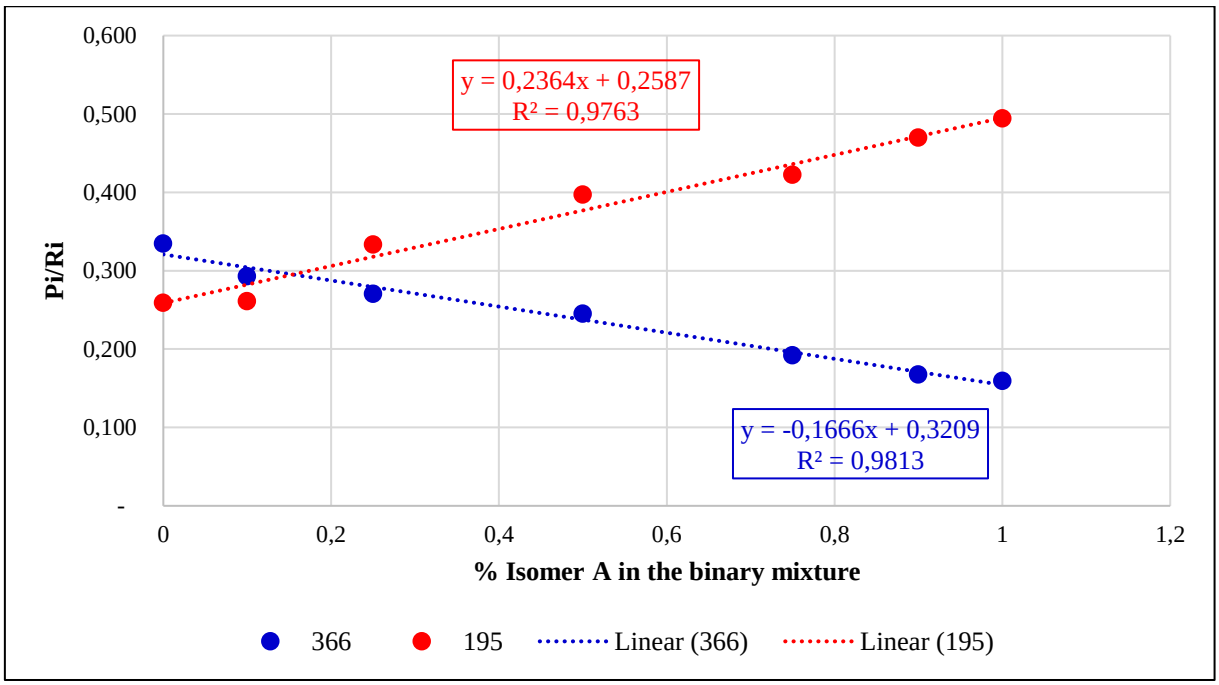

Figure 3.9: the linear correlation obtained by plotting the product ion vs reference ion ratio from the mixture of LB48 and GG13 of the most significant product ions (in this case 366 and 195 m/z) versus its theoretical composition versus its theoretical composition that confirm the possibility of recognition of isomers by the algorithm

Therefore, knowing the characteristic abundance ratios of the pure isomer, a deconvolution of these spectra is possible based on a series of linear regression equations as follows:

$$\left(\frac{Pi}{Ri}\right)_m = \sum_{x=1}^{n} \left(\frac{Pi}{Ri}\right)_x * [\%]_x$$

where $(Pi/Ri)_m$ is the abundance ratio between the product ion (Pi) and the reference ion (Ri) measured (m) in the sample; $(Pi/Ri)_x$ are the characteristic abundance ratios between the product ion and the reference ion of each pure isomer; and $[\%]_x$ is the concentration (%) of each isomer in the sample. In the binary mixture of isomers (A-B) a single equation related to the sole product ion ratio (Pi/Ri) could be enough. Indeed, by assuming that only the isomer pair constitutes the MS/MS spectrum, the concentration of B is calculated as B % = (1 – A) %. However, in this case the possible contribution of signals from unknown isomers (or any interferent having the same product and reference ions) is neglected. Therefore, to avoid ill-conditioned algorithm, the resolution of the mixtures of n isomers is a matrix composed at least by n equations is required (LEDA). Of course, it is mandatory to choose only product ions that show higher differences between the isomers. It is worth to emphasize that the CID experiments of LB48 shown the production of 242 m/z product ion that is “specific” of this compound

because it is made up of the Ar2 group and the carbon chain attached to it that is different for its positional isomer (the GG13 has a different length) making it a possible diagnostic ion for the determination of the LB48 even in a mixture. However, considering all the panel of the analytes in study, not everyone shown its "specific" product ion, then it was decided that the use of the LEDA algorithm was a more specific tool for this kind of investigation. All computations for the deconvolution MS/MS data are processed using an Excel™ macro.

3.2. MATHERIAL AND METHODS

The analyses were carried out with a Varian 1200 L triple quadrupole system (able to perform MS/MS experiments) coupled with two Prostar 210 pumps (each one can manage one solvent line), a Prostar 410 autosampler and an ESI source. All the raw data collected were processed by Varian Workstation (version 6.8) software.

3.2.1. CHEMICALS

The P-gp-CA hybrid inhibitors were obtained as reported in ref. 18. Acetonitrile (Chromasolv), formic acid, ammonium formate (MS grade), NaCl, KCl, Na_2HPO_4 2 H_2O, KH_2PO_4 (reagent grade), verapamil hydrochloride and ketoprofen (analytical standard) were purchased by Merck (Milan, Italy). Ketoprofen ethyl ester (KEE) was obtained by Fisher's reaction from ketoprofen and ethanol. Ultrapure water or mQ water (resistivity 18 M Ω cm) was obtained from Millipore's Simplicity system (Milan, Italy). Phosphate buffer solution (PBS) was prepared by dissolving in ultrapure water the reported salts at following concentrations: 8.01 g L^{-1} of NaCl, 0.2 g L^{-1} of KCl, 1.78 g L^{-1} of Na_2HPO_4 * 2 H_2O, and 0.27 g L^{-1} of KH_2PO_4. The human plasma was collected from healthy volunteers, pooled, and kept at -80 ◦C until use.

3.2.1. CHROMATOGRAPHY

The chromatographic parameters used to perform the analysis for this project were tuned in order to minimize the run time and so, increase the productivity. It was evaluated different length of columns, different solvent, different speed of gradient and column temperature. The column used was a Phenomenex Luna C18 20 mm length, 2 mm internal diameter and 3 μm particle size. It was employed a gradient using a binary mobile phase and the flow was fixed at

0.25 ml min^{-1}. The used solvent were 10 mM formic acid and 5 mM ammonium formate in mQ water:acetonitrile 90:10 (solvent A) and 10 mM formic acid and 5mM ammonium formate in mQ water:acetonitrile 10:90 (solvent B). The gradient program worked as follows:

Time (min)	A (%)	B (%)
00:00	90	10
04:00	10	90
06:00	10	90
06:01	90	10
08:00	90	10

Table 3.1: program of elution gradient

The column temperature was maintained at 40 °C and the injection volume was 5 μL.

3.2.2. MASS SPECTROMETRY PARAMETER

For these studies the source used was an ESI source operating in positive ion and using the following settings: 5kV needle, 42 psi nebulizing gas, 600 V shield, and 20 psi drying gas at 280 °C. The ERMS experiments were performed to study the fragmentation of molecular species of each analyte and build its breakdown curves. The ERMS experiments were carried out by a series of product ion scan (MS/MS) analysis, increasing the collision voltage (CV) stepwise in the range 5–50 V. Each MS/MS spectra were acquired in the m/z range from 50 to 650, scan time of 600 ms and argon was used as collisional gas. The ERMS experiments were performed by introducing working solution 1 of each analyte, via syringe pump at 10 μL min^{-1}; the protonated molecule was isolated, and the abundance of product ions were monitored. The ERMS data were used to build the breakdown curves that describe the fragmentation of precursor ion in relation to the collision voltage applied. The breakdown curves were obtained by plotting the relative intensity values (averaging about 15–20 scans) of each signal present in the MS/MS spectra acquired for each CV. The breakdown curves have served for chose the MRM transitions to analyze the samples. The choice of the MRM was made to obtain the best

results, higher sensitivity and selectivity and also to be able to apply the LEDA algorithm. The transitions were built following the most significant fragments obtained at the energy with the highest yield. In order to evaluate the chemical stability of studied compounds, a dedicate MRM method was arranged for each pair of isomers with the specific MS/MS transitions of the IS and the monitored isomers, each acquired for 100 ms (dwell time).

Compound	Precursor ion (m/z)	Reference ion (m/z) [CV (V)]	Quantifier ion (m/z) [CV (V)]	Qualifier ion (m/z) [CV (V)]
IS	455	-	165 [30]	303 [30]
CRF22 CRF35	579	579 [10]	221 [25]	341 [20]
CRF32 GG3	626	626 [10]	221 [30]	388 [30]
CRF33 GG4	607	607 [10]	221 [30]	406 [25]
GG12 GG15	577	577 [10]	205 [25]	376 [25]
GG1 GG5	593	593 [10]	221 [30]	392 [25]
LB48 GG13	567	567 [10]	195 [30]	366 [25]

Table 3.2: MRM parameters

3.2.3. STANDARD SOLUTION, CALIBRATION CURVES AND SAMPLE PREPARATION

Considering its similar structure, as Internal Standard (IS), it was used Verapamil. Stock solutions of analytes and verapamil hydrochloride (internal standard or IS) were prepared in acetonitrile at 1.0 mg mL-1 and stored at 4 ◦C. Working solutions of each analyte were freshly prepared by diluting stock solutions up to a concentration of 1.0 μg mL^{-1} and 0.1 μg mL^{-1} (working solutions 1 and 2, respectively) in mixture of mQ water:acetonitrile 50:50 (v/v). The IS working solution was prepared in acetonitrile at 33 ng mL-1 (IS solution). A six-level calibration curve was prepared by adding proper volumes of working solution (1 or 2) of each analyte to 300 μL of IS solution. The obtained solutions were dried under a gentle nitrogen stream and dissolved in 1.0 mL of 10 mM of formic acid in mQ water:acetonitrile 80:20 (v/v)

solution. Final concentrations of calibration levels of each analyte were: 2.5, 5.0, 10.0, 25.0, 50.0, and 100.0 ng mL^{-1}. All calibration levels were analyzed six times by HPLC-MS/MS system with the proper conditions. Finally, the spiked solution of each analyte, used in the sample preparation of chemical stability study, was separately prepared by diluting the respective stock solutions in mQ water:acetonitrile 80:20 (v/v) solution, to obtain a final concentration of 10 μM.

Each sample was prepared by addition of 10 μL of spiked solution to 100 μL of tested matrix (PBS or human plasma) in 1.5 mL microcentrifuge tube. The obtained solution corresponds to 1 μM of analyte that undergo to degradation study. Each set of samples was prepared in triplicate and incubated for four different times, 0, 30, 60, and 120 min at 37 ◦C. Therefore, each stability profile of studied analyte was represented by a batch of 12 samples (4 incubation times 3 replicates). During the test, some compounds showed a fast plasma degradation time (<30 min), hence, to correctly evaluate the half-life ($t_{1/2}$) values, their incubation times were reduced to 0, 2, 5 and 10 min. After the incubation, 300 μL of IS solution was added to the sample and then centrifuged (room temperature for 5 min at 800 g). Then, the supernatant was transferred in autosampler vials, dried under a gentle stream of nitrogen and dissolved in 1.0 mL of 10 mM of formic acid in mQ water:acetonitrile 80:20 solution [30]. Each sample batch were included the blank samples of tested matrices (PBS and human plasma), prepared as described above, but by adding only the IS solution. Thus, the analysis of the blank samples can check any interference in the analyte MRM signals due to the matrix components. Three sets of six replicates for each analyte were prepared to evaluate the matrix effect (ME) and the analyte recovery (RE) of the proposed method [31]. The same evaluation was extended to the IS to verify its reliability as quantitative reference. Set A was prepared by mixing 10 μL of spiked solution with 300 μL of IS solution. Set B was obtained by mixing 100 μL of plasma with 300 μL of acetonitrile and, after centrifugation and separation of the supernatant, by adding 10 μL of spiked solution of each analyte or 300 μL of IS solution. Set C, instead, was prepared by mixing 10 μL of spiked solution with 300 μL of IS solution and 100 μL of plasma, then centrifuging and collecting the supernatant. The obtained solutions were transferred in autosampler vials, dried under a gentle nitrogen stream and dissolved in 1 mL of 10 mM of formic acid solution in mQ water:acetonitrile 80:20. Following the procedure described above, the expected concentrations of the samples (degradation, ME and RE sets) ranged between 50 and 60 ng mL-1 (depending on the MW of the studied compound), values on which the calibration curve was centred. In order to estimate precision and accuracy of the methods, a new series of samples at three concentration levels (low, medium and high levels), corresponding to 25, 50 and 100 ng mL-1 respectively, were prepared in six replicates for each

compound following the procedures described above from the stock solutions in human plasma matrix. Then, the final solution of blank and all sets of samples, prepared as described above, were analyzed by proper HPLC-MS/MS method.

3.2.4. VALIDATION OF HPLC-MS/MS METHOD

Calibration curves of analytes were obtained by plotting the peak area ratios (PAR), between analyte and IS quantitation ions, versus the nominal concentration of the calibration solution. A linear regression analysis was applied to obtain the best fitting function between the calibration points. In order to obtain reliable limit of detection (LOD) values, the standard deviation (SD) of response and slope approach was employed [32]. The estimated SDs of responses of each analyte were obtained by the calculated SD of y-intercepts (SDY-I) of regression lines [30]. The ME and RE values were determined by comparing the absolute peak areas of analytes of the three sets of samples (set A, B, and C), prepared as described in the Chapter 3.2.3, following the formulas shown below [31]:

ME(%) = (B/A) x 100

RE(%) = (C/B) x 100

Precision and accuracy of the HPLC-MS/MS methods were determined by analysis of the three concentration levels (low, medium, and high) for each analyte in human plasma matrix. The accuracy was determined calculating the recovery (%) between the determined and added amounts. The precision was evaluated through the relative standard deviation (RSD) of the quantitative data of the replicate analysis of each level.

3.2.5. MS/MS EXPERIMENTS

The ERMS experiments were performed to highlight the fragmentation patterns between the positional isomers and build their breakdown curves. These experiments were performed by doing a series of Product Ion scan (MS/MS) analysis, increasing the collision voltage (CV) from 5 to 50 V. Each MS/MS spectra were acquired in the m/z range from 50 to 650 (the mass of the analytes is between 578 and 625 Da), argon was used as collisional gas and the scan time was set at 600 ms. Each analyte, prepared as working solution 1 described in Chapter 3.2.3, were introduced by a syringe pump at 10 mL min-1, then, the precursor ion were isolated and the abundance of the product ions were recorded. The ERMS data were used to build the

breakdown curves that represent the fragmentation energetics for each compound in study. Breakdown curves are a relative intensity versus CV chart and each point is represented by a mean of 15-20 scans.

3.2.6. LEDA ALGORITHM

The deconvolution was performed by applying the algorithm either to the area abundances, obtained from the integrated peak intensities of each MRM channel, or to individual MS/MS data point of the chromatographic sample profile. In the first case, the LEDA provides the relative amounts (%) of each know component present in the sample. In the second approach, each MRM signals are deconvoluted 'scan-by-scan' and assigned to the present isomers, allowing a graphical separation of the processed chromatographic profiles. The characteristic abundance ratios were calculated, for each pure isomer, by data obtained from the highest level of the calibration curve (100 ng mL^{-1}) by HPLC-MS/MS methods described above. The ratios between Pi vs. Ri selected in the MRM methods were calculated and the resulted values were reported in Table 3.3. The LEDA algorithm performances were checked by processing the MS/MS data obtained from the analysis of the set C samples, prepared in Chapter 3.2.3, and verified by its application in post-processing analysis of the samples.

Compound	Pi/Ri (1)	Ratio 1 value ± SD	Pi/Ri (2)	Ratio 2 value ± SD
CRF22	221/579	1.28 ± 0.05	341/579	0.06 ± 0.01
CRF35		1.00 ± 0.02		0.12 ± 0.01
CRF32	221/626	0.95 ± 0.05	388/626	0.16 ± 0.01
GG3		1.16 ± 0.08		0.03 ± 0.01
CRF33	221/607	1.17 ± 0.04	406/607	0.01 ± 0.01
GG4		0.85 ± 0.02		0.42 ± 0.01
GG12	205/577	0.84 ± 0.01	376/577	0.31 ± 0.02
GG15		0.49 ± 0.05		0.08 ± 0.01
GG1	221/593	0.89 ± 0.03	392/593	0,33 ± 0.01
GG5		0.45 ± 0.02		0.16 ± 0.01
LB48	195/567	0.49 ± 0.01	366/567	0.16 ± 0.01
GG13		0.26 ± 0.02		0.34 ± 0.01

Table 3.3: Pi/Ri values used for LEDA algorithm

3.3. RESULTS

3.3.1. CHROMATOGRAPHY

In the preliminary tests, it was evaluated the possibility of chromatographic separation of the compound in study. This was partially achieved by employing specific parameter for each pair of isomers such as long columns, specific stationary and mobile phases and different speed of the gradient elution but despite this, it was not accomplished for all the couples. As it was said in the Introduction the goal was to increase the productivity considering the high number of samples to be prepared, analyzed, and processed for the stability tests. Eventually it was decided to use the MS/MS features and the application of LEDA algorithm to achieve the determination of the isomers and develop a unique HPLC method for all the compounds. In this approach, the chromatographic column was used only to avoid or limit the interference of sample matrix towards the analyte ionization process (matrix effects). The use of a short column and a fast elution gradient let us to analyze and process a large number of samples (estimated to be 150-160 per day), avoiding all the specific methods setup for each couple of position isomers, with the same reliability of common HPLC-MS/MS methods.

The obtained chromatograms showed a suitable separation between the IS and the analytes in addition to the different characteristic MRM transitions. Anyway, as it was said an acceptable separation among the isomers ($R \geq 1.5$) was not reached.

All chromatographic parameters (i.e. retention times, peaks width, efficiency etc.) for each analyte were calculated and reported in Table 3.4.

Compound	Rt (min)	± 2 SD (min)	Width (min)	N (plates)	R
IS	3.13	0.02	0.20	3959	-
CRF22	2.92	0.02	0.20	3409	0.3
CRF35	2.99	0.01	0.21	3578	
CRF32	3.43	0.02	0.21	4133	0.1
GG3	3.45	0.02	0.21	4294	
CRF33	3.17	0.01	0.20	3885	0.2
GG4	3.21	0.01	0.20	4076	
GG12	3.64	0.02	0.23	4062	0.6
GG15	3.78	0.03	0.22	4614	

GG1 GG5	3.13 3.23	0.02 0.02	0.20 0.20	3917 4073	0.5
LB48 GG13	2.97 3.08	0.01 0.01	0.20 0.20	3620 3807	0.5

Table 3.4: Chromatographic parameters of each analyte

It is worth to emphasize that in this case the calculation of N was employed only for an evaluation of efficiency reached/achieved by the chromatographic system used.

Furthermore, the chromatographic profiles of all the compound in study are reported in Figure 3.10-3.15.

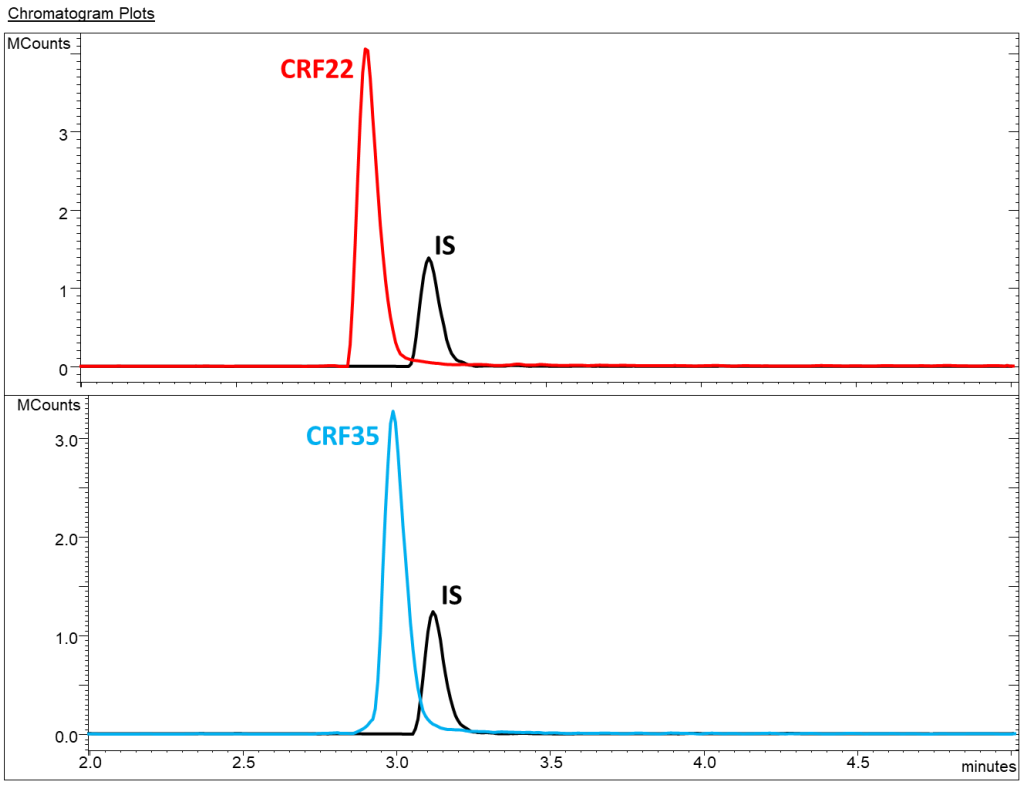

Figure 3.10: Chromatographic profiles of the HPLC-MS/MS analysis of CRF22-CRF35 isomers.

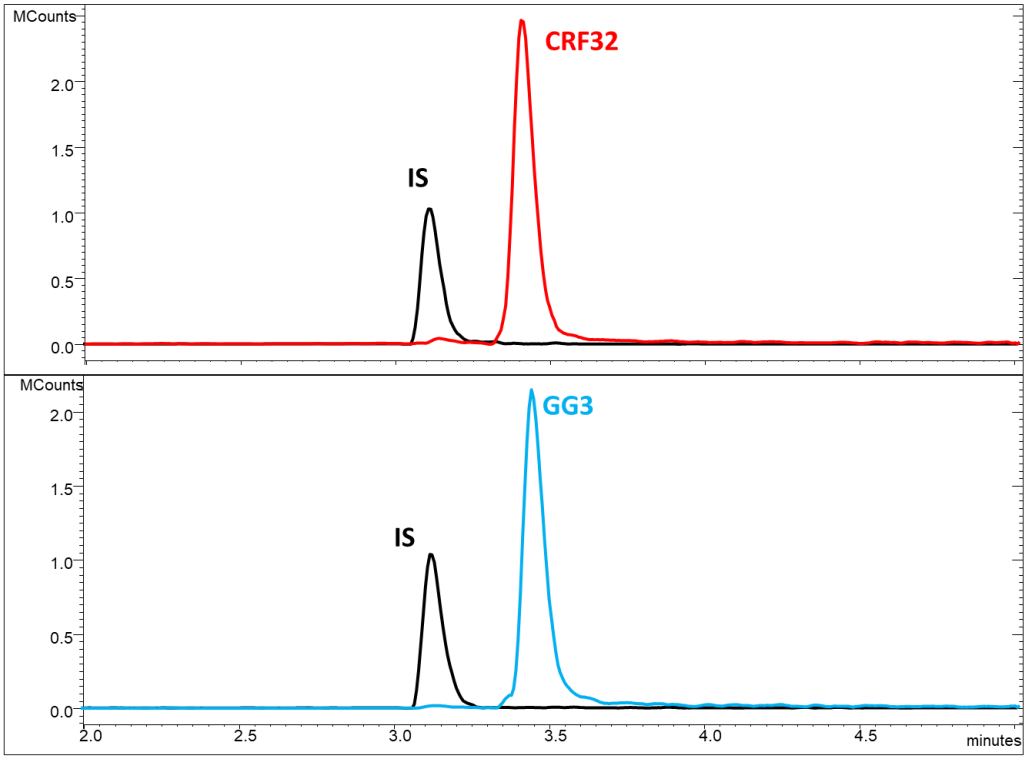

Figure 3.11: Chromatographic profiles of the HPLC-MS/MS analysis of CRF32-GG3 isomers.

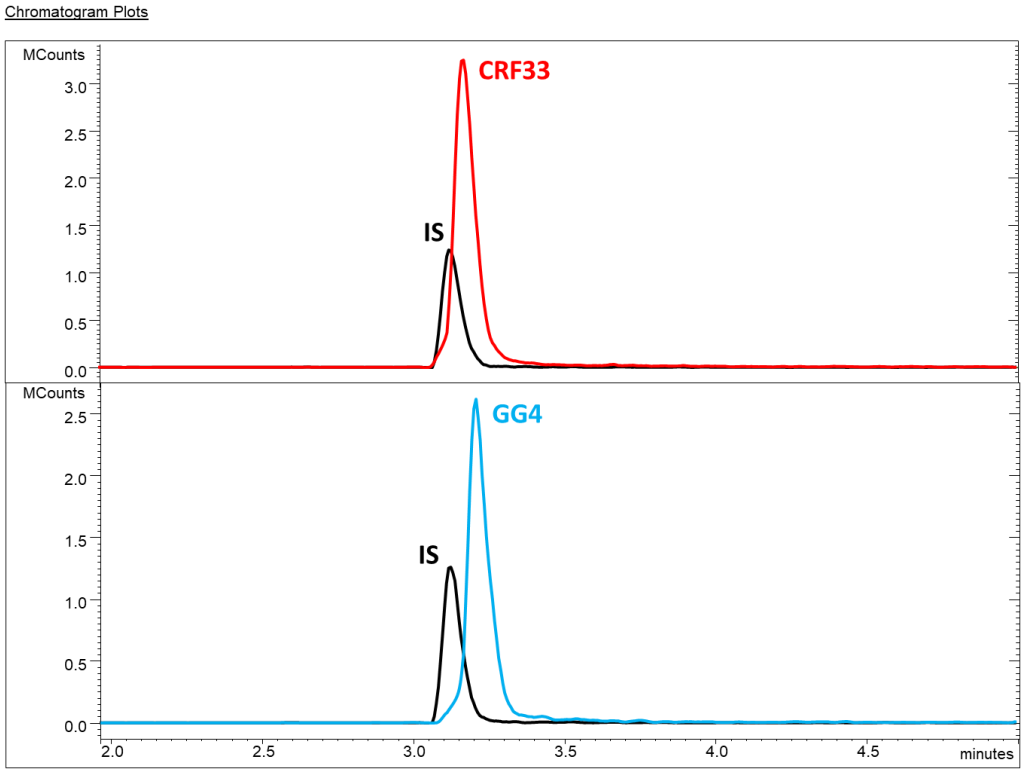

Figure 3.12: Chromatographic profiles of the HPLC-MS/MS analysis of CRF33-GG4 isomers.

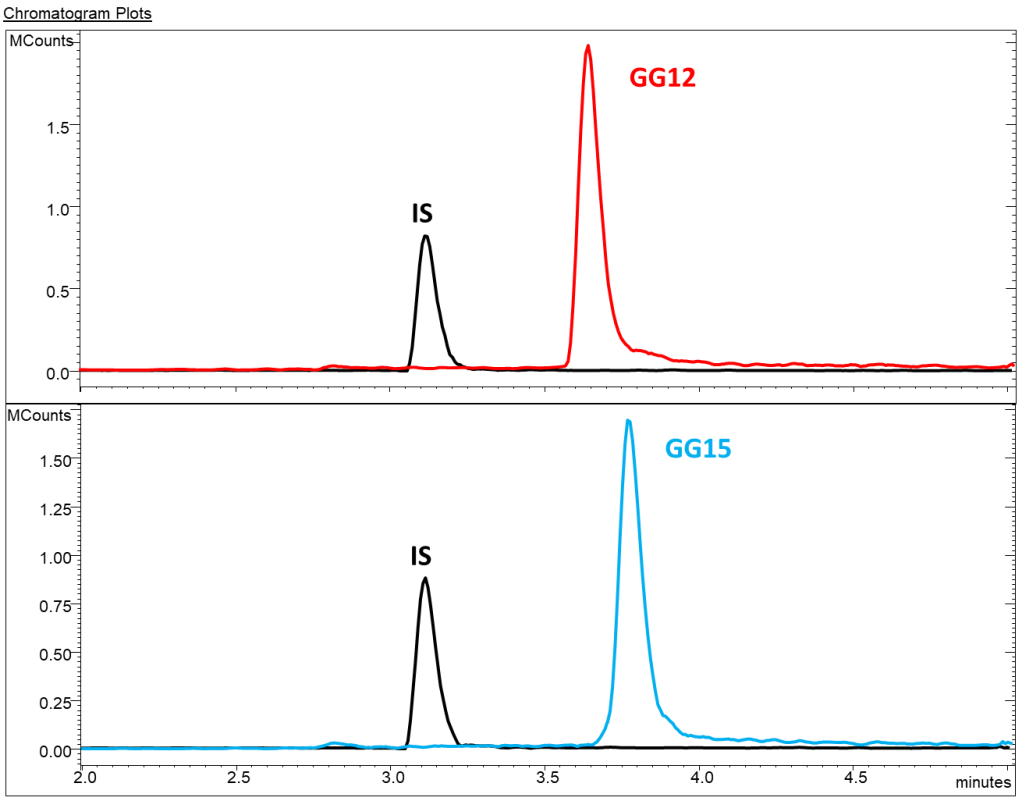

Figure 3.13: Chromatographic profiles of the HPLC-MS/MS analysis of GG12-GG15 isomers.

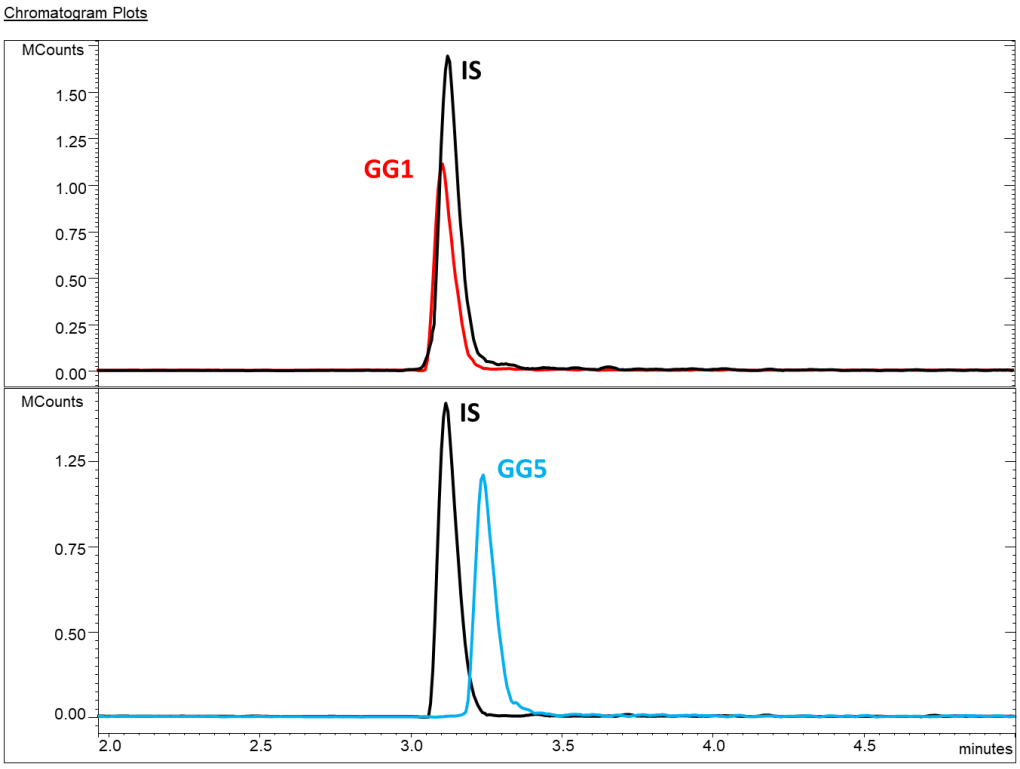

Figure 3.14: Chromatographic profiles of the HPLC-MS/MS analysis of GG1-GG5 isomers.

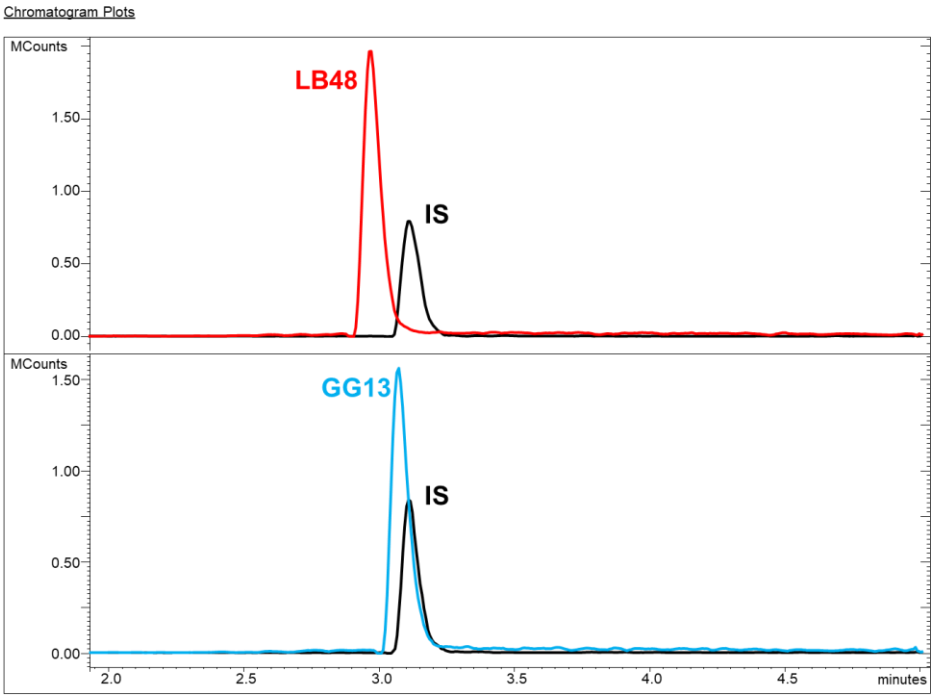

Figure 3.15: Chromatographic profiles of the HPLC-MS/MS analysis of LB48-GG13 isomers.

From these results it is possible to highlight how the proposed HPLC method achieved a poor efficiency (N ≃ 4000), mostly due to short column used. This choice let to exploit a rapid elution gradient, brief time to rinse the column, restoring the initial condition and, consequently, a fast chromatographic run. Therefore, the goal to develop a fast and simple chromatography method was achieved. At this point, in order to obtain the right specificity to obtain significant results from the stability tests, the MS/MS features for each analyte were explored.

3.3.2. COLLISION-INDUCED DISSOSIATION STUDY

The analytes in study (Figure 3.4), in positive ions ESI-MS conditions, showed a signal of the adduct with the proton. So, each isomer pair were detected at the same *m/z* value. The adduction with the proton was hypothesized on the tertiary amine group shared by all compounds. Therefore, to obtain a MS signal characterization of all analytes, some MS/MS experiments were done. In fact, to highlight the possible intrinsic differences in the molecular stability of the analytes, a series of ERMS experiments (Chapter 3.2.5) were performed. By computing all the data obtained by these experiments, the collision breakdown curves were plotted and the most significant and abundant product ions for each pair were selected. All the collision breakdown curves were showed in Figure 3.16-3.21.

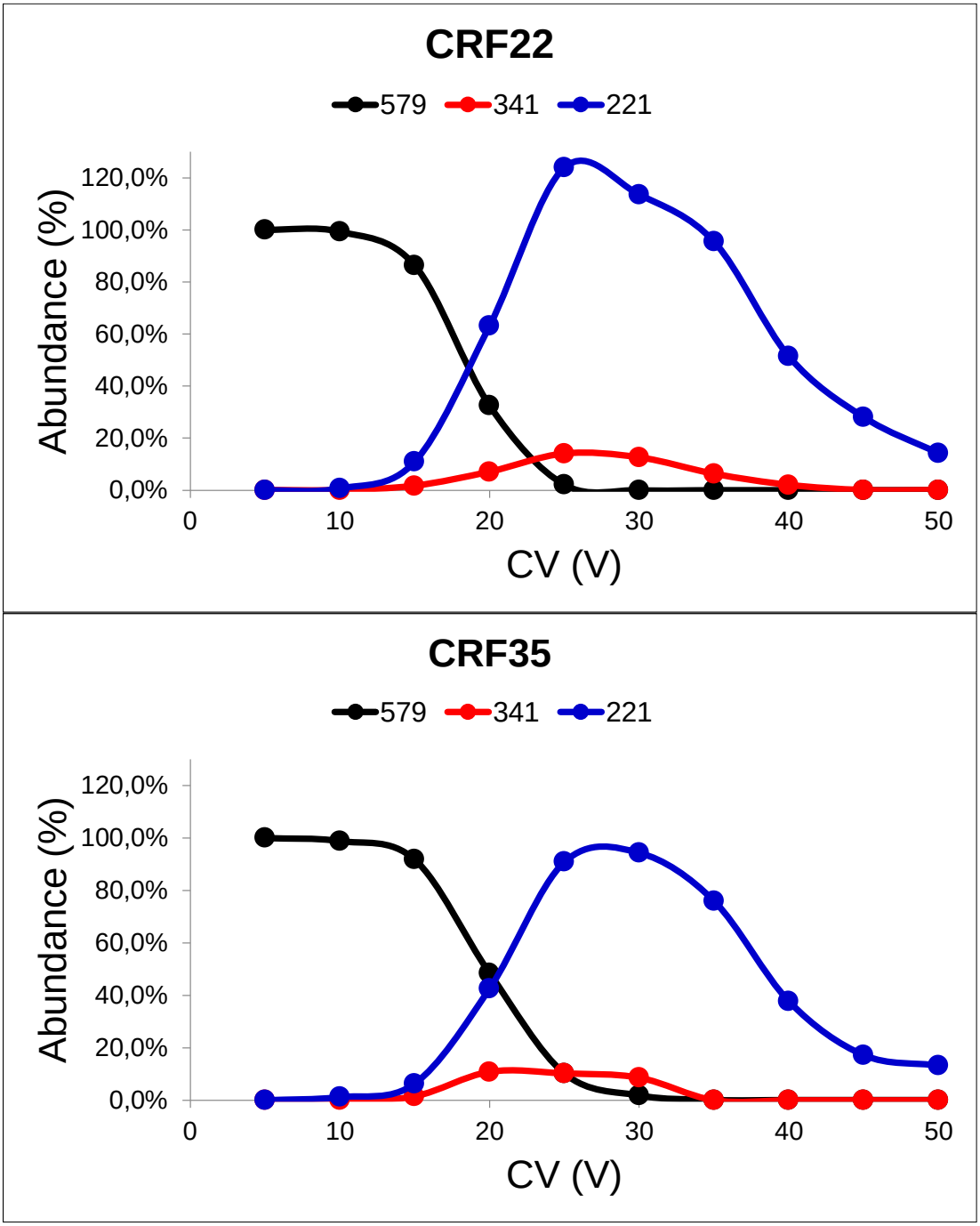

Figure 3.16: Collision induced dissociation of CRF22-CRF35 isomers.

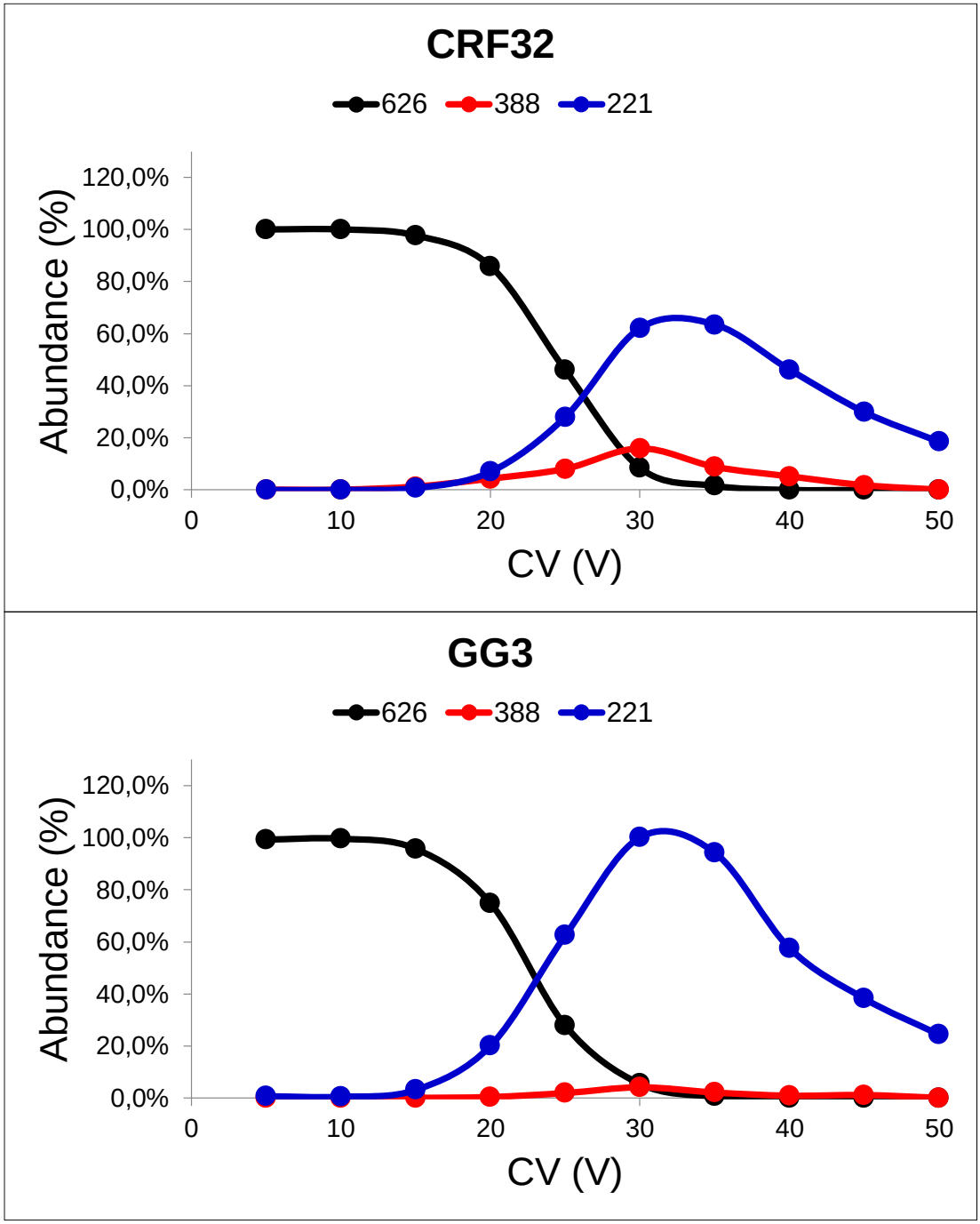

Figure 3.17: Collision induced dissociation of CRF32-GG3 isomers.

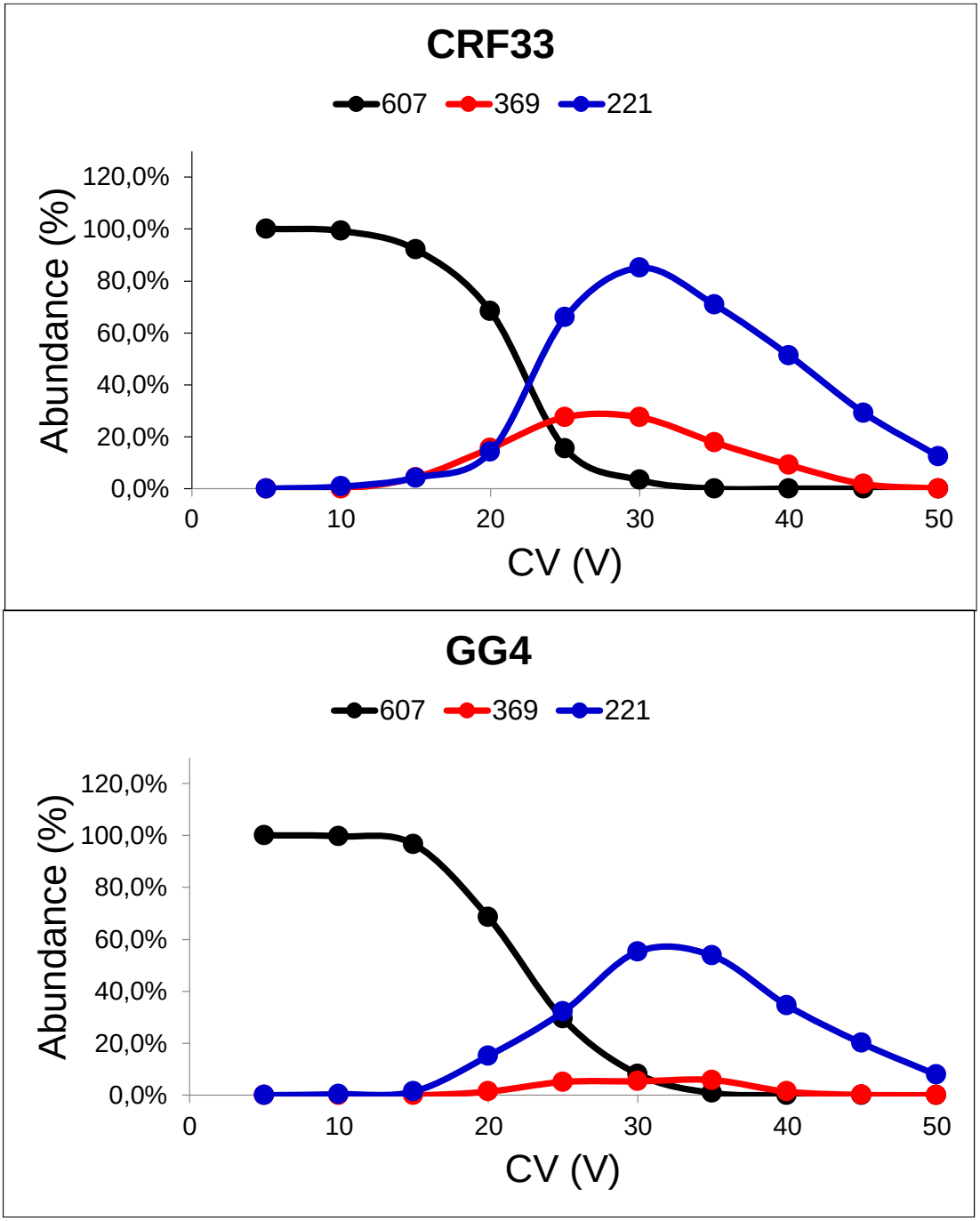

Figure 3.18: Collision induced dissociation of CRF33-GG4 isomers.

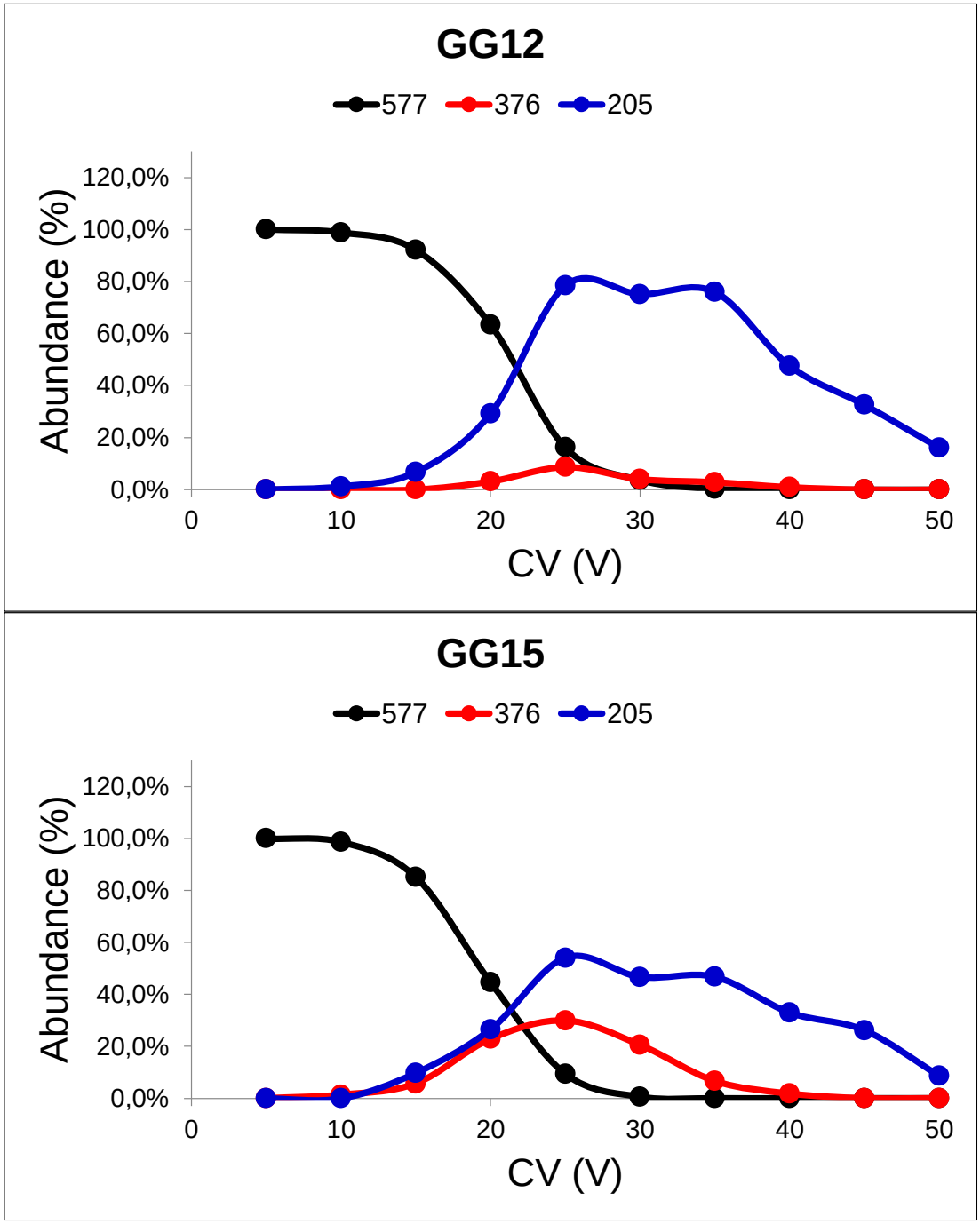

Figure 3.19: Collision induced dissociation of GG12-GG15 isomers.

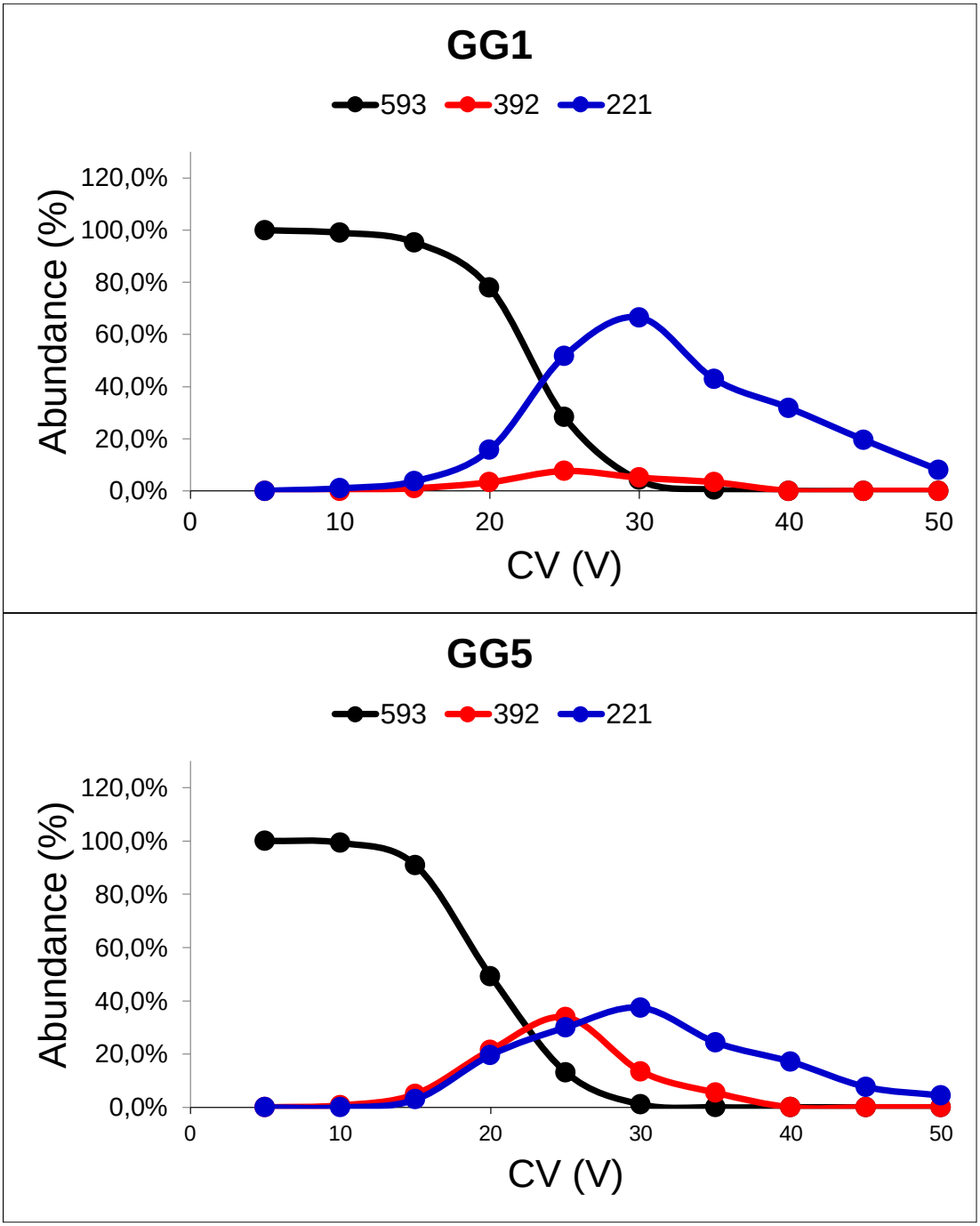

Figure 3.20: Collision induced dissociation of GG1-GG5 isomers.

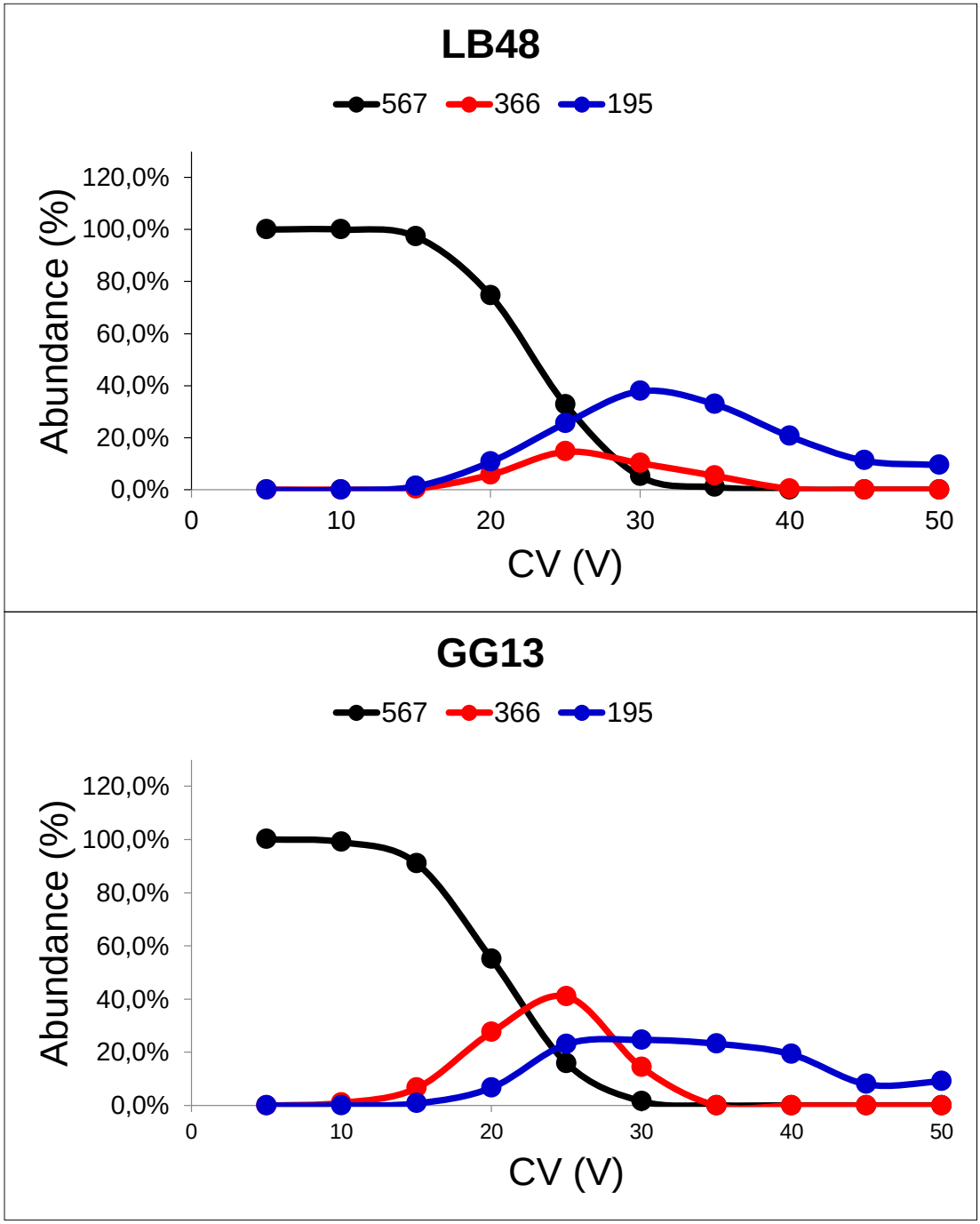

Figure 3.21: Collision induced dissociation of LB48-GG13 isomers.

From these experiments it was showed that, all the P-gp/CA hybrids showed a common fragmentation pathway, related to the cleavage of the ester groups (Figure 3.22).

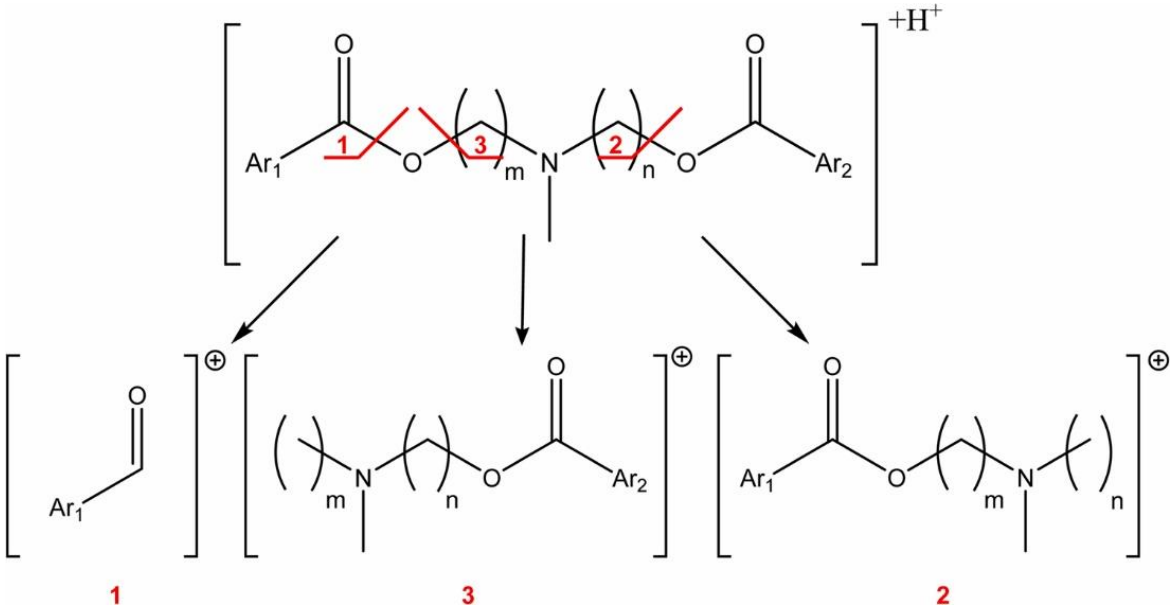

Figure 3.22: Fragmentation pathway shared by all compounds in study

The most intense signal, for all compounds, was obtained by the cleavage 1 with the formation of product ion 1 and the corresponding neutral alkyl-alcohol structure. Conversely, the second ion transition occurred by the Ar2 ester group cleavage but, in this case, with the formation of the product ion 2 structure and the carboxylic acid of Ar2. However, CRF22-CRF35 and CRF32-GG3 showed a different way. In fact, these two pair showed the breaking 3 as favored, with formation of ion 3 and the carboxylic acid of Ar1. It was interesting to note that, in the general ion structures, the product ions 2 and 3 have maintained the information about the differences between the isomers, useful to their distinction. Finally, in some cases (CRF22 and GG3) it is possible to notice that the signal that represents the product ion 221 m/z is higher that the signal of the precursor ion. Of course, this does not mean that the quantity of this product ion is actually higher than the precursor ion. In this case the geometry of the system employed (the collision cell is bent 90°) can facilitate the passage of a specific packet of ions (for example the product ion 221 *m/z*) respect to another one (the precursor ion). The stability of the ion itself could be another explanation for this behavior.

3.3.3. LINEARITY AND LOD

The obtained linear regressions coefficients, the determination coefficient (R^2) and the estimated Limit of Detection (LOD) values for each analyte are reported in Table 3.5.

Compound	Slope (PAR/ng mL^{-1})	Intercept (PAR)	R^2	LOD (ng mL^{-1})
CRF22	0.039	0.077	0.997	4.4
CRF35	0.028	0.028	0.999	2.1
CRF32	0.022	0.004	0.999	0.8
GG3	0.027	0.044	0.998	3.7
CRF33	0.032	0.011	0.999	2.2
GG4	0.023	0.023	0.998	3.8
GG12	0.022	0.022	0.998	3.9
GG15	0.010	0.003	0.999	0.6
GG1	0.017	0.016	0.999	2.6
GG5	0.008	0.004	0.999	2.1
LB48	0.012	0.005	0.999	0.9
GG13	0.005	0.001	0.999	2.1

Table 3.5: Calibration curve parameters (slope, intercept, determination coefficient) and limit of detection value (LOD) obtained for each compound. (PAR = Peak Area Ratio, R^2 = determination coefficient, LOD = Limit of Detection).

These results show that the obtained slope values for each isomer are significantly different; therefore, it is crucial to assign properly the signal to the processed isomer, in order to avoid quantitative errors. The LOD value of each compound was calculated on the SD of quantitation ion signal, neglecting either the intensity value or the evaluation of the background noise, that can be variable and dependent upon several factors. In this way, it was possible to obtain LOD values each time that the calibration curve was performed, enabling the monitoring of the instrumental performances between different analyzes batches. Moreover, the obtained LOD values strengthened the reliability of the low concentration levels chosen for the calibration curves, allowing the analyte detection in the samples less than 10% (< 0.1 μM) as compared with the spiked concentration (1 μM).

3.3.4. MATRIX EFFECT, RECOVERY, AND LEDA RELIABILITY

ME and RE values were calculated as described in Chapter 3.2.4 and reported in Table 3.6.

Compound	ME±SD (%)	RE±SD (%)	LEDA±SD (%)
IS	99 ± 5	101 ± 6	
CRF22	96 ± 12	95 ± 6	100 ± 1
CRF35	96 ± 2	104 ± 12	99 ± 1
CRF32	97 ± 6	103 ± 6	99 ± 1
GG3	99 ± 6	98 ± 4	99 ± 2
CRF33	103 ± 4	103 ± 6	99 ± 1
GG4	102 ± 5	102 ± 8	99 ± 2
GG12	99 ± 6	108 ± 5	98 ± 1
GG15	103 ± 7	101 ± 4	97 ± 3
GG1	106 ± 7	88 ± 5	99 ± 1
GG5	105 ± 6	102 ± 7	99 ± 2
LB48	104 ± 6	105 ± 9	100 ± 1
GG13	105 ± 6	102 ± 7	98 ± 2

Table 3.6: ME and RE values

From these results it is possible to highlight that the ME values ranging from 96% to 106% demonstrating that the signal abundance of each compound was not significantly different both in human plasma (set B) and in neat solvents (set A) samples. This means that, even if the chromatographic approach using short columns and fast gradient elution was sufficient to avoid the possible effect of the plasma matrix on the ionization efficiency. In addition, RE values, obtained calculating the ratio between set C and set B describing the recovery during the sample preparation, showed values ranging from 88% to 108%. These results, confirm that the sample preparation was suitable in the extraction of the analytes from the matrix. Also, it is important to emphasize that the ME and RE values obtained for the IS were close to 100% for both, showing that it was an appropriate choice to monitoring the studied compounds.

The LEDA reliability was evaluated by processing the MS/MS data, obtained from set C of each analyte, identifying which isomer was present, as well as its purity. The algorithm

elaborated each MRM signals, separating their components and assigning the correct abundance to the identified isomers. The purity value was calculated by applying LEDA to the integrated peak area of the analyte in the sample and represents the percentage of the MS/MS signal assigned of studied compound, with a threshold that can be represented by the SD of the values. The obtained purity (%) data and corresponding SD are reported in Table 3.6. In order to verify the performances of LEDA, the set C samples were also processed 'scan-by-scan', so applying the algorithm for each data point of the chromatogram. These "reconstructions" of the chromatographic profile by the algorithm were reported in Figure 3.23-3.28.

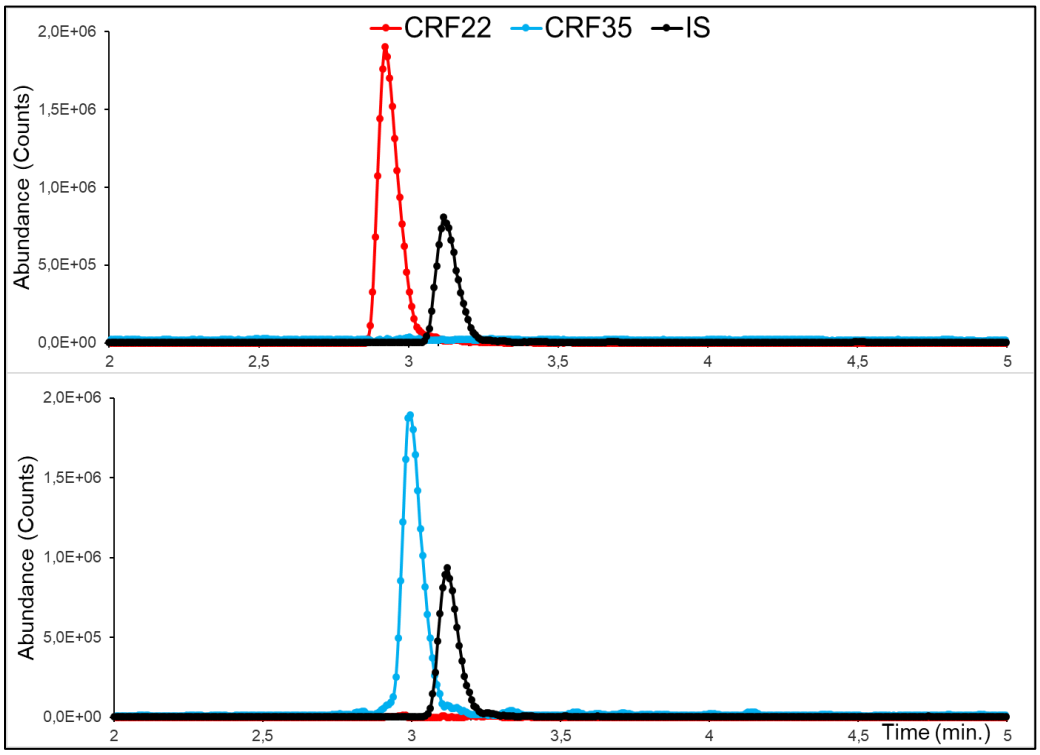

Figure 3.23: point-by-point LEDA reconstruction of CRF22 and CRF35 samples.

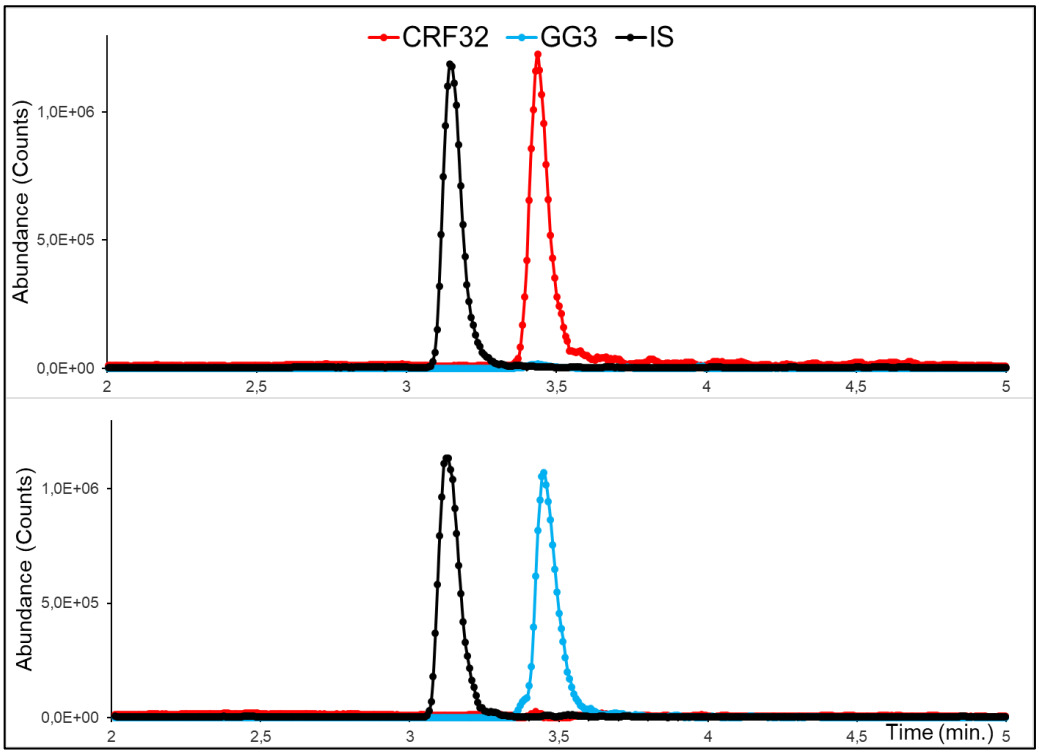

Figure 3.24: point-by-point LEDA reconstruction of CRF32 and GG3 samples.

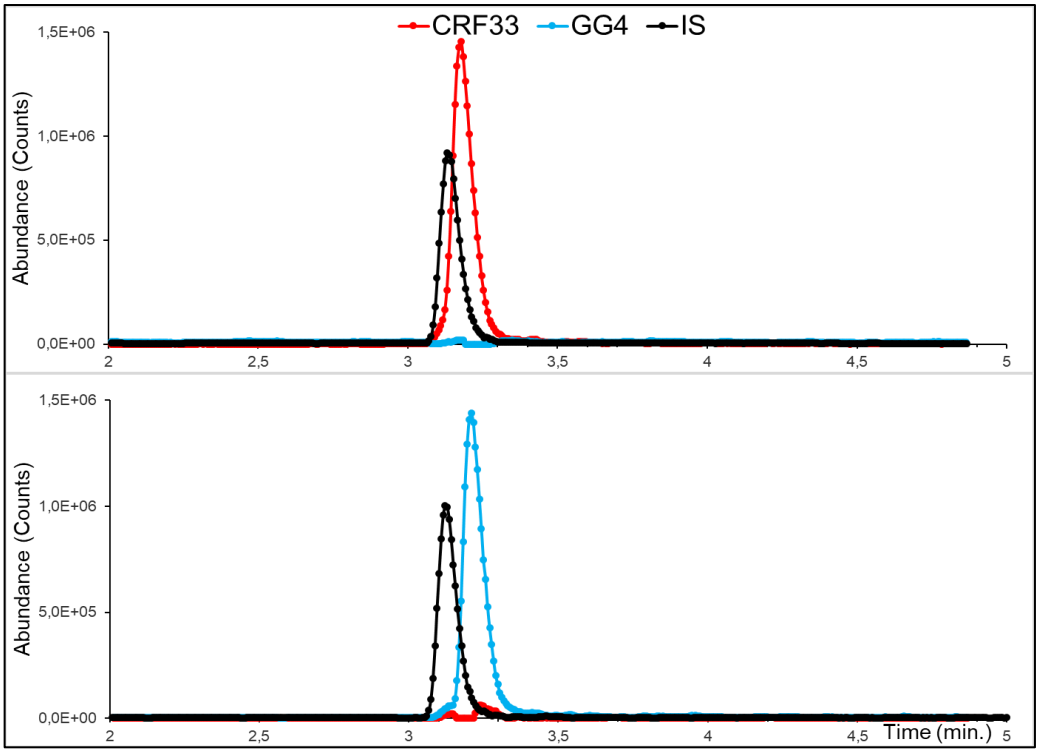

Figure 3.25: point-by-point LEDA reconstruction of CRF33 and GG4 samples.

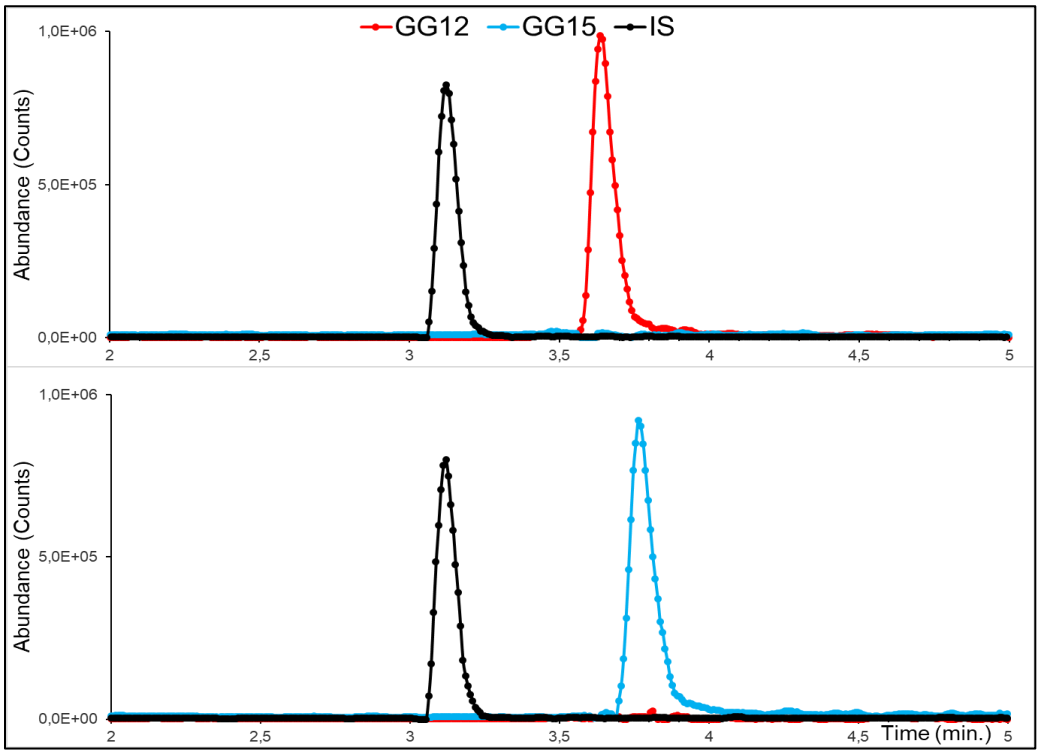

Figure 3.26: point-by-point LEDA reconstruction of GG12 and GG15 samples.

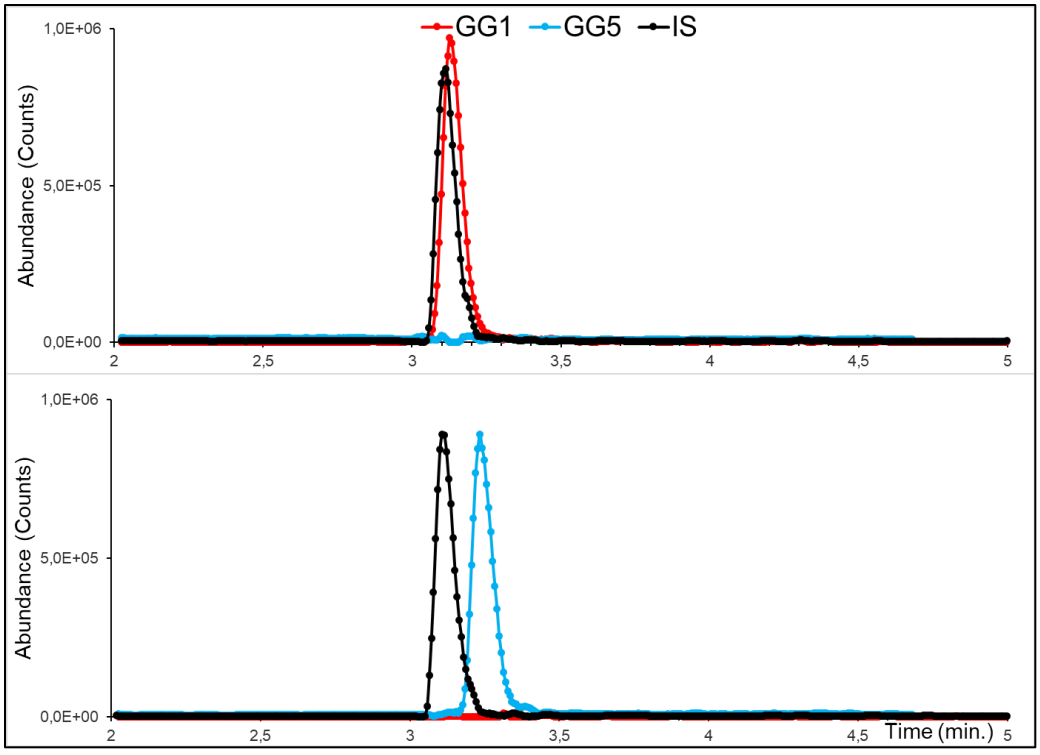

Figure 3.27: point-by-point LEDA reconstruction of GG1 and GG5 samples.

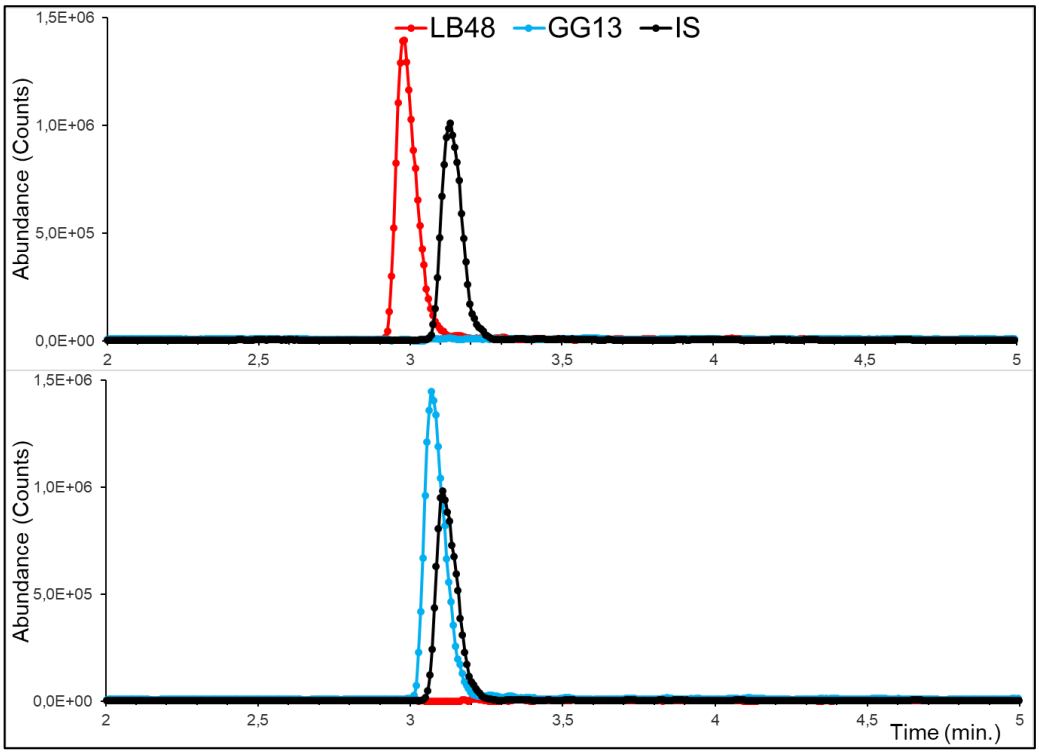

Figure 3.28: point-by-point LEDA reconstruction of LB48 and GG13 samples.

The LEDA purity results (>97%) and the reconstructed profiles demonstrate that the post-processing algorithm was able to distinguish between the isomers and to ensure the correct signal assignment. Then, all samples involved in the stability study were processed with the LEDA tool to assure the specificity of the HPLC-MS/MS methods, checking for possible procedural errors (wrong spiking solution, vial labelling, position in autosampler, etc.).

3.3.5. ACCURACY AND PRECISION

Accuracy was obtained by analyzing a series of human plasma samples, at three concentration levels, for each studied compound while precision was calculated from the analysis of each sample in six replicates (Relative Standard Deviation, RSD). All these samples were analyzed with the same HPLC-MS/MS method described before and reported in Table 3.7.

Compound	Low level	Medium level	High level
	Recovery ± RSD (%)	Recovery ± RSD (%)	Recovery ± RSD (%)
CRF22	105 ± 3	107 ± 3	98 ± 1
CRF35	103 ± 5	103 ± 7	99 ± 2
CRF32	92 ± 6	101 ± 2	100 ± 6
GG3	106 ± 7	107 ± 2	98 ± 4
CRF33	96 ± 7	104 ± 8	97 ± 5
GG4	99 ± 5	107 ± 5	98 ± 4
GG12	98 ± 4	93 ± 4	102 ± 6
GG15	100 ± 10	99 ± 6	100 ± 6
GG1	108 ± 13	100 ± 9	99 ± 2
GG5	107 ± 8	97 ± 5	100 ± 5
LB48	101 ± 4	99 ± 5	100 ± 7
GG13	104 ± 10	100 ± 3	100 ± 6

Table 3.7: accuracy and precision

The obtained results for all the analytes allow to be confident on their determination in the degradation experiment samples.

3.3.6. CHEMICAL STABILITY TEST

All compounds in study contain two ester bonds, that can be hydrolyzed by esterase enzymes, then a human plasma stability test was deemed necessary. Moreover, a stability test in PBS was performed to establish a possible spontaneous hydrolysis and support the human plasma tests. The hydrolytic activity of each batch of plasma used was evaluated with Ketoprofen Ethyl-Ester reference compound using the same HPLC-MS/MS method described before [33]. The stability charts were built plotting the concentration of each analyte in both matrices versus the time of incubation. Generally, when the substrate concentration was smaller than the Michaelis–Menten constant (K_M), the enzymatic degradation rate is described to a first-order kinetics. Therefore, by converting the quantitative results as natural logarithm, the natural logarithm of concentrations can be plotted versus incubation times and, the slope of the linear function

obtained (degradation plot), will represents the degradation rate constant (k). Then, the $t_{1/2}$ was calculated as follows:

$$t_{1/2} = \frac{\ln (0.5\mu M)}{k}$$

The KEE degradation plot (Figure 3.29) showed a comparable decrease with the one found in literature ($t_{1/2}$ 106 min) confirming the enzymatic activity of the plasma batches employed.

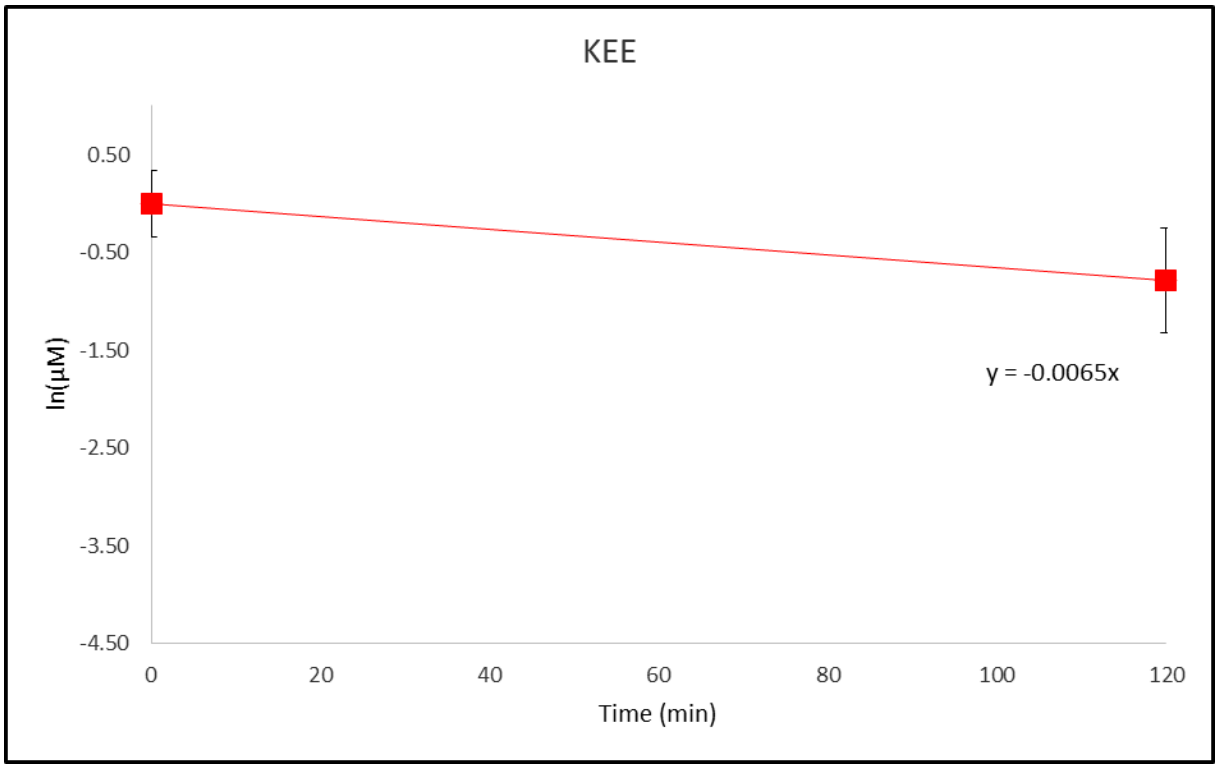

Figure 3.29: KEE degradation (control) in H-pl

Furthermore, all compound in study proved to be stable in PBS while showed a remarkable degradation rate in human plasma, except for GG15 that demonstrated to be stable over 240 minutes (Figure 3.30-3.35).

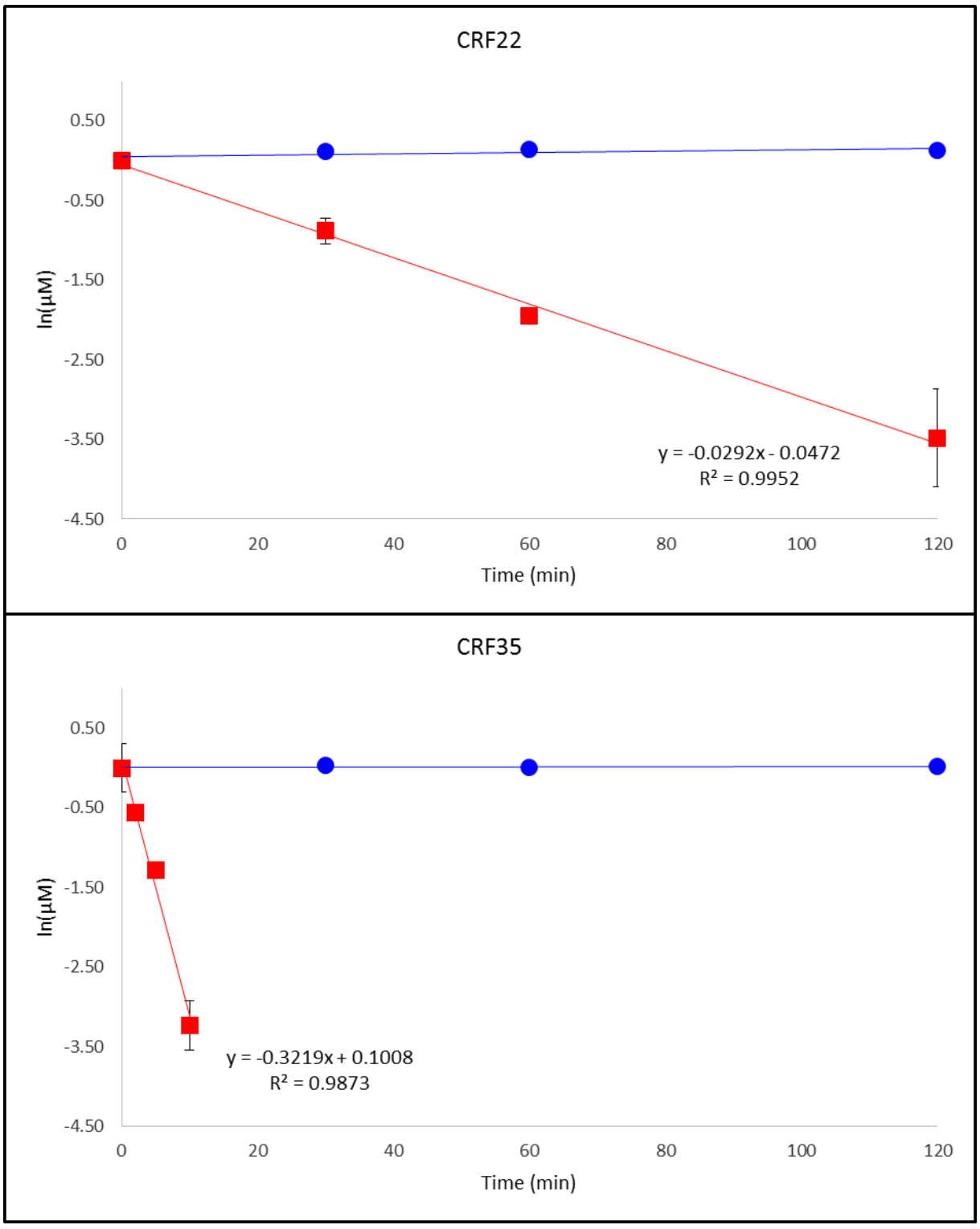

Figure 3.30: degradation profiles of CRF22 and CRF35. The red line and red square represent the degradation in H-pl while the blue line and blue dot represent the stability in PBS

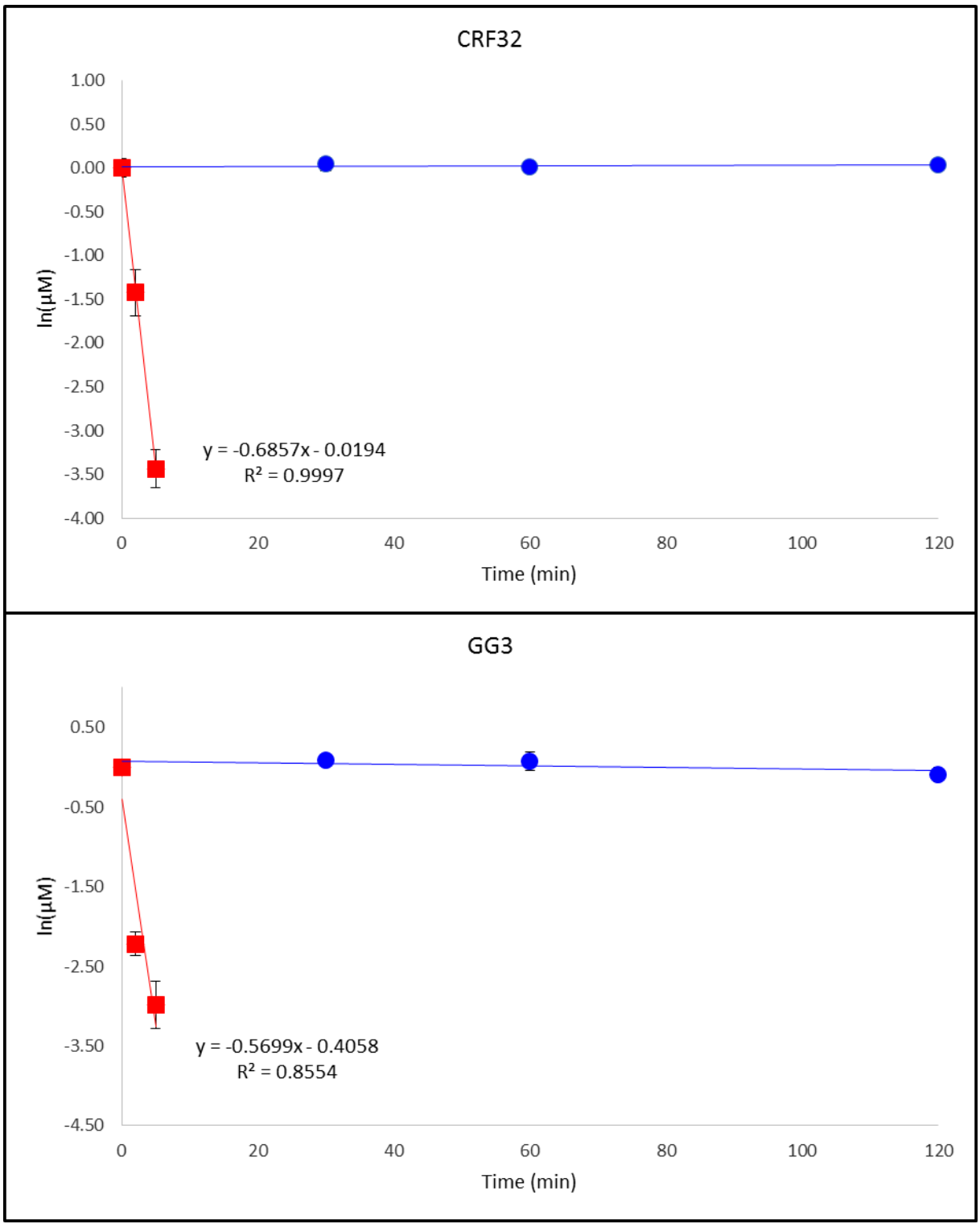

Figure 3.31: degradation profiles of CRF32 and GG3. The red line and red square represent the degradation in H-pl while the blue line and blue dot represent the stability in PBS

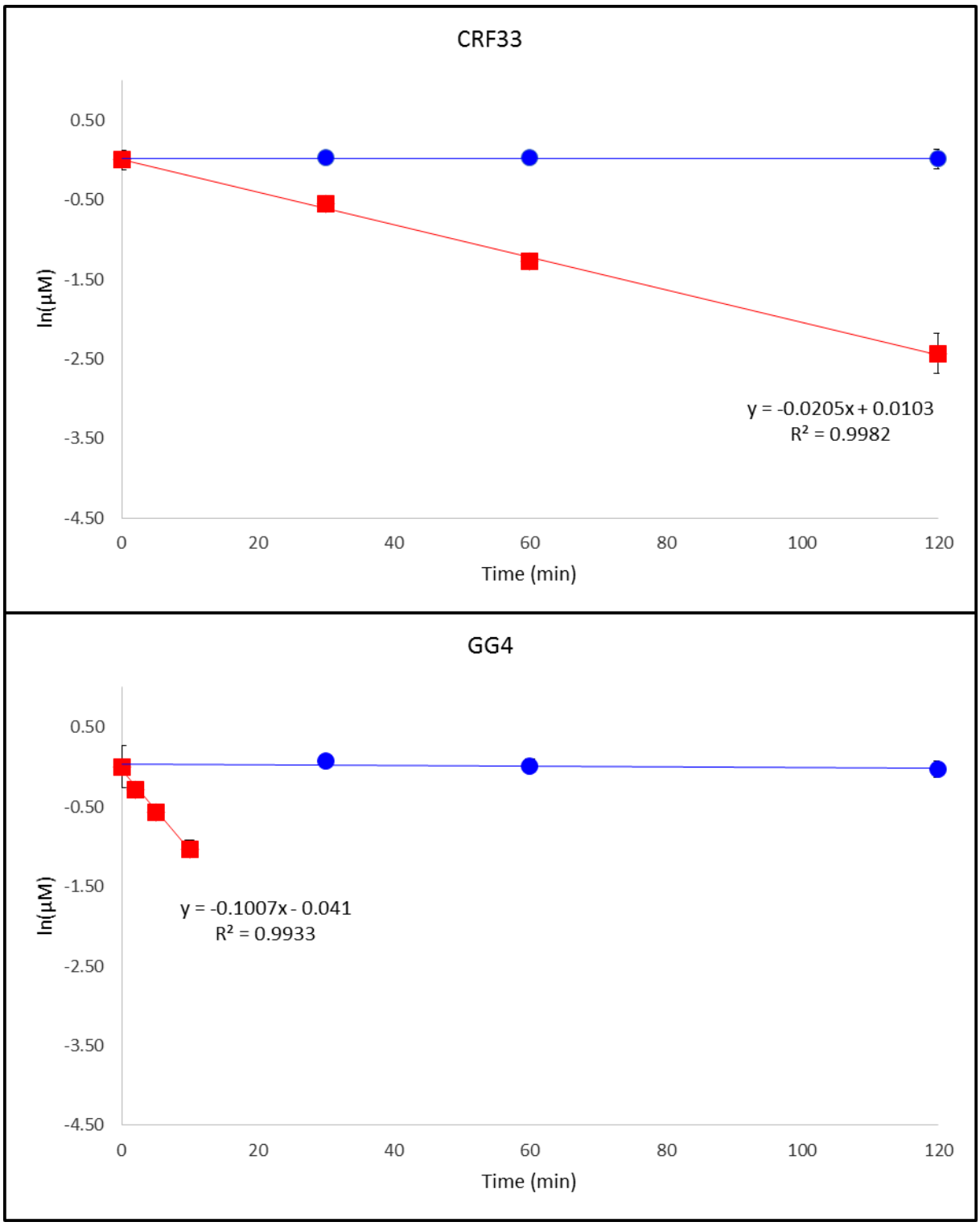

Figure 3.32: degradation profiles of CRF33 and GG4. The red line and red square represent the degradation in H-pl while the blue line and blue dot represent the stability in PBS

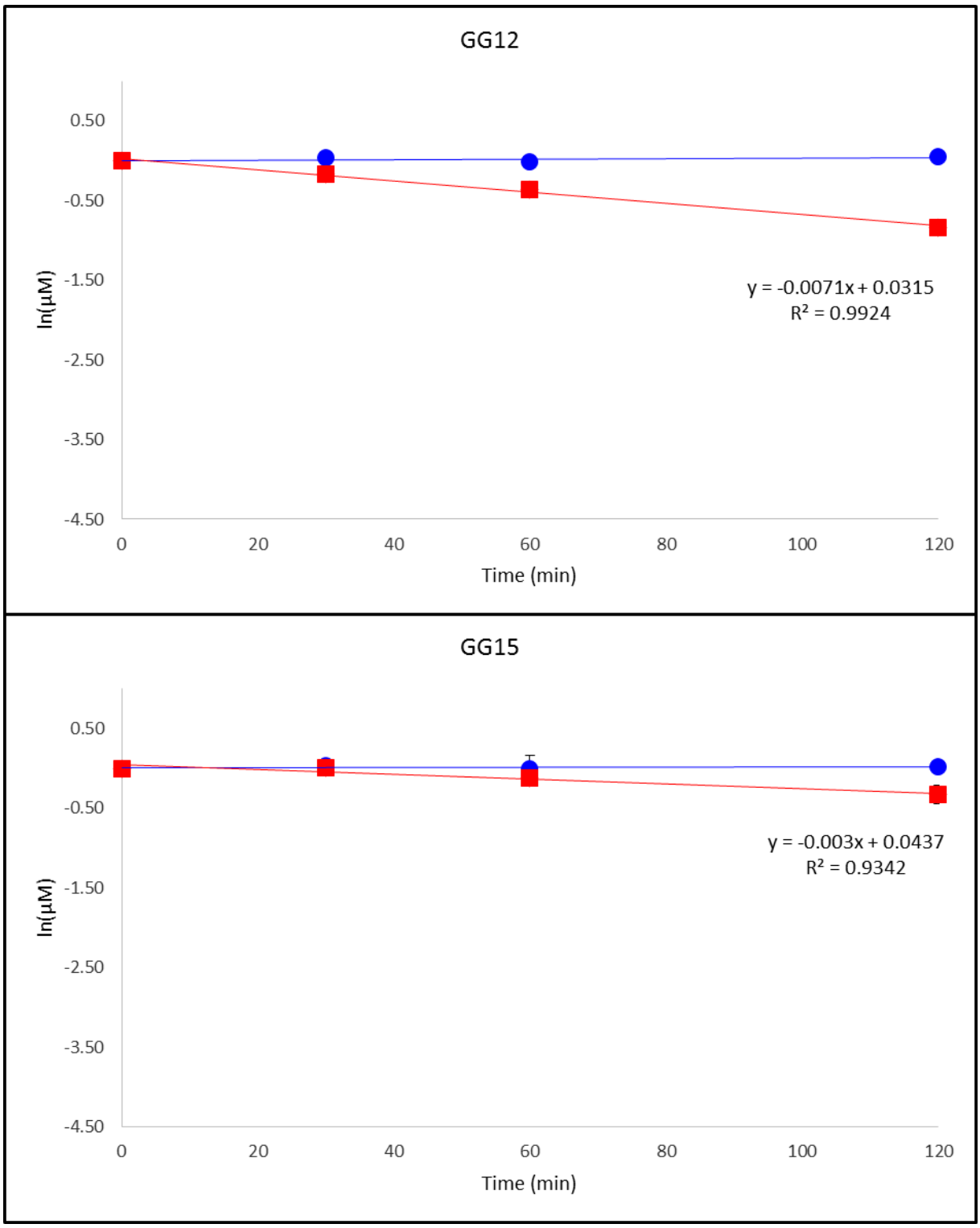

Figure 3.33: degradation profiles of GG12 and GG15. The red line and red square represent the degradation in H-pl while the blue line and blue dot represent the stability in PBS

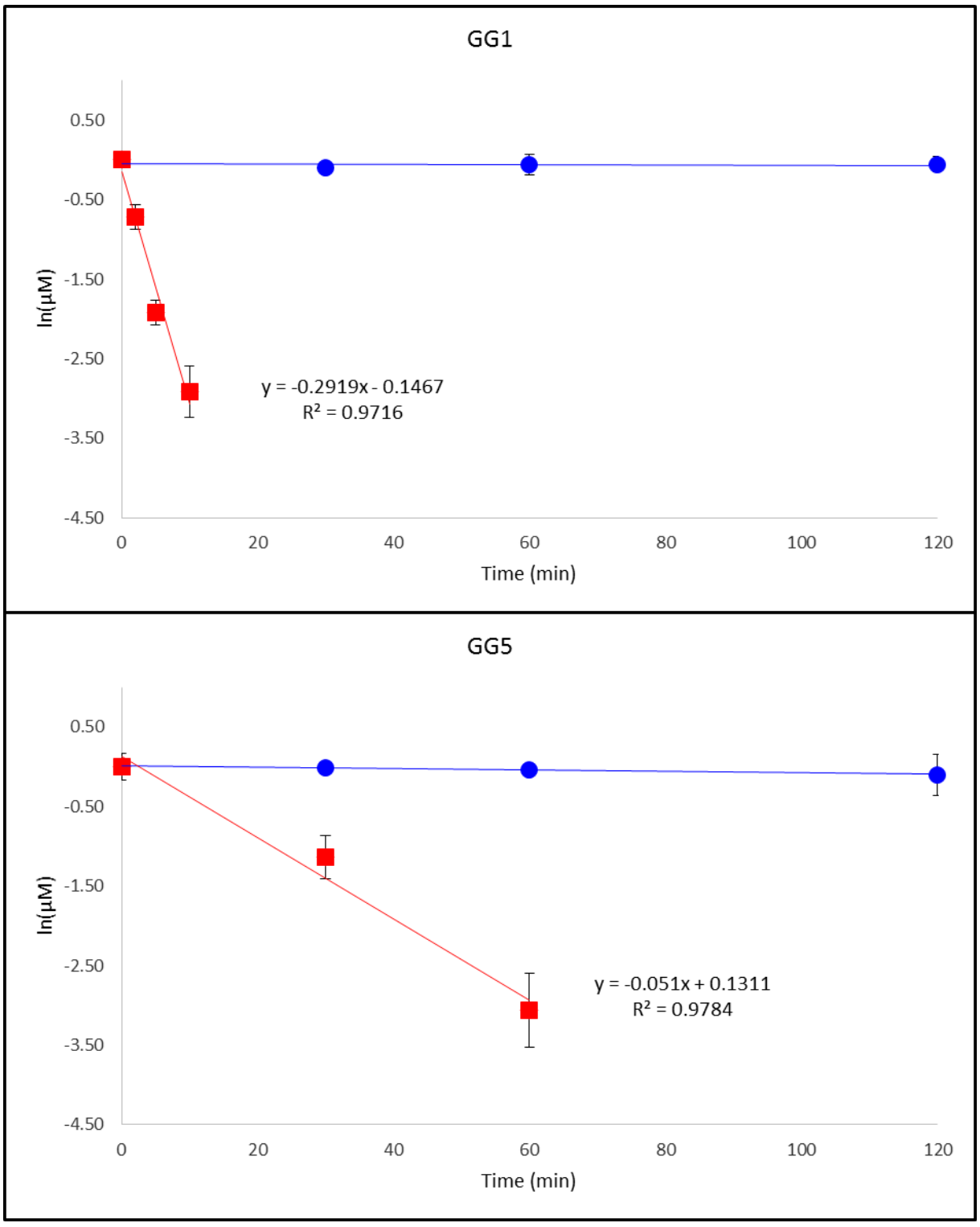

Figure 3.34: degradation profiles of GG1 and GG5. The red line and red square represent the degradation in H-pl while the blue line and blue dot represent the stability in PBS

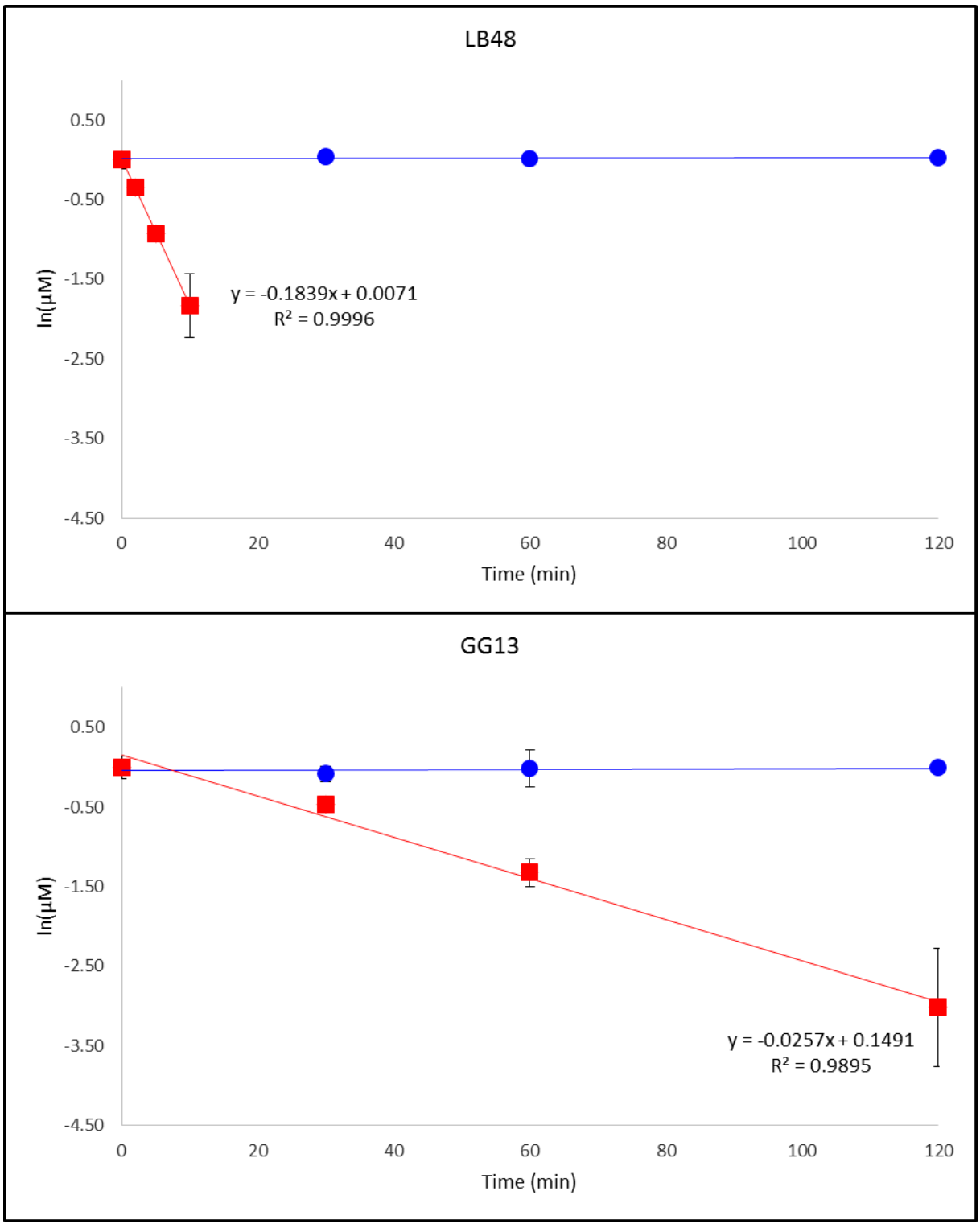

Figure 3.35: degradation profiles of LB48 and GG13. The red line and red square represent the degradation in H-pl while the blue line and blue dot represent the stability in PBS

The calculated results over 120 min have been considered affected by a significant error considering that the highest time involved in the study was 120 min. Therefore, this kind of

results were indicated as ≥ 120 min. All $t_{1/2}$ values of studied isomers were reported in Table 3.8.

Compound	PBS $t_{1/2}$ (min.)	H-pl $t_{1/2}$ (min.)
CRF22	≥120	22 ± 3
CRF35	≥120	3 ± 1
CRF32	≥120	1 ± 1
GG3	≥120	1 ± 1
CRF33	≥120	35 ± 6
GG4	≥120	6 ± 1
GG12	≥120	102 ± 7
GG15	≥120	≥240
GG1	≥120	2 ± 1
GG5	≥120	17 ± 5
LB48	≥120	4 ± 1
GG13	≥120	34 ± 7

Table 3.8: $t_{1/2}$ values obtained

The comparison between the $t_{1/2}$ values highlights a significant difference of degradation rate among the isomers; hence, it is even more important to ensure the analyte signal attribution to characterize its behavior. In fact, especially in the isomer tests, it should be possible to have a device that avoids eventual mistakes during the sample manipulation or in the compilation of autosampler sample-list, when they are preparing a large number of samples. The LEDA postprocessing algorithm solves these problems by ensuring the correct MS/MS signal attribution to the compound present in the analyzed sample working as a "quality control" tool.

3.4. CONCLUSION

In this project it was proposed a new approach using a HPLC fast and simple method using the MS/MS feature of the instrument and the application of LEDA to achieve the right selectivity to distinguish positional isomers. LEDA mathematical algorithm, introduced to process the acquired data, demonstrated to be reliable to recognize and to separate the possibly components present in the MS/MS signals avoiding any possible errors (wrong spiking solution, vial labelling, position in autosampler, etc.). After its validation, it was applied as a "quality control" tool for a chemical stability study in PBS and H-pl samples of a series of isomeric compounds

(P-gp/CA hybrids inhibitors) characterized by two ester groups in their structures. As it was presented at the beginning of this work, these hybrids were previously tested to prove their double activity. The inhibition of P-gp activity was evaluated by measuring the uptake of the P-gp substrate rhodamine-123 (Rhd 123) in K562/DOX and LoVo/DOX cells, in the absence or in presence of compounds by a flow cytometric test. Furthermore, An SX.18MV-R Applied Photophysics (Oxford, UK) stopped-flow instrument has been used to assay the catalytic/inhibition of various CA isozymes [10]. The results obtained are summarized in Table 3.9.

	FR[a]		K_I (nM)[b]			
Name	**3 μM**	**30 μM**	**hCA I**	**hCA II**	**hCA IX**	**hCA XII**
CRF22	1.08	1.83	447.2	554.8	210.6	94.3
CRF35	1.13	3.90	56.6	203.7	215.3	33.1
CRF32	1.99	5.45	>10000	>10000	26.6	94.3
GG3	1.39	1.98	>10000	>10000	40.2	33.1
CRF33	1.00	4.99	62.6	424.8	226.5	62.6
GG4	1.01	2.58	84.5	14.0	33.9	58.6
GG12	1.08	2.03	616.7	422.4	28.2	41.7
GG15	1.45	4.25	237.9	475.5	20.6	35.2
GG1	1.06	3.23	509.6	8.4	39.7	57.6
GG5	1.30	3.70	533.2	48.9	68.4	8.0
LB48	1.42	2.88	83.5	8.9	25.3	31.3
GG13	1.44	3.50	42.7	90.2	117.0	23.5
Ver	3.30	4.71				
AAZ	1.00	1.00	250.0	12.0	25.0	5.7

Table 3.9: [a] Inhibition of the P-gp transport activity on K562/DOX cells expressed as FR that is the ratio between the average fluorescence intensity of rhodamine in the presence and in absence of modulators (FR = Rhd uptake + modulator/Rhd uptake – modulator). [b] Mean from 3 different assays, by a stopped flow technique (errors were in the range of ± 5-10 % of the reported values).

From these results it is possible to highlight a very interesting affinity for some of the compounds in study. In the contrary, from the drug plasma stability test we demonstrated the low stability in human plasma. For these reasons, new p-gp/CA hybrid inhibitors were hypothesized and synthesized to be stable in human plasma [34]. These new compounds are represented by a coumarin group linked to the tertiary amine instead of a methyl (Figure 3.36).

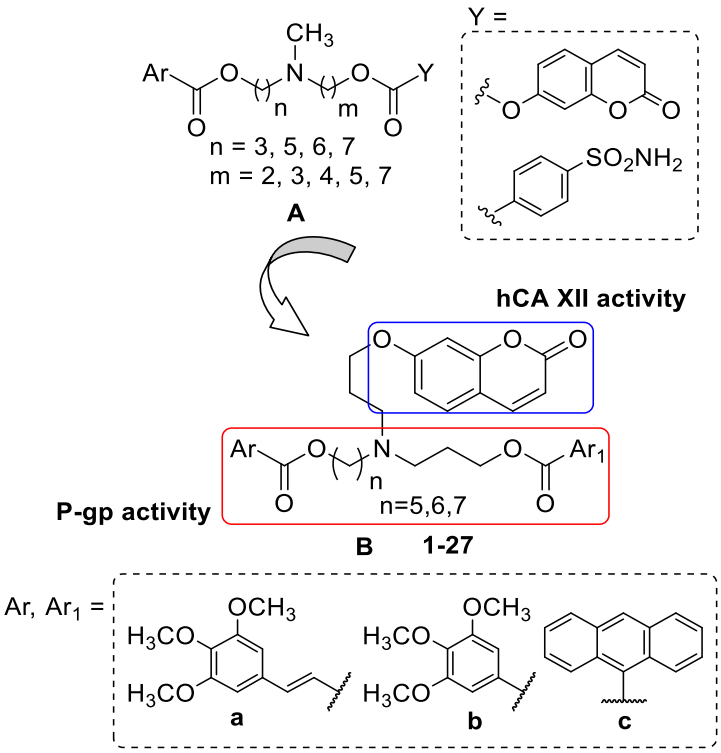

Figure 3.36: new hybrids synthesized

For these new compounds were also performed the drag stability test and it was demonstrated that the whole panel (composed by 27 new hybrids), were stable in human plasma within the 120 minutes employed in the experiment. The evaluation of the activity was repeated for these new hybrids showing interesting results (Table 3.10).

Compounds				***K*i (nM)**[a]				**RF**[b]	
N	**n**	**Ar**	**Ar1**	**hCA I**	**hCA II**	**hCA IX**	**hCA XII**	**1 μM**	**3 μM**
1	5	a	a	>10000	>10000	39.5	34.6	9.5	25.7
2	5	a	b	>10000	>10000	24.2	16.2	3.3	7.7
3	5	a	c	>10000	>10000	7.9	44.9	3.1	8.4
4	5	b	a	>10000	>10000	58.8	22.3	6.9	25.7
5	5	b	b	>10000	>10000	40.7	8.9	5.2	12.3
6	5	b	c	>10000	>10000	36.2	30.8	3.1	7.7
7	5	c	a	>10000	>10000	104.5	56.4	3.6	8.9
8	5	c	b	>10000	>10000	93.7	55.2	2.4	7.1
9	5	c	c	>10000	>10000	136.8	73.4	1.0	1.0

10	6	a	a	>10000	>10000	8.1	32.4	22.5	30.0
11	6	a	b	>10000	>10000	50.2	21.6	8.2	45.0
12	6	a	c	>10000	>10000	26.8	66.3	2.2	9.0
13	6	b	a	>10000	>10000	71.7	10.1	1.1	11.1
14	6	b	b	>10000	>10000	82.7	6.8	6.4	16.0
15	6	b	c	>10000	>10000	54.1	43.3	3.9	8.9
16	6	c	a	>10000	>10000	148.3	74.0	4.3	13.6
17	6	c	b	>10000	>10000	123.2	23.9	4.4	9.3
18	6	c	c	>10000	>10000	166.5	90.2	1.2	1.3
19	7	a	a	>10000	>10000	27.8	50.9	1.8	26.7
20	7	a	b	>10000	>10000	5.2	17.2	8.0	26.7
21	7	a	c	>10000	>10000	14.2	37.6	2.0	3.0
22	7	b	a	>10000	>10000	43.8	4.6	16.0	22.8
23	7	b	b	>10000	>10000	18.3	31.7	8.0	20.0
24	7	b	c	>10000	>10000	38.5	62.5	2.3	6.1
25	7	c	a	>10000	>10000	71.1	113.1	3.0	6.4
26	7	c	b	>10000	>10000	41.3	10.1	2.0	6.1
27	7	c	c	>10000	>10000	102.2	83.8	1.0	2.4
AAZ				250.0	12.0	25.0	5.7	-	-
Ver				-	-	-	-	1.2	3.0

Table 3.10: new hybrids activity results

In conclusion, this study gave an important support in the study and development of new hybrid inhibitors.

With regards to the method, the used chromatographic parameters were tuned to minimize the run time, without requiring high efficiency or resolution between the analytes, in fact, the column was used only to avoid or limit the interference of sample matrix towards the analyte ionization process (matrix effect). LEDA mathematical tool proved to be reliable to recognize and to separate the possible components present in the sample. Its reliability, checked by elaboration of HPLC-MS/MS analysis of a series of plasma samples (sets C) spiked with the studied compounds, ranging between 97% and 100% with a max SD of 3%. The obtained MEs values (ME 96% - 106%) demonstrate that the chromatographic set up (short column and fast elution gradient) was proper to avoid the matrix interferences while REs values (RE 88% -

108%) indicate a reliable sample preparation, despite only a protein precipitation was carried out. The calculated accuracy was between 92 and 108% while precision was evaluated below 13% confirming the adequacy of the method in the determination of these new P-gp/CA hybrid inhibitors in degradation samples. Finally, the general procedure proposed was found adequate to study a series of isomer compounds without their chromatographic separation but applying and developing the MS/MS features. For this purpose, the LEDA post-processing algorithm was introduced to allow the use of sole and simple chromatographic conditions, that leads to an increased productivity without losing determination specificity.

3.5. FURTHER APPLICATIONS

Considering the high performance obtained from LEDA algorithm it was decided to apply it in a new work that was just published [35]. Specifically, it was decided to evaluate the activity of hydrolytic human plasma enzymes towards the simultaneous presence of two possible substrate compounds to see if, when they are together, there are any interferences phenomena. In order to achieve this, it was evaluated the stability of two pair of positional isomers spiked in human plasma in couple or alone. The structure of these four compounds in study are reported in Figure 3.37.

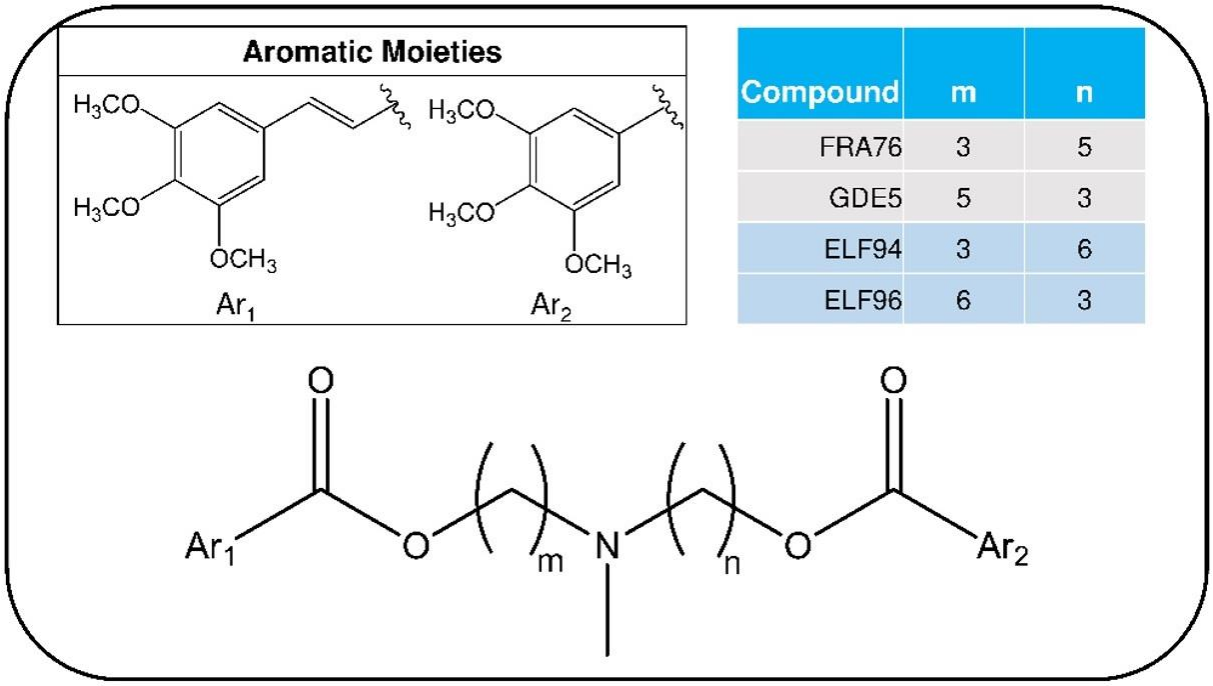

Compound	m	n
FRA76	3	5
GDE5	5	3
ELF94	3	6
ELF96	6	3

Figure 3.37: structures of the compounds involved in the new application of LEDA

As reported in previous LEDA applycation, it was studied the fragmentation energetics of each pure compound performing EMRS experiments and CID graphs were built (Figures 3.38-3.39).

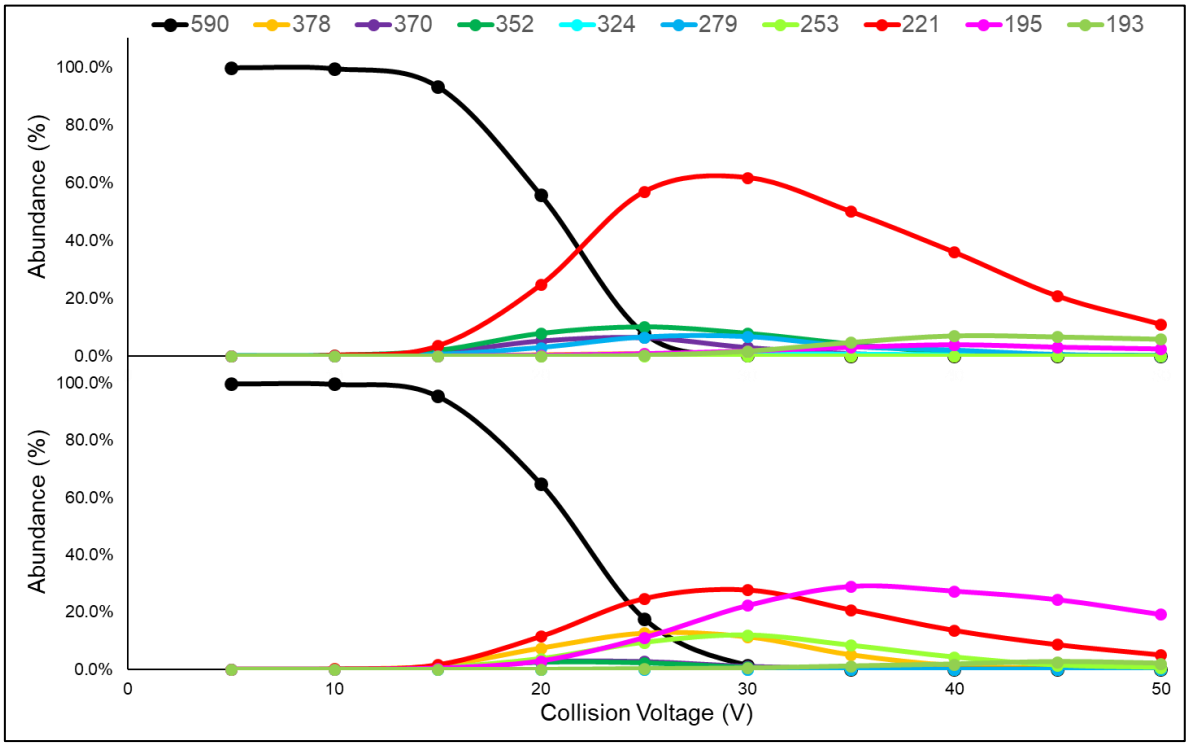

Figure 3.38: CID of FRA76 (up) and GDE5 (down)

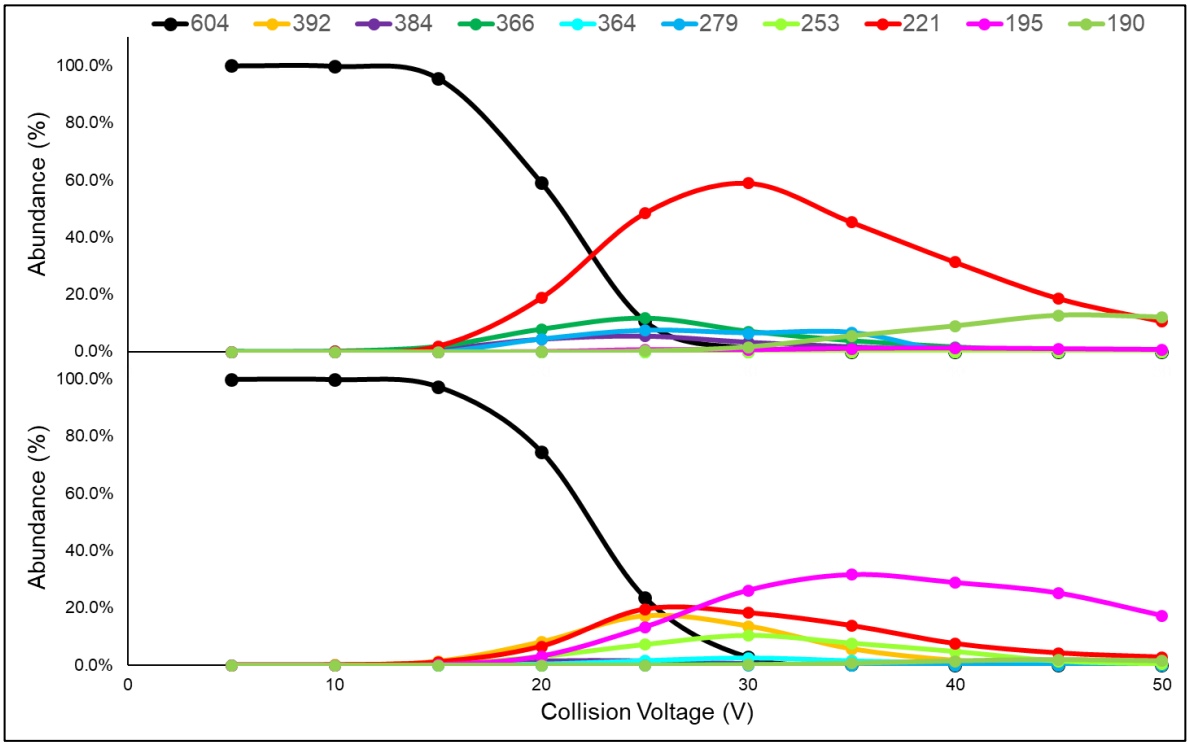

Figure 3.39: CID of ELF94 (up) and ELF96 (down)

Based on the collision breakdown curves of each couple of isomers, six most representative Pis (>10% fragmentation yield) could be selected. Four of these Pis were related to the bond cleavage of the ester groups, following the general scheme proposed in figure 3.40.

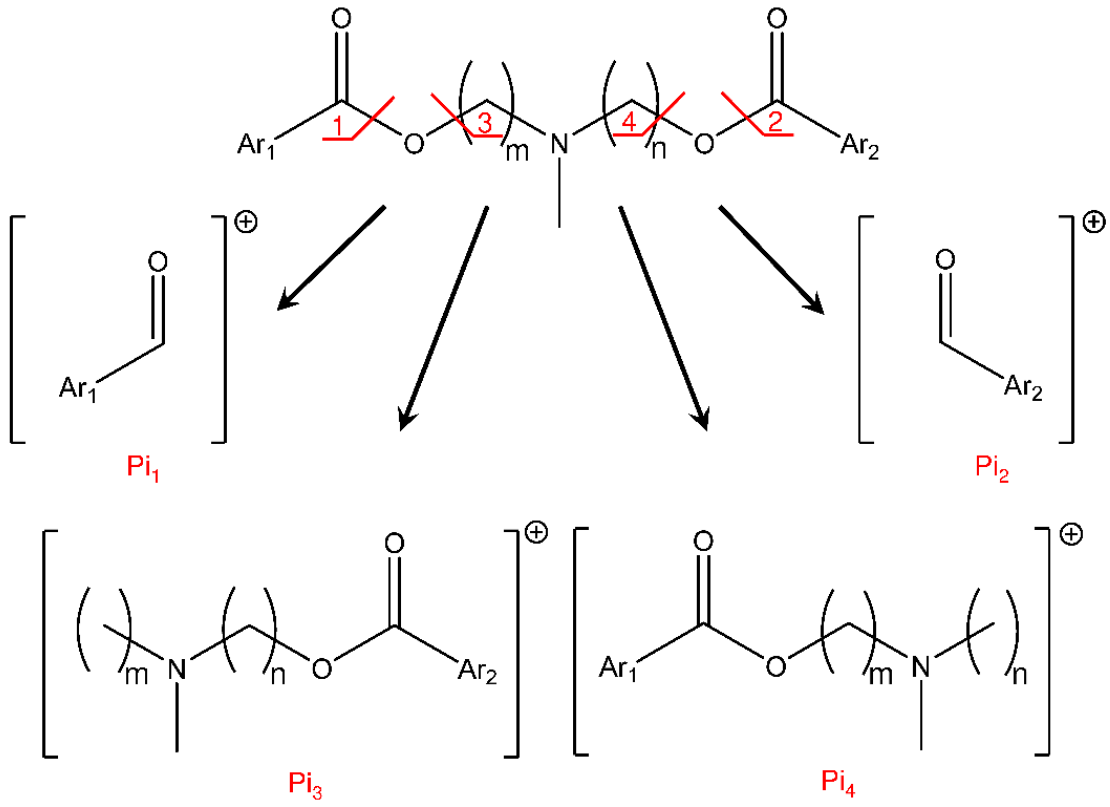

Figure 3.40: common fragmentation pathway proposed for the studied P-gp inhibitors

The MS/MS most intense signals, for all compounds, were obtained by the bond cleavage 1 and/or 2 with the formation of Pi_1 and/or Pi_2 and the corresponding neutral alkyl-alcohol structure. Pi_1 and Pi_2 (*m/z* 221 or 195 respectively) show the same structure regardless the precursor compound, but their maximum abundances are different and characteristic for each isomer (Figure 3.41).

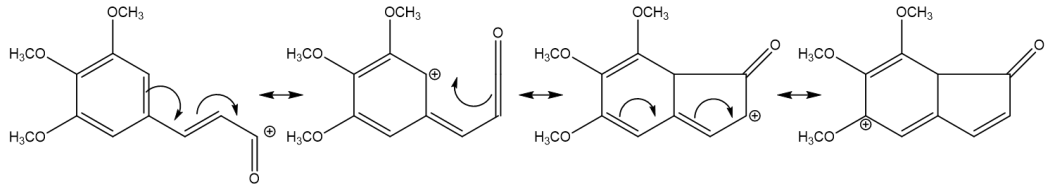

Chemical Formula: $C_{12}H_{13}O_4^+$
Exact Mass: 221.08

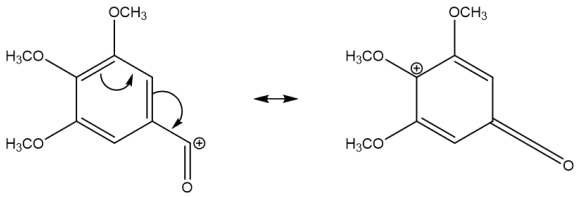

Chemical Formula: $C_{10}H_{11}O_4^+$
Exact Mass: 195.07

Figure 3.41: proposed molecular structure of Pi_1 and Pi_2

On the other hand, it was interesting to note that, the ion structures of the Pi_3 and Pi_4 maintained the information about the differences between the isomers and would have been useful to their distinction. Unfortunately, these Pis show a poor formation yield (< 20%), reducing their isomers recognition ability. Finally, other two Pis were observed (Pi_5 and Pi_6) that can be related to the bond cleavage between the tertiary amine group and the propyl chain linked to the aromatic moiety (Ar_1 or Ar_2), but their formation yield is less than 20% as well. Also in this case, the structures of the ions are the same, regardless the considered isomer, but their relative abundances are different (Figures 3.42-3.43).

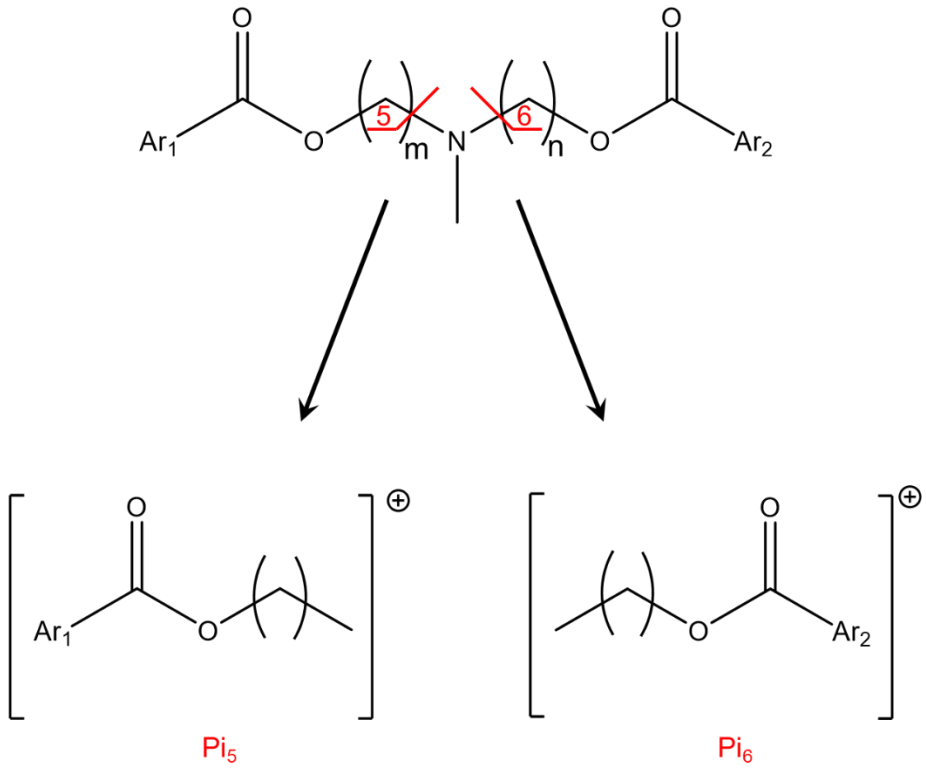

Figure 3.42: fragmentation hypothesis of the studied P-gp inhibitors with formation of Pi_5 and Pi_6

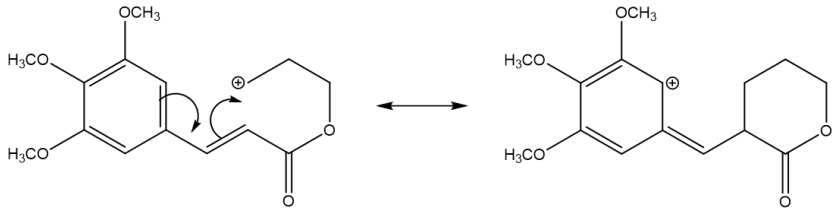

Chemical Formula: $C_{15}H_{19}O_5^+$
Exact Mass: 279.12

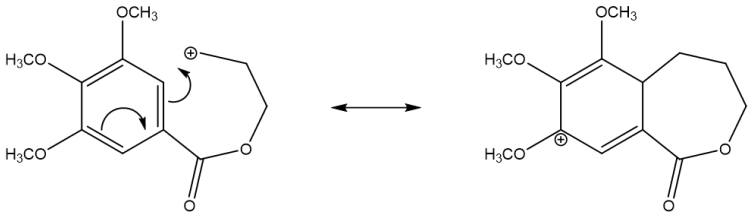

Chemical Formula: $C_{13}H_{17}O_5^+$
Exact Mass: 253.11

Figure 3.43: proposed molecular structure of Pi_5 and Pi_6

Maintaining the same approach, the employed chromatography method was the same as described in chapter 3.2.1 and the chromatographic profiles obtained for each analyte are reported in Figure 3.44-3.45.

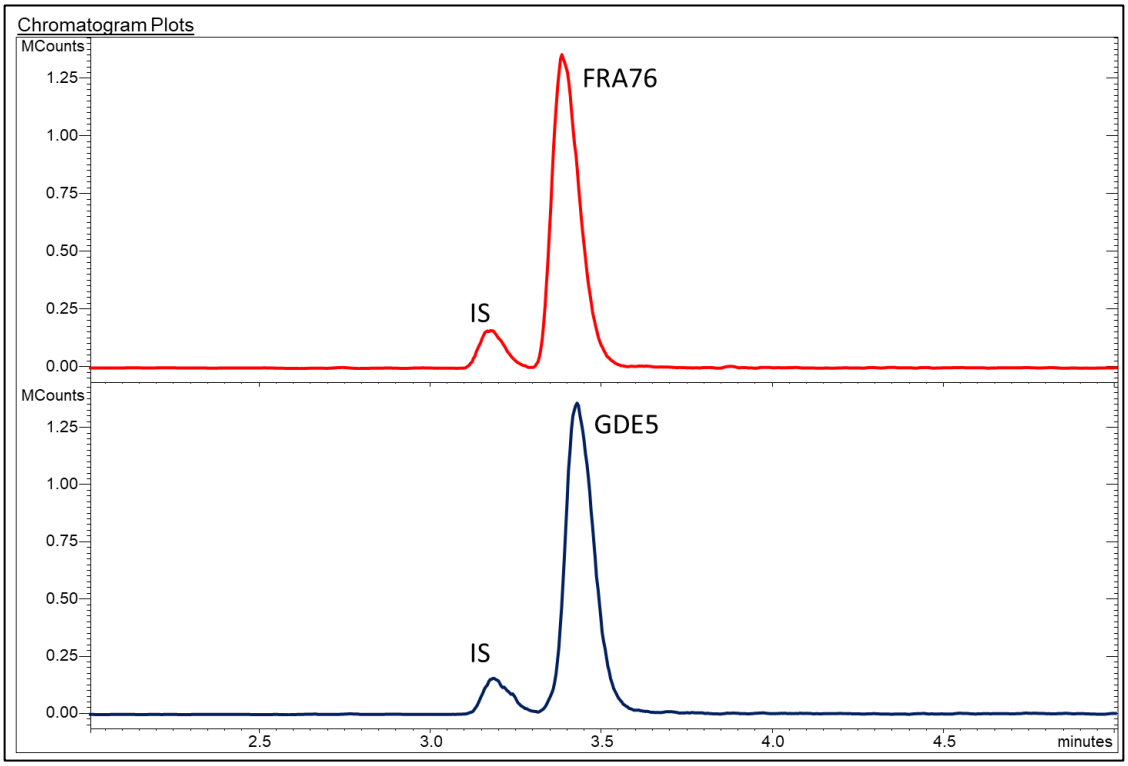

Figure 3.44: chromatographic profile of FRA76 (up) and GDE5 (down)

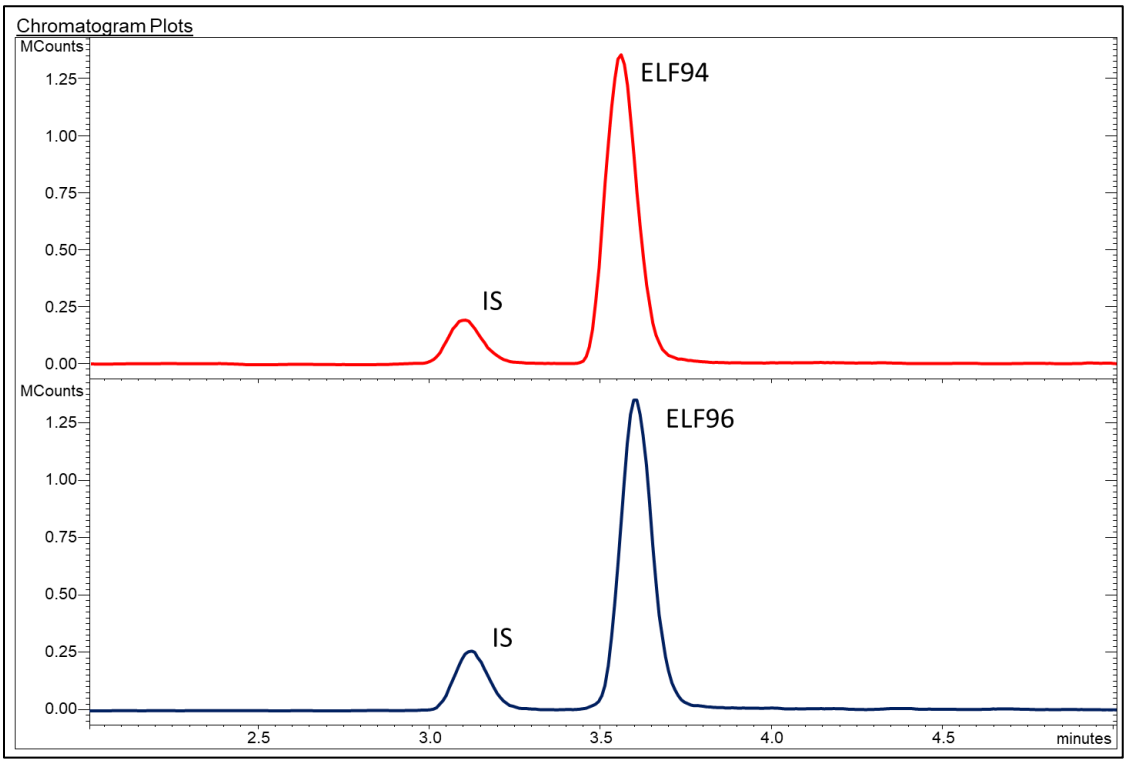

Figure 3.45: chromatographic profile of ELF94 (up) and ELF96 (down)

The obtained chromatographic profiles showed an appropriate distinction between the internal standard (IS) and the analytes, also due to the different characteristic ion transition (MRM signals), but in any case an acceptable separation among the isomers was not reached. The peak parametrs (i.e. retention times, peak width, efficiency, etc.) for each analyte are reported in Table 3.11.

	Rt (min.)	**2 SD (min.)**	**Base Width (min.)**	**2 SD (min.)**	**N**	**RSD (%)**
IS	3.14	0.02	0.18	0.02	4804	10%
FRA76	3.35	0.02	0.19	0.02	4909	8%
GDE5	3.35	0.02	0.20	0.02	4472	7%
ELF94	3.53	0.02	0.19	0.02	5689	10%
ELF96	3.53	0.02	0.19	0.02	5511	9%

Table11: chromatographic paramters such as retention time (Rt)) ± Error (2 standard deviation or 2 SD), base peaks width (Base Width), efficiency (N) and related relative standard deviation (RSD %) for each analyte obtained apply the proposed HPLC-MS/MS approach

Also in this application, the proposed HPLC method achieved a poor efficiency (N ≈ 5000) that cannot distinguish the studied positional isomers; then a dedicated "mathematical devices" must be used to obtain a suitable distinction (analytical specificity) between the tested compounds and ensure their proper monitoring during the degradation experiment.

The sample preparation for the stability test and validation was the same as the one described in chapter 3.2.3. The drug stability test of each compound spiked seperately in human plasma showed interesting results. For each pair of isomers one of the two demonstrated to be stable while its positional isomer showed a degradation (Figures 3.46-3.49).

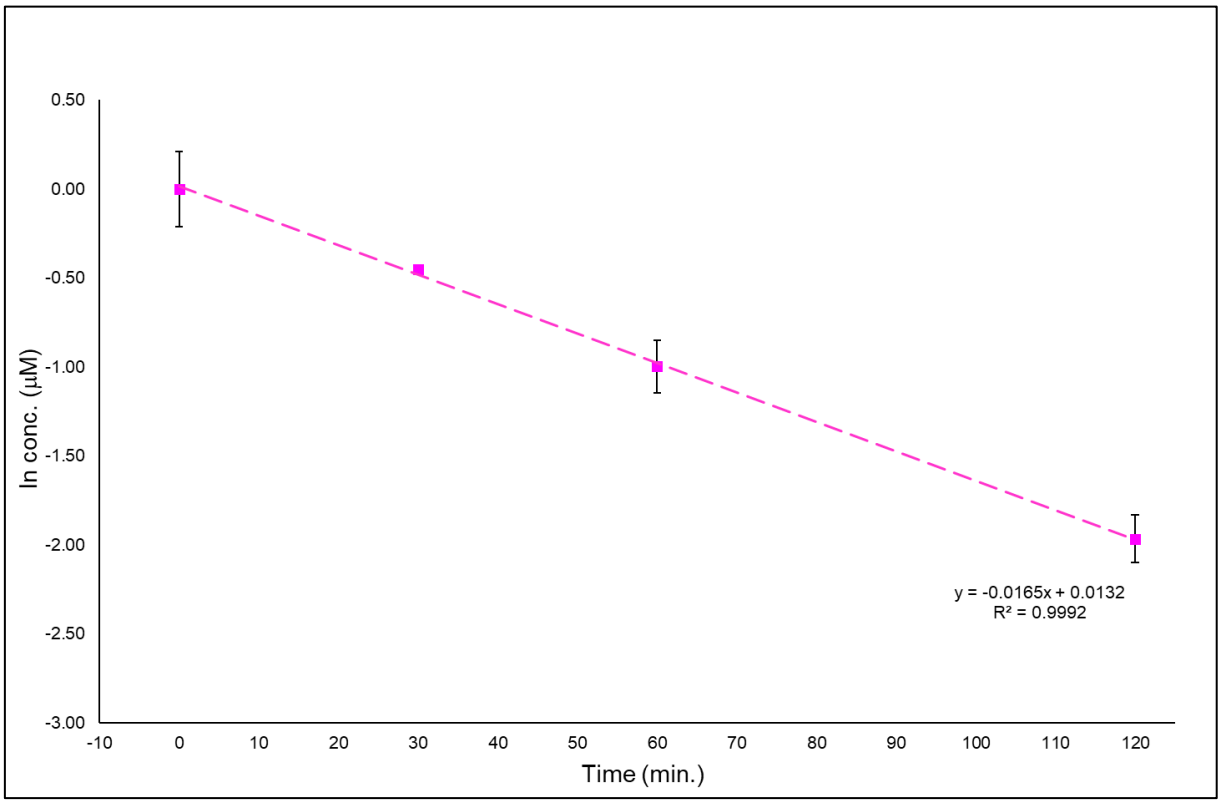

Figure 3.46: degradation plots obtained by conventional quantitative method of the human plasma samples spiked with FRA76 (pink square) isomer.

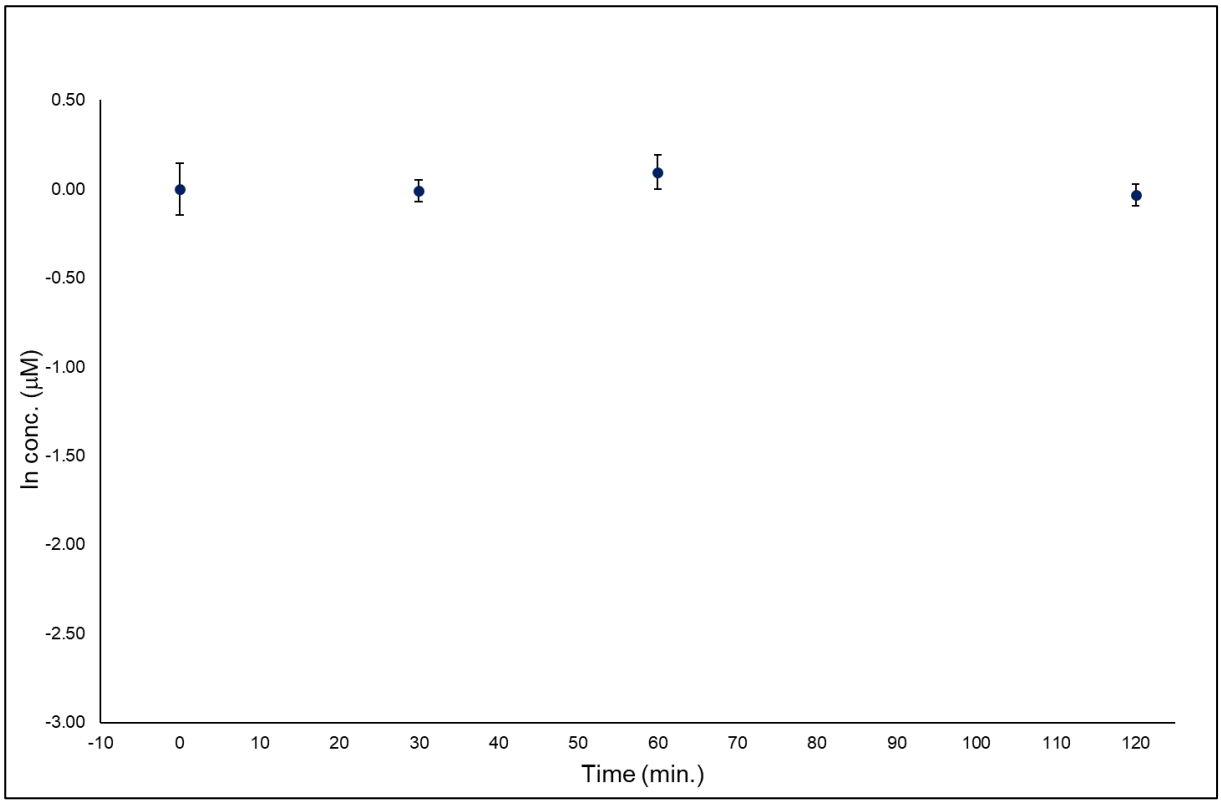

Figure 3.47: degradation plots obtained by conventional quantitative method of the human plasma samples spiked with GDE5 (blue circles) isomer.

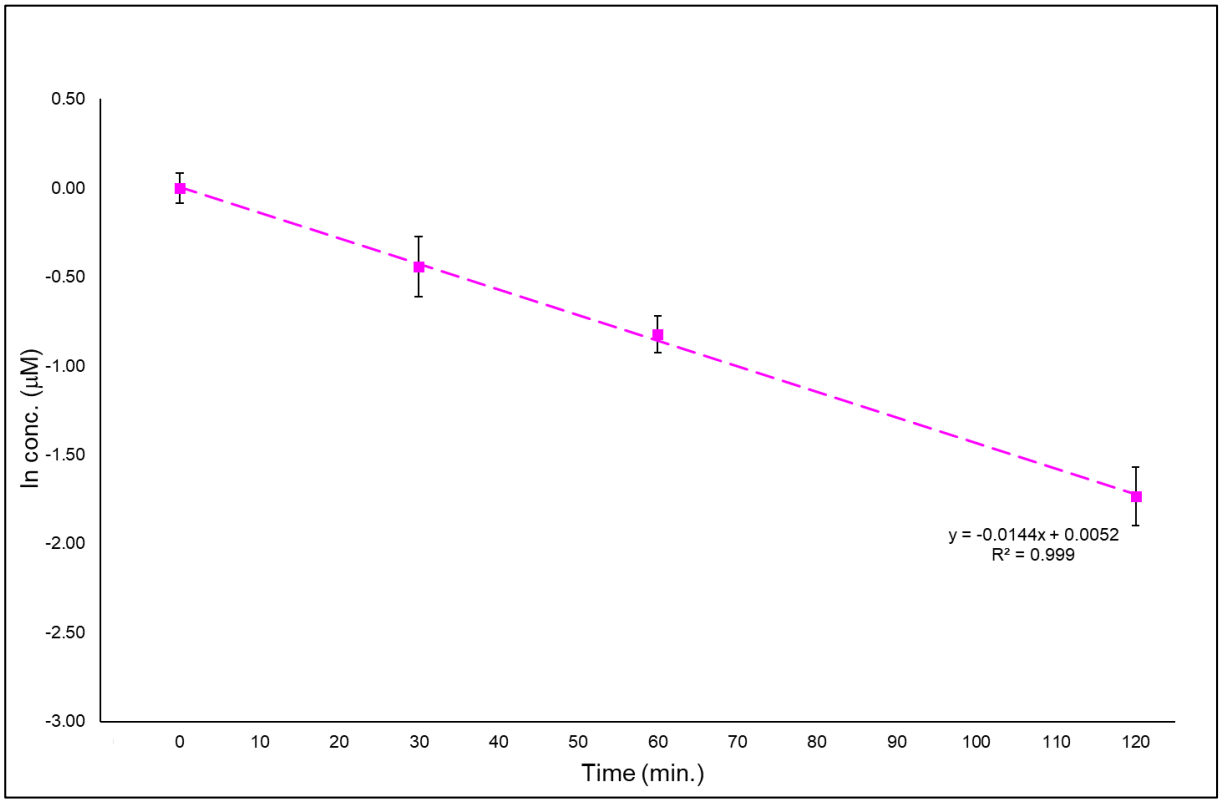

Figure 3.48: degradation plots obtained by conventional quantitative method of the human plasma samples spiked with ELF94 (pink square) isomer.

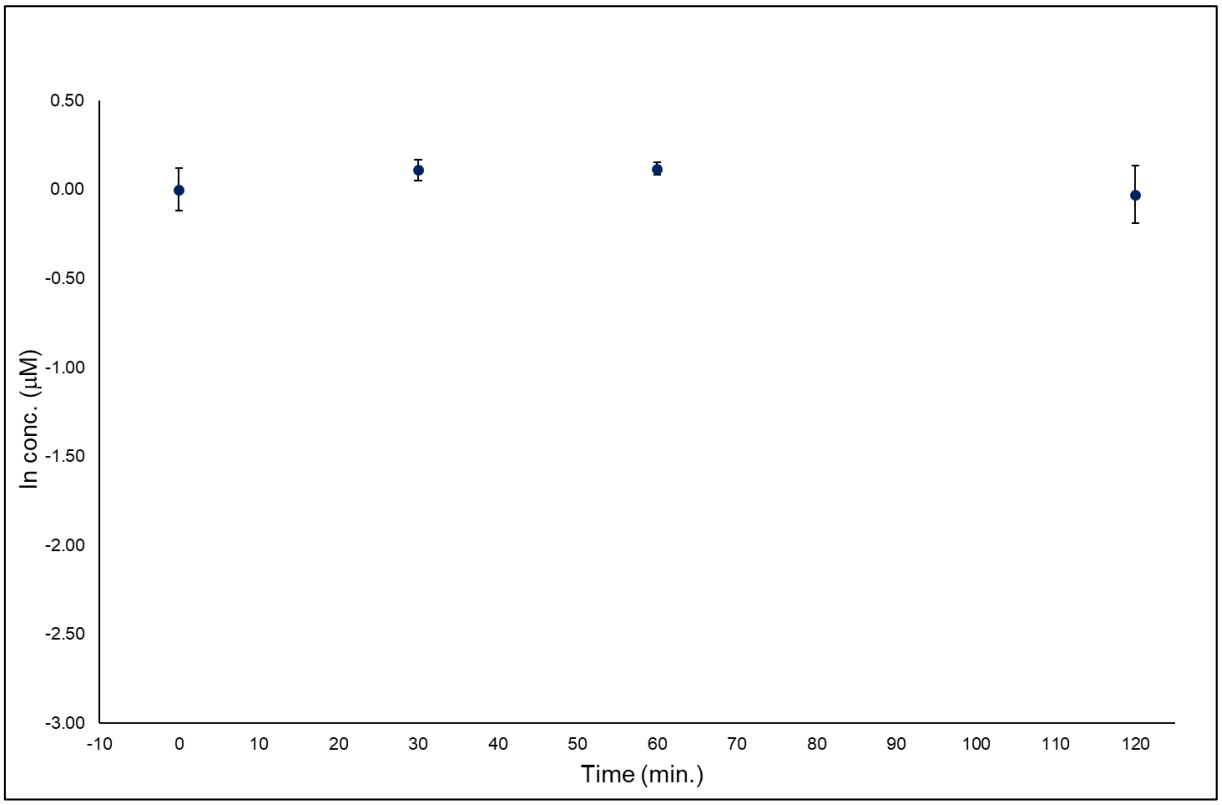

Figure 3.48: degradation plots obtained by conventional quantitative method of the human plasma samples spiked with ELF96 (blue circles) isomer.

Then the drug plasma stability experiment were repeated spiking each pair of isomers togther and, in this case, considering that the coelute we applied the LEDA algorithm to reconstruct the chromatogram so it was possible to integrate each peak represented its analyte. All the results obtained in this drug stability study are reported in Table 3.12.

Compound	**$t_{1/2}$ ± 2SD (min)**	**k ± 2SD (ln(mM)/min)**	**Mix $t_{1/2}$ ± 2SD (ln(mM)/min**	**Mix k ± 2SD (ln(mM)/min**
FRA76	43 ± 16	-0,017 ± 0,001	32 ± 18	-0,019 ± 0,003
GDE5	>240	<0,001	>240	<0,001
ELF94	49 ± 18	-0,014 ± 0,001	34 ± 14	-0,023 ± 0,005
ELF96	>240	<0,001	>240	<0,001

Table 3.12: half time values obtained from testing each analyte separately vs in mixture

The obtained results confirmed the hydrolysis of substrate-isomer (FRA76 and ELF94) by plasma enzymes, while the concentration of stable isomer (GDE5 and ELF96) remained constant in all sample sets tested (Figures 3.50 and 3.51).

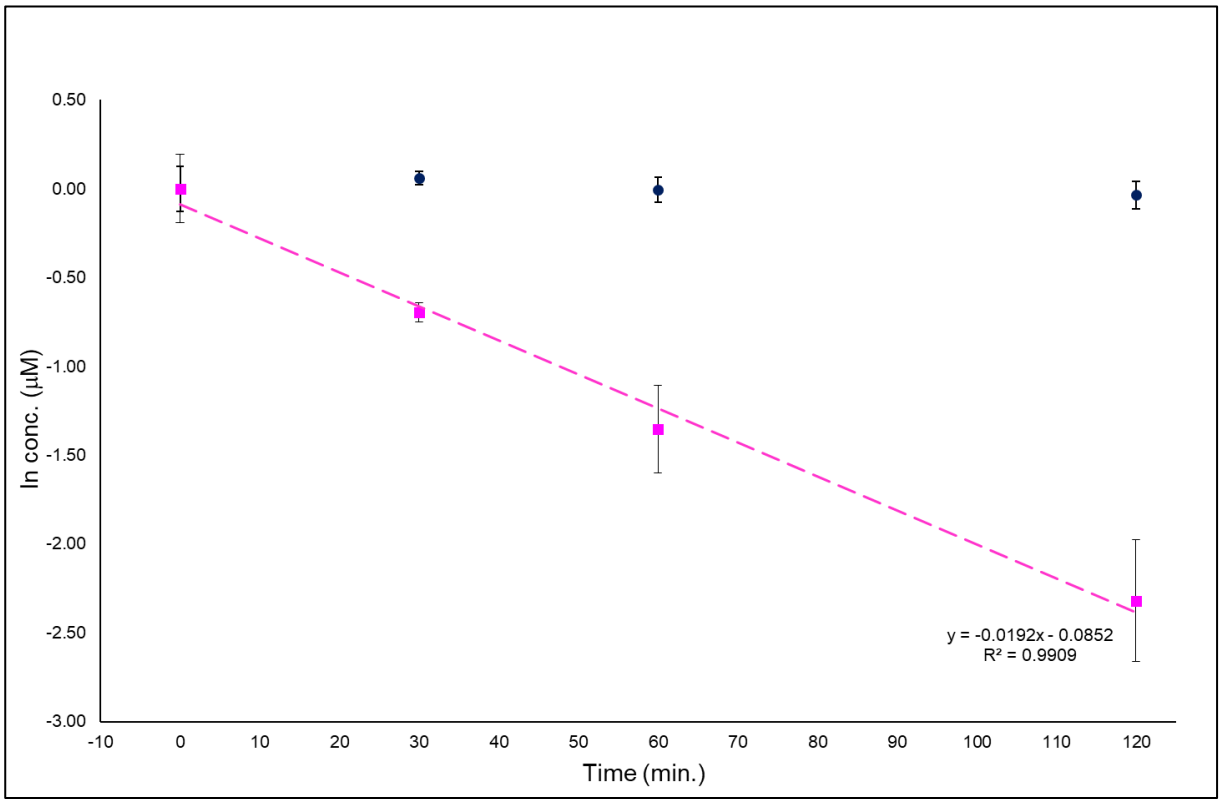

Figure 3.50: degradation plots obtained by LEDA elaboration of the human plasma samples spiked with mixtures of FRA76 (pink square) and GDE5 (blue circles)

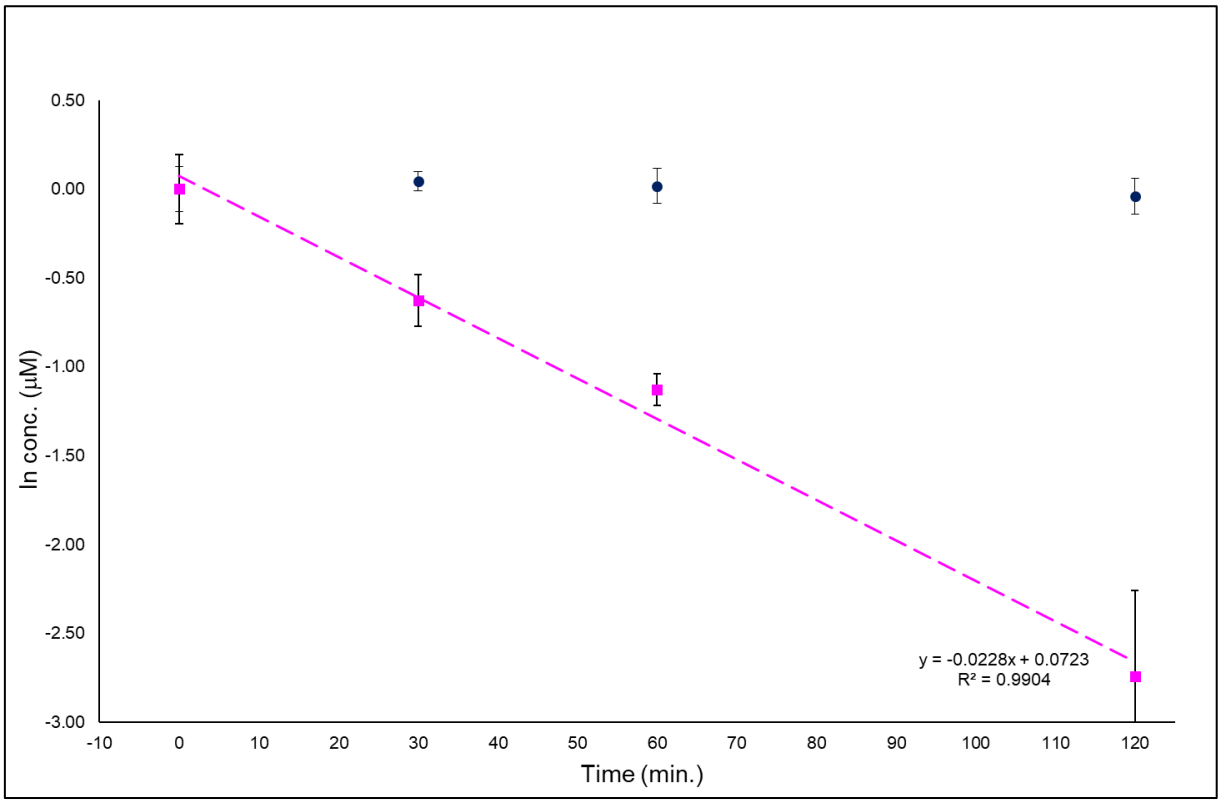

Figure 3.51: degradation plots obtained by LEDA elaboration of the human plasma samples spiked with mixtures of ELF94 (pink square) and ELF96 (blue circles)

The comparison of the degradation parameters ($t_{1/2}$ and k values) reported in Table 3.12 highlights some differences between the absolute values of the data obtained from the sets of samples (i.e. FRA76 $t_{1/2}$ 43 and 32 min.), but these differences are statistically non-significant (considering the error values, the confidence range of the measurements overlaps).

To verify the efficiency of the LEDA algorithm, the set of plasma samples spiked with an equimolar mixture of isomers was processed by 'scan-by-scan' method, allowing the graphical separation of the isomers present in the chromatographic profiles. In this case, the computation of the LEDA matrix was repeated on each MS/MS data point acquired; consequently, a relative abundance of the Ri signal for each isomer was assigned. By considering a generic chromatographic profile, the performance of the algorithm was appreciated in the deconvolution of unresolved peak of Ri signal that delivered its abundance between the isomers (LEDA reconstructed chromatographic profiles). In Figure 3.52, an example of LEDA reconstructed chromatographic profiles of the human plasma sample spiked with the mixture of ELF94-ELF96 isomers at the incubation time of 0 minutes was shown.

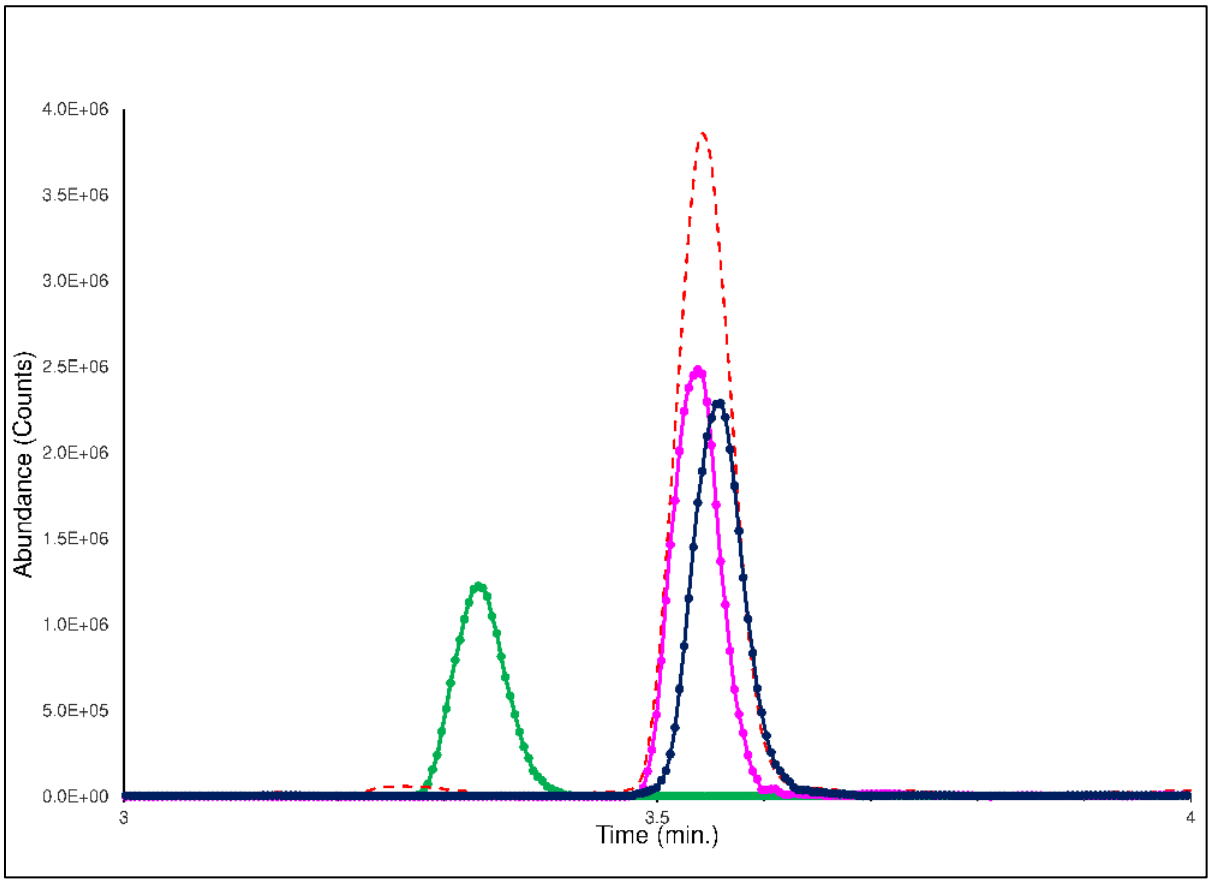

Figure 3.52: The LEDA reconstructed chromatographic profiles of the human plasma sample spiked with the mixture of ELF94 (pink line) and ELF96 (blue line) isomers at the incubation time 0 minutes. The IS (green line) and Ri (red dotted line) signals were also reported.

In Figure 3.42, the reconstructed profiles showed an equal abundance of the isomers in the Ri signal, as of the mixture solution added, verifying that at the incubation time 0 minutes the plasma enzymes did not work. Increasing the incubation times, the reconstructed profiles of substrate-isomer (in case ELF94) reported a decrease of the peak intensity, while the peak of the stable isomer (in case ELF96) maintained the same abundance (Figure 3.53-3.55).

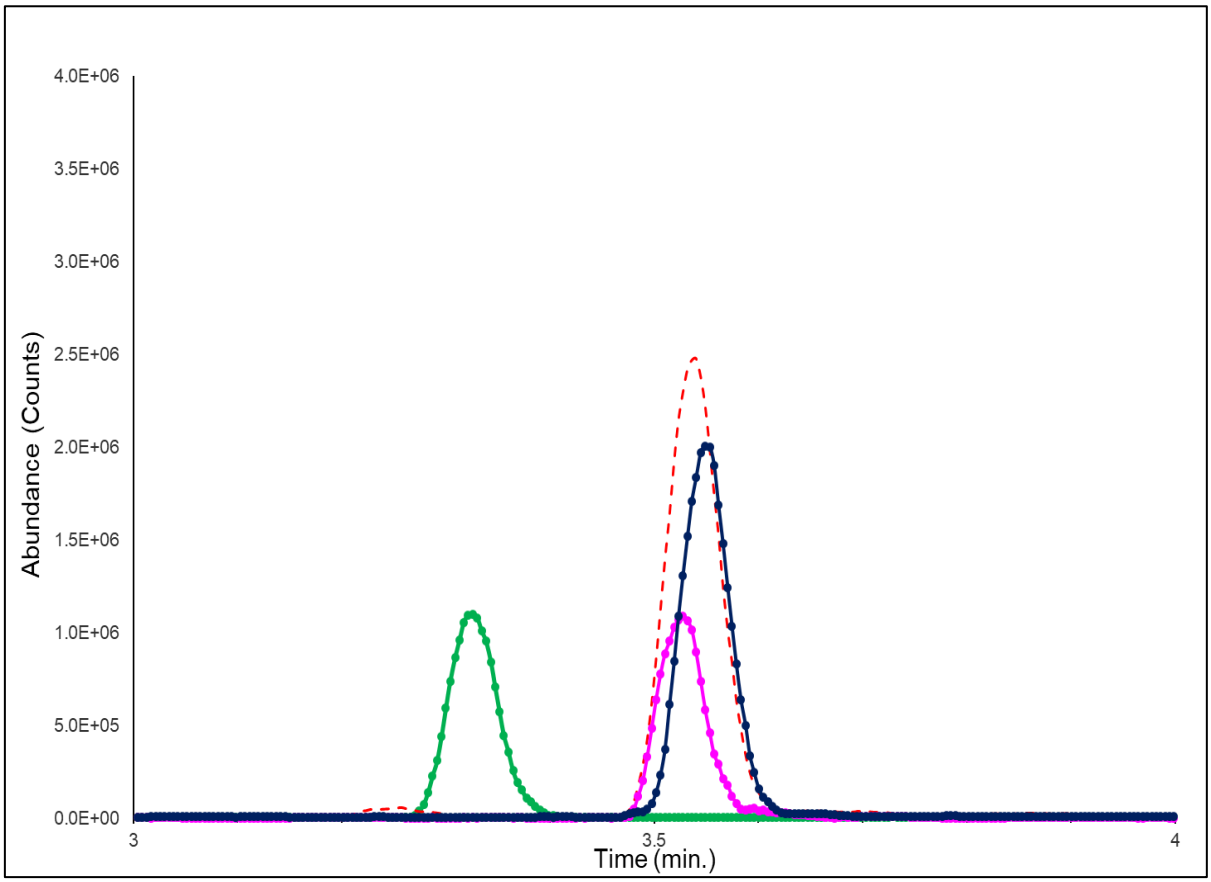

Figure 3.53: The LEDA reconstructed chromatographic profiles of the human plasma sample spiked with the mixture of ELF94 (pink line) and ELF96 (blue line) isomers at the incubation time 30 minutes. The IS (green line) and Ri (red dotted line) signals were also reported.

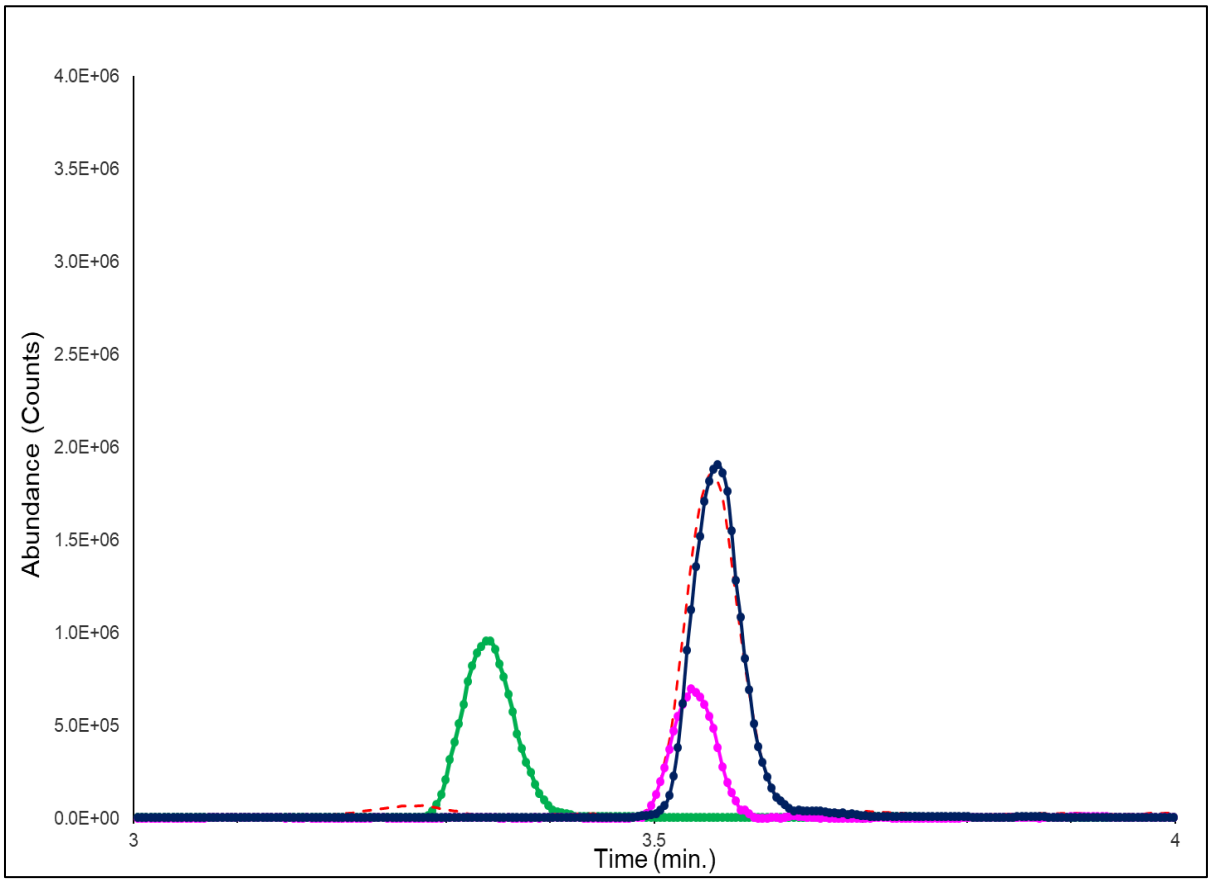

Figure 3.54: The LEDA reconstructed chromatographic profiles of the human plasma sample spiked with the mixture of ELF94 (pink line) and ELF96 (blue line) isomers at the incubation time 60 minutes. The IS (green line) and Ri (red dotted line) signals were also reported.

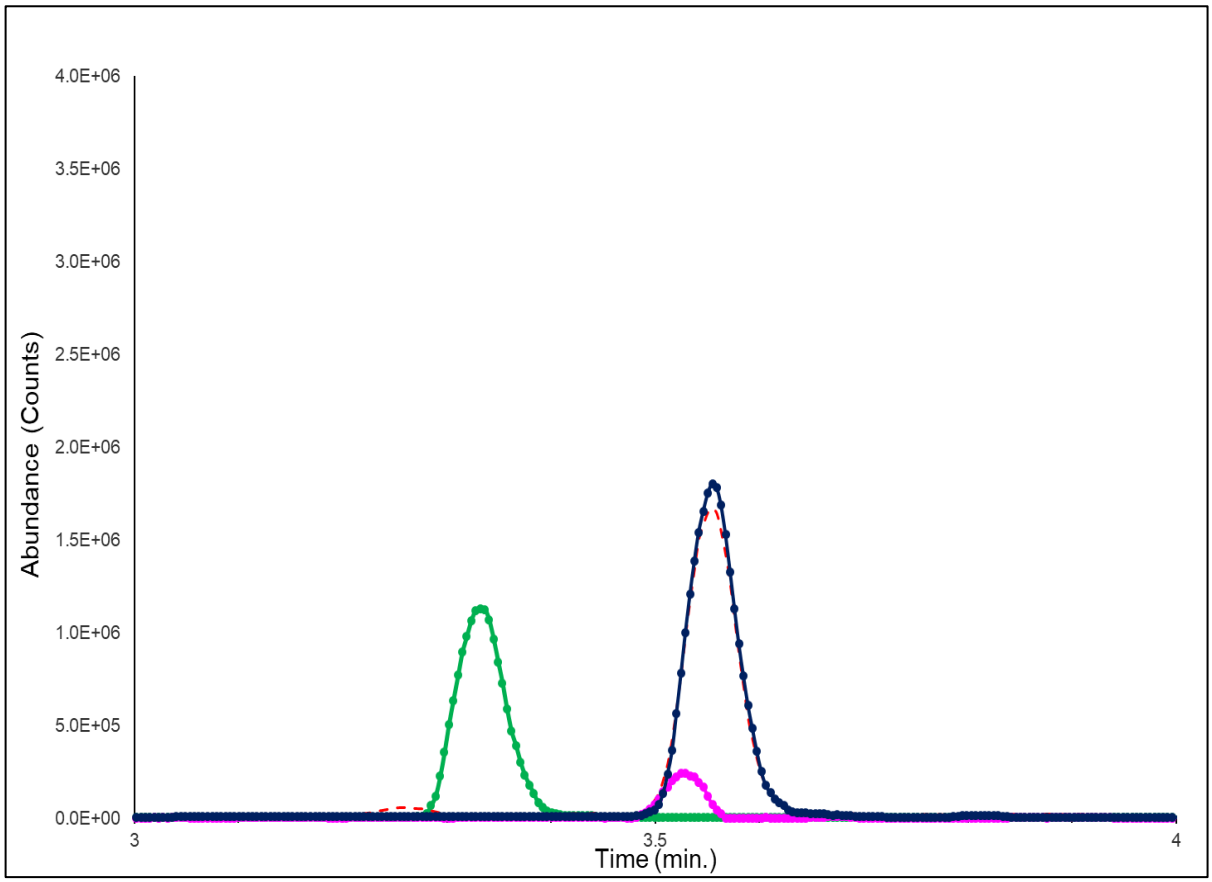

Figure 3.55: The LEDA reconstructed chromatographic profiles of the human plasma sample spiked with the mixture of ELF94 (pink line) and ELF96 (blue line) isomers at the incubation time 60 minutes. The IS (green line) and Ri (red dotted line) signals were also reported.

Therefore, the LEDA 'scan-by-scan' processing method confirmed the data obtained in previous elaboration (peak area integration) and demonstrated its reliability by distinguishing the abundance of each isomer present in the unresolved Ri signal. The LEDA reconstructed chromatographic profiles of FRA76 and GDE5 were reported in Figure 3.56-3.59.

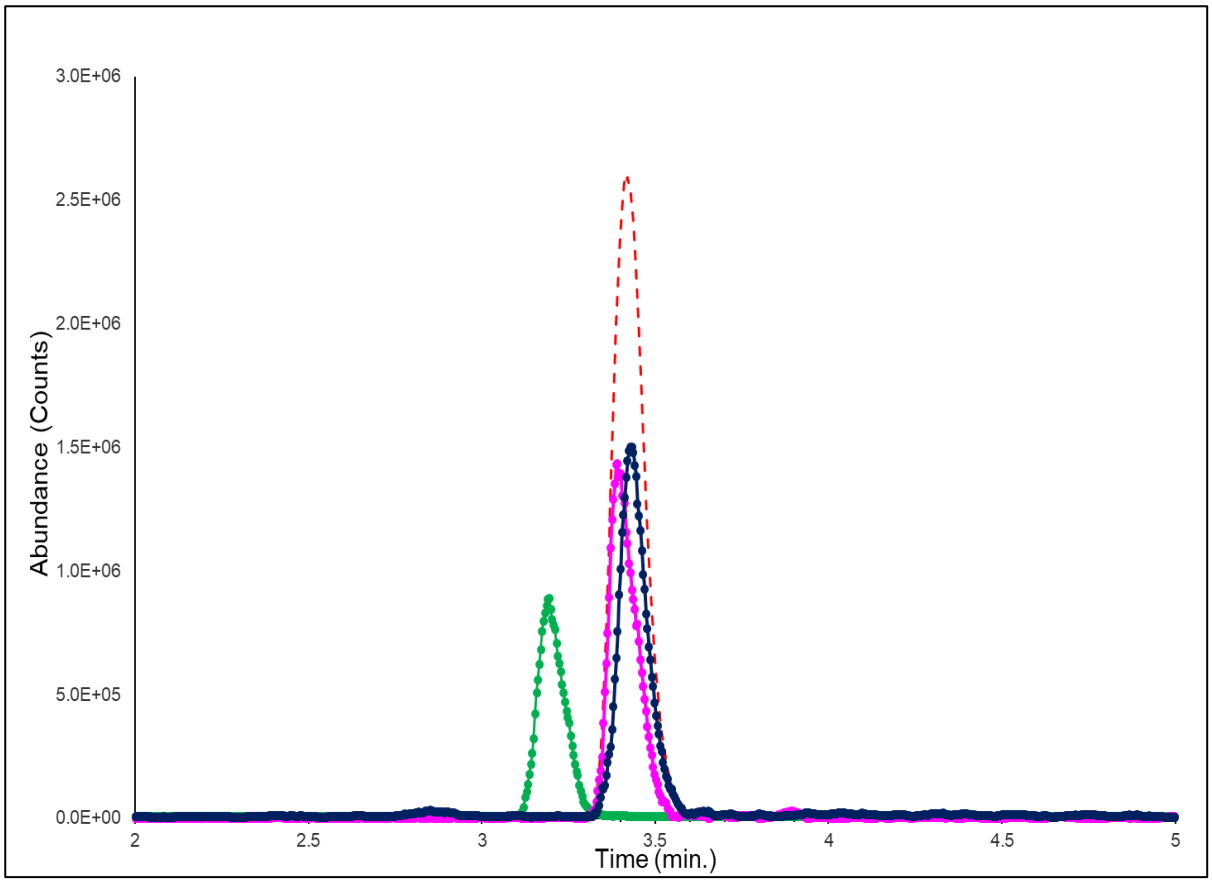

Figure 3.56: The LEDA reconstructed chromatographic profiles of the human plasma sample spiked with the mixture of FRA76 (pink line) and GDE5 (blu line) isomers at incubation time 0 minutes. The IS (green line) and Ri (red dotted line) signals were also reported.

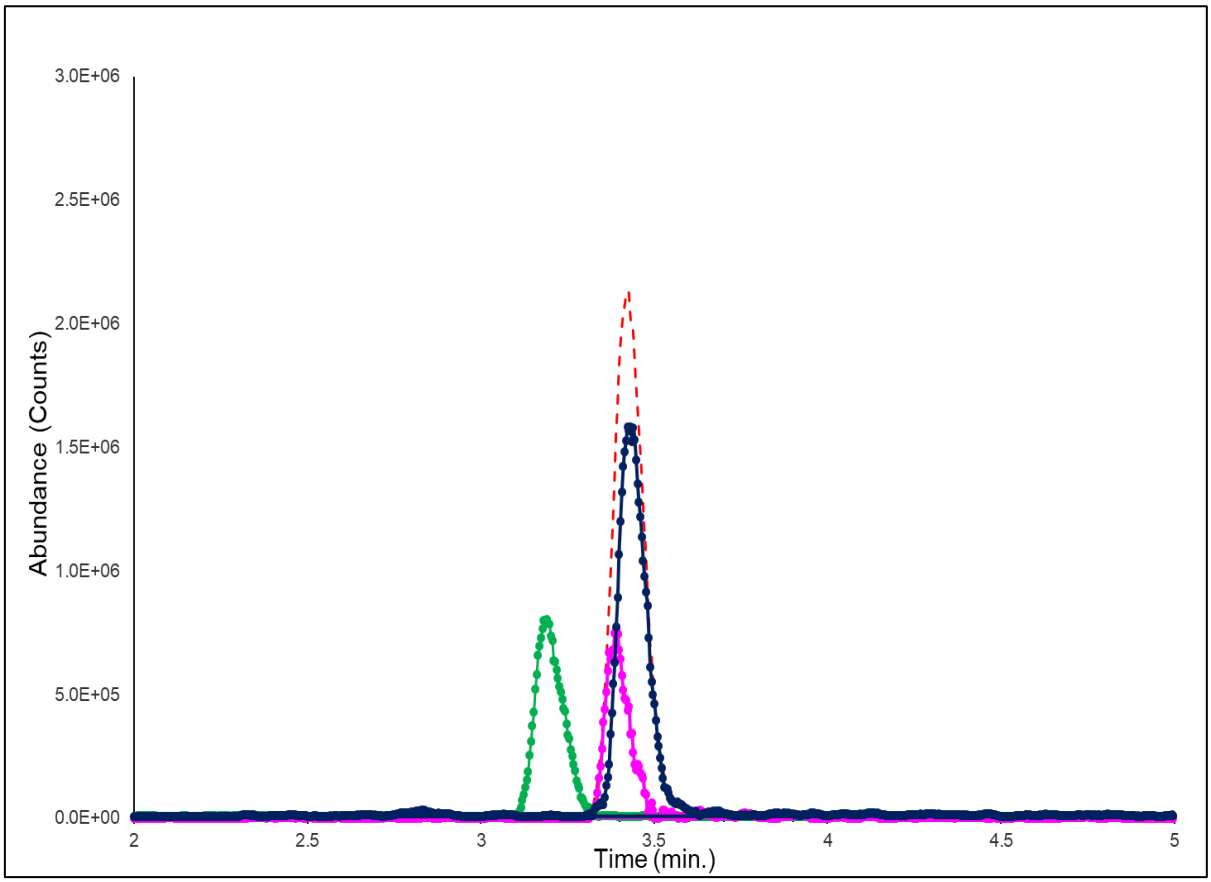

Figure 3.57: The LEDA reconstructed chromatographic profiles of the human plasma sample spiked with the mixture of FRA76 (pink line) and GDE5 (blu line) isomers at incubation time 30 minutes. The IS (green line) and Ri (red dotted line) signals were also reported.

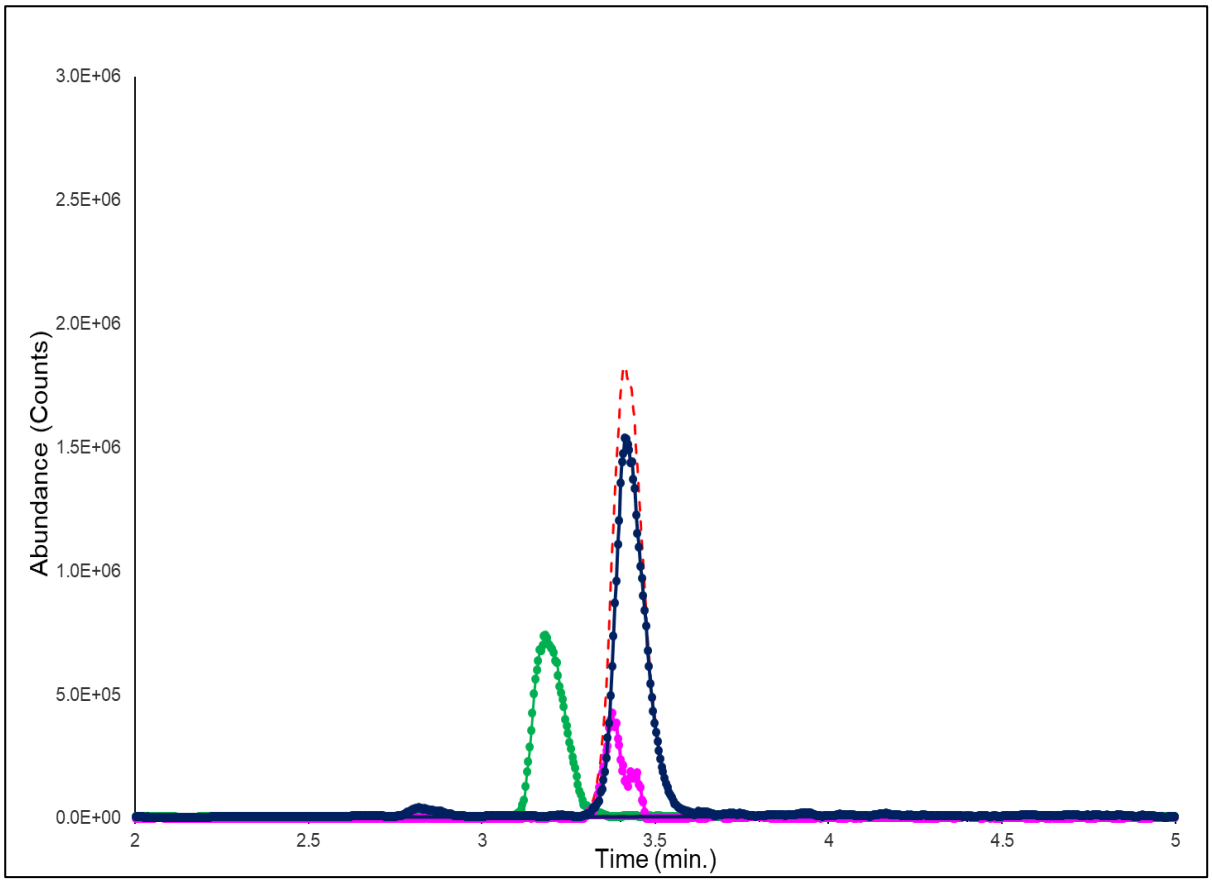

Figure 3.58: The LEDA reconstructed chromatographic profiles of the human plasma sample spiked with the mixture of FRA76 (pink line) and GDE5 (blu line) isomers at incubation time 60 minutes. The IS (green line) and Ri (red dotted line) signals were also reported.

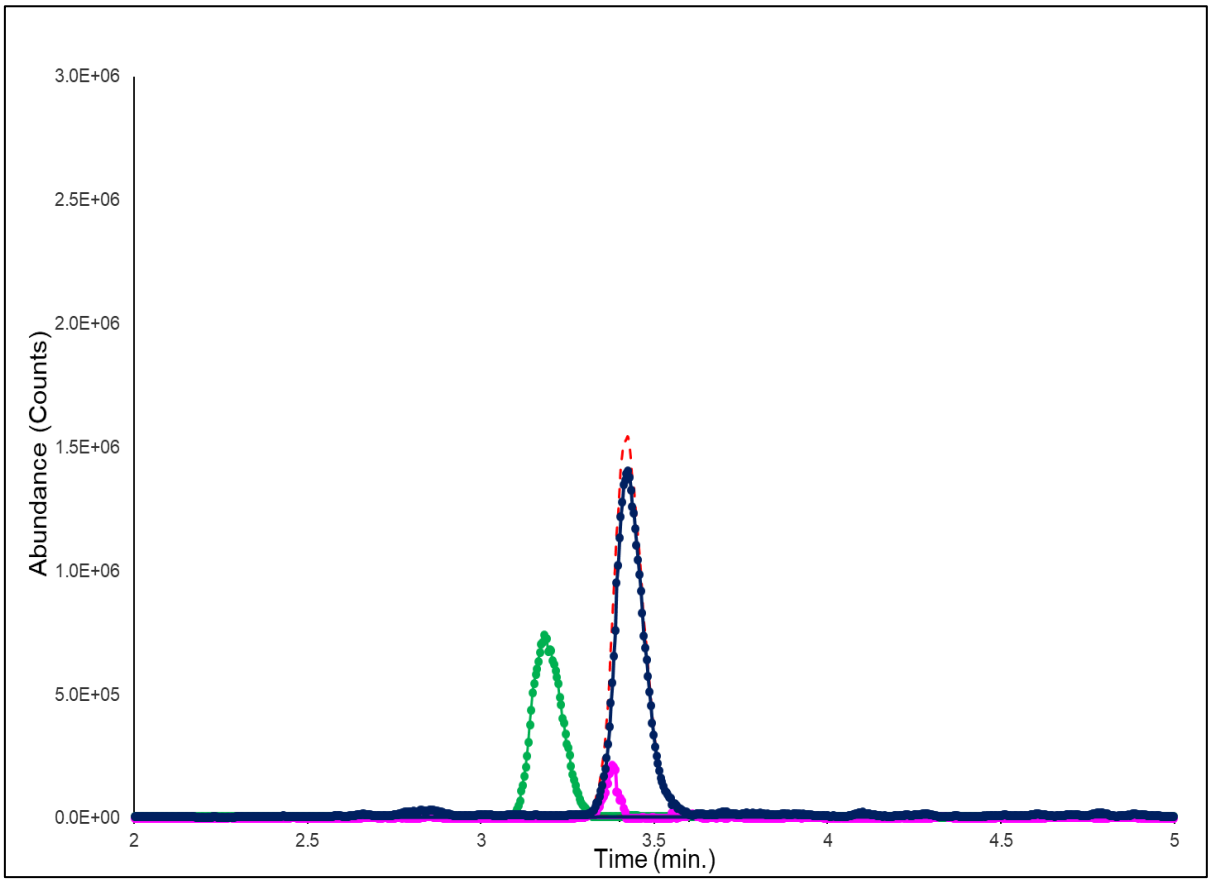

Figure 3.59: The LEDA reconstructed chromatographic profiles of the human plasma sample spiked with the mixture of FRA76 (pink line) and GDE5 (blu line) isomers at incubation time 120 minutes. The IS (green line) and Ri (red dotted line) signals were also reported.

In the proposed HPLC-MS/MS approach, the use of mathematical algorithm (LEDA) solves and separates the MS/MS spectra from the unresolved chromatographic peak of a pair of isomers. The development of LEDA involved an investigation on the energetics of fragmentation pathway allowed to select the better product ion for each analyte in terms of both sensitivity of detection and specificity, i.e. the capability to distinguish between isomeric compounds. Noteworthy that the choice of characteristic product ions and optimal abundance ratios plays an important role for the application of LEDA approach to a multi-component mixture analysis. The developed method was applied in a human plasma drug stability study of two couple of isomers to verify its effectiveness. The obtained results confirm the ability of LEDA approach to distinguish the isomers allowing the evaluation of their behavior in plasma samples. It is to emphasize that the investigation was carried out with a conventional HPLC-MS/MS system, without using expensive ultra-efficient chromatography systems or ancillary MS techniques (i.e. MS ion mobility). In the proposed approach, we have explored the

potentiality of MS/MS technique introducing the “energetic dimension” of the experiment, which proved to be fruitfully employed to solve MS problems in the isomers’ recognition.

4. PROJECT 2: DEVELOPMENT OF AN ID/GC-MS METHOD FOR THE QUANTITATIVE EVALUATION OF FATTY ACIDS IN PLASMA TO CONFRONT HEALTHY PATIENTS AND COLORECTAL CANCER PATIENTS

The goal of this project is to develop an analytical method to determine the quantity of free fatty acids (FFAs) in human plasma in order to study the differences between healthy patients and colorectal cancer patients. Several methods have been developed for previous studies but most of them can only determine the short-chain fatty acids (SCFAs), a product of the metabolism of the symbiotic gut microbiota and the host but recently it was also highlighted that in some gastrointestinal diseases the levels of octanoic and decanoic acids (medium-chain fatty acids MCFA) can change. For these reasons, a method that can determine both SCFAs and MCFAs could be useful to study possible interconnection between microbiota and metabolic alterations during hosts' disease. Considering the volatile properties of this compounds and the importance to obtain a high sensitivity, accuracy and precision from the method it was decided to develop an isotopic dilution gas-chromatography coupled mass spectrometry (ID/GC-MS).

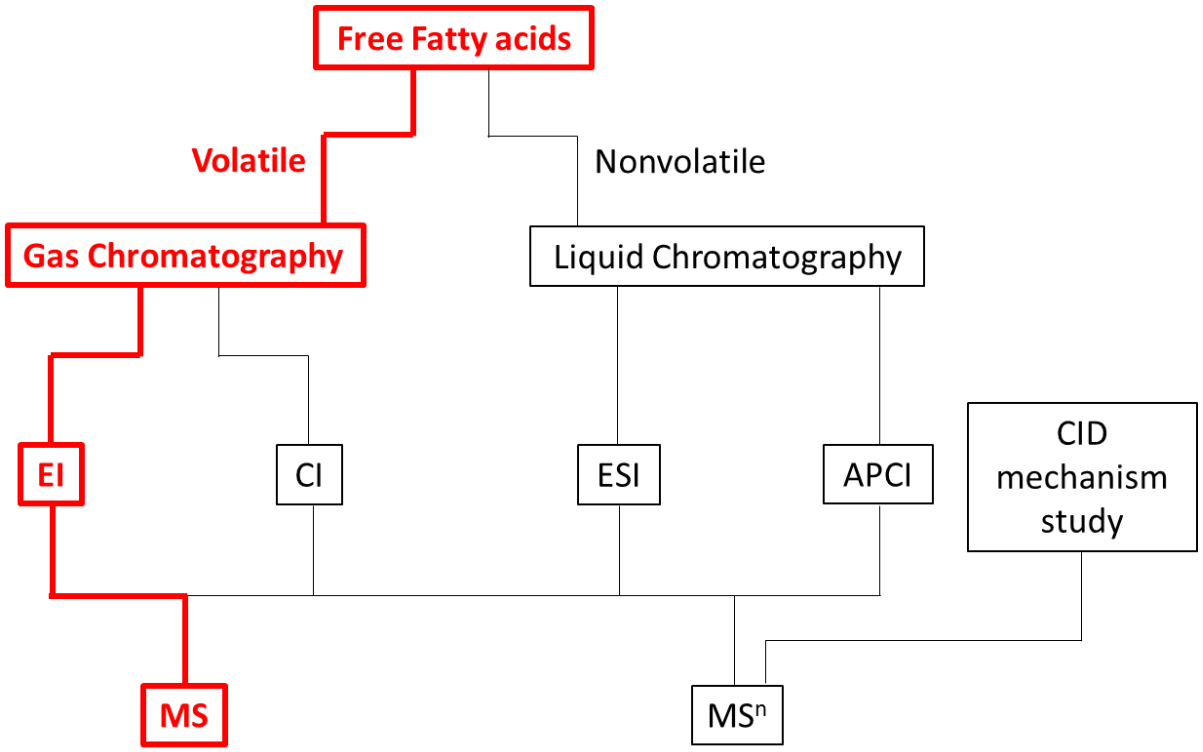

Figure 4.1: scheme of the system employed for Project 2

It was also decided to extend the panel of the analyte from C2 to C18, then SCFAs, MSFAs and Long Chain Fatty Acids (LCFAs). To minimize sample manipulation procedures, an efficient, sensible and low time-consuming procedure was developed, which relies in a simple liquid-liquid extraction before the determination of underivatized free acids (FFAs) by Single Ion Monitoring (SIM) acquisition. The proposed ID/GC-MS method was applied in a case study to evaluate the FFAs as specific markers for both microbiota and host alterations in CRC patients. Obtained results highlight the advantage of present method for its rapidity, simplicity, and robustness [36].

4.1. INTRODUCTION

A substantial body of evidence supports that the gut microbiota (GM) plays a pivotal role in the regulation of several metabolic, endocrine and immune functions of the host and its dysbiosis has been closely associated with several localized and systemic diseases[37]. Interestingly, one way by which the GM interact with the host physiology is the production of metabolites and, to date, short-chain fatty acids (SCFAs), are the main end-products obtained by the microbial fermentation of dietary fibers and resistant starch that exerts important effects on host health and disease[38]. In detail, SCFAs, which are constituted of 2 to 6 carbons exert their functions mainly through the inhibition of histone deacetylases (HDACs) and the activation of G-protein-coupled receptors (GPCRs). Since HDACs regulate gene expression, their inhibition has a vast array of downstream consequences while GPCRs activated by SCFAs are involved in the regulation of metabolism, cell proliferation and function and immune processes[39]. In the last years, different studies have documented an alteration in SCFAs' composition in multiple human pathologies, such as intestinal bowel disease (IBD)[40], irritable bowel, syndrome [41], and colorectal cancer [42]. Therefore, SCFAs represent a novel target to measure intestinal health and they have been proposed as potential diagnostic biomarkers because of their fast, reliable and cheap evaluation in stool samples.

Considering that SCFAs can cross the intestinal epithelium and enter systemic circulation [43], many research recently focused on the qualitative and quantitative evaluation of plasmatic free fatty acids (FFAs) that, in addition to SCFAs, they comprised medium chain fatty acids (MCFAs) and long chain fatty acids (LCFAs) and are generally encountered in the diet are important regulators of energy metabolism, gene expression, ion channels and pump activities and immune processes[44, 45]. In particular, altered levels of plasma FFAs have been associated with Crohn's disease, autoimmune disorders, and various types of cancer and so they currently

represent important systemic biomarkers for screening of different human pathologic conditions [46].

Fatty Acids (FAs) are a class of organic compounds, characterized by a hydrophilic group (the carboxylic acid) and a lipophilic one (aliphatic chain).

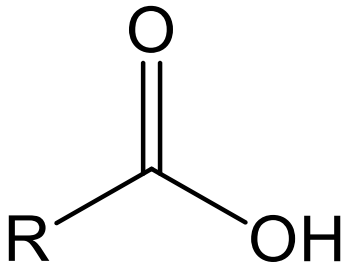

Figure 4.2: general structure of fatty acids

There are many ways to classify for this kind of compounds but for the sake of this project it will be used the classification by the number of carbons in the tail. In fact, this classification divides these molecules in short-chain fatty acids (SCFAs, < 6 C), medium-chain fatty acids (MCFAs, C6-C12) and long-chain fatty acids (LCFAs, > C12). By Free Fatty Acids (FFAs), instead, represent the fatty acids in plasma (but also in the feces) that are not bound with other compounds. As a matter of fact, they are usually bound to serum albumin and function as substrates for β-oxidation, take part to signaling events, and modulate host energy metabolism and inflammatory response. Furthermore, SCFAs are produced by gut microbial fermentation from unabsorbed/undigested food components in the small intestine, while MCFA and LCFA generally came from the diet [47]. Among the SCFA produced by gut microbiota into large bowel, acetic acid (C2), propionic acid (C3), and butyric acid (C4) are the most abundant ones, representing around 90–95% of total SCFAs in colon lumen. Acetate and butyrate may be converted to acetyl-CoA and used to form lipids and ketone bodies or may also enter the citric acid cycle and become utilized for glucose production via gluconeogenesis. SCFAs act also as an important molecular signal between the microbiota and the host [48]. Recently, it was also discovered that receptors expressed at the surface of gut epithelial cells, adipocytes, enteroendocrine L-cells, innate immune cells, and neurons, have been discovered across for which short chain fatty acids SCFAs appear to be the natural ligands [49]. While acid acetic can pass through into the peripheral circulation, butyric acid is the preferred fuel utilized by coloncytes and the primary site of butyrate sequestration in the body is the gut epithelium. Butyrate seems to have a dual role, referred in literature as “butyrate paradox”. In fact, it induces

proliferation in healthy colonocytes but terminal differentiation and apoptosis in transformed cells [50]. These interesting results produced several studies to highlight changes in FFAs in different pathologies respect to healthy individuals [51]. Furthermore, recently two studies highlighted the increase of the levels of decanoic acid (C10) in patients with CRC [52, 53]. For these reasons the aim of this project was to develop a sensitive, reliable, and cheap method to determine FFAs (free short, medium, and long chain fatty acids) in human plasma. In literature, few methods to analyze FFAs in HPLC are presented. Metha et al. in 1998 and Nishikiori et al. in 2014 presented two different methods to analyze FFAs employing a liquid chromatography technique[54, 55]. In our laboratory several HPLC was available but for our goal these techniques showed many criticalities. First of all, the panel of analytes of these two methods is restricted only to long chain fatty acids. In fact, analyze short chain fatty acids in HPLC can be tricky due to the difficulty to retain them and also for the high interference that can be found (i.e. acetic acid is commonly as buffer for liquid chromatography).

On the contrary, to achieve our target, it was decided to develop an isotopic dilution gas-chromatography coupled mass spectrometry (ID/GC-MS) method. Furthermore, to minimize the sample preparation, it was decided to perform a simple liquid-liquid extraction. In this way, it is possible to replicate this method in every routine laboratory with a low productive and economic impact.

4.2. MATHERIAL AND METHODS

The experiments were carried out by using an Agilent GC-MS system composed with 5973 single quadrupole mass spectrometer, 6890 gas-chromatograph and 7673 autosampler.

4.2.1. CHEMICALS

Methyl-t-butyl ether or MTBE (Chromasolv grade), sodium chloride (NaCl), potassium chloride (KCl), sodium hydrogen phosphate dihydrate (Na_2HPO_4 2 H_2O), potassium dihydrogen phosphate (KH_2PO_4) and hydrochloric acid (Reagent grade), [$^2H_3$]acetic, [$^2H_3$]propionic, [$^2H_7$]iso-butyric, [$^2H_9$]iso-valeric and [$^2H_{15}$]octanoic, used as isotopologues internal standards (ISs), acetic, propionic, butyric, isobutyric, isovaleric, 2-methylbutyric, valeric, hexanoic, heptanoic, octanoic, nonanoic, decanoic, dodecanoic, tetradecanoic, hexadecanoic and octadecanoic acids (analytical standards grade) were purchased by Sigma-Aldrich (Milan, Italy). MilliQ water 18 MΩ cm was obtained from Millipore's Simplicity

system (Milan, Italy). Phosphate buffer solution (PBS) was prepared in milliQ water by dissolving: 8.01 g L^{-1} of NaCl, 0.2 g L^{-1} of KCl, 1.78 g L^{-1} of Na_2HPO_4 2 H_2O and 0.27 g L^{-1} of KH_2PO_4. Acidic solution, freshly prepared before each analysis session, was obtained by 1:1 (v/v) dilution of 37% hydrochloric acid (density 1.2 g mL^{-1}) with a 1.0 M of NaCl solution.

4.2.2. CHROMATOGRAPHY

The separation of the analytes was achieved by using a DB-FFAP (Agilent J&W) column 30 m length, 0.25 mm internal diameter and 0.25 μm of film thickness. The temperature gradient is reported in following table:

Oven Ramp	°C/min	Next °C	Hold min	Run Time
Initial		50	1.00	1.00
Ramp 1	30	150	0.00	4.33
Ramp 2	20	250	6,67	16.00

Table 4.1: GC temperature gradient

Injection volume was 1μL in splitless mode (splitless time 1 minute) at 280 °C, and the MS transfer line temperature was 280 °C. The carrier gas was helium (He) at a constant flow of 1 mL min^{-1}.

4.2.3. MASS SPECTROMETRY METHOD

Each pure analyte was analyzed in order to evaluate their spectra and choose the best fragments to detect. In fact, the MS acquisition was carried out in single ion monitoring (SIM) by applying a proper dwell time (40 ms for each ion monitored) to guarantee an acquisition frequency of 4 cycle s-1. Working in SIM instead of a normal Scan mode increases the signal to noise ratio (S/N), then the sensitivity of the method. All ion selected for the method were reported in Table 4.2:

Analytes (Acids)	R_t (min.)	Quant. Ion *(m/z)*	Qual. Ion *(m/z)*	IS [*m/z*]
Acetic Acid	5.34	60	-	$^2H_3$-Acetic Acid [77]
Propionic Acid	5.76	74	73	$^2H_5$-Propionic Acid [77]
iso-Butyric Acid	5.89	73	88	$^2H_7$-iso-Butyric Acid [77]
Butyric Acid	6.18	60	73	$^2H_5$-Propionic Acid [77]
iso-Valeric Acid	6.36	60	-	$^2H_9$-iso-Valeric Acid [63]
2-Methylbutyric Acid	6.37	74	-	$^2H_9$-iso-Valeric Acid [63]
Valeric Acid	6.69	60	73	$^2H_9$-iso-Valeric Acid [63]
Hexanoic Acid	7.19	60	73	$^2H_9$-iso-Valeric Acid [63]
Heptanoic Acid	7.69	60	73	$^2H_9$-iso-Valeric Acid [63]
Octanoic Acid	8.19	60	73	$^2H_{15}$-Octanoic Acid [63]
Nonanoic Acid	8.67	60	73	$^2H_{15}$-Octanoic Acid [63]
Decanoic Acid	9.15	60	73	$^2H_{15}$-Octanoic Acid [63]
Dodecanoic Acid	10.06	60	73	$^2H_{15}$-Octanoic Acid [63]
Tetradecanoic Acid	11.14	60	73	$^2H_{15}$-Octanoic Acid [63]
Hexadecanoic Acid	12.60	60	73	$^2H_{15}$-Octanoic Acid [63]
Octadecanoic Acid	14.80	60	73	$^2H_{15}$-Octanoic Acid [63]

Table 4.2: Selected ions for SIM experiments

4.2.4. STANDARD SOLUTIONS AND SAMPLES PREPARATION

Stock solutions of SCFAs and their ISs were prepared in mQ water at 50 mg mL-1, while MCFAs, LCFAs and [$^2H_{15}$] octanoic were prepared in acetone at 10 mg mL-1. Obtained stock solutions were stored at 4 ◦C until use. Since the amount FFAs in plasma samples span over a range of different orders of magnitude, analyte-specific concentration ranges were defined. Therefore, to build up easily these calibration levels, working mixtures of analytes and ISs in acetone (Mix 1 and ISs) were prepared, as reported in Table 4.3.

Analytes (Acids)	Mix 1 (µg mL-1)	IS (Acids)	IS (µg mL-1)
Acetic	5’000	$^2H_3$-Acetic	1’000
Propionic	50	$^2H_3$-Propionic	5
iso-Butyric	50	$^2H_7$-iso-Butyric	5
Butyric	10		

iso-Valeric	500	$^{2}H_{9}$-iso-Valeric	50
2-Methylbutyric	500		
Valeric	10		
Hexanoic	50		
Heptanoic	10		
Optanoic	500	$^{2}H_{15}$-Octanoic	25
Nonanoic	10		
Decanoic	500		
Dodecanoic	50		
Tetradecanoic	1’000		
Hexadecanoic	1’000		
Octadecanoic	1000		

Table 4.3: Mix 1 and IS solution composition

Mix 2 was prepared by dilution of Mix 1 (1:10). A six levels calibration curve was prepared by adding a proper volume of Mix 1 (or Mix 2) to 10 µL of ISs mixture. PBS was added to reach a final volume of 0.3 mL and then each solution was extracted with 0.1 mL of MTBE acidified with 20 µL of acidic solution. Each tube was shaken in vortex apparatus for 5 mins, centrifuged at 10’000 rpm for 5 mins, and finally the solvent layer was transferred in vial conical insert and analyzed three times by ID/GC-MS method. The calibration levels and FFAs mixtures were analyzed six times by the proposed method. For each analyte, different calibration ranges were employed to fit the expected plasma levels, which show huge differences among FFAs. The final concentrations for each analyte in the calibration levels are reported in Table 4.4.

Calibration levels (Acids)	**1 (µg mL^{-1})**	**2 (µg mL^{-1})**	**3 (µg mL^{-1})**	**4 (µg mL^{-1})**	**5 (µg mL^{-1})**	**6 (µg mL^{-1})**
Acetic	10.0	25.0	50.0	100	250	500
Propionic	0.10	0.25	0.50	1.00	2.50	5.00
iso-Butyric	0.10	0.25	0.50	1.00	2.50	5.00
Butyric	0.02	0.05	0.10	0.20	0.50	1.00
iso-Valeric	1.00	2.50	5.00	10.0	25.0	50.0
2-Methylbutyric	1.00	2.50	5.00	10.0	25.0	50.0

Valeric	0.02	0.05	0.10	0.20	0.50	1.00
Hexanoic	0.10	0.25	0.50	1.00	2.50	5.00
Heptanoic	0.02	0.05	0.10	0.20	0.50	1.00
Octanoic	1.00	2.50	5.00	10.0	25.0	50.0
Nonanoic	0.02	0.05	0.10	0.20	0.50	1.00
Decanoic	1.00	2.50	5.00	10.0	25.0	50.0
Dodecanoic	0.10	0.25	0.50	1.00	2.50	5.00
Tetradecanoic	2.00	5.00	10.0	20.0	50.0	100.0
Hexadecanoic	2.00	5.00	10.0	20.0	50.0	100.0
Octadecanoic	2.00	5.00	10.0	20.0	50.0	100.0

Table 4.4: final concentration of calibration curves

Method precision and accuracy evaluation were estimated using different stock solutions containing all the FFAs at three concentration levels, corresponding to 20% (low level), 50% (medium level) and 80% (high level) of the linearity range. Precision was evaluated as repeatability of replicate analysis of each level and was represented by the relative standard deviation value (RSD %). Accuracy was determined by the ratio between the calculated and the real amounts. Matrix effect of co-extracted plasma compounds was evaluated as ratio of Iss values between the samples and the calibration levels solutions having the same concentration. The abundance ratio of each IS in the sample vs. calibration level represent its signal recovery in human plasma and the matrix effects obtained for isotopologue ISs can be reasonably considered the same for the analytes. Finally, to obtain reliable limit of detection (LOD) and limit of quantitation (LOQ) values, the standard deviation of response and slope approach was employed. The estimated standard deviations of responses of each analyte were obtained by the calculated standard deviation of intercepts (SDY-I) of regression lines [32].

Plasma samples from 10 CRC patients (CRC stages I–II), 10 high grade dysplasia adenoma (ADE), and 13 healthy subjects (controls) who underwent colonoscopy -but for whom no pathological affliction was found were obtained from the Tissue Biobank of the first Surgical Clinic of Padua Hospital, Italy (Ethical Committee Approved Protocol Number: P488). Demographic data and patient characteristics are summarized in Table 4.5.

Subjects	Healthy subjects (controls) n = 13	ADE (>1 cm) n = 10	CRC (stages I-II) n = 10
Age (years)			
median	66	67	72
min-max	47-87	51-78	58-81
Gender			
Male	6	6	6
Female	7	4	4

Table 4.5: Demographic data of analyzed samples

Groups under study do not differ for sex (Chi-square test, p = 0.449) or age (ANOVA, p value = 0.119). Blood samples were collected using a DB Vacutainer® blood collection tube (Becton, Dickinson and Company, USA) with K3EDTA. Plasma was prepared by centrifugation at 3000 rpm for 10 min and stored at -80 ◦C until analysis. All blood samples have been collected after at least 12 h overnight fasting, to ensure the irrelevance of dietary fatty acids in the present study. Just before the analysis, each plasma sample was thawed and FFAs were extracted as follow: an aliquot of 300 µL of plasma sample was added of 10 µL of Iss mixture, 100 µL of MTBE and 20 µL acidic solution in 0.5 mL centrifuge tube. Afterwards, each tube was shaken in vortex apparatus for 5 mins, centrifuged at 10'000 rpm for 5 mins, and finally the solvent layer was transferred in vial conical insert and analyzed by ID/GC-MS.

Statistical analysis of all samples data was performed using GraphPad Prism, version 5.00, 2007 (GraphPad Software, Inc., La Jolla, CA, USA). Nonparametric univariate analysis (Kruskall-Wallis test and Dunn's multiple comparison post hoc test) was used to compare the fatty acid levels in the three groups. MetaboAnalyst 5.0 web tool (https://www.metaboanalyst.ca/) was employed to detect pattern of change in the fatty acid levels in the pathological sequence C>ADE>CRC early.

4.3. RESULTS

4.3.1. CHROMATOGRAPHY

The chromatographic method showed an adequate separation between the analytes of the panel and, when some compounds coeluted (specifically isovaleric and 2-methylbutyric acid), the extracted ion chromatogram of specific fragments ion allows their determination (Figure 4.3).

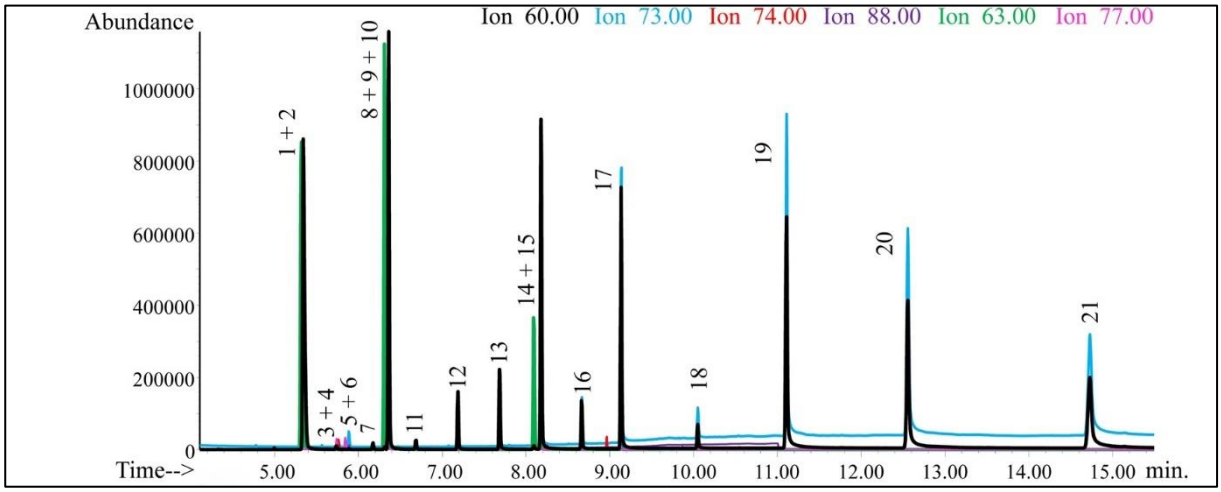

Figure 4.3: Chromatogram of a sample

As a matter of fact, all the ISs are not completely separated from their relative compounds but the different fragments ion allows their recognition. Another example is the coelution of 3 methyl- with 2 methyl-butanoic. Their determination is still possible due to their different characteristic ion fragment at *m/z* 60 and 74, respectively. Unfortunately, these isomers did not have further specific ions; hence the specificity can be ensured solely by the retention time and quantifier ions. Besides, this method is also able to separate and detect LCFAs, that are abundant in human plasma sample since they are coming from the diet.

The advantage in using a high polarity FFAP column is the possibility of analyzing the FFAs without any derivatization process, making the sample preparation simple and fast increasing productivity and decreasing the costs. Furthermore, Furthermore, thanks to the stationary phase, the selectivity value (α) obtained between consecutives homologs, is similar along the FFAs series, leading to correctly assign the chromatographic peak of each analyte by both retention times and the α value. All chromatographic parameters are reported in Table 4.6.

Acids	Rt (min)	±SD (min)	Width (min)	±SD (min)	N	α
Void volume	1.51					
Acetic	5.34	0.01	0.22	0.01	9414	
Propionic	5.76	0.01	0.11	0.01	48199	1.11
isoButyric	5.89	0.01	0.09	0.01	64192	
Butyric	6.18	0.01	0.10	0.01	62308	1.10
isoValeric	6.36	0.01	0.09	0.01	74939	
2-MethylButyric	6.37	0.01	0.09	0.01	73506	
Valeric	6.69	0.01	0.09	0.01	82837	1.11
Hexanoic	7.19	0.01	0.13	0.01	46810	1.10
Heptanoic	7.69	0.01	0.15	0.01	45040	1.09
Octanoic	8.19	0.01	0.19	0.01	30055	1.08
Nonanoic	8.67	0.01	0.20	0.01	28922	1.07
Decanoic	9.15	0.01	0.22	0.02	28170	1.07
Dodecanoic	10.06	0.01	0.25	0.02	25515	
Tetradecanoic	11.14	0.02	0.33	0.02	17792	
Hexadecanoic	12.60	0.03	0.37	0.02	18257	
Octadecanoic	14.80	0.05	0.45	0.02	17387	

Table 4.6: chromatographic parameters

4.3.2. MASS SPECTROMETRY PARAMETER

The aim of this method was to assure the sensitivity, specificity, and reliability in the determination of FFAs in complex biological matrices even using a low-resolution instrument that is normally present in most of the laboratories. Detection sensitivity was achieved by using the SIM acquisition mode, which allows the S/N increase limiting the matrix effect. Specificity, instead, was secured by the selection of the characteristic ions (quantifier and qualifier ions) for identification and quantitation of each analyte. Indeed, the isotopic dilution approach leads to a reliable and robust quantitative determination of analytes in complex matrices. Furthermore, FFAs are a series of homologous carboxylic acids that differ only for hydrocarbon chain length or saturation then, their electronic ionization (EI) spectra are similar. In general, most of the FFAs display in their mass spectrum the 60 and 73 *m/z* ions. The 60 *m/z* ion is the molecular

ion for the acetic acid moiety and derives from the McLafferty rearrangement in the carboxyl-function (Figure 4.4).

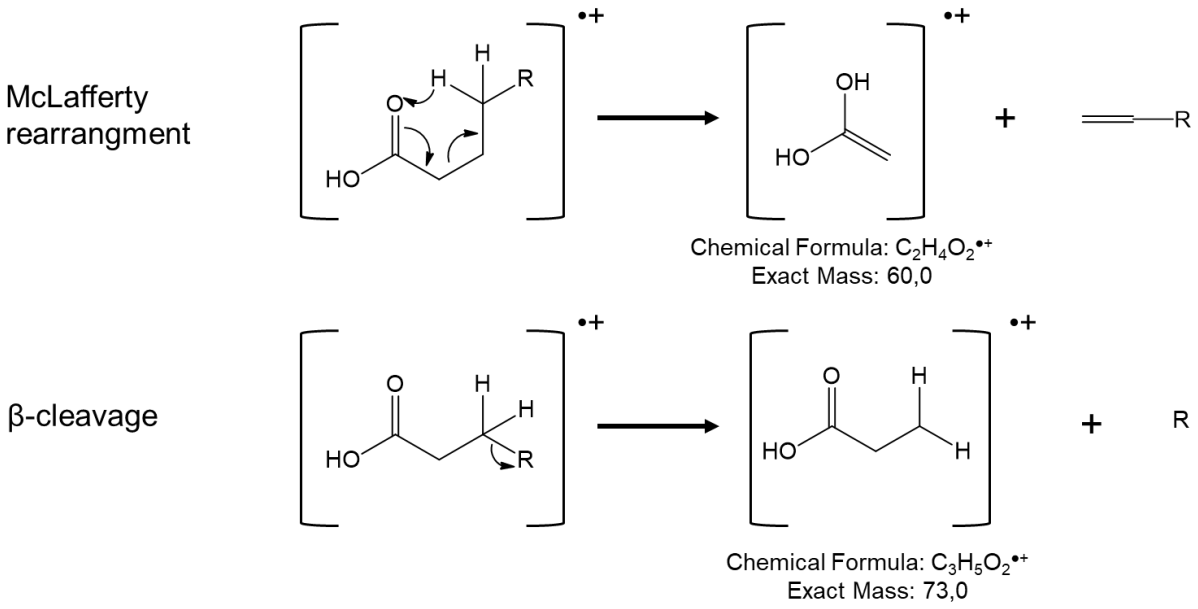

Figure 4.4: Proposed fragmentation of the analytes

In the other hand, the 73 *m/z* ion is generated by the cleavage of the sigma bond between the β carbons, with respect to the carboxyl-group, of hydrocarbon chain. The only exceptions are the acetic acid, that lacks the 73 *m/z* fragment, since its molecular weight is 60 Da, and propionic acid, that does not show the 60 *m/z* ion, since the impossibility of McLafferty rearrangement for this structure. Therefore, to increase specificity, the 74 and 88 *m/z* ions were included in the panel of monitored ions to allow the correct identification and quantification of propionic, isobutyric and the 2-methyl- or 2 ethylcarboxylic acids (e.g., 2-methylbutyric acid). Finally, ions at 63 and 77 *m/z* were monitored to detect and quantify the ISs.

4.3.3. SAMPLE ANALYSIS

The sample preparation was a simple Liquid Liquid Extraction (LLE) with MTBE where also a plasma denaturation take place. Specifically, the denaturation process was carried out by adding the acidic solution (Chapter 4.2.1) that allows the recovery of FFAs with the solvent extraction. In fact, these analytes need an acid pH in order to be undissociated, then soluble in

MTBE. The obtained linear regressions coefficients, the determination coefficient (R2) and the estimated LOD and LOQ values for each analyte are reported in Table 4.7.

Acids	Slope (PAR/mg L-1)	Intercept (PAR)	R2	LOD (mg L^{-1})	LOQ (mg L^{-1})
Acetic	0.009	0.086	0.999	7.58	22.75
Propionic	0.830	0.071	0.999	0.06	0.17
isoButyric	0.409	0.021	0.999	0.04	0.13
Butyric	2.445	0.082	0.999	0.02	0.05
isoValeric	0.070	0.181	0.988	0.72	2.15
2-Methylbutyric	0.056	0.121	0.990	0.60	1.81
Valeric	0.108	0.002	0.999	0.01	0.03
Hexanoic	0.386	0.011	0.999	0.03	0.09
Heptanoic	2.798	0.007	0.999	0.01	0.03
Octanoic	0.188	0.294	0.993	0.08	0.23
Nonanoic	1.740	0.046	0.999	0.01	0.04
Decanoic	0.145	0.219	0.994	0.16	0.49
Dodecanoic	0.207	0.002	0.999	0.05	0.16
Tetradecanoic	0.102	0.479	0.989	0.71	2.12
Hexadecanoic	0.101	1.099	0.995	1.61	4.84
Octadecanoic	0.100	0.527	0.999	1.37	4.12

Table 4.7: Calibration parameters for each analyte

It is possible to highlight that the detection limits calculated were less than 100 μg L^{-1} for most of the analytes. The exceptions were acetic, hexadecenoic and octadecanoic acids that reached higher values (>1 mg L^{-1}).

Accuracy and Precision data obtained were reported in Table 4.8.

Acids	Low Level		Mid Level		High Level	
	Accuracy	RSD	Accuracy	RSD	Accuracy	RSD

Acetic	94%	1.4%	98%	0.1%	99%	1.2%
Propionic	97%	2.5%	99%	2.0%	99%	0.1%
isoButyric	97%	1.7%	100%	0.3%	99%	0.5%
Butyric	93%	6.1%	97%	5.1%	100%	0.9%
isoValeric	97%	1.2%	86%	1.3%	96%	8.0%
2-MethylButyric	99%	2.4%	89%	0.5%	97%	7.5%
Valeric	98%	6.3%	98%	5.6%	99%	3.1%
Hexanoic	100%	4.0%	98%	1.5%	100%	4.4%
Heptanoic	99%	1.7%	98%	1.0%	100%	4.1%
Octanoic	96%	1.2%	92%	2.5%	97%	12.0%
Nonanoic	95%	1.7%	99%	1.6%	99%	4.5%
Decanoic	96%	1.6%	91%	1.5%	97%	12.0%
Dodecanoic	99%	3.7%	97%	2.0%	100%	3.9%
Tetradecanoic	99%	1.6%	84%	3.8%	93%	9.2%
Hexadecanoic	99%	6.5%	91%	1.3%	98%	12.4%
Octadecanoic	97%	11.1%	100%	0.8%	99%	5.3%

Table 4.8: Accuracy and Precision

Accuracy ranged between 84 and 100% while precision, represented by the RSD, between 0.1 and 12% at the concentration level tested.

The matrix effect (ME %) for the ISs were calculated according to Matuszewski et al [31] and the values oscillated between 87 and 98% indicating that the plasma matrix did not interfere on the results. Because of FFAs are naturally present in human plasma, the ME % has been calculated using the isotopologues internal standards spiked with 10 µL of ISs Mix 2. The ME % values of each IS are reported in Table 4.9.

IS compound	**[$^2H_3$]Acetic**	**[$^2H_3$]Propionic**	**[$^2H_7$]iso-Butyric**	**[$^2H_9$]iso-Valeric**	**[$^2H_{15}$]Octanoic**
Calibration level solutions (n=36)					
Average	2774792	1845012	166577	608858	192659
SD	174560	115070	11050	42239	13338
RSD %	6.3%	6.2%	6.6%	6.9%	6.9%
Human plasma samples (n=40)					
Average	2406413	1740508	161666	594447	182860

SD RSD %	195517 8.1%	113329 6.5%	10342 6.4%	38377 6.5%	17995 9.8%
ME%	87%	94%	97%	98%	95%

Table 4.9: ME calculated on IS abundances

To better understand the result will be discussed by the length classification (short, medium, and long).

The results of both branched and linear chain fatty from C2 to C5 are reported in Figure 4.5.

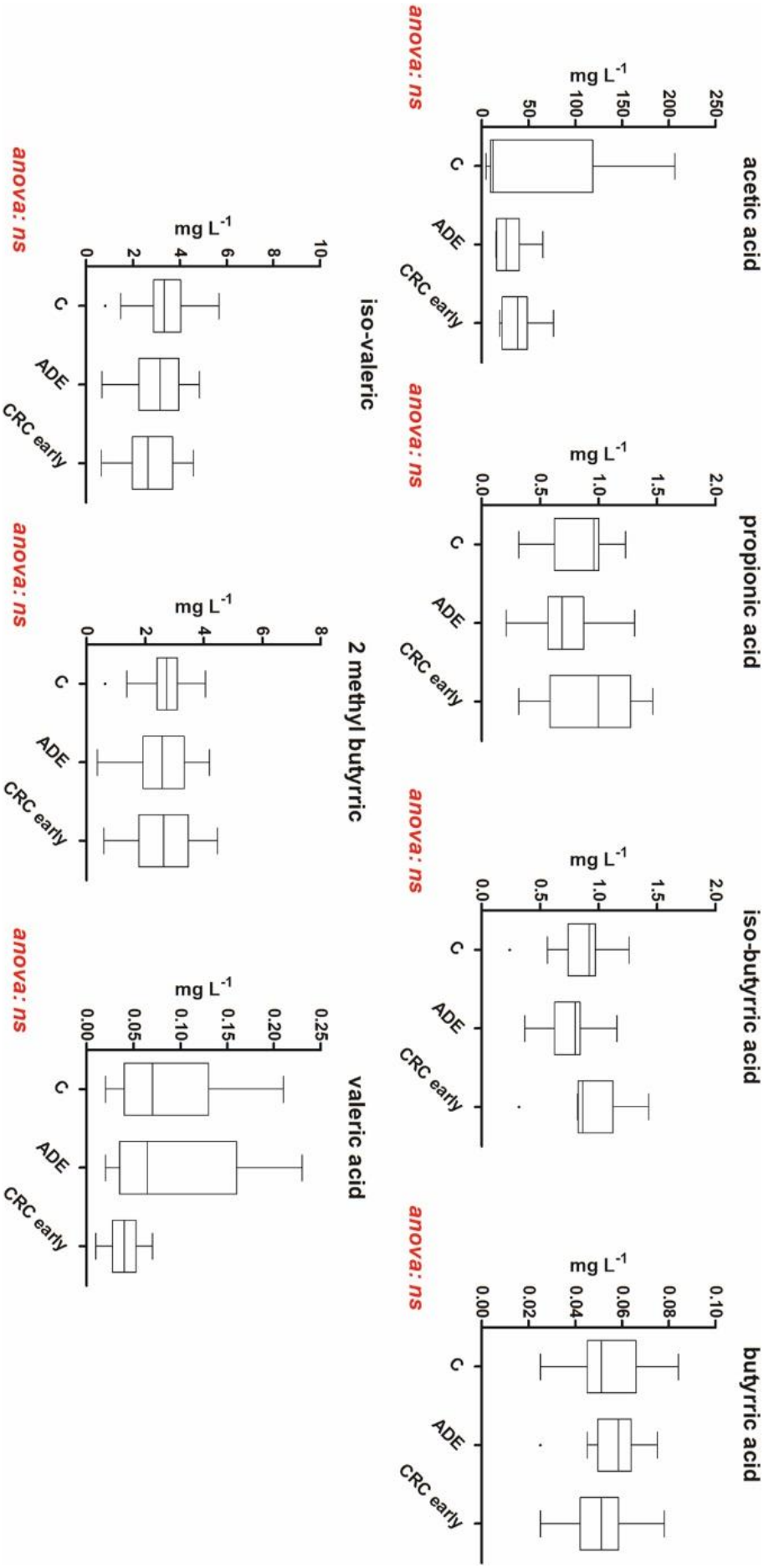

Figure 4.5: SCFAs results

Data shows comparable SCFAs levels among the different classes of patients (controls, ADE, and CRC). At first sight, the lack of a specific SCFA signature in the plasma of CRC patients seems to contrast with the dysbiosis associated to this pathology. Indeed, it is now recognized that SCFAs content in stools of CRC patients is strictly related to the modifications in the microbiota composition [56]. To date, SCFAs quantification in plasma samples of CRC patients has been provided only by Adewiah et al. who quantified, and reported, lower level of acetate, propionate and butyrate acids fourteen subjects with CRC [57].

In regards the medium chain fatty acids (from C6 to C12), all the results are reported in Figure 4.6.

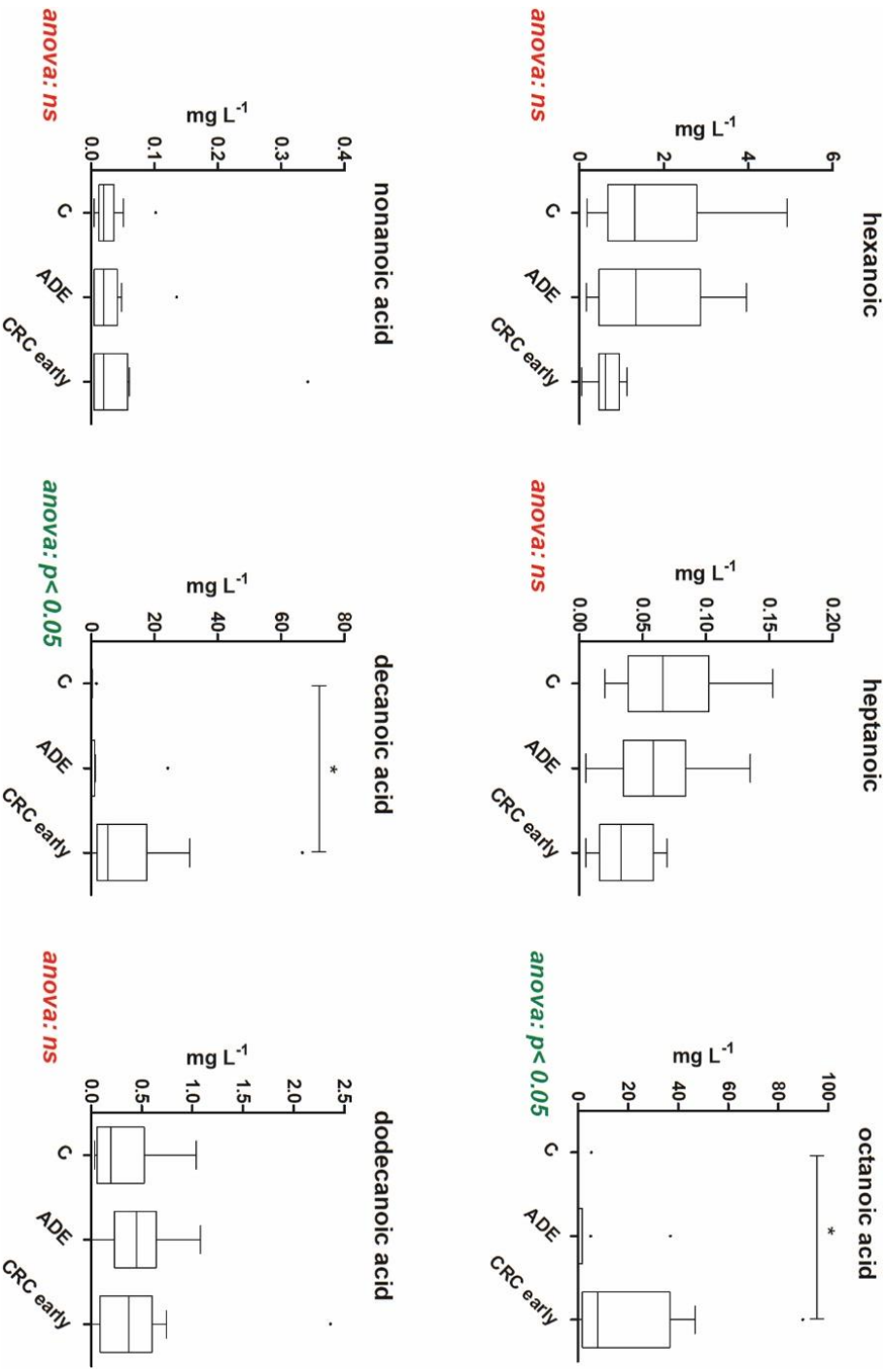

Figure 4.6: MCFAs results

In regards the MCFAs a trend did not seem to be in any of the analytes. With difference to SCFAs, in MCFA there is not a consistent trend for all the fatty acids quantified. Anyway, the quantity of hexanoic and heptanoic acids were found to be higher in controls and adenoma patients. Conversely, levels of octanoic and decanoic acid were significantly higher in early CRC patients than controls (Dunn's multiple comparison test, $p < 0.05$). Despite the low sample size (n = 33 subjects), data presented here are in good agreement with those found in our

previous study [52], further confirming the validity of these results. Finally, no significant differences in nonanoic and dodecanoic acids has been found.

Furthermore, this method also included the determination of LCFAs (C14 to C18). These group are among the most analytes studied in the literature, and their levels in both healthy and pathological subjects are reported. In the analyzed samples no differences in LCFAs were found in agreement with previous works [58]. The data are reported in Figure 4.7.

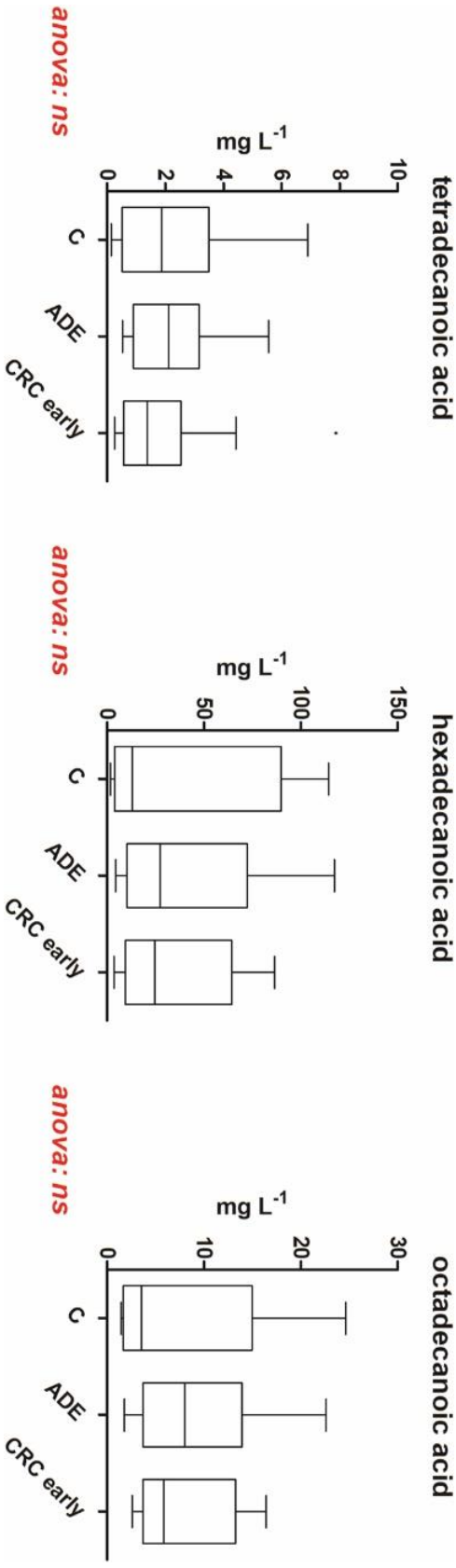

Figure 4.7: LCFAs results

Therefore, we have then focused our attention on possible associations between CRC early onset and progression and changes in plasma free fatty acids. The following statistical analysis were performed by Dr. Crotti's group. Specifically, SCFAs and MCFAs have been quantified in plasma samples as a possible hallmark of microbiota and host' metabolic alterations. Among the quantified analytes, putative biomarkers should be associable to the pathological sequence: healthy subjects (C) → high-grade dysplasia adenoma, ADE (i.e., pre-cancerous lesions at high risk to develop CRC) → CRC early stages (stages I-II). To verify this hypothesis, it was employed the *PatternHunter* tool of Metaboanalyst 5.0 website (www.metaboanalyst.ca/). Results presented in Table 4.7 reveal the presence of two different cluster of plasma free fatty acids alteration.

Compound	r	p-value
Valeric Acid	-0.38759	0.0258
Heptanoic Acid	-0.36598	0.0362
Hexanoic Acid	-0.3654	0.0365
isoValeric Acid	-0.17974	
2-Methylbutyric Acid	-0.0336	
Butyric Acid	-0.00422	
Tetradecanoic Acid	-0.00305	
Dodecanoic Acid	-0.023373	
Nonanoic Acid	-0.042217	
Octadecanoic Acid	-0.090561	
iso-Butyric Acid	-0.091528	
Hexadecanoic Acid	-0.0927	
Propionic Acid	-0.099281	
Acetic Acid	-0.19916	
Decanoic Acid	-0.5499	0.0009
Octanoic Acid	-0.60139	0.0002

Table 4.7: Pattern of decreased (r < 0) or increased (r > 0) fatty acids plasma levels in the pathological sequence: C>ADE>CRC. Statistically significant p values from the Pearson' correlation test are reported.

Indeed, circulating levels of SCFA and MCFA, but not LCFA have significant changes associable to the sequence C → ADE → CRC. In particular, among SCFAs, the valeric acid decrease showed the strongest correlation associable to the pathological sequence (r: -0.38759,

p = 0.0258). A recent study, similarly, showed reduced levels of valeric acid in CRC patients, thus confirming our observations [59]. Among microbiota-derived SCFAs, valeric acid raise interest because of its gut protective activities, the improvement of gastrointestinal function and the enhancement of integrity of intestinal epithelium [60]. Additionally, valeric acid possesses an inhibitory effect against the histone deacetylase (HDAC) enzyme, whose activity has been implicated in a variety of diseases, including colon cancer and inflammatory pathologies [61]. Surprisingly, other key SCFAs involved in the maintaining the stability of gut microbiota, the integrity of intestinal epithelium, and the chemoprevention against CRC doesn't show any correlation (e.g., butyric acid). SCFAs stool content in colorectal cancer has been accurately investigated by several studies, revealing a large variability in the fecal SCFAs signatures [62]. Despite stool profiling is for sure a good way to identify intestinal bacteria and metabolites in colorectal cancer patients or subject at risk, SCFAs production rates and their concentration in the large bowel lumen are related to several factors, including their slow intraluminal diffusion rate, their rapid mucosal absorption, and their local metabolism by epithelial cells[63]. Consequently, final amount of SCFAs in stool can be affected along the intestinal transit by both rates of production and disappearance [63]. For these reasons, the proposed ID/GC-MS method would be easily translated towards a minimally invasive methodology for the detection of gut-microbiota/intestinal homeostasis alterations. Plasma MCFAs have distinct, but opposite trend, in the analyzed samples. Smaller MCFAs, like hexanoic and heptanoic fatty acids, still have a statistically significant pattern of decrease in the sequence C → ADE → CRC (r: -0.36598, p = 0.0362 and r = -0.3654, p = 0.0365 for C6 and C7, respectively). The decrease trend of hexanoic acid, which is close to that of valeric acid, can be justified by the bivalent nature of this compound which share fermentative origin and biological effects similar to those of SCFA[64]. On the contrary, both octanoic and decanoic fatty acids showed a pattern of increase. In our previous study, performed using a different method and in a larger patients' cohort, we already observed the same trend, thus confirming the results' validity[52]. Octanoic and decanoic acids are active compounds involved in energetic metabolism [65]. In different cell models it has been demonstrated that decanoic acids only is capable to increase the flux of glucose to lactate thought the so-called Warburg Effect, which is characteristic of cancer cells [65]. On the contrary, octanoic acid is prevalently involved in mitochondrial metabolism and in the synthesis of ketone bodies [65].

4.4. CONCLUSION

The proposed ID/GC-MS method was developed to assure the sensitivity, the specificity and reliability of the determination of FFAs in complex biological matrices by using a low-resolution instrument, normally present in most of the laboratory with a very low productive and economic impact. The goal was to highlight a possible interconnection in human plasma between the microbiota and host's metabolic alterations. It was decided to perform a simple and fast sample preparation, an LLE before the determination of FFAs by SIM. The results revealed the presence of a possible biomarkers panel capable to summarize the pathological sequence C>ADE>CRC, showing significant differences in some SCFAs (C2-C5) and MCFAs (C6-C12) levels. Moreover, no differences of free LCFAs (C14-C18) were observed confirming being in line with previous works. Despite the small sample size of study that did not allow us to reach definitive conclusions, it was highlighted the possibility of using these plasma FFAs to monitor the local CRC microenvironment. We expect that such a panel would be useful for the identification of non-symptomatic subject at risk to develop CRC and the speed up the early CRC diagnosis, helping clinicians to correctly evaluate non-specific symptoms associated to stages I and II. In conclusion, the proposed ID/GC-MS method proved to be adequate in the study of FFAs in human plasma with a high productivity, sensitivity, and selectivity. The goal to develop an easy, fast, and relatively cheap method was achieved. Finally, the method demonstrated to be applicable to study FFAs in different matrices. This allowed to perform further different studies.

4.5. FURTHER APPLICATIONS

This method showed a great versatility and was applied to perform different investigations. Specifically, due to the application of this method in different collaborations, it was possible to publish 6 works [46, 66, 67, 68, 69,] while other four are under review. Coming up, will be briefly reported two different published studies that helped to elucidate different branches of studies (biological and dietary). First, it was evaluated a possible variation in the FFAs plasma levels between healthy individuals and patients with different diseases (celiac disease, CD, colorectal cancer, CRC, and adenomatous polyposis, AP) [46]. In this case it was performed a Dirichlet-multinomial regression in order to highlight disease-specific FFA signature. HC showed a different composition of FFAs than CRC, AP, and CD patients. Furthermore, the partial least squares discriminant analysis (PLS-DA) confirmed perfect overlap between the CRC and AP

patients and separation of HC from the diseased groups. The Dirichlet-multinomial regression identified only strong positive association between CD and butyric acid. Another application involved the analysis of SCFAs in feces of patients with fibromyalgia (FM) with difference diets [67]. Specifically, the patients were assigned to consume either Khorasan or control wheat products for 8 weeks and then, following an 8-week washout period, crossed. The replacement diet based on ancient Khorasan wheat results in beneficial GM compositional and functional modifications that positively correlate with an improvement of FM symptomatology. The opportunity to employ this method to different investigation and also different matrices (fecal water) confirmed the high performances achieved from this method. Furthermore, the easy sample preparation let us to prepare and analyze a large number of samples per day obtaining a large amount of data in few days. This method continues to be used for different studies and the results will be published in the future.

5. PROJECT 3: DEVELOPMENT OF AN ID/2D-HILIC-HPLC-MS/MS METHOD TO DETERMINE HISTAMINE FOR STUDYING THE EFFECT OF N-PALMITOYLETHANOLAMINE ON MORPHINE TOLERANCE

My involvement in this project started from a previous investigation [70] where histamine in rat plasma was quantified in the model of pain studies. My work instead, was to quantify histamine in culture medium to better elucidate the inhibitory effect of N-palmitoylethanolamine (PEA) against the development of morphine tolerance of these cells. The robustness of the method has allowed us not to change the chromatographic and mass spectrometry parameters but only the range of concentration of the calibration curve. Histamine determination and quantification can be an interesting tool in biological and clinical studies but due to its structural properties it can be challenging. Specifically, histamine, is a small polar organic compound. For this reason, it is not possible to analyze it in GC without derivatization. Therefore, for the same reason, a RPLC method does not allow the retention of histamine. Thus, we decided to develop a 2D-HILIC-HPLC-MS/MS method to quantify histamine in culture media for elucidating the role of N-palmitoylethanolamine on morphine tolerance. This 2D method allowed to perform a SPE on-line, "cleaning" and "concentrating" the samples. Furthermore, this technique let to change the injection volume between 5 and 50 μL without loss in the chromatographic performance. This is a very important tool because it gave the opportunity to use the same chromatographic and mass spectrometry parameters even if the different matrices to analyze had different concentrations of histamine.

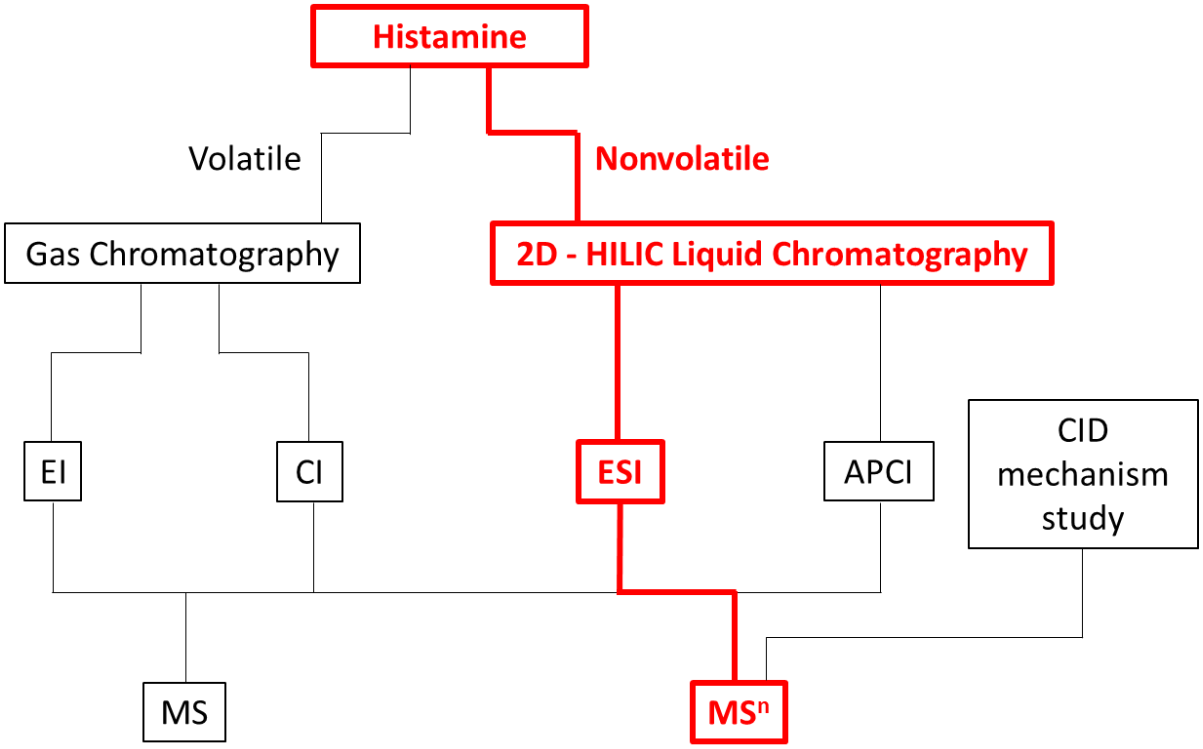

Figure 5.1: scheme of the system employed for Project 3

5.1. INTRODUCTION

Since glial cells are involved in opioid tolerance whereas mast cells (MCs) are one of the pivotal targets of N-palmitoylethanolamine (PEA), it was hypothesized that PEA is able to control the crosstalk between these cells [70]. A rat MC line, RBL-2H3 cells, and a primary culture of rat cortical astrocytes were used. Morphine treatment (30 mM, 30 min) significantly increased MC degranulation, which was prevented by pre-treatment with ultramicronized PEA (PEA, 100 μM, 18h), as evaluated by β-hexosaminidase assay, histamine quantification, tryptase expression, as well as CCL2 and TNFα mRNAs. In this study, our goal was the determination and quantitation of Histamine in culture media in order to elucidate the inhibitory effect of PEA against the development of morphine tolerance of these cells.

Histamine or 2-(1H-Imidazol-4-yl)ethanamine is a small organic compound known for its role in the inflammatory response. In fact, it is involved in local immune responses, as well as regulating physiological functions in the gut and acting as a neurotransmitter for the brain, spinal cord, and uterus. Most histamine in the body is generated in granules in mast cells and, if sensitized by IgE antibodies attached to their membranes, degranulate when exposed to the appropriate antigen [71]. In this study, the challenge was to find the retention of Histamine. This analyte is too polar to be analyzed in GC but also in RPLC with reverse phase. It is possible to

analyze histamine with GC-MS, but it needs to be derivatized, leading thus to an advanced sample manipulation [72]. Furthermore, some research groups were able to develop a LC method to analyze histamine [73, 74], involving HILIC chromatography or very complicated 2D-LC methods. In this project, we proposed an ID/2D-LC-MS/MS method using ZIC-HILIC columns in order to perform an On-line Solid Phase Extraction (SPE). As mentioned above, HILIC, like NPLC, uses polar stationary phases such as bare silica or short-chain amino and cyano phases. This afforded the retention and separation of polar or charged compounds. This method led to a minimum sample manipulation (e.g., protein precipitation) and also to a very good sensitivity. In fact, the 2D system let us to inject higher volumes (up to 50 μL) in case of a very low histamine quantity in the samples. The method showed high sensitivity and productivity.

5.2. MATHERIAL AND METHODS

The analyses were carried out with a Varian 1200 L triple quadrupole system (able to perform MS/MS experiments) coupled with three Prostar 210 pumps (each one can manage one solvent line), a Prostar 410 autosampler and an ESI source. All the raw data collected were processed by Varian Workstation (version 6.8) software. The system is equipped with two 6-port valves that let the instrument perform an on-line SPE, so a 2D liquid chromatography.

5.2.1. CHEMICALS

Histamine dihydrochloride, Histamine-α,α,β,β-d4 dihydrochloride, Acetonitrile (Chromasolv), formic acid, and ammonium formate (MS grade) were purchased from Merck (Milan, Italy). Ultrapure water or mQ water (resistivity 18 M Ω cm) was obtained from Millipore's Simplicity system (Milan, Italy).

5.2.2. CHROMATOGRAPHY

The columns used in the final method were: 1) the SeQuant® ZIC-HILIC Guard 20x2.1mm as loading column and 2) the SeQuant® ZIC-HILIC 50x2.1mm, 3.5µm, 100Å as analytic column. The solvents were: 1) Solvent A: mQ water:acetonitrile 9:1 solution added with 5mM HCOOH and 15mM $HCOONH_4$; 2) Solvent B: mQ water:acetonitrile 1:9 solution added with 15mM HCOOH and 5mM $HCOONH_4$; and 3) Solvent C (used for sample loading): mQ

water:acetonitrile 1:9 solution added with 17,5mM HCOOH 2,5mM $HCOONH_4$. The final loading time was 2 minutes at 0.5 mL min^{-1}, and it was tuned evaluating the t_m of histamine in 90% of solvent B. It was demonstrated that until 2 minutes the analyte is completely retained with the starting solvent composition. After two minutes the valve change position and the gradient started in counter-flow from the load column to the analytic column. The gradient started from 90% of solvent B to 20% of solvent B in 10% min-1 and kept for 3 minutes, then it returns in the initial condition in 0.1 minutes for a total run time of 25 minutes. The chromatographic method is reported in Table 5.1.

Time (min.)	A (%)	B (%)	Flow A+B (mL min^{-1})	Flow C (mL min^{-1})	Valve Position
0.00	10	90	0.25	0.5	Load
2.00	10	90	0.25	0.5	Inject
9.00	80	20	0.25	0.5	
12.00	80	20	0.25	0.5	
12.01	10	90	0.25	0.5	Load
25.00	10	90	0.25	0.5	

Table 5.1: chromatographic gradient with valve position switch time.

To better understand how the injection valve works in 2D-HPLC system, a scheme is reported in Figure 5.2.

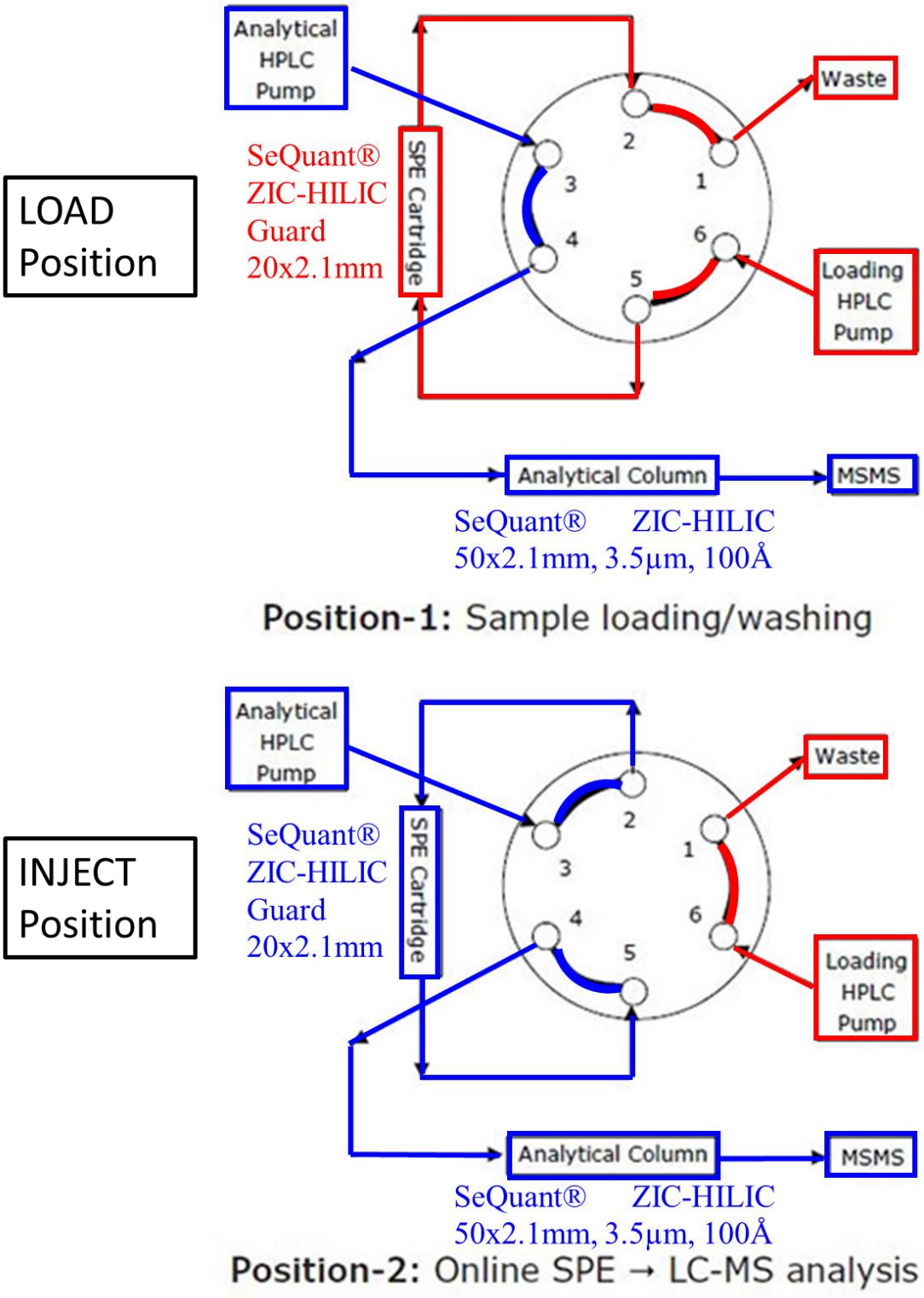

Figure 5.2: the injection valve position in 2D-HPLC system.

Injection volume was 50µL.

5.2.3. MASS SPECTROMETRY PARAMETER

The source used was an ESI source operating in positive ion and using the following settings: 5kV needle, 42 psi nebulizing gas, 600 V shield, and 20 psi drying gas at 280 °C. The ERMS experiments were performed to study the fragmentation of Histamine and [$^2H_4$]-histamine and build their breakdown curves. The ERMS experiments were carried out by a series of product ion scan (MS/MS) analysis, increasing the collision voltage (CV) stepwise in the range 5–50 V. Each MS/MS spectra were acquired in the m/z range from 50 to 130, scan time of 600 ms and argon was used as collisional gas. The ERMS experiments were performed by introducing working solution 1 of each analyte, via syringe pump at 10 μL min -1; the protonated molecule was isolated, and the abundance of product ions were monitored. The ERMS data were used to build the breakdown curves that describe the fragmentation of precursor ion in relation to the collision voltage applied. The breakdown curves were obtained by plotting the relative intensity values (averaging about 15–20 scans) of each signal present in the MS/MS spectra acquired for each CV. In order to increase the sensitivity and the selectivity it was decided to work in MRM. The MRM transitions are reported in Table 5.2.

Name	Precursor Ion (m/z)	Quantifier Ion (m/z)	Qualifier Ion (m/z)
[$^2H_4$]-histamine (IS)	116.0	99.0	-
Histamine	112.0	95.0	68.0

Table 5.2: MRM parameters.

5.2.4. STANDARD SOLUTION, CALIBRATION CURVES AND SAMPLE PREPARATION

Considering that it is its isotopologue, as Internal Standard (IS), it was used [$^2H_4$]-histamine. Stock solutions of histamine and [$^2H_4$]-histamine (internal standard or IS) were prepared in 10 mM HCOOH in mQ water at 1.0 mg mL^{-1} and stored at 4 ◦C. Working solutions of each analyte were freshly prepared by diluting stock solutions up to a concentration of 1.0 μg mL^{-1} and 0.1 μg mL^{-1} (working solutions 1 and 2, respectively) in mixture of mQ water:acetonitrile 50:50 (v/v). The IS working solution was prepared in acetonitrile at 1.0 μg mL^{-1} (IS solution). A six-level calibration curve was prepared by adding proper volumes of working solution (1 or 2) of each analyte to 10 μL of IS solution. The obtained solutions were dried under a gentle nitrogen

stream and dissolved in 1.0 mL of 10 mM of formic acid in mQ water:acetonitrile 50:50 (v/v) solution. Final concentrations of calibration levels of each analyte were: 2.5, 5.0, 10.0, 25.0, 50.0, and 100.0 ng mL^{-1}. All calibration levels were analyzed six times by the 2D-LC-MS/MS method described. Each sample was prepared by adding at 100 μL of culture medium 10uL of IS solution. Then it was added 500 μL of 10 mM HCOOH in acetonitrile doing a protein precipitation. The obtained solutions were dried under a gentle nitrogen stream and dissolved in 1.0 mL of 10 mM of formic acid in mQ water:acetonitrile 50:50 (v/v) solution. Each sample batch were included the blank culture medium, prepared as described above, but by adding only the IS solution. Thus, the analysis of the blank samples can check any interference in the analyte MRM signals due to the matrix components. Three sets of six replicates for each analyte were prepared to evaluate the matrix effect (ME) and the analyte recovery (RE) of the proposed method [31]. In order to estimate precision and accuracy of the methods, a new series of samples at three concentration levels (low, medium and high levels), corresponding to 25, 50 and 100 ng mL-1 respectively, were prepared in six replicates for each compound following the procedures described above from the stock solutions in human plasma matrix. All these samples were analyzed with the method described above.

5.2.5. VALIDATION OF HPLC-MS/MS METHOD

Calibration curves of analytes were obtained by plotting the peak area ratios (PAR), between analyte and IS quantitation ions, versus the nominal concentration of the calibration solution. A linear regression analysis was applied to obtain the best fitting function between the calibration points. In order to obtain reliable limit of detection (LOD) values, the standard deviation (SD) of response and slope approach was employed [32]. The estimated SDs of responses of each analyte were obtained by the calculated SD of y-intercepts (SDY-I) of regression lines. The ME and RE values were determined by comparing the absolute peak areas of analytes of the three sets of samples (set A, B, and C), prepared as described in the Chapter 3.2.3, following the formulas shown below [31]:

$$ME(\%) = (B/A) \times 100$$

$$RE(\%) = (C/B) \times 100$$

Precision and accuracy of the HPLC-MS/MS methods were determined by analysis of the three concentration levels inside the calibration curve (low, medium, and high) for each analyte in the medium without the presence of histamine. The accuracy was determined calculating the

recovery (%) between the determined and added amounts. The precision was evaluated through the relative standard deviation (RSD) of the quantitative data of the replicate analysis of each level.

5.3. RESULTS

5.3.1. CHROMATOGRAPHY

Being a targeted analysis with only one analyte, the chromatography method was tuned to obtain a good retention, minimize the matrix effect and separate histamine from potential interfering compounds. First, it was evaluated how much time the loading column was able to retain histamine employing the 90% of solvent B. It was demonstrated that until two minutes histamine is retained at the head of the loading column then it started to slowly flow inside of it, then two minutes of loading time was set. The 2D system let to "clean" and "concentrate" the sample so it is possible to dilute and inject. The sample is cleaned and concentrate during the 2 minutes of loading and then, after the valve change position the analyte is elute in counter-flow where it goes in the analytic column and finally in the mass spectrometer. An example of a chromatogram is reported in Figure 5.3.

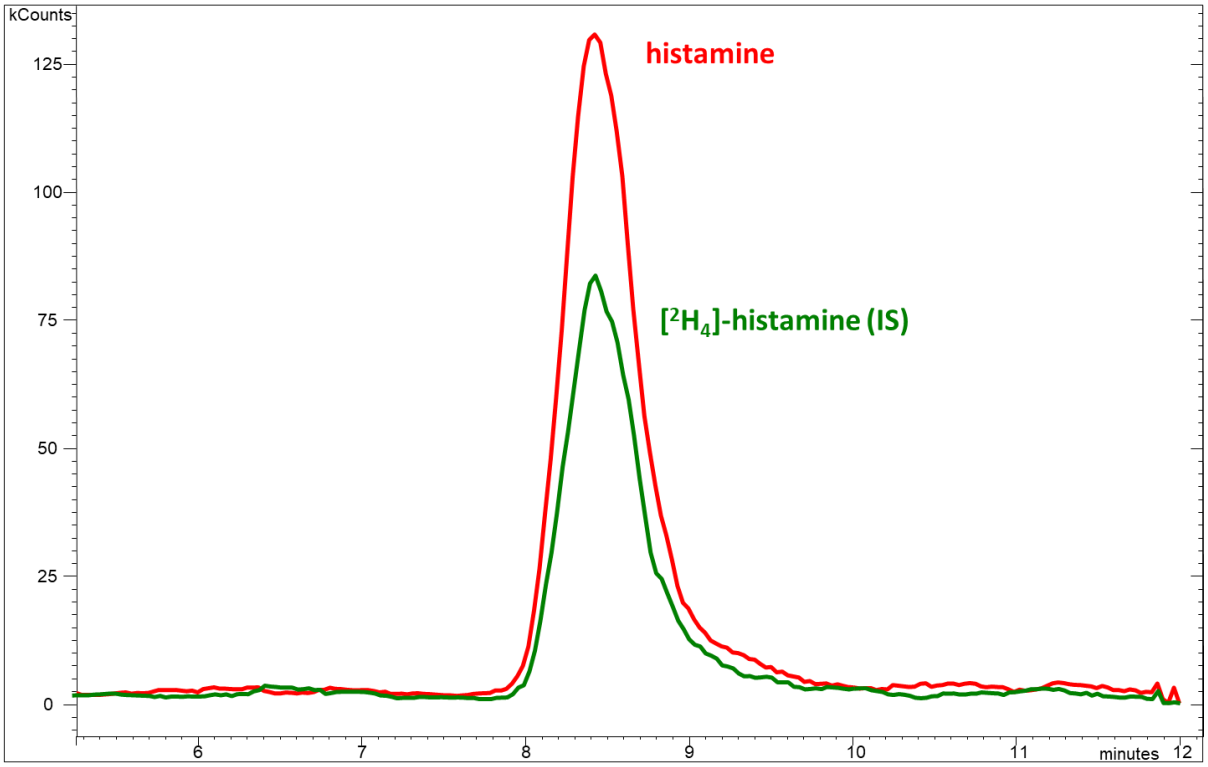

Figure 5.3: the chromatographic profile of a sample analyzed with the ID/2D-HILIC-HPLC-MS/MS proposed method.

5.3.2. MASS SPECTROMETRY ANALYSIS

The collision breakdown curves showed a very fast fragmentation generating two main ion fragments: 95 and 68 *m/z* used as quantitative and qualitative ion respectively (Figure 5.4).

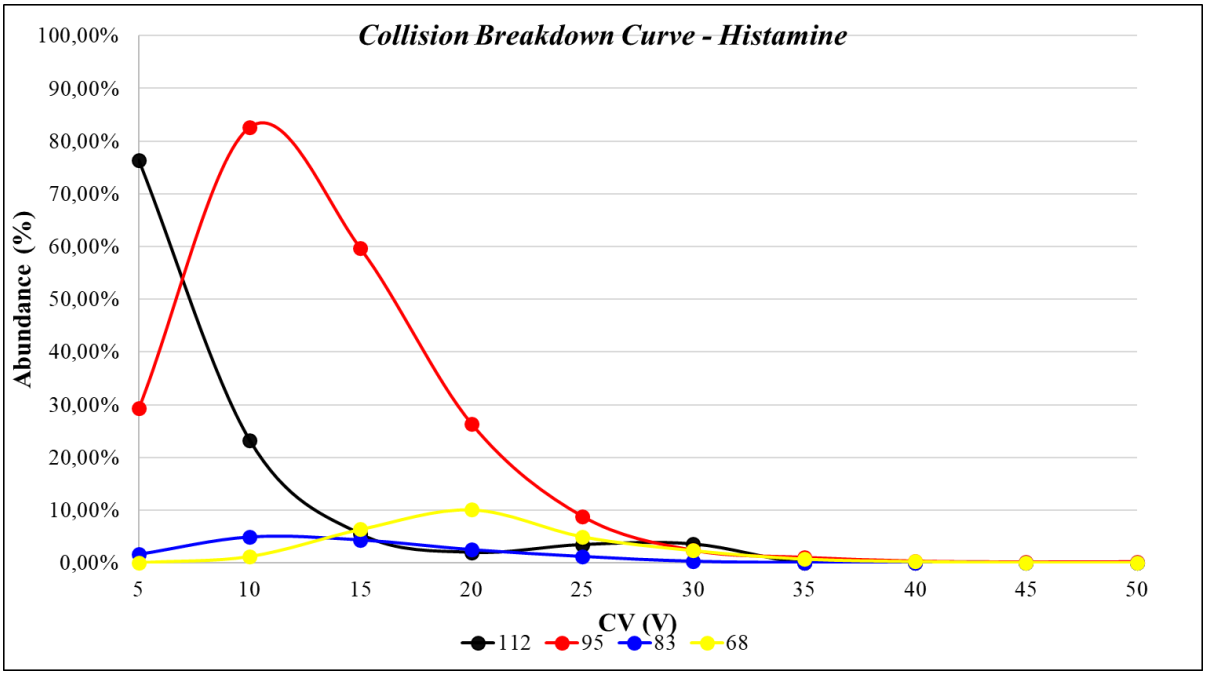

Figure 5.4: Collision breakdown curve of histamine.

In Figure 5.5 it was reported the structures of the proposed fragment ions (fragment ion 95 m/z is confirmed by a previous study [75]).

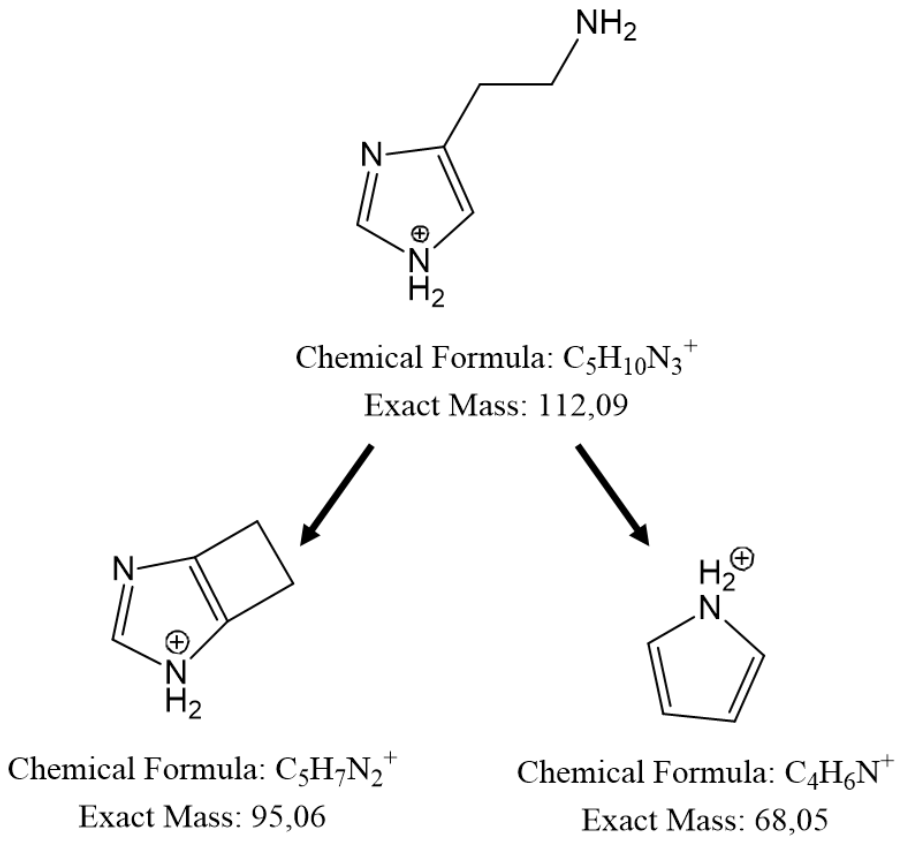

Figure 5.5: proposed fragment ion structures for histamine

In this regard the IS, the only fragment found from the CID experiment was the 99 *m/z*, that demonstrated that it retains all 4 deuterium. This behavior can confirm the structure proposed for the ion 95 *m/z* of histamine (Figure 5.6).

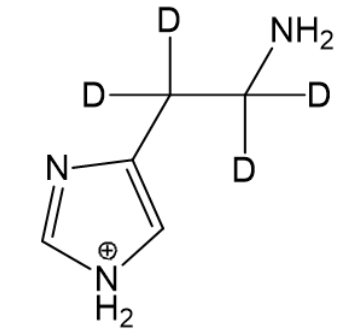

Chemical Formula: $C_5H_6D_4N_3^+$
Exact Mass: 116,11

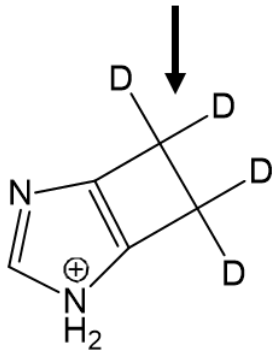

Chemical Formula: $C_5H_3D_4N_2^+$
Exact Mass: 99,09

Figure 5.6: proposed fragment ion structures for [$^2H_4$]-histamine(IS)

Considering that histamine and the IS coeluted we also check if they interfere each other analyzed them separately but with all the MRM transition (for histamine and [$^2H_4$]-histamine). This experiment demonstrated that histamine and IS do not interfere with each other.

5.3.3. LINEARITY, LOD, LOQ AND VALIDATION

The obtained linear regressions coefficient, the determination coefficient (R^2) and the estimated Limit of Detection (LOD) values for each analyte are reported in Table 5.3.

Name	Slope (PAR/ng mL^{-1})	Intercept (PAR)	R^2	LOD (ng mL^{-1})
Histamine	0.0968	0.1047	0.9968	4.4

Table 5.3: linear regression coefficients and LOD

The calibration curve, instead, is reported in Figure 5.7.

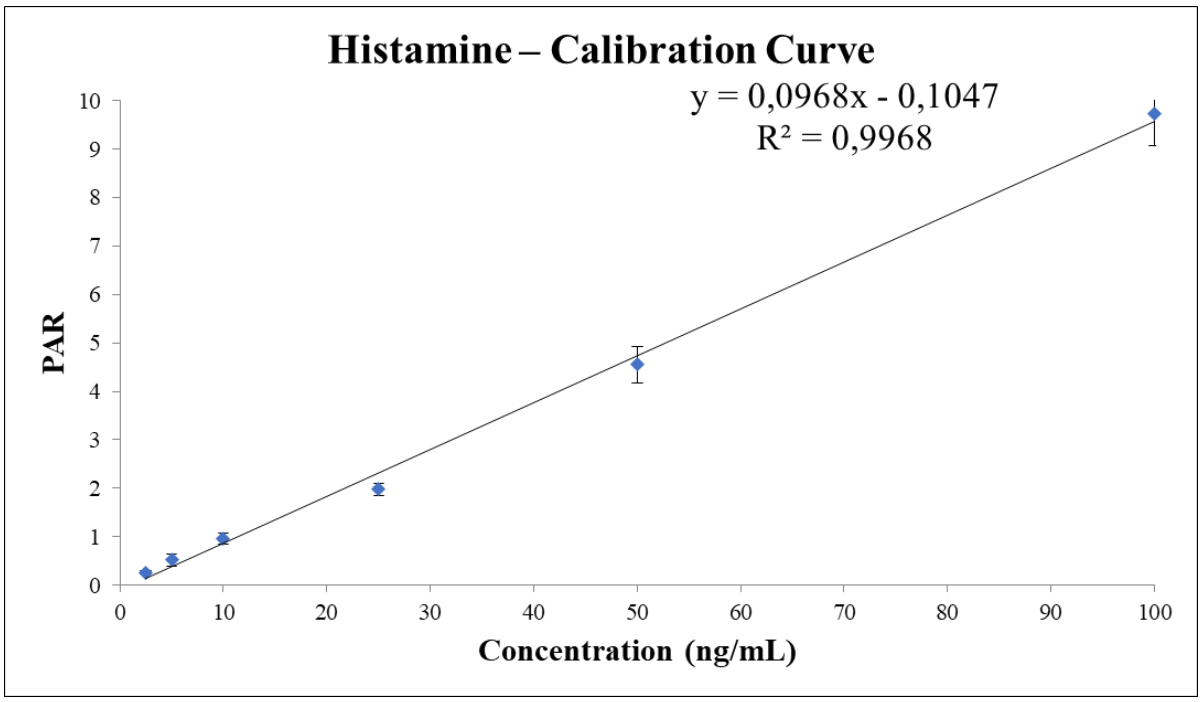

Figure 5.7: calibration curve for histamine

The LOD value of each compound was calculated on the SD of quantitation ion signal, neglecting either the intensity value or the evaluation of the background noise, that can be variable and dependent upon several factors. In this way, it was possible to obtain LOD values each time that the calibration curve was performed, enabling the monitoring of the instrumental performances between different analyzes batches. Moreover, the obtained LOD values strengthened the reliability of the low concentration levels chosen for the calibration curves, allowing to detect histamine in sample even when the quantity is very low. Therefore, ME and RE are reported in table 5.4.

Name	ME (%)	RE (%)
Histamine	114	98

Table 5.4: ME & RE values for histamine

Finally, accuracy and precision were calculated preparing a series of specific samples as reported in chapter 5.2.4 and the results are reported in Table 5.5.

Compound	Low level	Medium level	High level
	Recovery ± RSD (%)	Recovery ± RSD (%)	Recovery ± RSD (%)
Histamine	97 ± 5	101 ± 4	96 ± 4

Table 5.5: Accuracy & Precision(RSD) values for histamine

5.3.4. SAMPLES ANALYSIS

The need to develop this method started from the will of elucidating the inhibitory effect of PEA against the development of morphine tolerance. In fact, it was already shown that morphine activates mast cells (MCs) in vivo and enhances histamine release [76, 77] while PEA down-modulates MC degranulation [78] and astrocyte activity. Furthermore, the final goal of this study was to investigate if a crosstalk exists between astrocytes and MCs during morphine treatment and if PEA is able to regulate this signal.

In a very wide study, our part involved the quantification of histamine in culture medium where RBL-2H3 cell line have grown after different treatments. The first series of samples were treated as follow and the medium was picked up after 10 minutes from the treatment:

Sample 1) Control

Sample 2) Control + (morph 30 μM)

Sample 3) PEA 100 μM + (control)

Sample 4) PEA 100 μM + (PEA 100 μM)

Sample 5) PEA 100 μM + (PEA 100 μM + morph 30 μM)

The results obtained from this samples are reported in Figure 5.8.

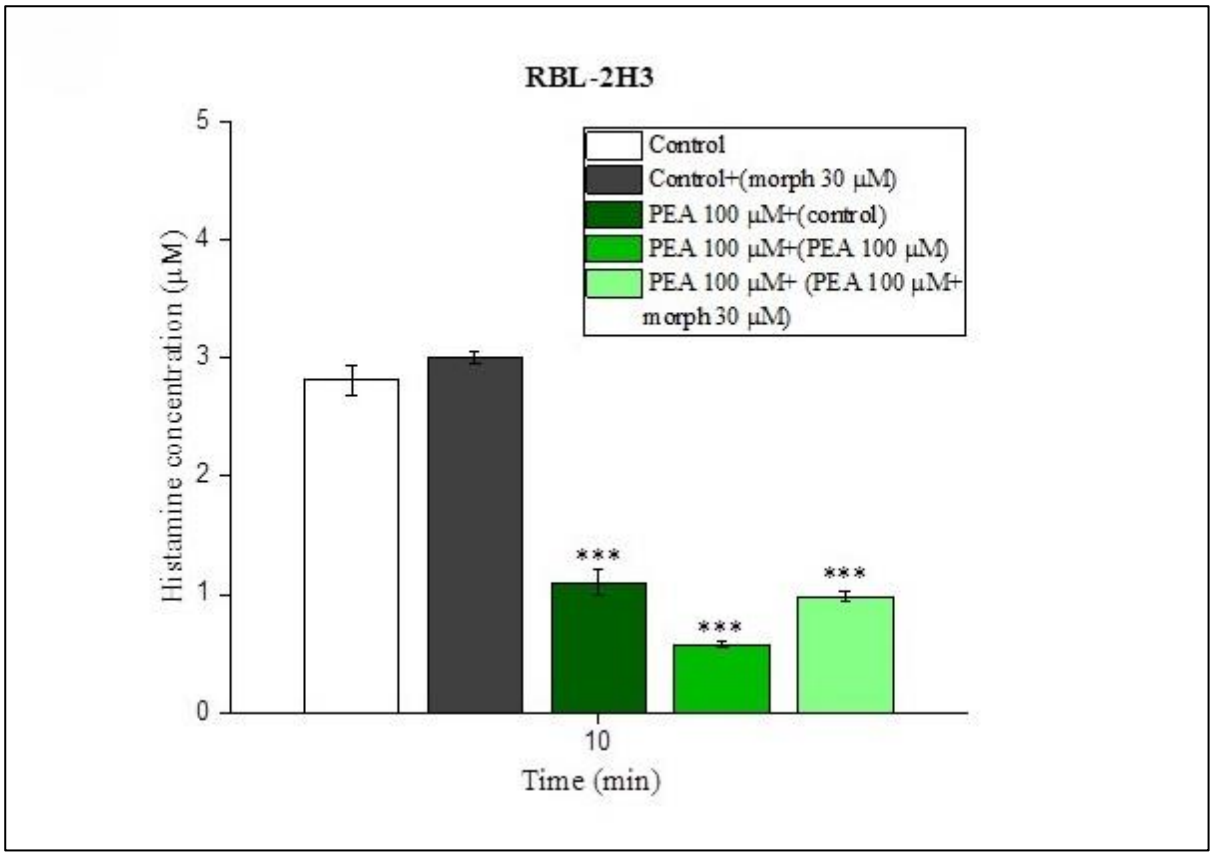

Figure 5.8: results from the first batch of samples

From these results it is possible to highlight that PEA-treated cells released a significantly lower amount of histamine compared to controls confirming the down-modulation of MC degranulation and astrocyte activity.

The second batch of samples were treated as follows: the RBL-2H3 cells were pre-sensitized and pre-treated with PEA 100 µM for 18 hours, and the next day stimulated with Bovine Serum Albumine (DNP-BSA) 625 ng/ml for 30 minutes, 2, 6 and 24 hours and the results are showed in Figure 5.9.

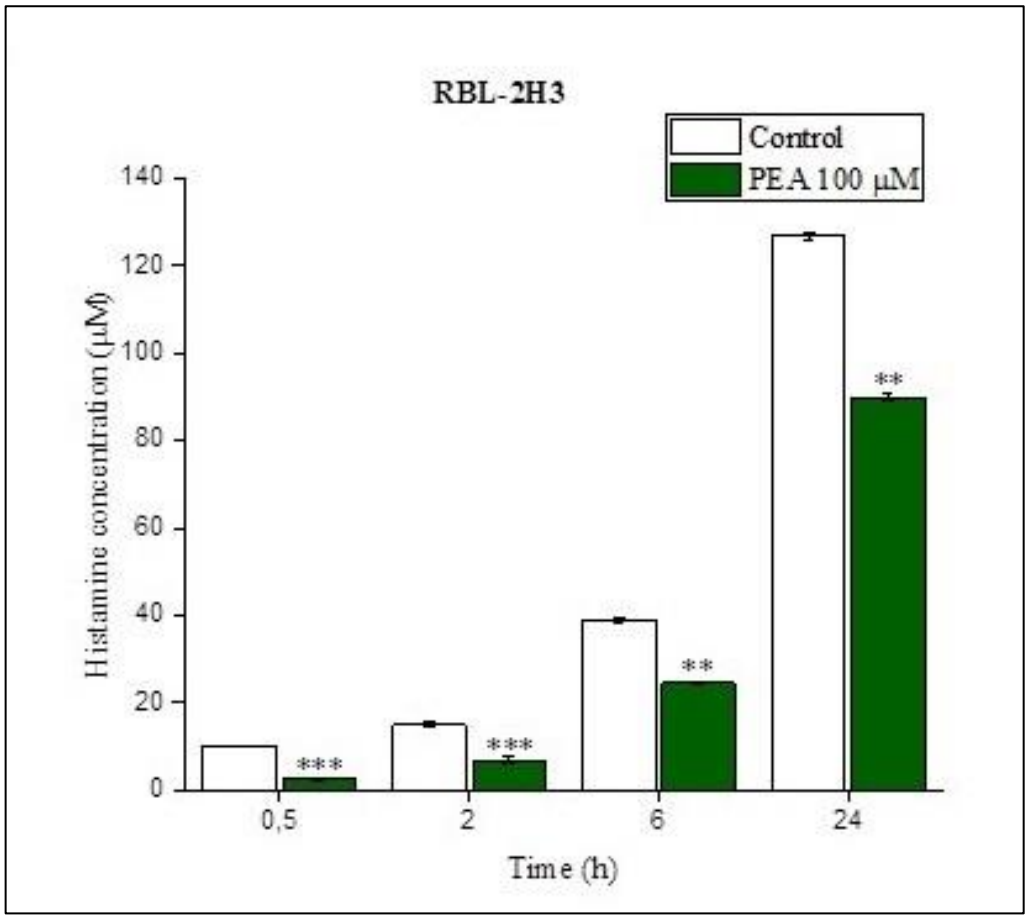

Figure 5.9: results from the second batch of samples

Even in this case the cells treated with PEA showed a lower production in histamine confirming the down-modulating effect of PEA to the degranulation of MC, then a decrease in histamine release. All these results must be deepened doing more biological studies but this preliminary data are very promising.

5.4. CONCLUSIONS

The analysis of histamine can be an interesting tool in pharmacology and biology, but it is also a challenge due to its physico-chemical properties. In fact, its polarity makes it impossible to analyze it in RPLC or GC without derivatization. In this project a new 2D-HPLC-MS/MS method was proposed, performing an on-line SPE. This choice let to a minimum manipulation of the samples (a simple dilution) and a very high sensitivity since it was possible to variate the injection volume (up to 50 μL) and a high dynamicity allowed us to analyze different matrices without changing the method. Matrix effect and recovery were evaluated as 114% and 98%

respectively. Moreover, the accuracy for the three-level tested was quantified as 97%, 101% and 96% with a precision always less than 5%. Finally, this method was applied to quantify histamine in media with RBL-2H3 cells to better elucidate the role of PEA in morphine tolerance. The results showed that the medium where this cell line was treated with PEA contained a less concentration of histamine. More experiments will be performed in order to better elucidate this mechanism.

5.5. FURTHER APPLICATIONS

Considering the versatility showed by this method, we applied in another work for a different study. In this case, the aim of the work was to quantify histamine in rat plasma of two different types of animals: wild type and the so called K.O. rats (with a mutation that block the synthesis of histamine). The sample preparation was proved to be suitable even in this work, but the calibration curve was changed to be accurate for a very low quantity of histamine that was expected in that matrix. Specifically, the six-point calibration curve was made at the following concentrations: 1.5, 2.5, 5, 10, 25 and 50 ng mL^{-1}. The LOD obtained was 0.3 ng mL^{-1}. The results (reported in Table 5.6) were very interesting.

Sample name	Concentration (ng mL^{-1})
HDC +/+ 9NS-ABX 17/2 WT plasma	114.2
HDC +/+ 8NS-ABX 16/2 WT plasma	55.7
HDC +/+ 7NS-ABX 19/2 WT plasma	79.1
HDC -/- 10NS-ABX 10/2 KO plasma	4.4
HDC -/- 2NS-ABX 2/2 KO plasma	6.2
HDC +/+ 4NS-ABX 14/2 WT plasma	48.3
HDC -/- 8NS-ABX 8/2 KO plasma	6.0
HDC -/- 9NS-ABX 9/2 KO plasma	3.9
HDC -/- 5NS-ABX 5/2 KO plasma	2.9
HDC -/- 6NS-ABX 6/2 KO plasma	3.2
HDC -/- 3NS-ABX 3/2 KO plasma	2.6
HDC +/+ 3NS-ABX 13/2 WT plasma	133.1
HDC -/- 1NS-ABX 1/2 KO plasma	3.1
HDC -/- 7NS-ABX 7/2 KO plasma	4.9
HDC +/+ 5NS-ABX 15/2 WT plasma	21.9

HDC +/+ 1NS-ABX 11/2 WT plasma	149.5
HDC +/+ 2NS-ABX 12/2 WT plasma	35.9
HDC -/- 4NS-ABX 4/2 KO plasma	6.1
HDC +/+ 6NS-ABX 18/2 WT plasma	38.3

Table 5.6: first batch of rat plasma samples

Sample name	Concentration (ng mL^{-1})
HDC -/- 3 SD-NO ABX KO	4.9
HDC -/- 5 SD-NO ABX KO	7.5
HDC +/+ 1 SD-NO ABX WT	64.6
HDC -/- 4 SD-NO ABX KO	3.4
HDC +/+ 5 SD-NO ABX WT	60.7
HDC +/+ 2 SD-NO ABX WT	75.4
HDC -/- 2 SD-NO ABX KO	6.7
HDC +/+ 6 SD-NO ABX WT	52.3
HDC -/- 1 SD-NO ABX KO	5.4
HDC -/- 6 SD-NO ABX KO	6.0
HDC +/+ 4 SD-NO ABX WT	69.6
HDC +/+ 7 SD-NO ABX WT	45.0
HDC +/+ 3 SD-NO ABX WT	49.8

Table 5.7: first batch of rat plasma samples

Sample name	Concentration (ng mL^{-1})
7 KO S0B1	32.1
17 WT 1B2	335.1
16 WT 1B1	444.6
18 WT 2A1	78.1
5 KO B0A1	40.4
3 KO B9B1	16.6
14 WT 1A1	881.3
9 KO B0C1	28.8
10 KO B0C2	23.1
11 WT 100A1	315.3
2 KO 89A2	30.6
13 WT 100A3	243.1
15 WT 1A2	224.9
8 KO 90B2	40.4
19 WT 2A2	85.1
4 KO 89B2	23.1

6 KO 90A2	22.9
1 KO 89A1	19.7
12 WT 100A2	433.9

Table 5.8: first batch of rat plasma samples

It is possible to highlight that all the samples of the wild type rats had a concentration of histamine higher than the K.O. ones but the interesting result it is that the mutated rats had a very low concentration of histamine but never zero as it was expected.

It was hypothesized that this low quantity of histamine present in the K.O. rats can come from the diet or/and it is produced by the microbiota of the host. More experiments must be done and are planned to better explain these curious results.

6 PROJECT 4: EVALUATION OF CID FRAGMENTATION OF LEU-ENKEPHALIN IN A LINEAR TRIPLE QUADRUPOLE VARYING THE PRESSURE AND THE COLLISION GAS INSIDE THE COLLISION CELL (WORK IN PROGRESS)

This project was performed in the laboratory of Prof. Memboeuf at Université de Bretagne Occidentale in Brest (France) in my three months abroad experience. As it was reported in Chapter 2.4, the MS/MS experiment can be summarized in three steps: 1) selection of the precursor ion, 2) its fragmentation and 3) analysis of the fragments obtained. The selection of the precursor ion and the analysis of the product ions formed are strongly influenced by the type of mass analyzer used; then, the experiments allowed are limited by the instrumental setup present in the laboratory. Regarding the fragmentation of the precursor ion, can be investigated the features of the process in order to optimize, develop and apply these finds in the standard procedures to improve the reliability and the effectiveness of MS/MS methods. In our case, CID mechanism was studied by evaluating the type, shape and quantity of collisional gas employed. Usually, the instrument manufactures calibrate the CID process in the instrument using only one collision gas and a limited range of pressure inside the collision cell. Furthermore, it is well known that the fragmentation patterns are influenced by the different gases used in the collision gas and their pressure, in addition to the geometry and the length of the collision cells. Since during my PhD work most of the projects involved the use of the MS/MS features through CID experiments using standard parameters (gas pressure and collision gas suggested by the manufacturer) it was found interesting explore what changing these parameters can provide. In fact, optimizing these parameters could be a tool to improve analytical performances for some specific analyte. For these reasons, the goal of this project was to explore the different CID experiments obtained by subject the Leu-enkephalin to collision with different pressures and different gas inside the collision cell using a linear triple quadrupole (Quattro II Micromass/Waters). This instrument presents a modification that allows the control of the pressure inside of the collision cell and an easy change of the collision gas. Furthermore, the CID data obtained can be express in different ways. In this study it was used the Survival Yield (SY) technique.

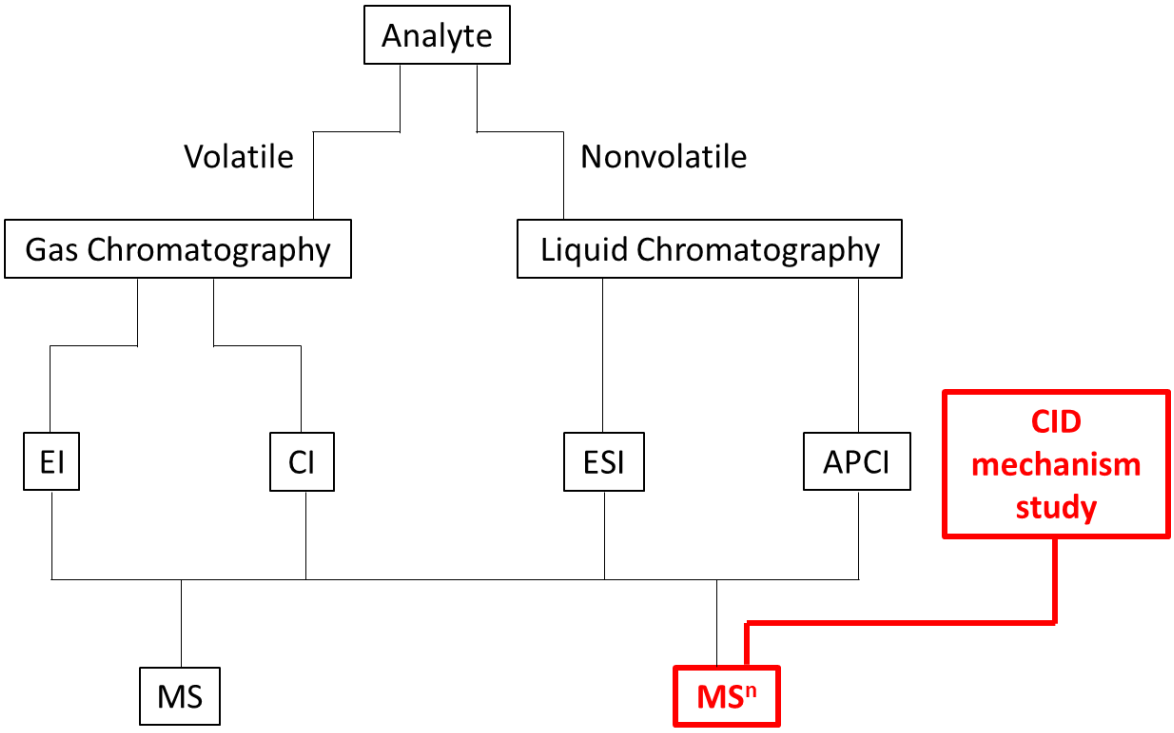

Figure 6.1: scheme of the system employed for Project 4

6.1 INTRODUCTION

In 2013, Tabet et al. studied the pressure effect on internal energy distribution of Leu-enkephalin performing MS/MS experiments with a triple quadrupole [79].

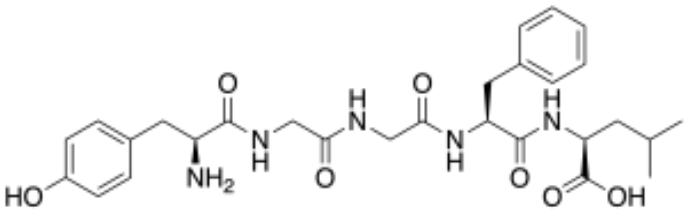

Figure 6.2: structure of Leu-enkephalin

The data obtained were processed with the Survival Yield technique, but also different procedures were employed. Finally, it was carried out different kinetic models to correlate the experimental data with simulated internal energy of precursor ions. In this work it was only employed three different pressures in the q2 and one collision gas (Argon). Starting from this paper it was decided to extend this investigation increasing the number of pressures inside the

collision cell tested and furthermore, it was decided to extend the number of collision gases. The collision gases used were the series of noble gases, namely Helium (He), Neon (Ne), Argon (Ar), Krypton (Kr), Xenon (Xe) and the bimolecular, Nitrogen (N_2) and Oxygen (O_2) gases.
Survival Yield (SY) is a process data technique to study the energetics of fragmentation of the molecules subjected to MS/MS experiments. Differently from the collision breakdown curves used in my previously reported studies where, plotting the abundances of the precursor ion and the fragment ions versus the collision voltage, it is possible to evaluate all the fragments ions produced by the fragmentation of precursor ions, SY curves only follow the part of precursor ions surviving the excitation process by calculating the SY value:

$$SY = \frac{I_{precursor}}{I_{precursor} + \sum I_{products}}$$

where "*I*" represents the absolute abundance of precursor or product ions [80]. Then, for the lower collision voltage, where usually there is not any fragmentation, SY value will be 1 (because the intensity of products ions will be 0), while the increase of the collision voltage will lead to a decrease of SY values until it will reach 0 (all the precursor ion is fragmentated). So, plotting each SY value versus its collision voltage it is possible to build a SY curve as I reported in Figure 6.1.

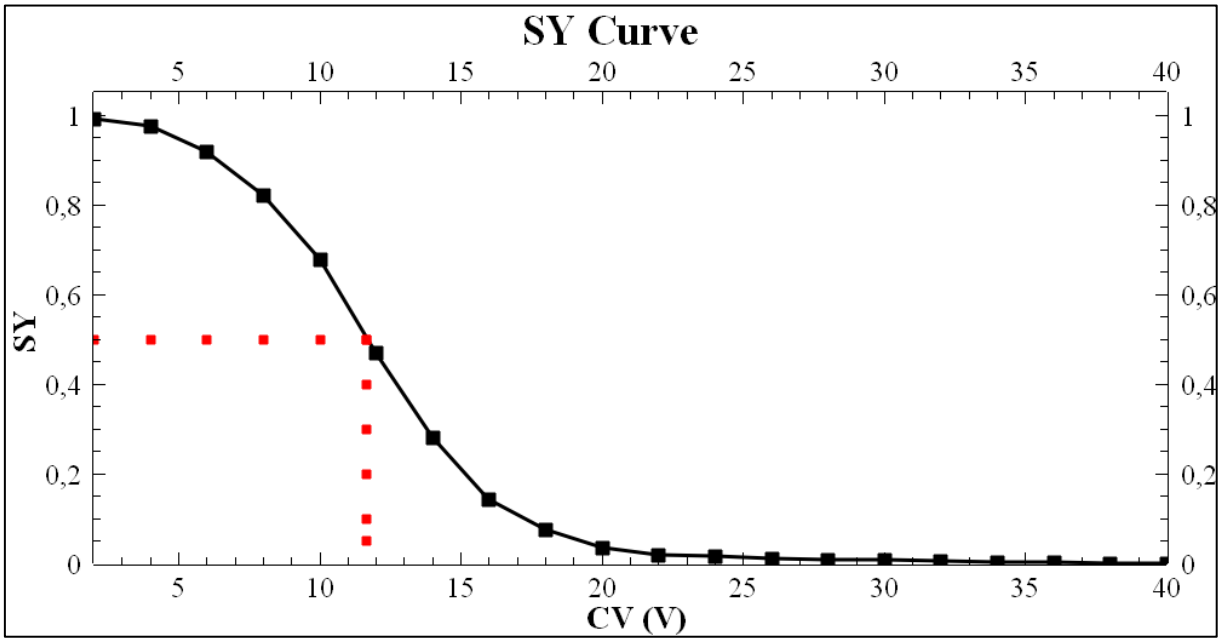

Figure 6.2: example of a SY curve

From a SY curve it is possible to calculate the CV50, so the energy needed to fragment a precursor ion at 50%.

6.2 MATERIAL AND METHODS

The instrument used for this investigation was a Quattro II (Micromass/Waters) equipped with an ESI Z-spray ion source with a specific modification to easy control the pressure inside of the collision cell and to easily change the collision gas. The sample was introduced directly by a Legato 1000 KD Scientific syringe pump.

6.2.1 CHEMICALS

Leu-enkephalin was purchased from Sigma-Aldrich as well as methanol solvent. Water mQ (18MΩ-cm) was obtained by Milli-Q instrument. Gases were purchased from Air liquid at best grade available (Alphagaz 2). The gases properties are reported in Table 6.1.

Gas	Purity (%)	Mass (g mol^{-1})	Polarizability	Correction Factor (Pirani Gauge)
He	≥99,999%	4.003	0.205	1
Ne	≥99,999%	19.992	0.396	1.5
N_2	≥99,999%	28.006	1.74	1
O_2	≥99,999%	31.990	1.581	1
Ar	≥99,999%	39.962	1.64	1.7
Kr	≥99,999%	83.911	2.48	2.6
Xe	≥99,999%	131.904	4.122	3.25

Table 6.1: gases used informations (see text for references)

All the parameters reported in table came from the manual of the Pirani gauge supplier but there were no polarizability and Correction Factor information for Helium and Xenon (values in red). The polarizability values were obtained from chapter 162 of "Physics of Solid Surfaces" Volume 45[81]. In regards of the missing correction factors, it was decided to extrapolate them from the linear correlation obtained by plotting the data from the manual of the Pirani gauge supplier versus the values from "On the gas species dependence of Pirani vacuum gauges"[82]. In this manuscript, it was calculated the correction factor for all the noble gases in another Pirani gauge. Then it was plotted the three correction factors in common (Ne, Ar and Kr) from the

manual of the Pirani gauge used for this experiment and the ones from the manuscript obtaining a linear function (Figure 6.3).

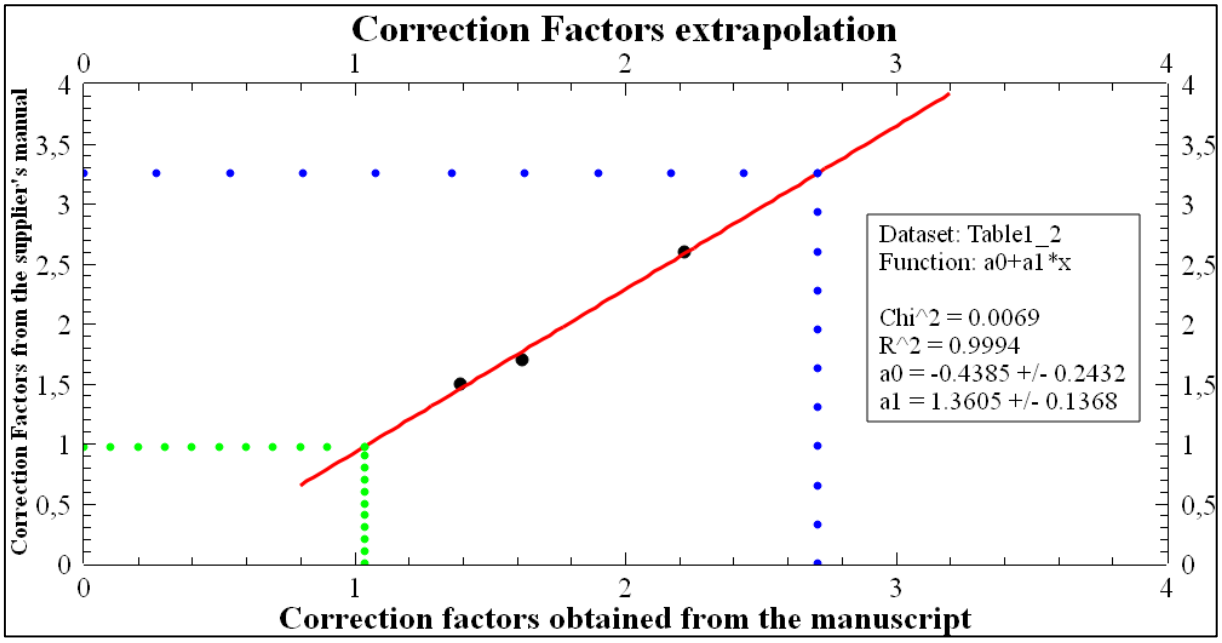

Figure 6.3: extrapolation of the missing CF. The green dots represent the CF extrapolation for Helium while the blue dots represent the CF extrapolation for Xenon

From the equation obtained and the correction factors for Helium and Xenon in the manuscript it was extrapolated the ones from the Pirani gauge employed for this experiment. It is worth to note that the correction factors extrapolated are theoretical and they were used to have a more realistic pressure because the Pirani gauge used was calibrated for Argon.

6.2.2 MASS SPECTROMETRY PARAMETERS

The sample described in chapter 6.2.3 was initially analyzed in scan mode showing the formation of the $[M+H]^+$ ion (556 *m/z*) as base peak with a little production of the $[M+Na]^+$ ion (578 *m/z*, less than 5%).

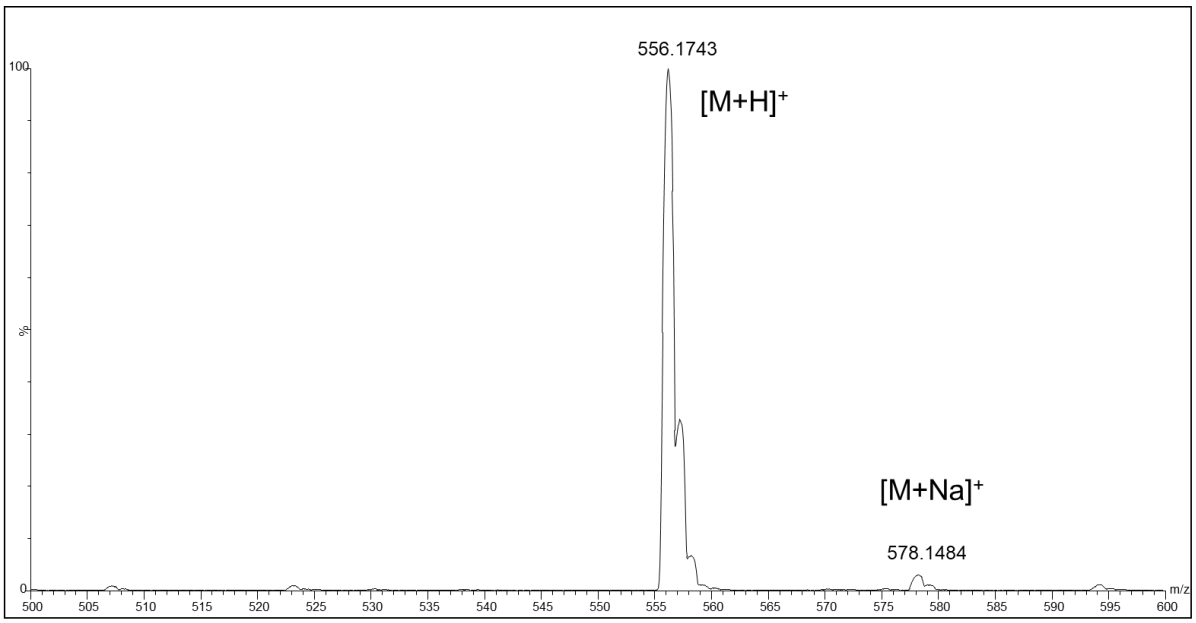

Figure 6.4: MS spectra of Leu-Enkephalin

Then the precursor ion $[M+H]^+$ was isolated and all the parameters were optimized in order to obtain the highest and most stable signal possible. The final MS parameters are reported in Table 6.2-6.4.

1. Source	
Capillary	4
Cone	35
Extractor	2
RF Lens	0
Source Block Temp.	90
Desolvation Temp.	120

Table 6.2: source parameters

2. MS1	
LM Res	10
HM Res	15
IEnergy 1	0.2
IE Ramp 1	10
Lens 6	5
Multiplier 1	650

Table 6.3: MS1 Parameters

3. MS2	
LM Res	12
HM Res	12
Collision	5
IEnergy 2	3.7

IE Ramp 2	0
Lens 8	0
Lens 9	0
Multiplier 2	650

Table 6.4: MS2 parameters

The MS/MS experiments were performed in Product Ion Scan isolating monoisotopically the 556 m/z ($[M+H]^+$), increasing the collision voltage by 2 volts up to 96 Volts (160 for Helium) and recording all the product ions from 80 to 560 m/z. The PIS experiments for each CV were recorded for 1 minute. The gas inside the gas cell was managed by using two valves, working between $1.1 \cdot 10^{-04}$ and $3.0 \cdot 10^{-02}$ mbar.

6.2.3 SAMPLE PREPARATION

The LE sample was prepared at 5 μM in 70% CH_3OH, 30% H_2O with 0.1% formic acid. The compound in study was directly injected by a syringe pump at 5 μL min^{-1}.

6.2.4 DATA PROCESSING

Data were processed with the SY technique. The SY value was calculated, for each voltage of CV, with the equation reported in chapter 6.1. All the SY values obtained were plotted versus their CV obtaining the SY curves. The SY curve is usually described as a sigmoid and, from it, it is possible to calculate the CV50, then the voltage of CV where the precursor ion is fragmented at 50%. All the survival yield curves were built with SciDAVis free software [https://sourceforge.net/projects/scidavis/, 10/20/2022]. The CV50 values were calculated with the same software using the Boltzmann equation function present in the software (described as follows).

$$(A1 - A2)/(1 + \exp\left(\frac{x - x0}{dx}\right)) + A2$$

A1 represents the higher point of the sigmoid (usually SY=1) while A2 represents the lower point of the sigmoid (SY=0 if it happens full fragmentation of the precursor ion). For the sigmoid that reached a SY value of 0 it was not fixed any parameter of the equation and it was let the equation of the instrument apply its calculation algorithm. On the contrary for the sigmoid that did not reach a SY value of 0 it was fixed the A2 value to the lowest SY value of the curve. Doing so, the line obtained was found to be more fitting.

It is important to emphasize that the instrument gauges are calibrated for Argon pressure so, in the following diagrams, the pressures for the other gases were calculated using the correction factors from table x in chapter 6.2.1.

6.3 RESULTS

Unfortunately, this work is still a work in progress, but preliminary result will be presented in chapter 6.3.1.

6.3.1 RESULTS DISCUSSION

The first experiment was performed with Argon as collision gas changing 23 different pressures. So, for each pressure the precursor ion was isolated and then subjected to an increasing CV and recorded for 1 minute. Moreover, for each spectra obtained it was calculated and plotted versus its collision voltage to obtain the SY curve. All the SY curves obtained from the different pressures were collected in the same chart (Figure 6.5).

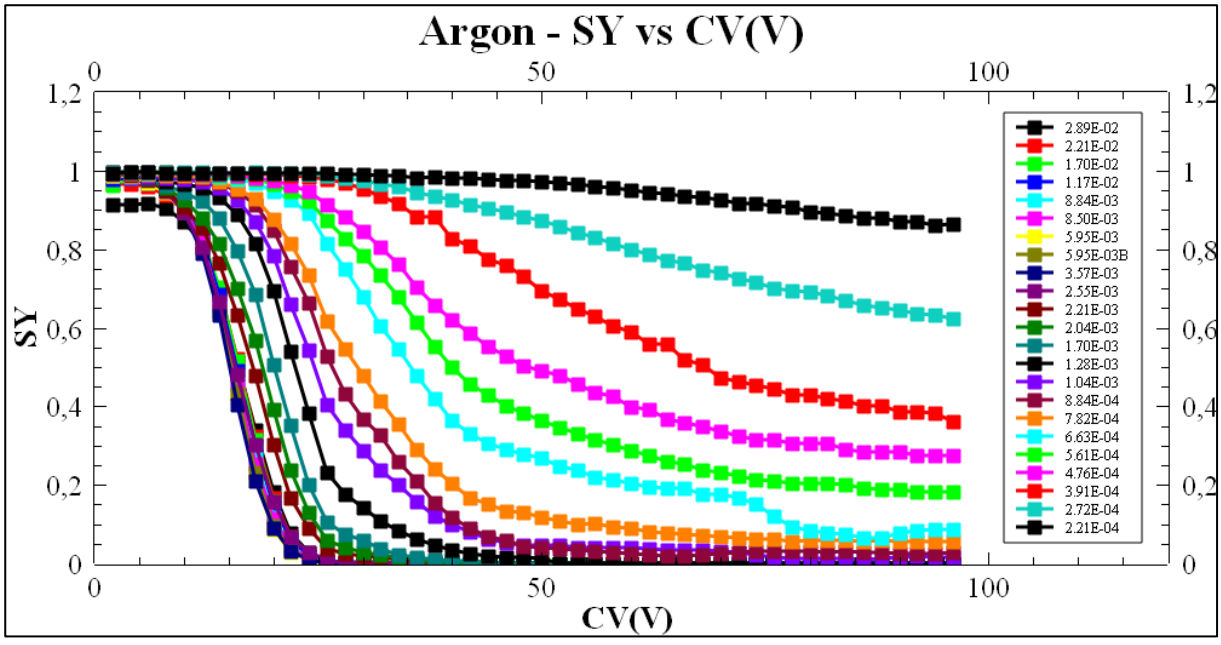

Figure 6.5: SY curves for each pressure using Argon

The choice to start with Argon was made because it is the most used one and usually the most recommended by the instrument suppliers.

From this chart is possible to highlight that for higher pressures lower acceleration voltage is necessary to obtain the complete fragmentation of the precursor ions while, on the contrary, for

lower pressures higher voltages are necessary and, for the lowest pressures, complete fragmentation is not achievable. This is because with larger pressures the accelerated ions inside the q2 are subjected to a lot of collisions with the gas, so they need less CV to have fragmentation while for lower pressures the accelerated ions need more CV to have enough collisions but sometimes is not enough. As it was said, for each SY curve is possible to calculate the CV50 by using the Boltzmann equation function on SciDAVis software.

The same experiment was then repeated for the other noble gases involved in this experiment and the charts obtained were reported in Figure 6.6-6.9.

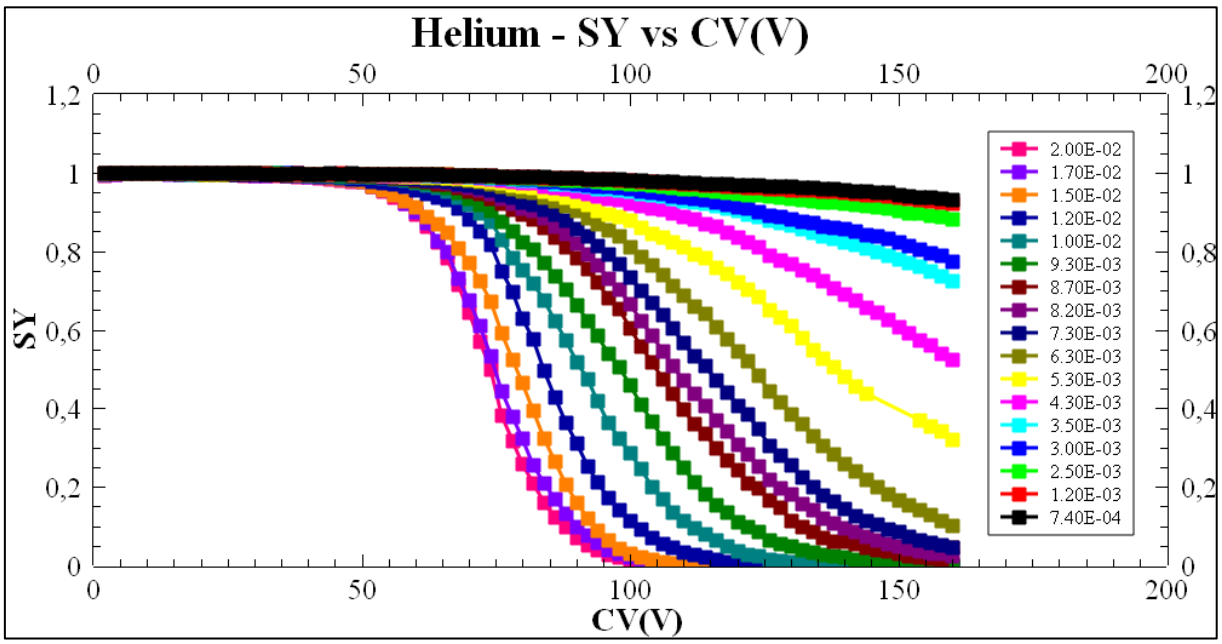

Figure 6.6: SY curves for each pressure using Helium

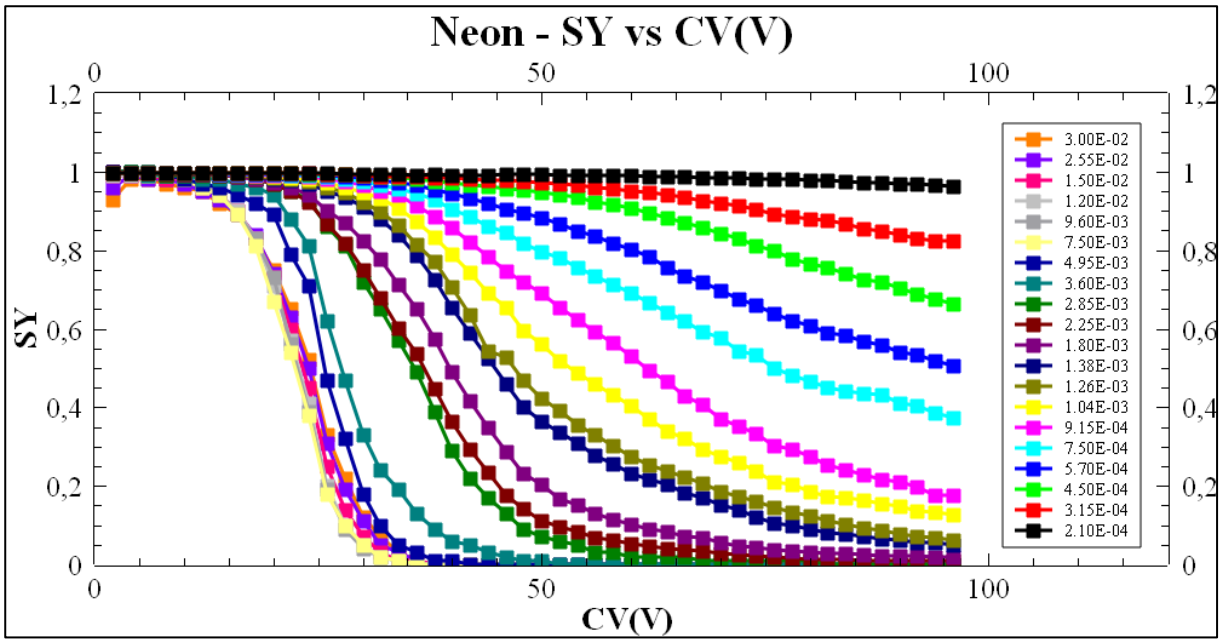

Figure 6.7: SY curves for each pressure using Neon

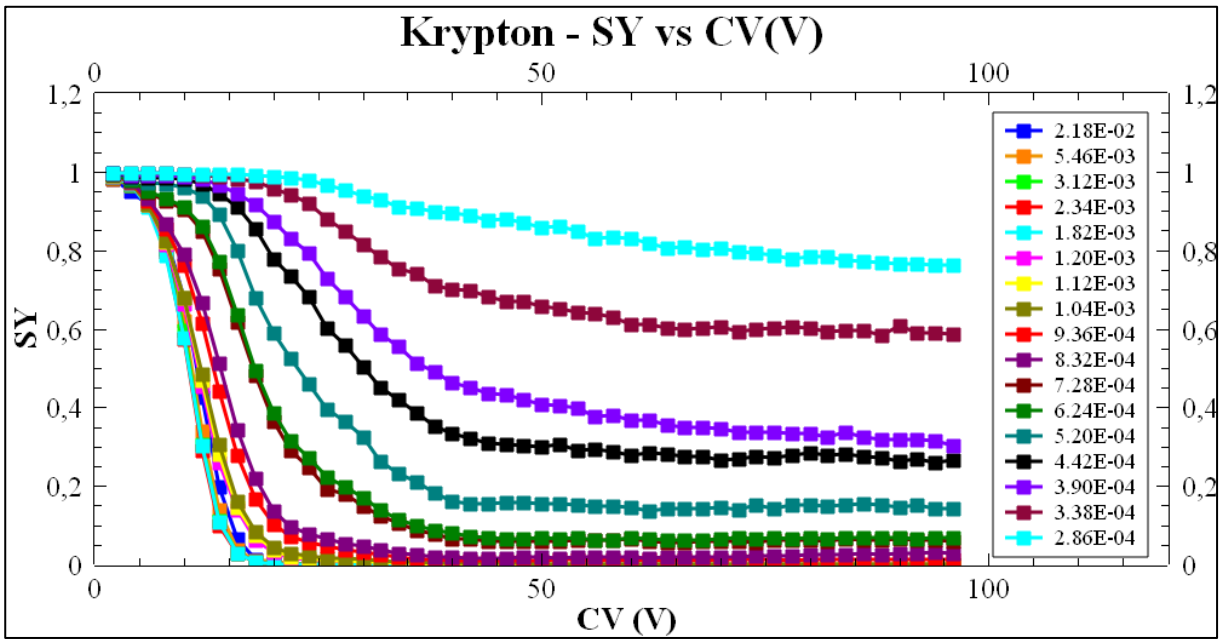

Figure 6.8: SY curves for each pressure using Krypton

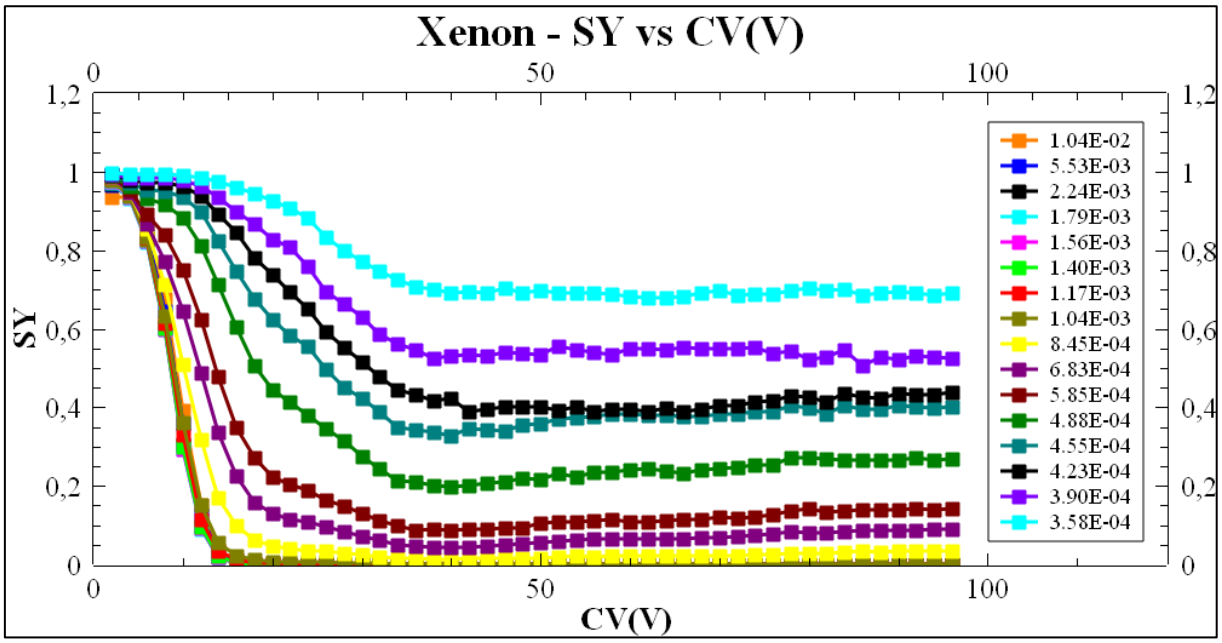

Figure 6.9: SY curves for each pressure using Xenon

For these charts, we observed the same behavior obtained by the experiments in Argon but, depending on the mass of the gases, different CV50 values. In fact, the larger is the mass of the collision gas, the lower is the CV necessary to achieve the same fragmentation degree. Furthermore, it was highlighted that at the highest pressure applied the SY curve shift a little bit on the right, then the CV50 value increases. This behavior was found with different extent in all monoatomic collision gases tested, except for He. For this behavior two theories were made: 1) in a very high-pressure situation we have a quencher effect like Helium in the ion traps; 2) scattering phenomenon occurs that decreases the signal of fragment ions generated.

It is important to highlight that for Xenon (Figure 6.9) seems like that increasing the CV the SY values increases. In this case it was hypothesized that the phenomenon of scattering is so widespread (bigger collision gas and high collision voltages) that it vitiating the calculation of SY.

Furthermore, the experiment was also repeated for the two diatomic gases involved (N2 and O2) and the charts obtained were reported in Figure 6.10-6.11.

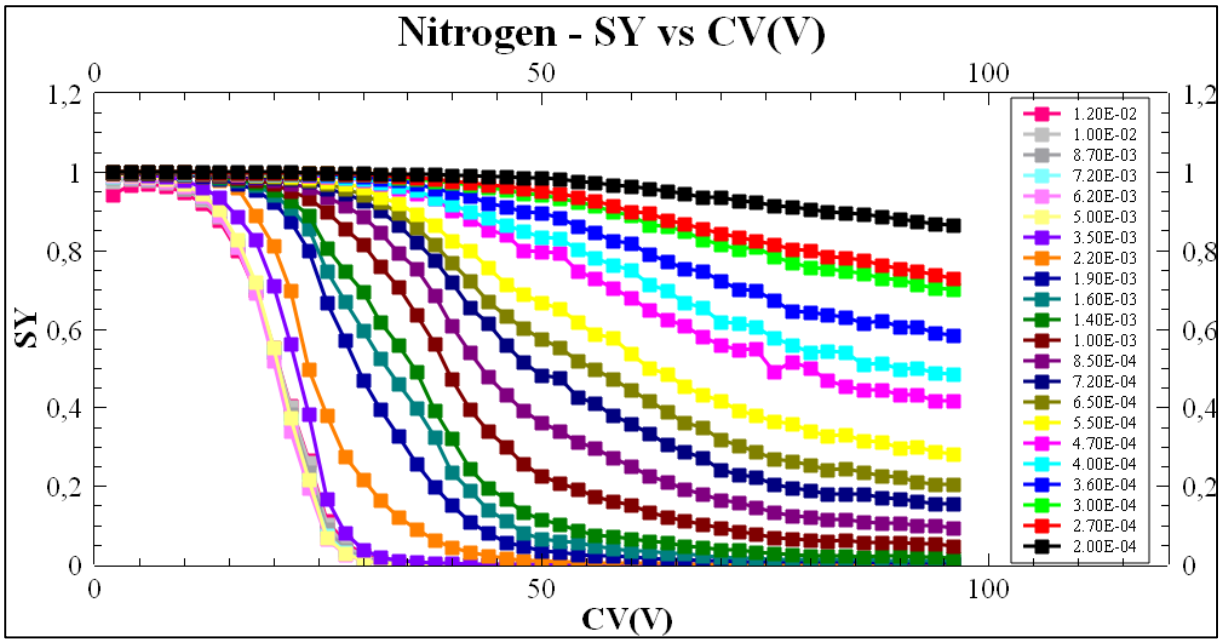

Figure 6.10: SY curves for each pressure using Nitrogen

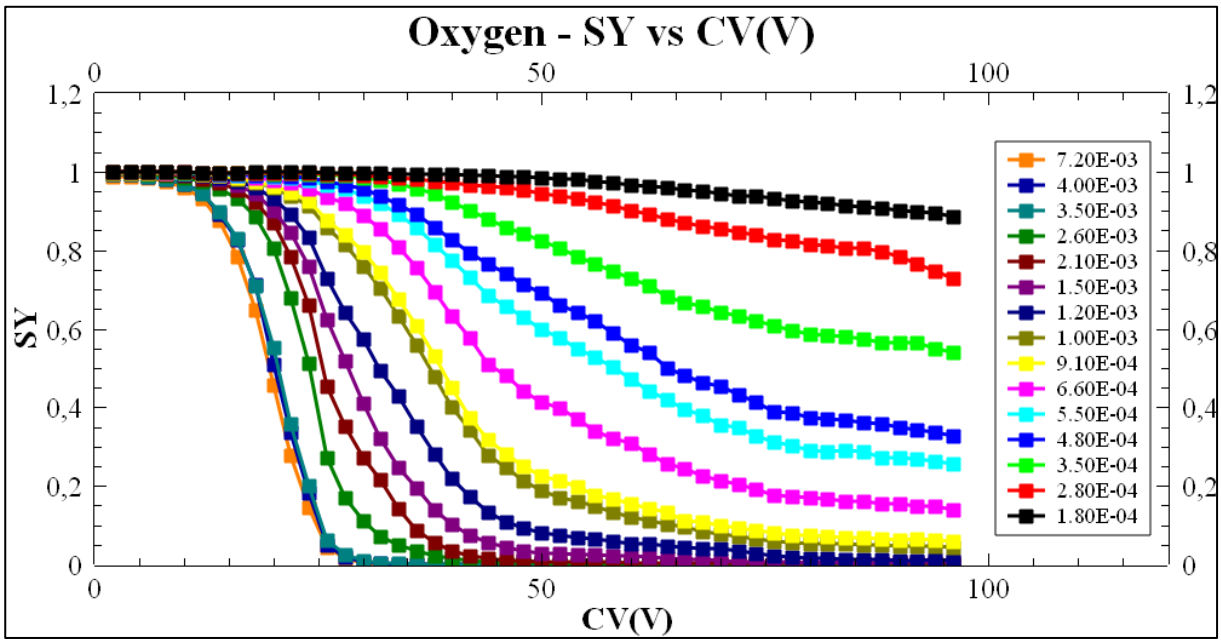

Figure 6.11: SY curves for each pressure using Oxygen

Then, it was decided to confront the SY curves obtained from similar pressure but different gases. The pressures used for each collision gas are reported in Table 6.5 while the chart obtained is reported in Figure 6.12.

Name	Pressure (mbar)
Xe	1.04E-03
Kr	1.04E-03
Ar	1.04E-03
O_2	1.00E-03
N_2	1.00E-03
Ne	1.04E-03
He	1.20E-03
Average	1.05E-03
SD	6.84E-05
RSD	6.52%

Table 6.5: similar pressure employed with different gases

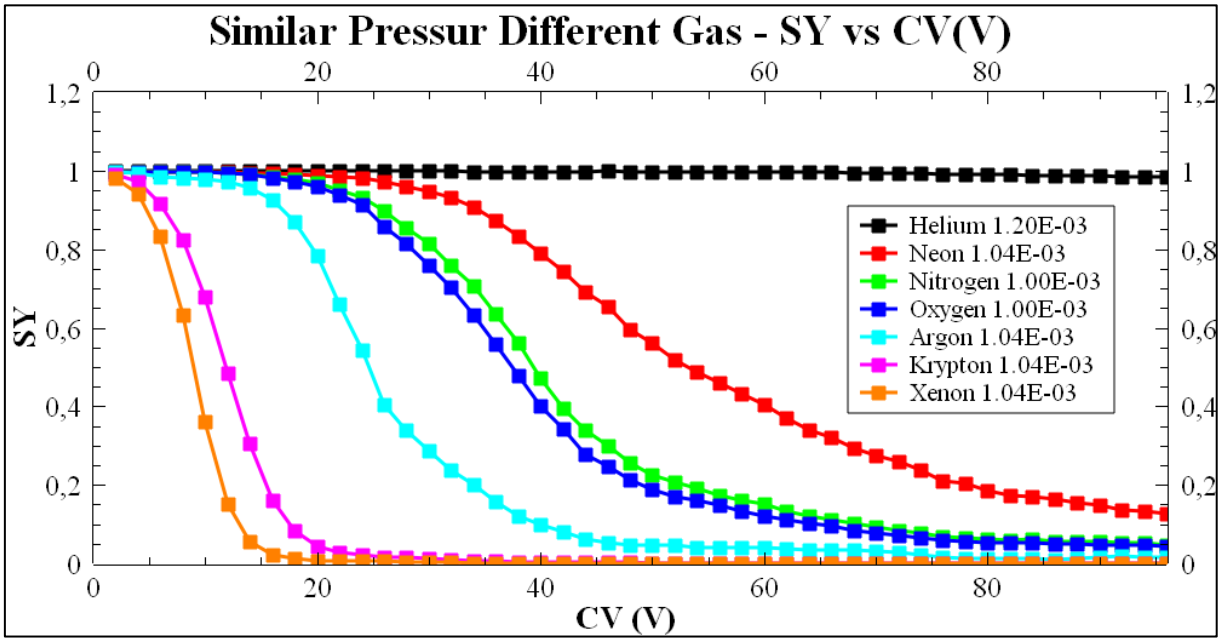

Figure 6.12: SY curves obtained with similar pressure but different gases

From this chart it is possible to highlight that, working with the same pressure inside the q2, higher is the mass of the gas involved lower is the CV energy that is needed for a complete fragmentation of the precursor ion. This makes sense because an accelerated ion in the collision cell will receive more energy in a collision with a bigger molecule or atom of gas. In fact,

plotting the natural logarithm of the CV50 from each SY curves versus the natural logarithm of the mass of the collision gas it was obtained a linear correlation (Figure 6.13).

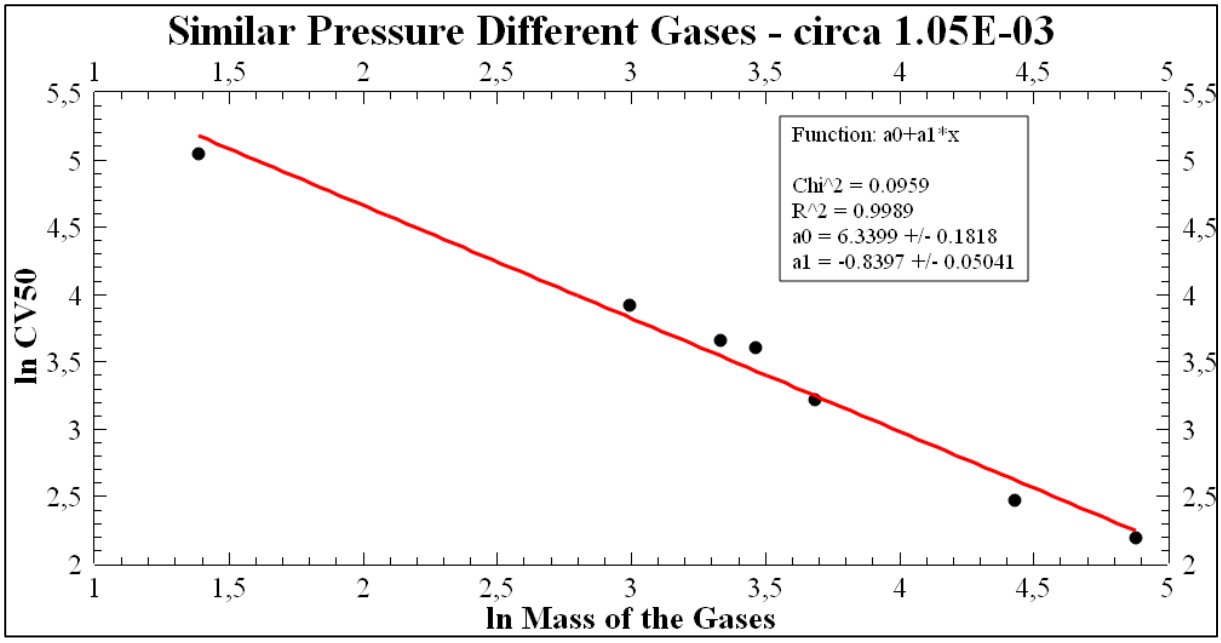

Figure 6.13: linearity obtained plotting the CV50 versus the mass of the gases

Furthermore, to confirm the quality of this experiment it was evaluated the Total Ion Count (TIC) for each CV employed and if there was any concentration effect. First, it was investigated the TIC obtained without any gas inside the collision cell with 3 different concentrations: 5μM (the one used for the experiments), 1μM and 10 μM (Figure 6.14).

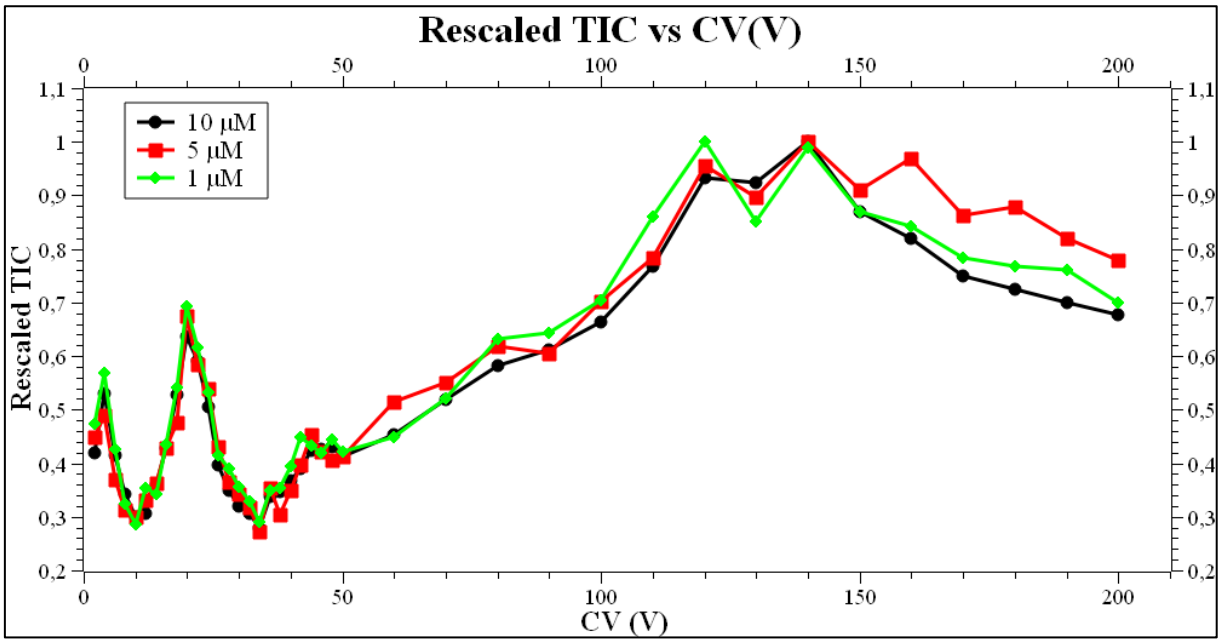

Figure 6.14: TIC obtained with no collision gas and for 3 different concentrations

From this evaluation it is possible to say that, without any gas inside the collision cell, the concentration of leu-enkephalin do not influence the intensity of the signal for each CV employed. The evaluation of the TIC was then repeated for all the gases and pressures employed. In Figure 6.15 it was reported the data obtained for Krypton and it showed a stable signal for high CVs indicating the goodness of the experiments.

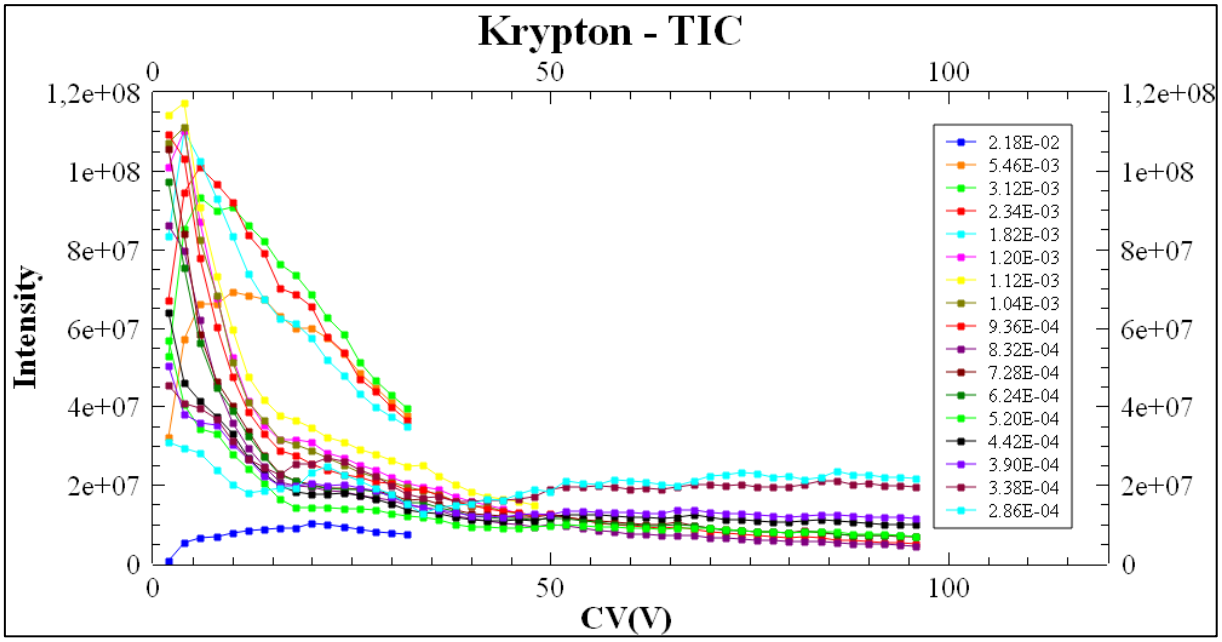

Figure 6.15: TIC obtained from the experiments with Krypton

The charts obtained from the other gases were not reported but they showed a comparable behavior.

6.3.2 PERSPECTIVE

This project involved the collection of a large amount of data and even though this is a work in progress some preliminary data has been explored. First, as expected, the increase of the pressure of collisional gas inside the collision cell led to a lower CV50 because of course, to obtain a fragmentation of the precursor ion, it needed a lower collision voltage. It was also highlighted, for the highest pressures, a right shift to the right of the SY curves with a consequent increase of the CV50 values. It was hypothesized two major events to explain this: 1) a quenching effect; and 2) a scattering effect. Furthermore, it was compared the SY curves obtained from different gases with similar pressures. Plotting the natural logarithm of the CV50 from those SY curve vs the natural logarithm of the mass of the gases it was obtained a linear correlation. However, it is possible to perform more data processing. For instance, performing kinetic modeling on the experimental data to better elucidate the findings and observed phenomena could be an interesting continuation. Moreover, it is also possible to perform data processing to carry out fundamental studies (for example evaluate the relation between the SY curves and the center of mass). Besides, could be an interesting evolution repeat these experiments in a different triple quadrupole equipped with different geometry and/or length of collision cell to evaluate the results obtained in terms of SY curves. These findings can be compared to previous results obtained in Brest to emphasize the possible convergences/similarities between two MS/MS systems.

7 CONCLUSIONS

In the last decades mass spectrometry has become one of the most employed analytical techniques for pharmaceutical, clinical, biological and environmental investigation due to its sensitivity and selectivity. Coupled with chromatography it allowed, in the last years, to elucidate and deepened plenty of arguments due to its high sensitivity, selectivity, robustness and dynamism.

The overall purpose of my project was to develop the best method for each different work using the instruments available in our laboratory. In fact, depending on the analyte/s to be studied it is important to pick the best separation method, ionization source and analyzer. Sometimes this is not even enough, and specific consumables or instrument can be a solution in addition to very complicated sample preparations, but it is very expensive and time consuming. Thus, in this work it was evaluated all the features available from our instruments

However, sometimes to achieve significant results, the employment of a classic application (chromatography with mass spectrometry) is not enough. But conversely, specific instruments or consumable can help in the development of a method. In contrast, this choice is very expensive. Instead, it is possible to take advantage of the MS/MS to solve some of these problems. For instance, it was already demonstrated that is possible to distinguish isomers performing advance MS/MS experiments [11] avoiding long and high-consumption methods. This philosophy was applied in my first project applying an algorithm called LEDA as a supportive tool in a drug stability test in human plasma where the panel of the analytes were pairs of isomers. It was demonstrated that studying the fragmentation patterns of each analyte singularly and building a specific mathematical matrix it was possible to resolve a mixture of isomers. Here, it was used as "quality control" tool to avoid any human error such as bad labeling or wrong autosampler position selected in the instrument. Furthermore, consider the high performances obtained from the algorithm it was decided to applying it to another investigation. This new application involved the evaluation of the stability in human plasma of two pair of positional isomers spiked together or on their own to see if they interfere each other when they are spiked together in human plasma.

The second project instead involved the development of an analytical method to determine the quantity of free fatty acids (FFAs) in human plasma in order to study the differences between healthy patients and colorectal cancer patients. In this case the "philosophy" to follow was the simplicity of the sample preparation and the analytical method. In fact, it was decided to analyze directly the free fatty acids (FFAs) without any derivatization with a GC-MS method. The

sample preparation consisted in a liquid-liquid extraction with MTBE that allowed further application of this method with different matrices without the need of any change.

For the third project the challenge was to develop a method to quantify histamine in culture media to elucidate the role of N-palmitoylethanolamine on morphine tolerance. Histamine is a small, polar organic compound so a RPLC method does not allow any retention. Some group developed a GC-MS method performing the derivatization of histamine while other groups succeeded to obtain a retention in LC employing a HILIC column. In this project we developed a 2D-HILIC-HPLC-MS/MS method performing an on-line SPE using two HILIC column: the first to load, clean and concentrate the sample the second to separate possible interference compounds present in the sample. This method reached a very high sensitivity and allowed the employment of a very simple sample preparation (dilution). The robustness of this method allowed its application to another project involving the quantification of histamine in plasma of two different types of rats (wild type and ko).

Finally, in the last project, it was explored the effect on changing the parameters of the collision cell in a triple quadrupole (type of gas and/or pressure) in the CID processes. This project was performed in my three months abroad experience at Universitè de Bretagne Occidentale in Prof. Memboeuf's laboratory, and it is still a work in progress.

8 BIBLIOGRAPHY

1. Baghel, U. S. & Singh, A. *Application of Mass Spectroscopy in Pharmaceutical and Biomedical Analysis Application of Mass Spectroscopy in Pharmaceutical and Biomedical Analysis*. doi:10.5772/intechopen.70655 (2017).

2. Watson, J. T. & Sparkman, O. D. *Introduction to Mass Spectrometry*. *Spectroscopic Methods and Analyses*. doi:10.1385/0-89603-215-9:191 (2003).

3. R. E. March & J. F. J. Todd. *Quadrupole Ion Trap Mass Spectrometry Second Edition Chemical Analysis.* (2005).

4. Vitha, M. F. *Chromatography principles and intrumentation* (2017).

5. Szumilak, M. & Wiktorowska-owczarek, A. Hybrid Drugs — A Strategy for Overcoming Anticancer Drug Resistance ? *Molecules* 1–31 (2021).

6. Bua, S. *et al.* Design and Synthesis of Novel Nonsteroidal Anti-In fl ammatory Drugs and Carbonic Anhydrase Inhibitors Hybrids (NSAIDs − CAIs) for the Treatment of Rheumatoid Arthritis. *J. Med. Chem.* doi:10.1021/acs.jmedchem.6b01607 (2017).

7. Menicatti, M. *et al.* 15. Resolution of co-eluting isomers of anti-inflammatory drugs conjugated to carbonic anhydrase inhibitors from plasma in liquid chromatography by energy-resolved tandem mass spectrometry. *J. Enzyme Inhib. Med. Chem.* **33**, 671–679 (2018).

8. Bua, S. *et al.* Bioisosteric Development of Multitarget Nonsteroidal Anti- In fl ammatory Drug − Carbonic Anhydrases Inhibitor Hybrids for the Management of Rheumatoid Arthritis. *J. Med. Chem.* doi:10.1021/acs.jmedchem.9b01130 (2020).

9. Kopecka, J., *et al*. P-glycoprotein-mediated chemoresistance is reversed by carbonic anhydrase XII inhibitors. *Oncotarget* **7**, 85861–85875 (2016).

10. Teodori, E. *et al.* Dual P-Glycoprotein and CA XII Inhibitors : A New Strategy to Reverse the P-gp Mediated Multidrag Resistance (MDR) in Cancer Cells. *Molecules* **1**, 1–26 (2020).

11. Crotti, S., *et al.* Tandem mass spectrometry approaches for recognition of isomeric compounds mixtures. *Mass Spec Rev.* doi:10.1002/mas.21757 (2022).

12. Kurimoto, A. *et al.* Analysis of Energy-Resolved Mass Spectra at MS n in a Pursuit To Characterize Structural Isomers of Oligosaccharides. **78**, 3461–3466 (2006).

13. Fouque, D. J. D., *et al.* Purification and quantification of an isomeric compound in a mixture by collisional excitation in multistage mass spectrometry experiments. *Anal. Chem.* **88**, 10821–10825 (2016).

14. Campbell, M. T., *et al.* Distinguishing Biologically Relevant Hexoses by Water Adduction to the Lithium-Cationized Molecule. *Anal. Chem.* **89**, 10504–10510 (2017).

15. Menicatti, M. *et al.* Resolution of co-eluting isomers of anti- inflammatory drugs conjugated to carbonic anhydrase inhibitors from plasma in liquid chromatography by energy-resolved tandem mass spectrometry. *J. Enzyme Inhib. Med. Chem.* **33**, 671–679 (2018).

16. Menicatti, M. *et al.* Determination of coeluted isomers in wine samples by application of MS/MS deconvolution analysis. *J. Mass Spectrom.* 2–9 doi:10.1002/jms.4607 (2020).

17. Pallecchi, M. *et al.* Application of LEDA algorithm for the recognition of P-glycoprotein and Carbonic Anhydrase hybrid inhibitors and evaluation of their plasma stability by HPLC-MS/MS analysis. *J. Pharm. Biomed. Anal.* **219**, 114887 (2022).

18. Hill, B. T. Drug resistance : An overview of the current state of the art. *Int. J. Oncol.*197–203 (1996).

19. McGuire, W. L. *Drug Resistance in Cancer Therapy Cancer Treatment and Research*. (1989).

20. Liu, Y., Han, *et al.* Ceramide glycosylation potentiates cellular multidrug. 719–730 (1999).

21. Dietel, M. What ’ s New in Cytostatic Drug Resistance and Pathology. *Pathol. Res. Pract.* **187**, 892–905 (1991).

22. Hammond, J. R., *et al.* Enhanced Efflux of [3H] Vinblastine from Chinese Hamster Ovary Cells Transfected with a Full-Length Complementary DNA Clone for the mdrl Gene. *Cancer Research* 3867–3871 (1989).

23. Beck, T. Mechanisms of multidrug resistance in human tumor cells . The roles of P-glycoprotein , DNA topoisomerase II , and other factors. *Cancer Treatment Reviews* **17**, (1990).

24. Scheper, R. J., *et al.* Overexpression of a Mr 110,000 Vesicular Protein in Non-P-Glycoprotein-mediated Multidrug Resistance. *Cancer Res.* 1475–1479 (1993).

25. Annereau, J. *et al.* Predicting drug sensitivity and resistance : Profiling ABC transporter genes in cancer cells. *Cancer Cell.* **6**, 129–137 (2004).

26. Kopecka, J. *et al.* Carbonic anhydrase XII is a new therapeutic target to overcome chemoresistance in cancer cells. *Oncotarget* (2015).

27. Chiche, J. *et al.* Hypoxia-inducible carbonic anhydrase IX and XII promote tumor cell growth by counteracting acidosis through the regulation of the intracellular pH. *Cancer Res.* **69**, 358–368 (2009).

28. Mboge, M. Y. *et al.* Selective inhibition of carbonic anhydrase IX over carbonic anhydrase XII in breast cancer cells using benzene sulfonamides: Disconnect between activity and growth inhibition. *PLoS One* **13**, 1–27 (2018).

29. Hockel, M., *et al.* Tumor Hypoxia : Definitions and Current Clinical, Biologic, and molecular aspects *J Natl Cancer Inst.* **93**, (2001).

30. Teodori, E. *et al.* Design, synthesis and biological evaluation of stereo- and regioisomers of amino aryl esters as multidrug resistance (MDR) reversers. *Eur. J. Med. Chem.* **182**, 111655 (2019).

31. Matuszewski, B. K. & Constanzer, M. L. Strategies for the Assessment of Matrix Effect in Quantitative Bioanalytical Methods Based on HPLC - MS / MS. *Anal. Chem.* **75**, 3019–3030 (2003).

32. Stefanini-Oresic, L. Validation of analytical procedures: ICH guidelines Q2(R2). *Farm. Glas.* **2**, 1–34 (2022).

33. Dei, S. *et al.* Modulation of the spacer in N,N-bis(alkanol)amine aryl ester heterodimers led to the discovery of a series of highly potent P-glycoprotein-based multidrug resistance (MDR) modulators. *Eur. J. Med. Chem.* **172**, 71–94 (2019).

34. Braconi, L. *et al.* New Dual P-Glycoprotein (P-gp) and Human Carbonic Anhydrase XII (hCA XII) Inhibitors as Multidrug Resistance (MDR) Reversers in Cancer Cells. doi:10.1021/acs.jmedchem.2c01175 (2022).

35. Pallecchi, M. *et al.* Simultaneous Degradation Study of Isomers in Human Plasma by HPLC-MS / MS and Application of LEDA Algorithm for Their Characterization. 1–19 (2022).

36. Bartolucci, G. *et al.* A method for assessing plasma free fatty acids from C2 to C18 and its application for the early detection of colorectal cancer. *J. Pharm. Biomed. Anal.* **215**,

114762 (2022).

37. Cong, J., Zhou, P. & Zhang, R. Intestinal Microbiota-Derived Short Chain Fatty Acids in Host Health and Disease. *Nutrients* **14**, 1–15 (2022).

38. Marchesi, J. R. *et al.* The gut microbiota and host health: A new clinical frontier. *Gut* **65**, 330–339 (2016).

39. Papackova, Z. & Cahova, M. Fatty acid signaling: The new function of intracellular lipases. *Int. J. Mol. Sci.* **16**, 3831–3855 (2015).

40. Huda-Faujan, N. . et al. The Impact of the Level of the Intestinal Short Chain Fatty Acids in Inflammatory Bowel Disease Patients Versus Healthy Subjects. *Open Biochem. J.* doi:10.1016/S0022-328X(00)84700-2 (2010).

41. Mohan, R. *et al.* Effects of Bifidobacterium lactis Bb12 supplementation on body weight, fecal pH, acetate, lactate, calprotectin, and IgA in preterm infants. *Pediatr. Res.* **64**, 418–422 (2008).

42. Niccolai, E. *et al.* Evaluation and comparison of short chain fatty acids composition in gut diseases. *World J. Gastroenterol.* **25**, 5543–5558 (2019).

43. Silva, Y. P., *et al.* The Role of Short-Chain Fatty Acids From Gut Microbiota in Gut-Brain Communication. *Front. Endocrinol. (Lausanne).* **11**, 1–14 (2020).

44. Schönfeld, P. & Wojtczak, L. Short- and medium-chain fatty acids in energy metabolism: The cellular perspective. *J. Lipid Res.* **57**, 943–954 (2016).

45. Wojciechowicz, M. L. & Ma'ayan, A. GPR84: an immune response dial? *Nat. Rev. Drug Discov.* **19**, 374 (2020).

46. Baldi, S. *et al.* Free Fatty Acids Signature in Human Intestinal Disorders : Significant Association between Butyric Acid and Celiac Disease. (2021).

47. Kimura, I., *et al.* Free Fatty Acid Receptors in Health and Disease. *Physiol Rev.* 171–210 doi:10.1152/physrev.00041.2018 (2019).

48. Morrison, D. J., *et al.* Formation of short chain fatty acids by the gut microbiota and their impact on human metabolism. *Gut Microbes* **7**, 189–200 (2016).

49. Tan, J. K., *et al.* Metabolite-Sensing G Protein – Coupled Receptors — Facilitators of Diet-Related Immune Regulation. *Annu. Rev. Immunol.* (2017).

50. Lupton, J. R. Microbial Degradation Products Influence Colon Cancer Risk: the Butyrate Controversy. *J. Nutr* **134**, 479–482 (2004).

51. Yao, L. *et al.* Quantitative analysis of short - chain fatty acids in human plasma and serum by GC – MS. *J. Pharm. Biomed. Anal.* 4391–4399 (2022).

52. Crotti, S. *et al.* Altered plasma levels of decanoic acid in colorectal cancer as a new diagnostic biomarker. *Anal. Bioanal. Chem.* 6321–6328 doi:10.1007/s00216-016-9743-1 (2016).

53. Uchiyama, K., *et al.* Serum metabolomics analysis for early detection of colorectal cancer. *J. Gastroenterol.* **52**, 677–694 (2017).

54. Mehta, A., Oeser, A. M. & Carlson, M. G. Rapid quantitation of free fatty acids in human plasma by high-performance liquid chromatography. *J. Chromatogr. B Biomed. Appl.* **719**, 9–23 (1998).

55. Nishikiori, M., Iizuka, H., Ichiba, H., Sadamoto, K. & Fukushima, T. Determination of free fatty acids in human serum by HPLC with fluorescence detection. *J. Chromatogr. Sci.* **53**, 537–541 (2015).

56. Ohigashi, S., *et al.* Changes of the Intestinal Microbiota , Short Chain Fatty Acids , and Fecal pH in Patients with Colorectal Cancer. *Dig. Dis. Sci.* 1717–1726 doi:10.1007/s10620-012-2526-4 (2013).

57. Yusuf, F., *et al.* Butyrate Acid as a Potential Marker for Diversity of Gut Microbiota in Colorectal Cancer Patients. *SKIC-MHS 2018* 27–30 doi:10.5220/0008790200270030 (2020).

58. Nkondjock, A., *et al.* Specific fatty acids and human colorectal cancer : an overview. *Cancer Detect. Prev.* **27**, 55–66 (2003).

59. Genua, F. *et al.* Association of circulating short chain fatty acid levels with colorectal adenomas and colorectal cancer. *Clin. Nutr. ESPEN* **46**, 297–304 (2021).

60. Li, Y. *et al.* Gut commensal derived-valeric acid protects against radiation injuries. *Gut Microbes* **11**, 789–806 (2020).

61. Hinnebusch, B. F., *et al.* The effects of short-chain fatty acids on human colon cancer cell phenotype are associated with histone hyperacetylation. *J. Nutr.* **132**, 1012–1017 (2002).

62. Hester, C. M. *et al.* Fecal microbes , short chain fatty acids , and colorectal cancer across racial / ethnic groups. *World J. Gastroenterol.* **21**, 2759–2769 (2015).

63. Sakata, T. Pitfalls in short- - chain fatty acid research : A methodological review. *Anim. Sci. J.* 3–13 doi:10.1111/asj.13118 (2019).

64. Schönfeld, P. & Wojtczak, L. Short- and medium-chain fatty acids in the energy metabolism – the cellular perspective *J. Lipid. Res.*(2016).

65. Damiano, F. *et al.* Decanoic Acid and Not Octanoic Acid Stimulates Fatty Acid Synthesis in U87MG Glioblastoma Cells : A Metabolomics Study. *Front. Neurosci.* **14**, 1–11 (2020).

66. Russo, E. Effects of viremia and CD4 recovery on gut "microbiome-immunity" axis in treatment-naïve HIV-1-infected patients undergoing antiretroviral therapy. *World J. Gastroenterol. Gastroenterol.* **9327**, (2022).

67. Baldi, S. *et al.* Effect of ancient Khorasan wheat on gut microbiota, inflammation, and short-chain fatty acid production in patients with fibromyalgia. *World J. Gastroenterol.* **28**, 1965–1980 (2022).

68. Russo, E. *et al.* Crohn's disease recurrence updates: first surgery vs. surgical relapse patients display different profiles of ileal microbiota and systemic microbial-associated inflammatory factors. *Front. Immunol.* **13**, 1–18 (2022).

69. Federica, R. *et al.* Characterization of the "gut microbiota-immunity axis" and microbial lipid metabolites in atrophic and potential celiac disease. *Front. Microbiol.* **13**, 1–13 (2022).

70. Micheli, L. *et al.* Effects of Ultramicronized N-Palmitoylethanolamine Supplementation on Tramadol and Oxycodone Analgesia and Tolerance Prevention. *Pharmaceutics* **14**, 1–20 (2022).

71. Thangam, E. B. *et al.* The role of histamine and histamine receptors in mast cell-mediated allergy and inflammation: The hunt for new therapeutic targets. *Front. Immunol.* **9**, 1–9 (2018).

72. Payne, N. A., Zirrolli, J. A. & Gerber, J. G. Analysis of Histamine and / VT-Methylhistamine in Plasma by Gas Chromatography-Negative Ionization Mass Spectrometry *Analytical Biochemistry*. **420**, 414–420 (1989).

73. Chimalakonda, K. C. *et al.* Development and validation of a liquid-chromatography

tandem mass spectrometry method to determine in vitro and in vivo histamine release. *J. Pharm. Biomed. Anal.* **102**, 494–499 (2015).

74. Guo, Y., *et al.* Histamine H1 receptor cell membrane chromatography online high-performance liquid chromatography with mass spectrometry method reveals houttuyfonate as an activator of the histamine H1 receptor. *J. Sep. Sci.* **37**, 3188–3194 (2014).

75. Moore, S., *et al.* Mass spectrometric characterisation and quantitation of selected low molecular mass compounds from the venom of Haplopelma lividum (Theraphosidae). *Rapid Commun. Mass Spectrom.*1747–1755 doi:10.1002/rcm (2009).

76. Nguyen, J. *et al.* Morphine stimulates cancer progression and mast cell activation and impairs survival in transgenic mice with breast cancer. *Br. J. Anaesth.* **113**, 4–13 (2014).

77. Vincent, L. *et al.* Mast cell activation contributes to sickle cell pathobiology and pain in mice. *Blood* **122**, 1853–1862 (2013).

78. Mazzari, S., *et al.* N-(2-Hydroxyethyl) hexadecanamide is orally active in reducing edema formation and inflammatory hyperalgesia by down-modulating mast cell activation. *Eur. J. Pharmacol.* **300**, 227–236 (1996).

79. Ichou, F. *et al.* Collision cell pressure effect on CID spectra pattern using triple quadrupole instruments: A RRKM modeling. *J. Mass Spectrom.* **48**, 179–186 (2013).

80. Jeanne Dit Fouque, D., Lartia, R., Maroto, A. & Memboeuf, A. Quantification of intramolecular click chemistry modified synthetic peptide isomers in mixtures using tandem mass spectrometry and the survival yield technique. *Anal. Bioanal. Chem.* **410**, 5765–5777 (2018).

81. Chiarotti, G. & Chiarandia, P. *Physics of Solid Surfaces*. *Physics of Solid Surfaces*. doi:10.1007/978-3-662-53908-8 (2018).

82. Jousten, K. On the gas species dependence of Pirani vacuum gauges. *J. Vac. Sci. Technol. A Vacuum, Surfaces, Film.* **26**, 352–359 (2008).